The Role of Epidermal Growth Factor Receptor in Feline Oral Squamous Cell Carcinoma

Gurå Therese Bergkvist

Thesis presented for degree of Doctor of Philosophy

The University of Edinburgh

2011

Abstract

Feline oral squamous cell carcinomas (FOSCCs) are locally aggressive tumours and a common cause of mortality and morbidity. Current treatment options are rarely successful and animals are frequently euthanised upon diagnosis due to their grave prognosis. Epidermal Growth Factor Receptor (EGFR) is a tyrosine kinase receptor which is frequently dysregulated in SCC of the head and neck (HNSCC) in man. Recent advances in human medicine have identified EGFR as a therapeutic target in HNSCC.

In this study the role of EGFR in FOSCC was investigated. Sixty seven biopsy samples were immunohistochemically labelled for EGFR and Ki67, a proliferation marker. The tyrosine kinase region of feline EGFR was cloned and sequenced, and six small interfering RNAs (siRNAs) targeting the tyrosine kinase region were developed. The most effective siRNA as well as an EGFR specific tyrosine kinase inhibitor, gefitinib, was then used on a feline SCC cell line (SCCF1), and the effect of EGFR targeting alone, or in combination with irradiation, on the cell line was determined.

The majority of the biopsy samples were labelled positively for EGFR and Ki67, and high proliferation corresponded with poor prognosis. The siRNA caused reduction in EGFR mRNA by Real-Time Polymerase Chain Reaction and protein levels as assessed by western blot analysis. Reduced cell proliferation and migration were also observed by proliferation assays and scratch assays respectively. Combining EGFR knockdown with irradiation caused an additive effect on the ability of the cell line to form colonies. These results support the role of EGFR as a potential therapeutic target in FOSCCs.

Table of Contents

List of Figures

Chapter 1

Chapter 2

Chapter 3

Chapter 4

Chapter 5

Chapter 6

List of Tables

Chapter 1

Chapter 2

Chapter 3

Chapter 4

Chapter 5

Chapter 6

Acknowledgements

First, I would like to thank my supervisors Dr Donald Yool and Prof David Argyle for all their support and guidance throughout my PhD. Thanks also go to all members of the Argyle Group for their help and support, in particularly Ms Daniela Gattegno, Mrs Rhona Muirhead, Dr Lisa Pang, Mrs Margaret Ross, Dr Matylda Sczaniecka and Dr Karen Tan. You have all been absolutely fabulous.

Several people helped with the immunohistochemistry study. Firstly, Mrs Alison Hayes from Animal Health Trust who provided us with feline oral biopsy samples and clinical histories. I would like to acknowledge and thank Mr Neil MacIntyre for performing all the labelling, without his knowledge and expertise this study would not have prevailed, and Mrs Linda Morrison who helped scoring the samples. In addition thanks go to Dr Darren Shaw for help with statistical analysis, and to Prof. Elspeth Milne and Dr. Sionagh Smith for their input.

Thanks to Prof Tomas J. Rosol who provided us with the SCCF1 cell line, Dr. Lisa Pang who performed a radiation study and three drug assays presented in this thesis (Figures 6.9, 6.10, 6.11 and Tables 6.2 & 6.3), and to Alejandro Cervantes who performed the western blot shown in Figure 6.4.

I would also like to extend my thank you to The Petplan Charitable Trust for their generous funding of this project.

Last, but not least, I would like to thank Dr Steven Tait, my husband and my rock then, now, and always. Thanks to my parents, Turid and Annar who always let their little girl go where she desired in life, my sister, Anne Camilla, for all her support and excellent shared travel and shopping experiences, and finally to Blue and Fram, my loyal dogs who know how to cheer me up whatever the weather or circumstance.

Declaration

I, Gurå Therese Bergkvist, do hereby declare that the work carried out in this thesis is original, was carried out by myself or with due acknowledgement, and has not been presented for award or degree at any other university.

Gurå Therese Bergkvist 26th January 2011

Abbreviations

ADAMs	adamalysins
AHT	Animal Health Trust
AK	actinic keratosis
ALDH 1	aldehyde dehydrogenase 1
AMV-RT	avian myeloblastosis virus reverse transcriptase
APS	ammonium persulphate
AR	amphiregulin
ATP	adenosine triphosphate
BAD	bcl-2-associated death promoter
bFGF	basic fibroblast growth factor
BISC	Bowenoid *in situ* carcinoma
BLAST	basic local alignment search tool
BrdUrd	5-bromo-2-deoxyuridine
BSA	bovine serum albumin
BTC	betacellulin
CFA	colony formation assay
Cp	crossing point
CR	complete response

CRC	colorectal cancer
CSC	cancer stem cells
Ct	cycle threshold
DAG	1,2-diacylglycerol
DF	dilution factor
DMEM	Dulbecco's Modified Eagle Medium
DMSO	dimethylsulphoxide
DNA	deoxyribonucleic acid
dNTP	deoxynucleotide triphosphates
DEPC	diethyl pyrocarbonate
dsDNA	double stranded DNA
dsRNA	double stranded RNA
DTT	dithiothreitol
E	efficiency (of primers)
EGF	epidermal growth factor
EGFR	epidermal growth factor receptor
EGFRvIII	epidermal growth factor receptor variant III
eIF2	eukaryotic initiation factor
EMT	epithelial to mesenchymal transition
EMST	epithelial-mesenchymal to stem-like transition
EPI	epiregulin
Eps15	epidermal growth factor receptor substrate 15

ErbB 2, 3, 4 v-erb-b 2,3,4	erythroblastic leukaemia viral oncogene homolog 2,3,4
ERK	extracellular signal–regulated kinase
esiRNA	endoribonuclease-prepared siRNA
ETS	environmental tobacco smoke
FACS	fluorescent-activated cell sorting
FAM	carboxy-fluorescein
FBS	foetal bovine serum
FeLV	feline leukaemia virus
FITC	fluorescein isothiocyanate
FIV	feline immunodeficiency virus
FOSCC	feline oral squamous cell carcinoma
FOXO	forkhead box protein O
GAB1	Grb2 associated-binding protein 1
GAP	GTPase activating protein
GAPDH	glyceraldehyde 3-phosphate dehydrogenase
GBM	glioblastoma multiforme
GDP	guanosine diphosphate
GFP	green fluorescent protein
GPCR	G protein coupled receptor
GTP	guanosine triphosphate
Grb2	growth factor receptor-bound protein 2

Gy	Gray
HB-EGF	heparin-binding epidermal growth factor
HCC	hepatocellular carcinoma
HER	human epidermal growth factor receptor
HGF	hepatocyte growth factor
HIF-1α	hypoxia induced factor 1α
HNSCC	head and neck squamous cell carcinoma
HPLC	high performance liquid chromatography
HPV	human papilloma virus
H-ras	Harvey rat sarcoma viral oncogene homolog
HRP	horseradish peroxidase
IGF-R1	insulin growth factor 1 receptor
ILK	integrin linked kinase
IMS	industrial methylated spirit
IP_3	inositol triphosphate
JAK	Janus kinase
Jcm^{-2}	Joules per square centimetre
kDa	kilo Dalton
K-ras	Kirsten rat sarcoma viral oncogene homolog
nt	nucleotides
mAbs	monoclonal antibodies
MACS	magnetic cell sorting

MAPK	mitogen-activated protein kinases
MBS	membrane binding solution
MDFI	median disease free interval
MET	mesenchymal to epithelial transition
MGB	minor groove binder
miRNA	micro RNA
MMPs	matrix metalloproteinases
MPFI	mean progression free interval
MPFS	median progression free survival
mRNA	messenger RNA
MS	median survival
mTOR	mammalian target of rapamycin
N/A	not applicable
NFκB	nuclear factor-κB
NRG	neuregulin
NSCLC	non-small cell lung cancer
NTP	nucleotide triphosphates
ODN	oligodeoxyribonucleic acid
O-RT	Omniscript reverse transcriptase
PBS	phosphate buffered saline
PBST	phosphate buffered saline Tween-20
PCR	polymerase chain reaction

PDGFRβ	platelet derived growth factor receptor β
PDK	phosphoinositide-dependent kinases
PDT	photodynamic therapy
PI	propidium iodide
PIP_2	phosphatidylinositol (4,5) biphosphate
PIP_3	phosphatidylinositol (3,4,5) triphosphate
PI3K	phosphatidylinositol 3-kinase
PKB	protein kinase B (Akt)
PKC	protein kinase C
PKR	protein kinase R
PLC	phospholipase C
PTB	phosphotyrosine binding domain
PTEN	phosphatase and tensin homologue
RAM	rabbit anti-mouse
ras	rat sarcoma viral oncogene homolog
R(D)SVS	Royal (Dick) School of Veterinary Studies
RE	relative expression
RISC	RNA-induced silencing complex
RNA	ribonucleic acid
RNAi	RNA interference
RNase	ribonuclease
rRT	recombinant reverse transcriptase

RT	room temperature
RT-PCR	reverse transcriptase polymerase chain reaction
RTK	receptor tyrosine kinase
SAR	swine anti-rabbit
SCC	squamous cell carcinoma
SD	standard deviation
SDS	sodium dodecyl sulphate
SDS-PAGE	sodium dodecyl sulphate polyacrylamide gel electrophoresis
SH2	Src homology-2 domain
shRNA	short hairpin RNA
siRNA	small interfering RNA
SOS	Son of Sevenless
SP	side population
ssDNA	single stranded DNA
ssRNA	single stranded RNA
STAT	signal transducers and activators of transcription
TAE	tris acetate ethylene-di-amine-tetra-acetate
TBS	tris-buffered saline
TBST	tris-buffered saline Tween-20
TE	tris ethylene-di-amine-tetra-acetate
TEMED	tetramethyl ethylene-di-amine

TGFα, β	transforming growth factor α, β
TKI	tyrosine kinase inhibitor
TNF	tumour necrosis factor
TNM	tumour node metastasis
UV	ultraviolet
VEGF	vascular endothelial growth factor
VEGFR	vascular endothelial growth factor receptor
WHO	World Health Organisation

Chapter 1:

Introduction

1.1 Feline squamous cell carcinoma

Squamous cell carcinoma (SCC) is an important feline tumour of epithelial cell origin, affecting a wide range of sites. Feline SCC has been reported to affect (in descending order of occurrence) the oropharynx (including the pharynx and tonsils), skin (including head, neck, trunk and digits), nasal cavity and paranasal sinuses, and rarely, the trachea and larynx (Stebbins et al., 1989, Miller et al., 1991, Mukaratirwa et al., 2001, Jakubiak et al., 2005). SCCs are frequently locally aggressive and only rarely metastasise to local lymph nodes and even less frequently to distant sites (Stebbins et al., 1989, Hayes et al., 2007).

Oral neoplasia accounts for up to 10% of all tumours diagnosed in the cat (Stebbins et al., 1989, Mauldin, 2001), and SCC is the most common tumour type at this site (Stebbins et al., 1989, Postorino-Reeves et al., 1993, Jones et al., 2003) accounting for 61.2% (Stebbins et al., 1989) to 75% (Kapatkin et al., 1991) of oral malignancies diagnosed.

Tonsillar tumours are quite rare, but when diagnosed, the majority are SCC (Morris and Dobson, 2001). Similarly, neoplastic laryngeal and tracheal masses are seen infrequently in cats (Saik et al., 1986, Jakubiak et al., 2005). Nevertheless, seven out of 19 cases with laryngeal masses reported in one study were confirmed as SCC (Jakubiak et al., 2005).

Cutaneous SCC is reported to be one of the most commonly diagnosed malignant skin tumours in the cat accounting for 7-50% of tumours (Dorn et al., 1971, Bostock, 1972, Priester, 1973, Macy and Reynolds, 1981, Miller et al., 1991, Sabattini et al., 2010), depending on geographical location (Sabattini et al., 2010).

1.1.1 Oropharyngeal, laryngeal and tracheal squamous cell carcinomas

1.1.1.1 Signalment and risk factors

Commonly, oral SCC affects older cats (Stebbins et al., 1989, Postorino-Reeves et al., 1993, Northrup et al., 2006, Hayes et al., 2007), although cats as young as three years of age have been reported in the literature (Stebbins et al., 1989). The mean ages of cases reported range from 11 to 15.4 years (Table 1.1). Apart from an increasing incidence with age, (Dorn et al., 1971, Bertone et al., 2003), no apparent sex or breed predilections were reported (Dorn et al., 1971, Postorino-Reeves et al., 1993, Morris and Dobson, 2001).

A variety of risk factors have been identified for the development of the disease in man including smoking, exposure to environmental tobacco smoke (ETS, i.e. passive smoking) and air pollution (Zhang et al., 2000b, Dobrossy, 2005). Other risk factors include human papillomavirus (HPV) infection, dietary deficiencies or imbalances and poor dental hygiene, (Zhang et al., 2000b, Dobrossy, 2005, Hashibe et al., 2007). A similar study in cats identified a trend for feline oral SCC to also be associated with ETS (Snyder et al., 2004). The study investigated the relationship between exposure to ETS and overexpression of the tumour suppression protein p53 in cats with SCC, and reported an association between p53 overexpression in the oral mucosa of cats and the development of oral SCCs (Snyder et al., 2004). This

association did not, however, reach statistical significance (Snyder et al., 2004). p53 has been found to be overexpressed in human tumours linked to carcinogens found in tobacco products (Snyder et al., 2004). These types of causal relationships frequently necessitate large sample sizes in order to reach statistical significance (Petrie and Watson, 2006a). Until larger scale studies can be undertaken, these relationships may well remain unproven.

Study	Total number of cases	Mean age♦	Median age♦	Age range♦
Bregazzi et al. 2001	7		15	
Fox et al. 2000	18	13.2		3.7-20
Postorino-Reeves et al. 1993	52	11.6	12	2.5-18
Hutson et al. 1992	7	11	10	8-16
Northrup et al. 2006	42		13.8	5-17.5
Hayes et al. 2007	54		13.3	7-20
Stebbins et al. 1989	227	12.5		3-21
Jones et al. 2003	8	15.4		13-19

Table 1.1: Summary of reported ages of cats affected by oral SCC. ♦ Age in years

Cat oral cavities are potentially exposed to high levels of environmental toxins due to their meticulous grooming behaviour (Ogilvie and Moore, 1996a, Bertone et al., 2003, Snyder et al., 2004). Bertone et al. (2003) investigated the relationship between oral SCC and environmental and lifestyle risk factors. They found that the use of flea collars and the feeding of wet food were statistically significantly associated with an increased risk of developing oral SCC.

Recently, the presence of papilloma virus DNA was identified in a small number of oral SCC biopsy samples (three out of 64 samples in total) using polymerase chain reaction (PCR) to detect viral DNA (Munday et al.,

2009, O'Neill et al., 2010). The low occurrence of papillomavirus DNA in these oral tumours suggests this to be only a minor risk factor in cats.

1.1.1.2 Affected areas

Oral SCC most commonly affects the sublingual region and tongue, commonly near the frenulum (Dorn and Priester, 1976, Dubielzieg, 1982, Stebbins et al., 1989). Oral SCC also affects the gingiva and these tumours frequently invade the underlying bone (Dubielzieg, 1982). Despite being locally very aggressive tumours, they are slow to metastasise (Dubielzieg, 1982, Stebbins et al., 1989). Tonsillar SCC metastasises to regional lymph nodes and distant organs more readily than oral SCC (Stebbins et al., 1989). Occasionally, SCC may arise in the epithelium of the mucosal surfaces of the cheek or lip. These neoplastic lesions are often more ulcerative than proliferative in nature (Morris and Dobson, 2001).

The majority of feline laryngeal tumours are either SCC or lymphomas (Saik et al., 1986, Jakubiak et al., 2005). They carry a very poor prognosis, with a median survival of five days following diagnosis, partly because they frequently present with signs of airway obstruction (Jakubiak et al., 2005).

1.1.1.3 Clinical and presenting signs

The most commonly reported clinical signs of feline oral SCC were facial asymmetry or facial mass, ptyalism (sometimes with haemorrhage), anorexia, inappetence, dysphagia and weight loss, behavioural changes (for example cessation of grooming), pawing at mouth, and other signs of oral pain (Fox et al., 2000, Bertone et al., 2003, Snyder et al., 2004, Northrup et al., 2006). Gagging was sometimes the presenting sign with tonsillar, laryngeal and tracheal SCC, as well as respiratory signs including dyspnoea, voice changes, coughing, wheezing and tachypnoea (Saik et al., 1986, Jakubiak et

al., 2005). Occasionally, teeth were noted to be loose or to fall out (Postorino-Reeves et al., 1993). If the tumours invaded the nasal cavity, a nasal discharge was sometimes apparent (Mauldin, 2001). Fifteen percent of the cases in one study were detected incidentally by a veterinary surgeon during routine clinical examinations or dental treatments (Hayes et al., 2007), so a proportion of cats did not exhibit clinical signs appreciable to the owners.

1.1.1.4 Treatment options, prognosis and survival times

Historically, the only treatment option available for oral SCC was surgery. Hence, only tumours amenable to surgical excision were treatable. Early studies reported oral SCCs to carry a poor prognosis with a mean survival of seven weeks following diagnosis, and found no correlation between the degree of differentiation of the tumours and survival (Bostock, 1972). Although this study consisted of a very small study population, subsequent reports have supported these conclusions. Overall, oral SCCs still only have around 10% one year survival rates with median survival between one and five months (Evans et al., 1991, Postorino-Reeves et al., 1993, Hayes et al., 2007).

Surgery remains the main stem of treatment, but is now often combined with other therapies. Successful surgery is likely to involve radical resection by mandibulectomy or maxillectomy (Birchard, 1996). One study with 21 cases treated by radical surgical excision reported a one year survival rate of 43% (Northrup et al., 2006). The surgeries caused considerable post-operative morbidity with half of the cats that had more than 50% of their mandible resected never regaining the ability to eat (Northrup et al., 2006). The authors reported overall high owner satisfaction, but many owners would find this level of morbidity unacceptable. Another small study of five cats achieved a median survival of six months following mandibular

resections (Bradley et al., 1984). Even better results were achieved when surgery was combined with radiotherapy giving a one year survival rate of 57% and a median survival of 14 months (Hutson et al., 1992). In this small study of only seven cases all cases with sublingual involvement had been excluded, as this tumour site has been associated with a poorer prognosis (Evans et al., 1991). The small number of cases and restrictive inclusion criteria of these studies means that the survival rates reported are not directly comparable to the earlier reports in the literature that estimated overall survival regardless of tumour site and treatment. Exclusions of certain tumours from survival analysis may skew data and may produce artificially high survival rates.

Study	Number of cats	Treatment combination	Remission rates	Survival rates
Bregazzi et al. 2001	2	Radiation and mitoxantrone	N/A, palliative study	60 days (42-97)
Evans et al. 1991	11	Radiation and intratumoural etanidazole	Partial remission 100% Days to progression ranged from 55-331 days	Median survival 116 days (19-389)
Jones et al. 2003	8	Radiation and gemcitabine	CR 2 PR 4 Median remission 42.5 days (11-85)	Median survival 111.5 days (11-234)
LeBlanc et al. 2004	8	Radiation and gemcitabine	Median remission time 91 days	
Postorino-Reeves et al. 1993	11	Radiation and cisplatin		Median survival 75 days

Table 1.2: Summary of remission and survival rates achieved for combination therapies reported in oral SCCs, N/A: not applicable.

Radiation therapy has been used alone and in combination with other therapies, but has not increased survival times considerably. The main benefits of radiation therapy include the ability to treat a large area without permanent disfigurement and the ability to include draining lymph nodes in

the radiation field (Postorino-Reeves et al., 1993). Side effects of radiation therapy may occur even at palliative doses (Bregazzi et al., 2001), and include osteonecrosis, permanent alopecia, stomatitis, halitosis, mucositis, anorexia and depression (Evans et al., 1991, Hutson et al., 1992, Ogilvie et al., 1993, Postorino-Reeves et al., 1993, LeBlanc et al., 2004).

In one study, radiotherapy alone produced median survival of three months (Postorino-Reeves et al., 1993) and when used in combination with mitoxantrone chemotherapy it produced complete remission in eight out of eleven cats with a median remission time of five and a half months (Ogilvie et al., 1993). Other combination therapies reported have been summarised in Table 1.2.

In human chemotherapy, cisplatin analogues are sometimes used as single agents in the treatment of head and neck cancers (Fox et al., 2000). In cats, one study used mitoxantrone as a single agent, but reported disappointing results with only one of 32 cats achieving complete remission before relapsing after two months (Ogilvie et al., 1993). Similar results were achieved using a cisplatin analogue as the single agent (Fox et al., 2000).

A more recent study evaluated the survival times of cats with oral SCC managed in non-specialist settings and given palliative care only. The one year survival rate was 9.5% and median survival time from presentation was 44 days (Hayes et al., 2007). The author concluded that if aggressive therapies for feline oral SCC are to be considered they must exceed the survival rates achieved with palliative therapy alone (Hayes et al., 2007). So far, no single treatment modality has convincingly improved survival times far beyond those reported with palliative therapy alone.

1.1.2 Cutaneous squamous cell carcinomas

The classification of cutaneous SCC in man is subject to a continual debate and is under constant review. There are inconsistencies in the literature in the naming of the different classes of tumours, causing some confusion when comparing results from different studies (Anwar et al., 2004). It follows that similar confusion exists in the veterinary literature, and different authors classify actinic keratosis, SCC *in situ* and feline Bowenoid *in situ* carcinomas (BISC) differently. For the purpose of this review, the cutaneous form of feline squamous cell carcinomas will be divided into three groups depending on the depth of invasion and their aetiology. SCC *in situ* will be divided into two separate groups, solar or actinic keratosis (AK) and feline BISC (Baer and Helton, 1993, Fox, 1995, Nespeca et al., 2006, Munday et al., 2007). Both of these types are generally confined to the epidermis (Baer and Helton, 1993, Munday et al., 2007) and are often considered to be pre-malignant lesions (O'Neill et al., 2010). Comparative studies of these two early lesions showed that BISC could reliably be diagnosed histologically, while the histologic diagnosis of lesions clinically suggestive of AK is more difficult (Favrot et al., 2009).

The last group is made up of the invasive SCC, which is characterised by invasion of the basement membrane, and is often considered an extension or progression from SCC *in situ* of the AK type, although invasive SCC can also develop from normal skin (Anwar et al., 2004). It is generally accepted that BISC differs from the others in its aetiology and prevalence (Favrot et al., 2009) and this entity will therefore be discussed separately.

1.1.2.1 Signalment and risk factors

As with most tumours, cutaneous SCCs have an increasing incidence with age (Priester, 1973, Miller et al., 1991). The reported ages of the affected

animals from the eight largest studies are summarised in Table 1.3. The mean age of affected animals ranged from 8.5 to 14 years and the median ages reported were 12 to 13 years. Cats as young as nine months were reported in some studies (Evans et al., 1985, Miller et al., 1991, Favrot et al., 2009). The youngest cats in some of these studies had AK, which is known to have a significantly earlier onset than BISC (Favrot et al., 2009). No increase in risk has been reported in relation to gender or neutering status (Dorn et al., 1971).

Study	Number of cats	Median age♦	Mean age♦	Age range♦
Theon et al. 1995	90		11.1	3-20
Carlisle and Gould 1982	88		8.5	1-17
O'Neill et al. 2010	84	13		0.75-25
Lana et al. 1997	61	12		5-17
Miller et al. 1991	52	12	11.6	1-19
Favrot et al. 2009	AK 22 BISC 23		AK 9.5 BISC 13.1	2-17
Theon et al. 1996	23		14	8-17

Table 1.3: Summary of reported ages of cats affected by cutaneous SCC. ♦ Age in years, AK: actinic keratosis, BISC: Bowenoid *in situ* carcinoma

A clear predisposition for cutaneous SCC is reported in white cats, which are 13.4 times more likely to develop this neoplasm compared to non-white cats (Dorn et al., 1971). An overview of the proportion of cats diagnosed with cutaneous SCC with lack of pigment in affected areas is given in Table 1.4.

The combination of lack of pigment in sparsely haired areas predisposes these cats to repeated sunburn, which in turn predisposes them to develop actinic or solar keratosis (Dorn et al., 1971, Favrot et al., 2009). AK

is thought to be a potential precursor to invasive SCC (Anwar et al., 2004). Siamese cats are less likely to develop AK, presumably because of their pigmented extremities (ears, eyelids, lips and nose) where these tumours commonly occur (Dorn et al., 1971, Priester, 1973). Access to the outdoors increases risk of sunlight exposure and hence tumour risk (Dorn et al., 1971, Macy and Reynolds, 1981, Lana et al., 1997), and in one study (Lana et al., 1997), 95% of all cats with cutaneous SCCs had outdoor access. It has been proposed that the reduced incidence of SCC reported in Siamese cats could be partly due to the fact that pedigree cats are often more likely to be kept indoors (Goodfellow et al., 2006).

Study	Total	Cats white/part white	%	Notes
Carlisle and Gould 1982	97	97	100	All cats had white areas to their nose (only nasal SCC reported)
Theon et al.1995	90	66	73.3	Proportion reported in article
Lana et al. 1997	61	58	95.1	Proportion reported in article
Nespeca et al. 2006	22	22	100	Number of samples taken from sun exposed or white areas
Favrot et al. 2009	22	22	100	Proportion reported in article

Table 1.4: Proportion of cats diagnosed with cutaneous SCC reported to have a white coat colour or unpigmented affected areas.

In man, immunocompromised patients are reported to be more prone to developing metastasis from invasive SCC compared to healthy individuals (Anwar et al., 2004) but no similar trend has been reported to date in the cat. No relationship has been found between Feline Leukaemia Virus (FeLV) and Feline Immunodeficiency Virus (FIV) infections and the development of cutaneous SCC (Lana et al., 1997). One study did identify an increased incidence of chronic lip ulceration following radiotherapy in FIV

positive cats with SCC of the nasal planum (Theon et al., 1995). However, these authors reported that treatment response rates were not influenced by FIV status and concluded that FIV status alone should not be used as a criterion to deny radiotherapy (Theon et al., 1995).

1.1.2.2 Affected areas

The largest study published reviewed 340 cases diagnosed with cutaneous neoplasia by biopsy or necropsy over a three-year period. This study found that 82% of SCC affected the head, 11% affected the limbs, 2 % affected the neck and another 2% affected the trunk while 3% affected other areas (Miller et al., 1991). Another study reported that 96% of 149 cases of histologically confirmed cutaneous SCC originated on the head or neck (Dorn et al., 1971).

The commonly affected areas on the head in order of prevalence are the pinnae, nasal planum, eyelids, chin and lips. These are the areas of sparser hair growth so they are more at risk of sunburn (Nespeca et al., 2006).

1.1.2.3 Clinical and presenting signs

Cutaneous SCC lesions tend to be slowly progressing, and this was reflected in the time interval reported between when the lesions were first noted by the owners and when the animals were first presented for treatment, ranging from a few days to two years, with an overall median time of three to six months (Lana et al., 1997, Goodfellow et al., 2006). On first presentation the owners often ascribed the lesions to a traumatic injury such as a cat scratch that never healed (Goodfellow et al., 2006). Early lesions seen with AK often appear as non-healing wounds, plaque-like to papillated in nature, often with scaling or crust formation (Favrot et al., 2009). These lesions progress over time and often become erosive and ulcerative (Lana et

al., 1997), appearing as shallow ulcers surrounded by elevated, indurated borders (Fox, 1995). Left untreated, the neoplastic lesion may remain the same size or spread and become larger in size and depth, sometimes invading underlying cartilage (Carlisle and Gould, 1982). The lesions may also become secondarily infected, which may lead to a sudden deterioration in appearance, prompting the owner to bring the animal to the veterinarian.

1.1.2.4 Treatment options, prognosis and survival

Several treatments are available for the treatment of cutaneous SCCs, and the preferred options depend on the area affected. Tumour staging influences the treatment options available, as does cost, owner preference, general health of the patient (which may, for example, limit the administration of multiple anaesthetics) and what treatments are available at the treatment centre (Lana et al., 1997, Thomson, 2007).

An overview of treatment options is summarised in Figure 1.1. In order to assess more accurately how different treatment options compare to each other a common assessment of tumour behaviour and invasiveness was required, and the Tumour Node Metastasis (TNM) staging protocol is most commonly used (Owen, 1980). Clinical stages of feline tumours of epidermal origin according to the World Health Organisation (WHO) classification are summarised in Table 1.5.

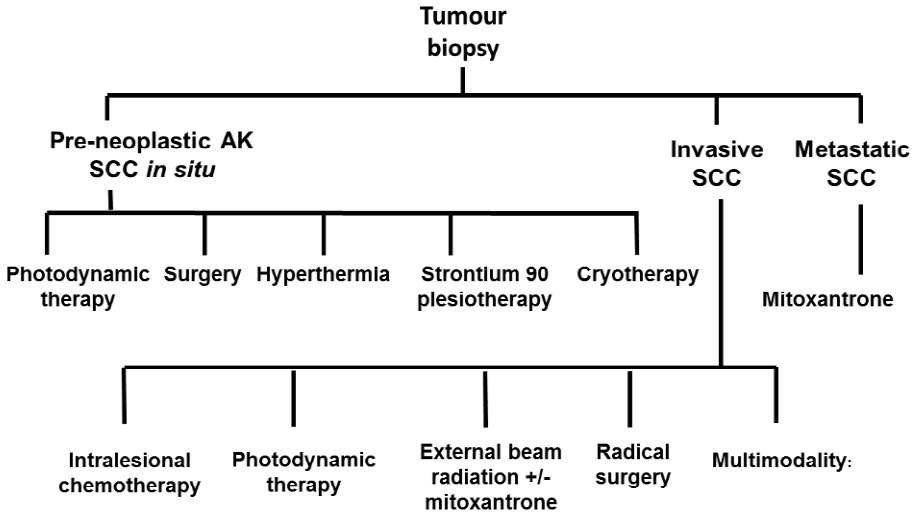

Figure 1.1: Diagram showing an overview of the treatment options available for cutaneous SCC. Adapted from Ogilvie & Moore (1996b).

Historically, surgery was the only treatment option available. Bostock reported in 1972 that cats with well differentiated cutaneous SCC had a good prognosis and in some cases were cured by surgical intervention, while cats with poorly differentiated tumours only survived on average for twelve weeks (Bostock, 1972).

For some tumours, surgery offers a relatively simple procedure with potentially low complication rates (Withrow and Straw, 1990). It is a widely available treatment which is cost effective and involves overall less total treatment time (Lana et al., 1997). Depending on area affected, surgery produces cosmetically acceptable results (Lana et al., 1997). Surgical excision of lesions allows for the histopathological examination of the surgical margin contributing to the prediction of the long term prognosis of the animal (Withrow and Straw, 1990, Lana et al., 1997, Thomson, 2007).

Site	Stage	Definition
Primary tumour	T_{is}	Pre-invasive carcinoma (carcinoma in situ)
	T_0	No evidence of tumour
	T_1	Tumour < 2 cm maximum diameter, superficial or exophytic
	T_2	Tumour 2-5 cm maximum diameter, or with minimal invasion irrespective of size
	T_3	Tumour >5 cm maximum diameter, or with invasion of subcutis, irrespective of size
	T_4	Tumour invading other structures such as fascia muscle, bone or cartilage
Regional lymph nodes	N_0	No evidence of RLN involvement
	N_1	Moveable ipsilateral nodes
		N_{1a} Nodes not considered to contain growth
		N_{1b} Nodes considered to contain growth
	N_2	Moveable contralateral or bilateral nodes
		N_{2a} Nodes not considered to contain growth
		N_{2b} Nodes considered to contain growth
	N_3	Fixed nodes
Distant metastasis	M_0	No evidence of distant metastasis
	M_1	Distant metastasis detected

Table 1.5: Clinical staging (TNM) of feline tumours of epidermal or dermal origin (Owen 1980).

Prognosis improves if a complete excision of tumour with a wide surgical margin is achieved, but depending on the tumour site this is not always possible (Fox, 1995). Excisions of the pinnae can give mean (Fox, 1995) or median (Lana et al., 1997) disease free intervals of two years. This is probably the most straightforward surgery to perform and it allows for potentially larger areas of tissue to be removed without interfering overtly with function (Lana et al., 1997). Regardless of treatment used, animals with

lesions confined to the pinnae had the greatest disease free intervals and the longest survival times (Lana et al., 1997).

Nasal planum resections caused more morbidity compared to pinnae resections (Withrow and Straw, 1990, Thomson, 2007), but the median disease free intervals and median survival times compared favourably to other treatment modalities (Lana et al., 1997). Surgery remains the most effective treatment for invasive SCC of stage T3 and T4 (Stell et al., 2001). In one study eight cats with highly invasive SCCs of the nasal planum were treated with surgery alone and three died within five months due to recurrence of tumours (Withrow and Straw, 1990). One died of unrelated causes with no recurrence after eight months; the remaining four cats were disease free with a mean follow up of 17.2 months (Withrow and Straw, 1990).

The lack of staging of the tumours in some of the studies (Withrow and Straw, 1990, Lana et al., 1997) makes a true comparison with other treatment modalities difficult. For example, in the study performed by Lana et al. (1997), surgery and cryosurgery had median survival rates twice that of the radiotherapy treated group, but details of the clinical stage of the tumours were not given. Cryosurgery is widely reported not to be effective in lesions larger than one centimetre (Ogilvie and Moore, 1996b), or four millimetres (Thomson, 2007) due to high recurrence rate. Some authors recommend that cryosurgery is never performed as it produces poor results (Fox, 1995) and may delay more effective treatments (Ogilvie and Moore, 1996b). The long median survival reported in the Lana study could be due to only low grade lesions (T_{IS} and T_1) being treated, compared to the lesions treated with irradiation and surgery. Without the clinical stages of the tumours in the different groups no meaningful comparison could be made.

Despite conflicting reports in the literature, cryosurgery is still being used to treat SCC. Cryosurgery was described as the destruction of tissues by the controlled use of freezing and thawing using liquid nitrogen or nitrous oxide (Thomson, 2007). The advantages of the technique reported were cost effectiveness and availability (Thomson, 2007), while the disadvantages were lack of surgical margins, protracted period required for the eschar detachment, and high and relatively rapid recurrence rate (Withrow and Straw, 1990, Lana et al., 1997, Thomson, 2007).

Study treatment	Tumour stage	Response rates	Survival rates	Disease free intervals
Cox et al.1991 Mix	Not given	All had initial regression	MS 12 months	Not given
Fidel et al. 2001 Proton irradiation	T_{1a} to T_{2b}	CR 60% T1a 100% T2b 33%	MS 31 months MPFS 14.4 months	MPFI 4.5 months
Goodfellow et al. 2006 Plesiotherapy	T_{is} to T_2	CR 87%	MS 25.6 months	MDFI 21.4 months
Lana et al. 1997 Mix	Not given	Not given	MS 12.5 months	MDFI 12 months
Theon et al. 1995 Orthovoltage	T_1 to T_4	Not given	MPFS 16.5 months	Not given

Table 1.6: Summary of reported survival times and disease free intervals for different radiation treatment protocols. CR: complete response, MS: median survival, MPFS: median progression free survival, MPFI: mean progression free interval, MDFI: median disease free interval.

Radiotherapy offers an alternative to surgery that produces excellent cosmetic outcomes (Thomson, 2007). The reported disadvantages of radiotherapy were availability (as it can only be offered in specialist settings), cost and the requirement for repeat general anaesthetics (Lana et al., 1997, Fidel et al., 2001). The first large scale report (88 cats) on the

efficacy of radiation therapy investigated two treatment regimens; irradiation at monthly intervals, and a schedule that consisted of three irradiations in one week (Carlisle and Gould, 1982). They reported superior results with weekly treatment schedules and poor response rates in larger and more invasive T_3 lesions (Carlisle and Gould, 1982). Later studies confirmed these findings, and also reported tumour stage to be a statistically significant prognostic indicator (Theon et al., 1995). A summary of reported survival times and response rates is presented in Table 1.6.

Recent advances in the field of photodynamic therapy (PDT) have produced some favourable results (Fox, 1995). PDT works by utilising two components, a photosensitizer and a light source of a specific wavelength to maximally activate the tumour localising photosensitizer (Frimberger et al., 1998, Stell et al., 2001, Buchholz et al., 2005). The photosensitizer is usually injected intravenously and has tumour seeking properties (Peaston et al., 1993), although topical photosensitizers are also available (Stell et al., 2001). Light at wavelengths of 600-900 nm of the red and infrared spectrum penetrates tissues best, so photosensitizers should ideally be activated in this range (Frimberger et al., 1998). Tumour destruction is achieved through three principal mechanisms: direct tumour kill via the release of free oxygen radicals and other cytotoxic substances, destruction of tumour-associated vasculature, and activation of the host's immune system against tumour cells (Peaston et al., 1993, Stell et al., 2001, Buchholz et al., 2005).

PDT is reserved for lower grade tumours, where it achieves acceptable response rates ranging from a 57% to 100% (Peaston et al., 1993, Magne et al., 1997, Frimberger et al., 1998, Stell et al., 2001, Buchholz et al., 2005). Response rates for T_3 and T_4 tumours are much lower (Peaston et al., 1993, Magne et al., 1997) . In one study, increasing the fluence from 100 Jcm^{-2} to 200 Jcm^{-2}

resulted in an improved overall response rate of 70% (Hahn et al., 1998). There was a statistically significant increase in median remission duration for the tumours treated at the higher fluence, achieving median remission times that compared favourably with other available treatments options for late stage tumours (Hahn et al., 1998).

Adverse effects of PDT treatments are mild and well tolerated, and include vomiting during injection of the photosensitizer, sneezing, reversible facial swelling, local infection, permanent alopecia, and variable length (from a few days to up to two weeks) of photosensitization (Roberts et al., 1991, Peaston et al., 1993, Magne et al., 1997, Frimberger et al., 1998, Hahn et al., 1998, Stell et al., 2001, Buchholz et al., 2005).

In summary, a range of therapies are available for the management of feline cutaneous SCC. Good results are achieved with complete surgical excision, but this is not always possible. A range of other therapies have also been evaluated, but local recurrence remains a common reason for treatment failure.

1.1.2.5 Prevention

Education of clients and veterinarians to identify and treat early lesions could improve response rates as early lesions have a better prognosis following treatment (Thomson, 2007). Other suggested preventative measures include tattooing (Withrow and Straw, 1990, Fox, 1995), henna tattooing (Thomson, 2007), applying sunscreen (Macy and Reynolds, 1981, Carlisle and Gould, 1982, Fox, 1995), and keeping cats indoors during maximum sunlight hours (Macy and Reynolds, 1981, Withrow and Straw, 1990) to limit sunlight exposure to the extremities. The main obstacle to

successful enforcement of these latter two measures may well be cat compliance (Fox, 1995).

1.1.2.6 Feline Bowenoid *in situ* carcinoma (BISC)

Feline BISC is morphologically similar to Bowen's disease in man; however, it is not identical and should therefore be referred to as Bowenoid or Bowen's-like disease (Favrot et al., 2009). It is a rare skin disease, predominantly affecting older cats. The lesions are usually multicentric and may occur at any site and are not associated with sun exposure (Baer and Helton, 1993, Favrot et al., 2009). The lesions usually occur as hyper-pigmented plaques (Wilhelm et al., 2006, Munday et al., 2007) that are often alopecic, slightly elevated and covered by crusts (Baer and Helton, 1993).

The lesions are distinguished from actinic keratosis on the basis of a history of no or little sun exposure and on the basis of distribution of lesions, as histologically the two lesions are very similar (Favrot et al., 2009). The aetiology of BISC is predominantly unknown, but papillomaviruses have been identified in a proportion of these tumours (Wilhelm et al., 2006, Munday et al., 2007, Favrot et al., 2009).

Treatment consists of surgical removal of the lesions, which do not tend to recur locally, although *de novo* lesions may develop. A proportion of these lesions may progress to invasive SCC if left untreated (Baer and Helton, 1993).

1.1.3 Squamous cell carcinomas of the nose and paranasal sinuses

Tumours of the nose and paranasal sinuses accounts for up to 4% of all neoplasms in the cat (Cox et al., 1991). These figures do not include tumours

of the nasal planum (Mukaratirwa et al., 2001). SCCs are the third most common nasal tumour in the cat, accounting for about ten percent of all nasal and paranasal tumours (Mukaratirwa et al., 2001, Tromblee et al., 2006). In one study, however, none of the sixteen tumours diagnosed in the nasal passages and sinuses were SCC (Cox et al., 1991).

These tumours are of unknown aetiology with no breed predisposition, but a male predisposition has been reported as well as an increased incidence with age (Cox et al., 1991, Mukaratirwa et al., 2001). Most commonly reported clinical signs include nasal and ocular discharge, epistaxis, upper respiratory signs such as stridor and stertor, seizures, sneezing, facial swelling, exophthalmos, and enophthalmos (Cox et al., 1991, Mukaratirwa et al., 2001, Malinowski, 2006).

Treatment modalities include surgery, irradiation, chemotherapy or combination therapies (Cox et al., 1991, Malinowski, 2006). Supportive care is important as affected cats have reduced ability to smell their food often leading to anorexia (Malinowski, 2006). The best treatment responses were achieved with a combination of surgery and orthovoltage therapy, but no large scale studies comparing different treatments have been performed (Malinowski, 2006).

1.2 Squamous cell carcinomas of the head and neck in man

Squamous cell carcinoma of the head and neck (HNSCC) accounts for more than 90% of upper aerodigestive tract malignancies in man (Dobrossy, 2005, Rogers et al., 2005, Reuter et al., 2007). The disease is locally aggressive with rapid spread to regional lymph nodes, and with high incidences of recurrence and *de novo* primary tumour formation (Reuter et al., 2007). The

most commonly affected sites are the larynx, followed by the oropharynx, hypopharynx and the oral cavity (Bentzen et al., 2005).

1.2.1 Risk factors

The aetiology of HNSCC is not fully understood, but epidemiological studies have identified several factors that independently or in combination are associated with an increased risk of disease (Dobrossy, 2005, Hashibe et al., 2007). The two major predisposing factors were tobacco use and alcohol consumption. Individually they account for a two- or three-fold increase in disease, but in combination they increase risk 15-fold (Dobrossy, 2005). When investigated as independent entities, smoking was shown to be the main contributor to risk (Hashibe et al., 2007). In addition, ETS exposure caused a dose dependant increase in risk (Zhang et al., 2000b). Up to three quarters of all HNSCCs diagnosed were attributable to a combination of smoking and alcohol drinking (Hashibe et al., 2007), rendering them *per se* preventable (Dobrossy, 2005).

Other reported risk factors for the development of HNSSC were human papillomavirus infection, oral leukoplakia, dietary deficiencies, poor dental hygiene and, atmospheric pollution (Dobrossy, 2005).

1.2.2 Current treatments and outcome

The management of HNSCC has improved over the past decades (Kramer et al., 2005, Rogers et al., 2005), resulting in better response rates to new treatment protocols (Reuter et al., 2007). There is little evidence, however, that this has significantly enhanced outcome (Ford and Grandis, 2003). A summary of the reported outcomes to different treatments of HNSCC is shown in Table 1.7.

Stage of disease & treatment	Expected outcome
Early stage disease Surgery and/or radiotherapy /chemotherapy	Approximately 80% cure rate
Resectable, advanced disease Surgery and radiotherapy/chemotherapy	50-60% develop local/regional recurrence 20% develop metastatic disease or secondary primaries
Unresectable, advanced disease	5 year survival of < 10%
Recurrent/metastatic disease	Median survival 4 months 1 year survival < 30%

Table 1.7: Summary of reported expected outcome for patients with HNSCC. Modified from Kirby et al. (2006) and Reuter et al. (2007)

1.3 Epidermal Growth Factor Receptor (EGFR)

1.3.1 Epidermal growth factor receptor family

The epidermal growth factor (EGF) receptor family makes up the first of six subfamilies of the receptor tyrosine kinases (RTK) superfamily of proteins (Graus-Porta et al., 1997, Holbro and Hynes, 2004). It compromises four members: the EGF receptor (EGFR) also known as ErbB1/HER1 (Ullrich et al., 1984), ErbB2/HER2, ErbB3/HER3 and ErbB4/HER4, collectively termed the ErbB receptors due to their homology with the avian erythroblastosis viral gene product (v-*erb*B) (Holbro and Hynes, 2004). These receptors share a similar structure consisting of a single-pass transmembrane protein of approximately 1200 amino acids (Figure 1.2) (Alberts et al., 1994, Jimeno and Hidalgo, 2005), with the EGFR protein being approximately 170kDa in size (Milano et al., 2008). The receptor extracellular domain consists of four subdomains: ligand binding domains L1 and L2, and two cysteine-rich domains C1 and C2. A single alpha-helix hydrophobic domain spans the cell membrane and intracellularly a region with tyrosine kinase function is

flanked by a carboxy-terminus with tyrosine phosphorylation sites (Yarden and Sliwkowski, 2001, Holbro and Hynes, 2004). A schematic diagram of the receptors with their phosphotyrosine residues and associated docking molecules is shown in Figure 1.3. The juxtamembrane region of EGFR exhibits a distinct set of sorting sequences that are involved in regulatory events such as internalisation and recycling of the receptor–ligand complex (Yarden and Sliwkowski, 2001, Jorissen et al., 2003, Wiley, 2003).

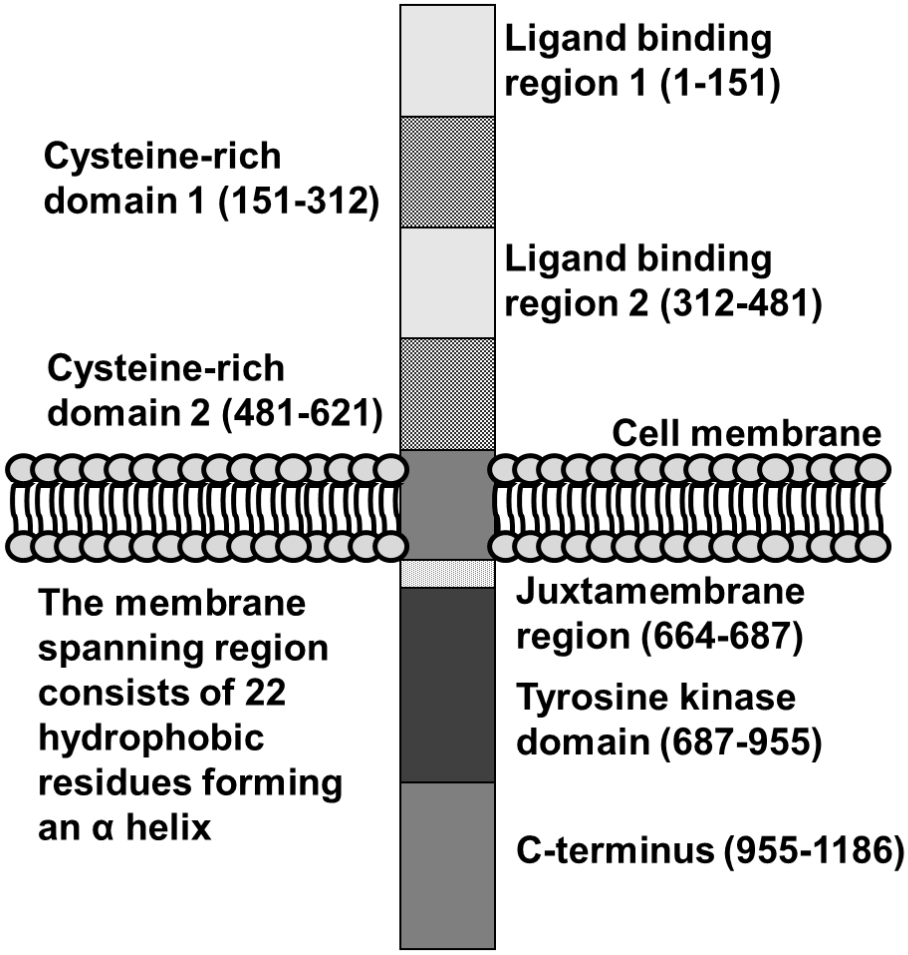

Figure 1.2: Schematic diagram of the structure of EGFR. All the members of the ErbB family have a similar structure of two ligand-binding domains and two cysteine-rich regions in the extracellular part of the receptor complex. ErbB2 has substitutions in the L1 and L2 domains, rendering it unable to bind ligand and ErbB3 has a substitution of a critical residue in the kinase domain rendering it inactive. Modified from Prigent (2006), see main text for more detail.

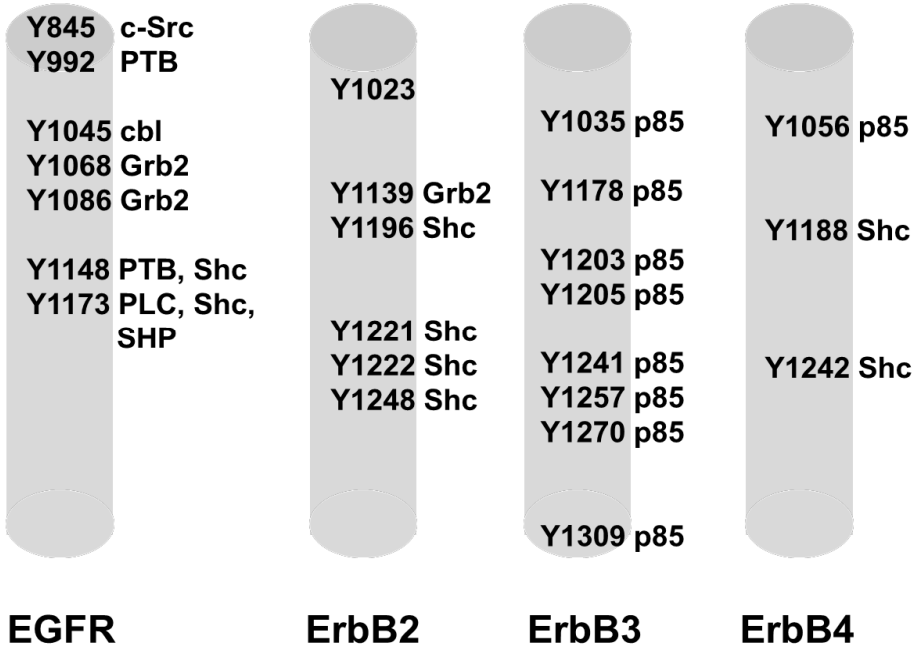

Figure 1.3: Schematic diagram showing ErbB receptor phosphorylation sites and their respective docking molecules. Cytosolic Src (c-Src) is able to phosphorylate EGFR in absence of ligand, while Cbl, an ubiquitin ligase is involved in receptor downregulation. Grb2 is an important molecule in the activation of the MAPK pathway, but often binds the receptors via the scaffolding molecule Shc. SHP phosphatases are important in RTK regulation, while p85 is the RTK interacting PI3K subunit. Modified from Prigent (2006) and Chaturvedi (2009), see text for more detail.

ErbB2 differs structurally in its extracellular domain from the other receptors, and so far, no exogenous ligand has been identified interacting with this receptor (Graus-Porta et al., 1997, Hynes and Lane, 2005). Graus-Porta (1997) demonstrated in a series of experiments that ligand-induced ErbB receptor heterodimerization follows a strict hierarchy, with ErbB2 being the preferred partner for all the other ErbB receptors. However, if ErbB2 is downregulated the other receptors are able to dimerize with each other (Graus-Porta et al., 1997). This has led to the hypothesis that the primary function of ErbB2 is as a co-receptor (Olayioye et al., 2000).

ErbB3 differs structurally from the other family members in the catalytic domain, rendering it devoid of intrinsic kinase activity (Holbro and Hynes, 2004). It is therefore dependent upon its heterodimerization partner to be transphosphorylated for downstream signalling to occur (Rogers et al., 2005).

1.3.2 EGFR function in normal development

EGFR and other members of the gene family are expressed in a wide range of epithelial and neuronal tissues during normal development and throughout life (Henson and Gibson, 2006, Sibilia et al., 2007). Gene knockout studies demonstrated that the gene family is crucial for normal embryonic development (Sibilia et al., 2007). EGFR receptor knockout mice die from day 11.5 of gestation to the early postnatal period due to multiple defects in epithelial organ development (Henson and Gibson, 2006, Sibilia et al., 2007). ErbB2, ErbB3, and ErbB4 gene knockout mice die during early to mid-gestation due to defects in cardiac, glial and neuronal development (Citri et al., 2003, Henson and Gibson, 2006, Sibilia et al., 2007).

1.3.3 ErbB receptor family ligands

To date, ten cognate ligands have been identified interacting with the receptor family, each containing an EGF-like domain (Nicholson et al., 2001, Prigent, 2006). They can broadly be divided into three groups depending on their receptor specificity (Table 1.8).

The members of this family of peptides are initially synthesised as large glycosylated membrane-associated precursors consisting of a hydrophobic signal peptide and a transmembrane domain (Salomon et al., 1995). Some ligands can act in a juxtacrine fashion when still tethered to the cell

membrane, but most require further processing (Rogers et al., 2005). The low molecular weight EGF peptide is found in the amino-terminus of the precursor from which it is proteolytically cleaved by matrix metalloproteinases (MMPs) and adamalysins (ADAMs), leading to shedding of soluble growth factors (Salomon et al., 1995). ErbB ligands generally act over short distances as autocrine or paracrine growth factors, except EGF which can also be found in many body fluids (Olayioye et al., 2000).

Group of ligands	Receptor binding specificity	
Group 1 Ligands that binds specifically to EGFR	Epidermal Growth Factor (EGF)	
	Transforming Growth Factor α (TGFα)	
	Amphiregulin (AR)♦	
Group 2 Ligands that have dual specificity to EGFR and ErbB4	Betacellulin (BTC)	
	Heparin-binding EGF (HB-EGF)	
	Epiregulin (EPI)	
Group 3 Ligands that bind to ErbB3 and ErbB4, the neuregulins	ErbB3 and ErbB4	Neuregulin (NRG) 1♣
		Neuregulin (NRG) 2
	ErbB 4 only	Neuregulin (NRG) 3
		Neuregulin (NRG) 4

♦ Some authors suggests that AR also activates ErbB4, Rogers et al. (2005)

♣ NRG-1 is also known as neu differentiation factor, heregulin, acetylcholine receptor inducing activity and glial growth factor, Olayioye et al. (2000)

Table 1.8: Binding specificity of the different ligands that interact with the ErbB family of receptors. Compiled from Hynes & Lane (2005) and Graus-Porta et al. 1997.

ErbB ligands exhibit distinct expression patterns that are specific to tissue type and developmental stage, providing additional control of the signalling pathways (Olayioye et al., 2000). Their biochemical properties also influence signalling diversity. ErbB ligands are bivalent and upon receptor binding, the ligand will influence the dimerization partner interaction (Lenferink et al., 1998, Olayioye et al., 2000). The ligands also exhibit

differential receptor binding affinities which influence signal duration and strength (Olayioye et al., 2000). In addition, ligands influence signalling through their differential pH stability (Lenferink et al., 1998, Wiley, 2003). Ligand-receptor complexes dissociate at ligand-dependent pH values, and this influences downstream trafficking of the receptor (Wiley, 2003) by, for example, targeting the receptor for recycling rather than degradation and contributing to receptor upregulation (Lenferink et al., 1998, Olayioye et al., 2000, Wiley, 2003).

1.3.4 ErbB receptor interactions and signalling and expression and their role in the pathogenesis of cancer

ErbB receptor signalling is induced by ligand binding to their extracellular domain causing conformational changes to the receptor (Prigent, 2006), which promote formation of homo- or heterodimers between receptor family members (Holbro and Hynes, 2004, Jimeno and Hidalgo, 2005). Dimerization is dictated by the nature of the ligands and the cell's complement of ErbB receptors (Olayioye et al., 2000) and follows a strict hierarchal pattern (Graus-Porta et al., 1997, Olayioye et al., 2000). Dimerization in turn activates the intracellular tyrosine kinase and leads to autophosphorylation of one or more of the tyrosine residues in the intracellular carboxy-terminus. These phosphorylated residues act as docking sites for several adaptor and docking molecules which in turn activate downstream pathways (Holbro and Hynes, 2004, Jimeno and Hidalgo, 2005).

Each ErbB receptor displays distinct specificities for different adaptor proteins or enzymes determined by the amino acids surrounding the autophosphorylation sites (Olayioye et al., 2000, Holbro and Hynes, 2004). The cytoplasmic mediators bind via their Src-homology 2 (SH2)-domains or

their phosphotyrosine-binding (PTB)-domains. The recruitment of these adaptor proteins and enzymes leads to activation of a variety of intracellular downstream signalling pathways (Rogers et al., 2005, Holbro and Hynes, 2004). The major EGFR downstream pathways include the mitogen-activated protein-kinase (MAPK) pathway, the phosphatidylinositol 3-kinase (PI3K) pathway, the signal transducers and activators of transcription (STAT) pathway and the phospholipase Cγ (PLCγ) pathway (Yarden and Sliwkowski, 2001, Jorissen et al., 2003, Rogers et al., 2005) (Figure 1.4). In addition, abundant cross talk exists between different receptor pathways both at the intracellular and the extracellular level (Rogers et al., 2005). Activation of these pathways leads to increased cell proliferation, angiogenesis, cell survival and invasive and migratory potential (Eriksen et al., 2004).

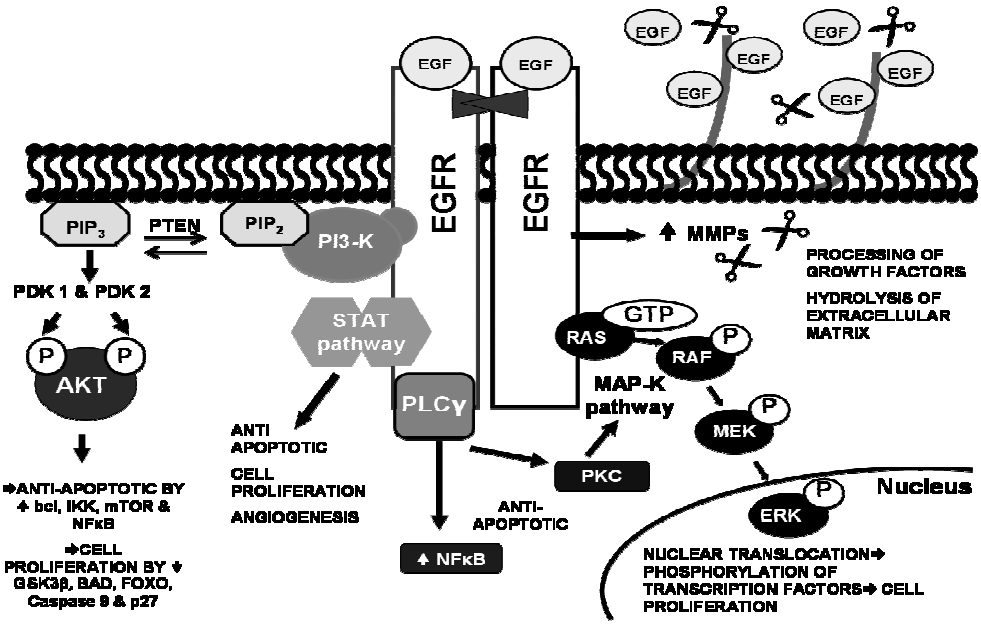

Figure 1.4: EGFR downstream pathways. Activation of PI3-K pathway leads to conversion of PIP_2 to PIP_3, the first step in a phosphorylation cascade ending in activation of Akt. It in turn activates anti-apoptotic proteins bcl, IKK and NFκβ and inhibits pro-apoptotic proteins FOXO and Caspase 9. Activation of mTOR and inhibition of cell cycle inhibitors GSK3β and p27 drives cell proliferation. MAPK pathway stimulates cell proliferation and STAT pathways inhibit apoptosis and stimulate angiogenesis and cell proliferation. The PLCγ pathway is implicated in cell survival and migration, and the MMP pathway is involved in processing of growth factors potentially causing an autocrine signalling loop and in the hydrolysis of basement membrane and extracellular matrix which may play a role in invasion.

Dysregulation of EGFR function and the overexpression of EGFR and its ligands were commonly reported features of epithelial malignancies. The major pathways, their role in cancer and other important mechanisms in the pathogenesis of EGFR are discussed further below.

1.3.4.1 The MAPK pathway promotes proliferation

All four ErbB receptors activate the MAPK pathway, but EGFR is the most important activator (Jorissen et al., 2003, Rogers et al., 2005). The pathway is a potent inducer of proliferation in cancer while its contributions towards invasive capability are thought to be limited (Thomas et al., 2003, Sharma et al., 2007). The pathway has also been implicated in transactivation of vascular endothelial growth factor (VEGF) receptors contributing to neoangiogenesis (Rogers et al., 2005).

Upon ligand activation and tyrosine kinase phosphorylation of tyrosine residues, the adaptor molecules growth factor receptor-bound protein 2 (Grb2) and Shc are recruited to the receptor. Grb2 interacts with EGFR either directly at tyrosine residues Y1068 or Y1086 via its SH2 domain, or indirectly by binding Shc which binds EGFR at Y1148 or Y1173 via its PTB domain (Jorissen et al., 2003, Prigent, 2006). It has been suggested that the Shc-Grb2 complex interaction is the major activation step (Sasaoka et al., 1994), but regardless of interaction involved, the Grb2 protein associates constitutively with the Son of Sevenless (SOS) protein, which regulates the activity of Ras (Sasaoka et al., 1994, Prigent, 2006). Ras is a guanosine triphosphate (GTP) binding protein, which, in its inactive state, is bound to guanosine diphosphate (GDP) and localised to the plasma membrane by a fatty acid chain modification (Egan and Weinberg, 1993, Prigent, 2006, Roberts and Der, 2007). The recruitment of the Grb2–SOS complex to the plasma membrane promotes their interaction. SOS catalyses the exchange of GTP to

GDP converting Ras into its active form (Roberts and Der, 2007). Ras remains active until its GTP is converted back to GDP by GTPase activating protein (GAP) (Roberts and Der, 2007). There are three mutated forms of Ras commonly found in cancer, and these proteins are GAP insensitive, rendering them constitutively activated (Prigent, 2006, Roberts and Der, 2007).

Ras-GTP activates the serine/threonine kinase raf-1, which in turn via a series of intermediate kinases phosphorylates the dual specificity kinases MEK1 and MEK2. The next step is the phosphorylation of extracellular signal–regulated kinase 1 (ERK1) and ERK2, which translocate to the nucleus where they regulate various transcription factors including cyclin D1, jun, fos and myc (Jorissen et al., 2003, Roberts and Der, 2007). Cyclin D1 is important in cell cycle progression and jun, fos and myc are proto-oncogenes. The pathway is further regulated by a negative feedback loop where the Grb2-Sos complex dissociates following ERK phosphorylation (Jorissen et al., 2003).

1.3.4.2 The PI3K pathway is the pro-survival arm downstream of EGFR

Phosphatidylinositol 3-kinase (PI3K) is one of the most important phospholipid modifying enzymes downstream of the RTKs (Jorissen et al., 2003). PI3K contains two subunits, the p85 units which carry a SH2 binding domain and the catalytic subunit p110 (Jorissen et al., 2003, Prigent, 2006).

The PI3K pathway is often termed the pro-survival pathway, as this is one of the main mechanisms tumour cells use to circumvent apoptosis (Rogers et al., 2005, Sharma et al., 2007). It is also thought to be the main mechanism conferring radiation resistance in HNSCC cells (Thomas et al.,

2003, Sharma et al., 2007), and it has been implicated as the main inducer of neoangiogenesis during tumour growth (Rogers et al., 2005).

The main activator of the PI3K pathway is ErbB3 (Olayioye et al., 2000), which has several binding sites for the p85 subunit (Prigent, 2006). EGFR has to date no reported direct binding sites for this subunit (Prigent, 2006), but EGFR specific ligands are still strong initiators of this pathway through three mechanisms (Jorissen et al., 2003, Prigent, 2006). Firstly, following ligand-induced heterodimerization between EGFR and ErbB3, the p85 subunit binds to the transphosphorylated ErbB3 tail (Prigent, 2006). Secondly, EGFR can interact with the p85 subunit via a scaffold protein, Grb2 associated-binding protein 1 (GAB1), and the adaptor protein Grb2 which binds EGFR via Y1068 and Y1086 (Prigent, 2006). Thirdly, the pathway can also be activated by Src, a cytosolic tyrosine kinase that phosphorylates novel sites within the kinase domain of the EGFR, providing a docking site for the p85 subunit (Jorissen et al., 2003, Prigent, 2006).

Upon activation, PI3K catalyses the conversion of phosphatidylinositol (4,5) biphosphate (PIP_2) to phosphatidylinositol (3,4,5) triphosphate (PIP_3) (Gupta et al., 2002, Jorissen et al., 2003, Prigent, 2006). PIP_3 is a second messenger which targets the serine/threonine kinase Akt (also referred to as protein kinase B [PKB]) (Jorissen et al., 2003, Rogers et al., 2005). PIP_3 localises Akt to the membrane where phosphoinositide-dependent kinases (PDKs) phosphorylate it at two sites, causing full activation of Akt (Gupta et al., 2002, Rogers et al., 2005). Downstream of Akt a multitude of proteins are substrates for Akt phosphorylation (Gupta et al., 2002, Jorissen et al., 2003, Rogers et al., 2005), including the forkhead box protein O (FOXO) family of transcription factors, which are implicated in promoting cell cycle progression by promoting cyclin D1 expression and repressing cell cycle

inhibitors like p27 (Jorissen et al., 2003, Prigent, 2006). Akt also inhibits bcl-2-associated death promoter (BAD), a pro-apoptotic protein (Rogers et al., 2005), activates mammalian target of rapamycin (mTOR), which induces protein synthesis (Sharma et al., 2007) and the pro-survival transcriptional regulator protein nuclear factor-κB (NFκB) (Rogers et al., 2005).

In normal tissues the pathway is regulated by the phosphatase and tensin homologue (PTEN), a tumour suppression protein that dephosphorylates PIP_3. In some tumours, PTEN is found to be mutated, which removes the negative regulator of the pathway causing continuous activation of the pathway (Rogers et al., 2005, Negri et al., 2010).

1.3.4.3 The STAT3 and STAT5b pathways drive cell survival and migration

STAT proteins were first identified as signal transducers downstream of cytokine receptors and they were dependent on the Janus kinase (JAK) family for activation (Jorissen et al., 2003). Later, it was shown that EGFR also mediates STAT phosphorylation in a JAK-independent manner (Song and Grandis, 2000).

Seven STAT proteins have been identified in mammals: STAT 1 to 4, 5a, 5b, and STAT 6 (Grandis et al., 2000). STAT 1 demonstrates a tumour suppression function, whereas STAT 3 and 5b behave as oncogenes and contribute to cell proliferation, survival and invasion (Xi et al., 2003, Rogers et al., 2005, Wheeler et al., 2010b).

Activation of the STAT3 pathway involves the binding of STAT SH2 domains to EGFR phosphorylation sites Y1068 and Y1086 (Grandis et al., 2000, Song and Grandis, 2000, Xi et al., 2003). This interaction leads to phosphorylation, dimerization and nuclear translocation of STAT (Grandis

et al., 2000, Song and Grandis, 2000). STAT 5b is activated in a similar manner (Xi et al., 2003), and combined they contribute to inhibition of apoptosis and progression of tumour cell growth in HNSCC (Song and Grandis, 2000, Xi et al., 2003). The downstream targets of STAT includes hypoxia induced factor (HIF-1α) (Wheeler et al., 2010b), the anti-apoptotic protein Bcl-xL (Xi et al., 2003) and cyclin D1, which is important in permitting cell cycle progression from checkpoint G1 to S-phase and consequent cell growth (Rogers et al., 2005).

1.3.4.4 The PLCγ pathway is implicated in tumour migration and invasion

PLCγ is capable of binding both EGFR and ErbB2 receptors (Rogers et al., 2005). It interacts directly with EGFR by binding phosphorylated tyrosine residues Y992 and Y1173 (Jorissen et al., 2003, Reuter et al., 2007). The activation of this pathway has been implicated in migration and invasion in HNSCC (Thomas et al., 2003, Rogers et al., 2005, Kalyankrishna and Grandis, 2006).

Once activated by associating with EGFR, PLCγ hydrolyses PIP_2 to inositol triphosphate (IP_3) and 1,2-diacylglycerol (DAG) (Jorissen et al., 2003, Thomas et al., 2003, Rogers et al., 2005). IP_3 induces calcium release from intracellular stores stimulating a number of calcium dependent enzymes. DAG activates the serine/threonine kinase Protein Kinase C (PKC) which in turn induces a number of signalling pathways including the MAPK pathways (Rogers et al., 2005).

1.3.4.5 Receptor crosstalk and minor signalling pathways also play important roles in cancer pathogenesis

There is an abundance of signalling pathways downstream of the ErbB family members (Olayioye et al., 2000). The complexity increases further as other RTK families are capable of transactivation and crosstalk with the ErbB receptors (Yarden and Sliwkowski, 2001, Holbro and Hynes, 2004). For example, EGFR may be activated by gastrin-releasing peptide receptor (Lui et al., 2003), insulin-like growth factor 1 receptor (IGF1-R), cell adhesion molecules and G protein coupled receptor (GPCR) (Rogers et al., 2005).

In the latter case, ligand bound GPCRs activate MMPs through a poorly understood mechanism. The MMPs proteolytically cleave ligand precursors which in turn cause EGFR activation and downstream signalling (Yarden and Sliwkowski, 2001, Holbro and Hynes, 2004, Rogers et al., 2005). The release of MMPs can also be stimulated via the MAPK pathway following binding of ligands (in descending order of potency) BTC, EGF and NRG to ErbB receptors (Rogers et al., 2005). This creates a positive feedback loop where the MAPK pathway activates the transcription of genes encoding ErbB ligands (Yarden and Sliwkowski, 2001, Rogers et al., 2005). MMPs are often overexpressed in HNSCC, and the degree of upregulation correlates with invasive potential of the tumour (Rogers et al., 2005).

GPCRs also transactivate EGFR through the activation of Src, a cytosolic tyrosine kinase (Rogers et al., 2005). Src phosphorylates tyrosine residues in the EGFR tyrosine kinase domain, treating the receptor as a passive scaffold not utilising its tyrosine kinase function, creating a ligand independent process (Rogers et al., 2005).

1.3.4.6 Switching off the response

An important level of cell signalling control is the ability to switch off a signal following activation. In comparison to the process of EGFR stimulation, the inactivation of signalling is poorly understood (Lenferink et al., 1998, Sorkin and Goh, 2009). Downregulation is the net result of receptor degradation and recycling (Levkowitz et al., 1998, Sorkin and Goh, 2009), and downregulation of receptor-ligand complexes is the main mechanism of receptor inactivation (Sorkin and Goh, 2009). The downregulation of EGFR differs from the other receptors in its family (Lenferink et al., 1998, Wiley, 2003), and it has been suggested that this is mediated through differential binding affinities at their carboxy tails (Olayioye et al., 2000, Sorkin and Goh, 2009). For example, cbl (Lenferink et al., 1998, Levkowitz et al., 1998, Olayioye et al., 2000) and epidermal growth factor receptor substrate 15 (Eps15) (Olayioye et al., 2000) only bind to activated EGFR. Cbl has been identified as an ubiquitin protein ligase responsible for receptor ubiquitination causing subsequent degradation (Olayioye et al., 2000, Wiley, 2003) while Eps15 (Olayioye et al., 2000) are thought to be important in the internalization of activated receptor-ligand complexes.

In normal cells, EGFR cluster over clathrin-coated regions of the plasma membrane, which rapidly internalize receptor-ligand complexes forming endocytic vesicles upon activation (Lenferink et al., 1998, Sigismund et al., 2008). The majority of EGFR signalling occurs within these endosomal compartments (Wiley, 2003). The route the receptor then follows is dependent on its ligand and dimerization partner (Lenferink et al., 1998) and the level of receptor ubiquitination (Sigismund et al., 2008). EGFR homodimers are targeted to the lysosome for degradation, while heterodimerization with ErbB2 will increase recycling of EGFR (Yarden and

Sliwkowski, 2001). ErbB2 has a slower rate of internalization compared to EGFR due to a lack of internalization signals in its carboxy terminal (Sorkin and Goh, 2009). Expression levels of ErbB2 also influence EGFR internalization with decreased EGFR degradation in cells overexpressing ErbB2 (Sorkin and Goh, 2009).

TGFα, in contrast to EGF, readily dissociates from EGFR inside the endosome even at moderately acidic pH, and thus directs the receptor preferentially to recycling regardless of its heterodimerization partner (Lenferink et al., 1998). In contrast, EGF dissociates poorly from EGFR at the same pH, causing ligand receptor complex to be sorted to the lysosome (Sorkin and Goh, 2009).

In HNSCC, EGFR, TGFα and Erb2 receptor are often all overexpressed (Grandis et al., 1998, Cavalot et al., 2007). As the concentration of ligands or expression levels of the receptor increase, the clathrin-independent pathways internalize activated EGFR which preferentially targets the receptor to degradation (Sigismund et al., 2008). However, saturation of endocytosis and the lysosomal sorting machinery will occur, further reducing receptor degradation rates (Levkowitz et al., 1998, Wiley, 2003).

1.3.5 Mechanisms of aberrant EGFR activation in cancer

1.3.5.1 EGFR overexpression is a major mechanism in oncogenesis

EGFR overexpression and dysregulation is an important feature in the pathogenesis of HNSCC in man. Grandis and Tweardy (1993) compared the levels of messenger RNA (mRNA) encoding EGFR and TGFα between biopsy samples of tumours and the adjacent histologically normal mucosa from cancer patients. Normal oral mucosae from non-cancer patients were

used as controls. The tumour tissues had a 69-fold increase of EGFR mRNA compared to controls, and the histologically normal mucosa adjacent to the tumour samples had a 29-fold increase in mRNA levels compared to controls. Levels of mRNA encoding TGFα showed similar trends and elevated levels of mRNA encoding both molecules were associated with increased protein expression (Grandis and Tweardy, 1993). These findings led to the concept of "field cancerization", where the changes in the levels of EGFR and its ligand were thought to be an early carcinogenic event in the development of HNSCC (Grandis and Tweardy, 1993). A dramatic upregulation of EGFR expression has also been observed during transformation from dysplasia to SCC (Shin et al., 1994). This field cancerization has been suggested as an explanation of why HNSCC patients are susceptible to developing *de novo* tumours following successful treatment of earlier lesions (Grandis and Tweardy, 1993, Baselga et al., 2005).

Overexpression of EGFR is frequently reported in HNSCC, and has been reported in 38-98% of tumours (Baselga et al., 2005, Kalyankrishna and Grandis, 2006). The great variation reported is likely due to the lack of standardised scoring methods. Most studies use different labelling techniques and antibodies, and often use arbitrary cut off points to define overexpression (Dei Tos and Ellis, 2005). A consensus on a standardised EGFR scoring system that could be widely used with high repeatability would greatly enhance our understanding of what constitutes EGFR overexpression.

Other ErbB family members have also been reported to be overexpressed in HNSCC (Lango et al., 2001, Kalyankrishna and Grandis, 2006). Increased ErbB2 and ErbB3 expression have been associated with decreased survival and increased nodal metastasis (Shintani et al., 1995,

Cavalot et al., 2007). The role of ErbB4 is still unclear, but it has also been reported to be overexpressed in HNSCC (Lango et al., 2001).

1.3.5.2 Autocrine ligand activation may be an early step in malignant transformation

Uncontrolled cell growth may be the result of a cell developing the ability to produce growth factors that stimulate its own proliferation (Grandis and Tweardy, 1993). This is thought to be an important early event in the pathogenesis of HNSCC (Jimeno and Hidalgo, 2005, Kalyankrishna and Grandis, 2006). This was supported by the findings that in normal mucosa from non-cancer patients, TGFα and EGFR were produced by adjacent cells, implying a paracrine stimulation pathway (Grandis et al., 1996). In contrast, in histologically normal mucosa from HNSCC patients, TGFα and EGFR were co-expressed in cells, suggesting a switch to an autocrine pathway (Grandis et al., 1996, Lui et al., 2003), rendering the cell self-sufficient in growth signals, one of the hallmarks of cancer (Hanahan and Weinberg, 2000).

1.3.5.3 EGFR gene amplification in HNSCC

One of the reported causes of EGFR overexpression is gene amplification (Salomon et al., 1995, Nicholson et al., 2001, Arteaga, 2003). Although EGFR overexpression commonly occurs in HNSCC, gene amplification does not seem to be the main mechanism behind this phenotype. In a small study of 33 HNSCC patients, 30 tumours overexpressed EGFR but only seven patients exhibited gene amplification, and that was only of a moderate degree (Mrhalova et al., 2005). Similarly, Grandis and Tweardy (1993) showed that ten HNSCC cell lines which overexpressed EGFR and TGFα mRNA did not show a significant increase in EGFR or TGFα gene dosage or any evidence of rearrangements of these

genes. They suggested the increases in mRNA in these tumours were due to an elevated transcription rate and possibly enhanced mRNA stability rather than gene amplification (Grandis and Tweardy, 1993).

1.4 EGFR as a therapeutic target

The role of EGFR as a potent driver of oncogenesis is well established, but there are several reasons why it has become a favoured therapeutic target (Arteaga, 2003, Kalyankrishna and Grandis, 2006). EGFR and its ligands are overexpressed in a range of tumours (Lurje and Lenz, 2009), and EGFR expressing tumours can be identified in diagnostic biopsies from patients, aiding in the selection of potentially responsive tumours (Arteaga, 2003). EGFR expression relative to normal tissues has been extensively studied in ten major solid cancers in man, namely ovarian, breast, bladder, cervical, HNSCC, oesophageal, colorectal, gastric, endometrial and non-small cell lung cancer (NSCLC) (Nicholson et al., 2001, Dei Tos and Ellis, 2005). In these tumours EGFR overexpression is associated with worse overall survival (Dei Tos and Ellis, 2005), although EGFR overexpression is only considered a strong prognostic indicator in HNSCC, ovarian, cervical, bladder and oesophageal cancers (Dei Tos and Ellis, 2005, Lurje and Lenz, 2009).

The lack of an obvious physiological role of EGFR in the adult further indicates that it is a potentially good drug target (Arteaga, 2003). Inhibition of EGFR signalling can be achieved through three main approaches: monoclonal antibodies (mAbs), tyrosine kinase inhibitors (TKIs) and inhibition of EGFR synthesis through antisense oligonucleotides or RNA interference (RNAi) (discussed separately in chapter 1.6.1) (Nozawa et al.,

2006, Reuter et al., 2007, Lai et al., 2009, Lurje and Lenz, 2009). Drugs used to target EGFR for the treatment of cancer in preclinical and clinical development are summarised in Table 1.9.

Drug (trade name)	Type	Current status
Gefitinib (Iressa)	TKI	Approved NSCLC. Phase II for breast, nasopharyngeal carcinoma, SCC of skin and oesophageal cancer.
Erlotinib (Tarceva)	TKI	Approved NSCLC, pancreatic cancer. Phase II for CRC, HCC, GBM, and oesophageal cancer.
Cetuximab (Erbitux)	Chimeric mAb	Approved HNSCC, CRC Phase III NSCLC, oesophageal cancer Phase II GBM, breast cancer
Panitumumab (Vectibix)	Humanised mAb	Approved CRC Phase III HNSCC, oesophageal cancer Phase II NSCLC, pancreatic cancer
Zalutumumab (HuMax-EGFr)	Human mAb	Phase III HNSCC

TKI = Tyrosine Kinase Inhibitors, NSCLC = non-small cell lung cancer, SCC = squamous cell carcinoma, CRC = colorectal cancer, HCC = hepatocellular carcinoma, GBM = glioblastoma multiforme.

Table 1.9: Examples of EGFR targeting cancer drugs at different stages of development. Compiled from (NCI, 2010).

1.4.1 Monoclonal Antibodies

Monoclonal antibody-based drugs compete with the EGFR ligands and bind to the extracellular domain of the receptor (Lurje and Lenz, 2009), where drug binding blocks dimerization and subsequent activation (Roberts and Der, 2007). The antibodies may also recruit Fc receptor-expressing immune effector cells leading to antibody-dependent cell-mediated cytotoxicity (Roberts and Der, 2007, Reuter et al., 2007, Lurje and Lenz, 2009). A number of EGFR mAbs have been developed, and each recognises distinct

sequences on the receptors and has different binding affinities, resulting in a range of biological activities (Roberts and Der, 2007).

The most important mAb in HNSCC to date is cetuximab, which was the first new treatment approved for HNSCC in over 30 years when it came on the market (Baselga, 2006). Cetuximab is a chimeric mouse-human IgG mAb that binds the EGFR extracellular domain blocking autophosphorylation and inducing downregulation of receptor from the cell surface. It may also block dimerization (Jimeno and Hidalgo, 2005, Bonner et al., 2006). Cetuximab induces cell cycle G1 arrest, inhibiting cell proliferation and tumour induced angiogenesis (Jimeno and Hidalgo, 2005, Bernier and Schneider, 2007). It has been used clinically in combination with radiotherapy, where it significantly prolonged locoregional control and survival (Bonner et al., 2006, Bernier and Schneider, 2007), or in conjunction with chemotherapy, where it was shown to increase overall survival and response rates as a second line therapy in patients refractory to platinum-based drug therapies (Baselga et al., 2005). The use of mAbs did not seem to increase the adverse effects of radiotherapy (Bonner et al., 2006) or chemotherapy (Baselga et al., 2005).

There are no reports of use of EGFR mAbs in veterinary patients or of the development of specific antibodies targeting EGFR for veterinary use. The available human monoclonal antibody based therapies may be ineffective for use in animal patients. These antibodies have been raised against the human EGFR receptor and may have reduced affinities for the corresponding receptor in animals. However, low affinity binding may still be effective or even superior to high affinity binding as high affinity binding can reduce tissue penetration or cause increased binding to normal tissues (Nissim and Chernajovsky, 2008). Perhaps more critically, the use of the

currently available monoclonal antibodies may be limited by host immune responses to the drugs. Currently in man, murine antibodies are used that have been modified to avoid these host responses, either by producing human-mouse chimeric antibodies or humanised murine antibodies (Nissim and Chernajovsky, 2008). If used in animals they are likely to cause anti-human antibody responses similar to the human anti-mouse antibody responses seen in man to murine antibodies (Nissim and Chernajovsky, 2008). Specific development of monoclonal antibodies targeting the EGF receptor in each individual species may be required to implement these therapies in veterinary oncology.

1.4.2 Tyrosine Kinase Inhibitors

These drugs were developed based on the observation that mutations in the ATP-binding pocket of the EGFR severely affected its tyrosine kinase function (Arteaga, 2003). The TKIs can be classified according to their selectivity for receptors (mono-, bi- or tri-functional) and their reversibility (reversible versus irreversible inhibitors) (Fry, 2003, Jimeno and Hidalgo, 2005, Reuter et al., 2007).

The mechanism of action of TKIs is predominantly by inhibiting the catalytic activity of the tyrosine kinase by blocking the ATP binding site (Roberts and Der, 2007, Lurje and Lenz, 2009). Two further mechanisms of action have also been proposed although these mechanisms are not fully understood (Fry, 2003). TKIs are thought to induce an inhibitor-mediated degradation of receptor and to cause interference with the signalling process by disrupting receptor dimerization (Fry, 2003). Advantages of TKIs include the ability to target ligand-independent signalling (necessary if EGFR activity has become dysregulated from ligand binding) and good oral bioavailability (Arteaga, 2003, Baselga and Swain, 2009).

Three TKIs are currently undergoing clinical trials for therapy of HNSCC, either as a monotherapy or in combination with radiation or chemotherapy (NCI, 2010, Reuter et al., 2007). Gefitinib (Iressa®, Astra Zeneca Pharmaceuticals, UK) is an EGFR selective and reversible TKI (Jimeno and Hidalgo, 2005) currently undergoing stage III clinical trials for the treatment of HNSCC (Reuter et al., 2007). It has been shown to exhibit additive and synergistic properties in combination with chemotherapy or irradiation (Huang et al., 2002, Reuter et al., 2007).

Although the TKI-based therapies may be more directly transferable between species, the efficacy and safety of these drugs has not been established in veterinary species and no specific TKIs targeting EGFR in animals have been marketed to date. However, there is a tri-functional TKI licenced for use in cutaneous mast cell tumours in dogs, toceranib sulphate (Palladia™, Pfizer), which inhibits KIT, VEGF receptor 2 and platelet derived growth factor receptor β (PDGFRβ) (London et al., 2009).

1.4.3 Side effects of EGFR targeting therapies

The main side effects of both of these groups of drugs are skin reactions and acne-like rash, fever, chills, asthenia, infusion reactions (mAbs only) and nausea (Baselga et al., 2005, Bonner et al., 2006). Patients that develop these reactions seem to respond more favourably to therapy, and the severity of the reaction corresponds with the response rate observed (Jimeno and Hidalgo, 2005, Lurje and Lenz, 2009).

1.4.4 Current use of EGFR targeting strategies

EGFR targeting drugs have been evaluated as single agent therapies, but may also have roles as part of multimodality therapy and in overcoming resistance to other therapies. Cancer cells surviving fractionated

radiotherapy have been shown to upregulate both EGFR and its ligand TGFα, indicating that EGFR upregulation may be an important mechanism used by cancer cells to circumvent the cytotoxic effects of radiotherapy (Thariat et al., 2007). The resistance of tumour cells to radiotherapy has also been shown to increase proportionally with EGFR expression in HNSCC (Bernier and Schneider, 2007, Thariat et al., 2007). In HNSCC, increased locoregional control and reduced mortality was reported when cetuximab was used in combination with radiotherapy compared to treatment with radiotherapy alone (Bonner et al., 2006). EGFR inhibitors have also been used in combination with chemotherapy in HNSCC (Baselga et al., 2005) and NSCLC (Mok et al., 2009). Some trials found no benefit from combination therapy of EGFR-TKI and chemotherapy in NSCLC, but others demonstrated that a subset of NSCLC with specific EGFR mutations respond favourably to EGFR inhibition (Pircher et al., 2010). Efforts are now focusing on finding reliable predictors of response to EGFR targeted therapies when used as both single agents and in multimodal therapies (Mok et al., 2009, Pircher et al., 2010).

1.4.5 Predictors of response to therapy

Initially the expectation was that there would be a straightforward relationship between level of EGFR expression and response to targeted therapies, mirroring the relationship in HER2 positive breast carcinomas where high HER2 expression is predictive of response to trastuzumab (an HER2-specific mAb) (Wheeler et al., 2010a). The relatively modest response rates of only 5-15% reported for EGFR targeted therapy in early trials were therefore disappointing (Lai et al., 2009), and patient selection based on immunohistochemical assessment of EGFR expression did not seem to predict response to therapy (Pircher et al., 2010, Wheeler et al., 2010a). In

some circumstances, EGFR expression levels were predictive, for example when an accelerated fractionation scheme (a fixed total dose is delivered in a fixed number of fractions during a shorter overall treatment time) was used to treat HNSCC the authors reported that patients with high EGFR expression received a significant benefit from this treatment type compared to patients with low or no EGFR expression (Eriksen et al., 2004, Bentzen et al., 2005). Further studies proved the benefit of cetuximab in combination with radiotherapy for HNSCC (Bonner et al., 2006), which then led to FDA approval for cetuximab in combination with radiotherapy the same year (Wheeler et al., 2010a).

As our understanding of the complex relationships governing EGFR signalling in different tumour types has evolved, the requirement for reliable molecular markers capable of predicting response to therapy has become apparent. A good example of this is the improvement seen in response rates to gefitinib treatment in NSCLC following the detection of EGFR activating mutations in a cohort of patients (Pircher et al., 2010, Wheeler et al., 2010a). This cohort had been identified based on their distinct clinical profile (patients that were female, of Asian origin who had never smoked and whose tumours were adenocarcinomas) (Pircher et al., 2010). The definitive role of two mutations in exons 19 and 21 affecting the receptor ATP binding pocket, which led to ligand-independent constitutive activation was finally determined in 2004 (Ratushny et al., 2009, Pircher et al., 2010). Due to the gain of function associated with these mutations, the tumours become EGFR-dependant, rendering them sensitive to TKI treatment (Ratushny et al., 2009), resulting in trials using these selection criteria achieving 50-70% response rates (Wheeler et al., 2010a).

Other predictive markers showing promise in solid tumours include markers of epithelial to mesenchymal transition (EMT) like E-cadherin and vimentin for HNSCC, pancreatic and colorectal cancers among others (Eyzaguirre et al., 2008, Haddad et al., 2009), EGFR copy number and K-ras mutations in colorectal cancer (Chen et al., 2010, Wheeler et al., 2010a) and H-ras mutations in HNSCC (Chen et al., 2010).

Interestingly, in a phase I trial of intratumoural antisense DNA therapy against EGFR in HNSCC, a response rate of 30% was achieved in patients already refractory to two standard therapies and in this study, response was correlated to high EGFR expression (Lai et al., 2009). The authors urged caution against over interpretation of these results, but this might suggest that targeting transcriptional regulation and downregulating protein levels may be more effective than blockade of EGFR-ligand binding or tyrosine phosphorylation (Lai et al., 2009).

1.4.6 Resistance to EGFR targeting therapies

Response to EGFR targeted therapies is limited by two mechanisms of resistance. Firstly, some cancer subsets have intrinsic resistance to EGFR targeted therapy despite expressing high levels of EGFR and show no response to treatment (Li et al., 2009). It is for this group of patients that the development of reliable predictive markers is crucial. Secondly, in the subgroups of cases that do show major clinical response to EGFR targeted therapy many develop an acquired resistance over time (Li et al., 2009).

Several mechanisms cause intrinsic resistance to EGFR targeted therapies, and they vary depending on tumour type. A relatively recent discovery is the presence of the mutant EGFR variant III (EGFRvIII) in up to 40% of HNSCC (Wheeler et al., 2010b). This mutation produces a

constitutively active truncated receptor lacking the extracellular ligand binding region, and has been associated with a proportion of glioblastoma multiforme (GBM) tumours in man (Gan et al., 2009). It has now been implicated in conferring resistance to cetuximab (Wheeler et al., 2010b) and radiotherapy (Ratushny et al., 2009) in HNSCC. Other mechanisms of intrinsic cellular resistance are mediated through inactivating mutations in PTEN in colorectal cancer (Negri et al., 2010, Mao et al., 2010), germ line polymorphisms in EGFR gene introns (Ratushny et al., 2009, Chen et al., 2010) and a more mesenchymal phenotype tumour (Haddad et al., 2009, Wheeler et al., 2010a).

Acquired resistance is mediated through a range of mechanisms, but most commonly through some form of oncogenic shift where the tumour compensates for EGFR blockade by shifting its reliance from the EGFR pathway to other pathways (Wheeler et al., 2010a). This could be through upregulation of other EGFR family members like ErbB2 (Erjala et al., 2006) and ErbB3 (Erjala et al., 2006, Wheeler et al., 2008, Chen et al., 2010) or through the activation of other RTK pathways. The main pathways implicated in circumventing EGFR targeting are altered VEGF receptor (VEGFR) expression conferring resistance to mAbs (Ratushny et al., 2009, Wheeler et al., 2010a), MET RTK amplification and its ligand hepatocyte growth factor (HGF) overexpression (Ratushny et al., 2009, Wheeler et al., 2010a), and transactivation of GPCR (Ratushny et al., 2009, Chen et al., 2010) and cytosolic Src (Chaturvedi et al., 2009). Transactivation of IGF1-R has been implicated in conferring intrinsic resistance to EGFR targeting therapies in NSCLC, but the phosphorylation and activation of IGF1-R has also been shown to increase in response to gefitinib in tumour models including

HNSCC, breast, prostate and colorectal cancer (Eyzaguirre et al., 2008), playing a role in acquired resistance in these tumours.

The occurrence of secondary mutations causing a methionine for threonine substitution in the kinase domain (T790M) has also been reported in acquired resistance to TKIs (Wheeler et al., 2010a). This mutation is found in NSCLC tumours containing the activating mutations associated with increased sensitivity to TKIs, but it is still not entirely clear whether this mutation arises in the population following treatment (Eyzaguirre et al., 2008) or whether this mutation was already present in a small subpopulation and was enriched for through positive selection during treatment (Eyzaguirre et al., 2008, Wheeler et al., 2010a). The latter option is currently the favoured explanation (Wheeler et al., 2010a).

Other mechanisms implicated in the occurrence of acquired resistance include impairment of receptor downregulation and deregulation of receptor ubiquitination (Wheeler et al., 2008, Li et al., 2009), cells undergoing EMT (Haddad et al., 2009, Chen et al., 2010) and EGFR nuclear translocation (Li et al., 2009). Further work is required to elucidate the main mechanisms of resistance by tumour cells to EGFR targeting therapies in order to target the tumour cells more strategically.

1.5 EGFR in veterinary medicine

Veterinary interest in EGFR as a potential prognostic indicator and possible therapeutic target is increasing, and a number of veterinary studies have been undertaken to investigate the role of EGFR in solid tumours. In man, EGFR has been implicated as an oncogenic driver in subsets of many tumours, including HNSCC (Grandis and Tweardy, 1993), NSCLC (Sharma et al., 2007), GBM (Gan et al., 2009), renal SCC, hepatocellular carcinoma

(Sibilia et al., 2007), ovarian, bladder, breast, pancreatic and colon cancers (Dei Tos and Ellis, 2005). Veterinary medicine is building on these advances in human medicine and several animal tumours have been investigated for EGFR expression. However, to date, there have been few studies that have directly evaluated if EGFR dysregulation is a key oncogenic driver and no studies that have evaluated EGFR targeted therapy in animals.

1.5.1 Squamous cell carcinomas

The expression of EGFR in feline oral SCC was investigated in an immunohistochemical study on archived biopsy samples and this demonstrated that 9 out of 13 samples had increased EGFR labelling (Looper et al., 2006). Recently, the expression of EGFR was evaluated in feline cutaneous SCC biopsy samples (Sabattini et al., 2010), and 14 out of 19 tumours had EGFR expression, but with great variation in intensity and proportion of positively labelled cells. The authors reported however, that cats with EGFR positive tumours had a significantly worse outcome with decreased disease-free intervals and survival (Sabattini et al., 2010).

Canine nasal carcinomas have also been evaluated for EGFR and VEGFR expression and both have been considered as potential therapeutic targets for the treatment of nasal tumours in the dog (Shiomitsu et al., 2009). EGFR was expressed in just over half of the tumour samples (Shiomitsu et al., 2009), and the authors speculated that EGFR and VEGFR targeted therapies in canine nasal tumours may be of value. Targeted therapies could potentially be used concurrently with standard therapies, for example by augmenting radiosensitivity of the tumours (Shiomitsu et al., 2009), but this hypothesis has not yet been tested.

Although these veterinary studies demonstrate that there is merit in evaluating EGFR-mediated signalling in SCCs, no studies have directly established if EGFR expression can be used as a marker of response to therapy or as a therapeutic target.

1.5.2 Mammary Tumours

EGFR is widely expressed in human breast cancers (Normanno et al., 2008), and feline and canine mammary carcinomas share many key features with the disease in man and have been cited as comparative models (Minke et al., 1991, De Maria et al., 2005, Gama et al., 2009, Queiroga et al., 2009). Both feline and canine mammary carcinomas have been reported to express EGFR (Minke et al., 1991, Rutteman et al., 1994, Donnay et al., 1996), but some authors report no correlation between EGFR expression and tumour aggressiveness (Rutteman et al., 1994, Donnay et al., 1996). A more recent study found that malignant tumours showed a significantly higher proportion of EGFR-expressing cells than benign tumours and that there were significant associations between EGFR expression and patient age and tumour size (Gama et al., 2009). Although not statistically significant, there appeared to be trends for reduced disease free survival and reduced overall survival in patients with malignant tumours that overexpressed EGFR compared to those with tumours which did not (Gama et al., 2009).

EGFR expression has also been evaluated in a xenotransplantation study of feline mammary carcinoma cell lines (Minke et al., 1991). This study demonstrated that a subpopulation of feline mammary carcinoma cells had increased tumourigenicity that correlated with high expression of functionally active EGFR associated with amplification of the *EGFR* gene (Minke et al., 1991). This study provides the clearest evidence that EGFR dysregulation may be a key oncogenic driver in some solid tumours in

animals, but dysregulation of EGFR has not been demonstrated in material from clinical cases of feline mammary carcinoma.

1.5.3 Brain tumours

In the dog, glial cell tumours account for 20% of CNS tumours (Thomas et al., 2009) and canine GBM shares many gross, microscopic and immunocytochemical features with the disease in human patients who often have *EGFR* gene mutations (Lipsitz et al., 2003, Stoica et al., 2004, Dickinson et al., 2006, Thomas et al., 2009, Higgins et al., 2010). EGFR expression in canine GBM has been reported in a subset of canine GBMs (Lipsitz et al., 2003, Stoica et al., 2004, Higgins et al., 2010), but no studies have evaluated the potential prognostic significance of EGFR expression in these tumours.

1.5.4 Lung cancer

One study has evaluated EGFR expression in a range of spontaneously arising and plutonium-induced lung tumours in dogs which may be comparable to human NSCLC (Gillett et al., 1992). In the canine study, EGFR was not expressed in unaffected lung, but was identified in 47% of tumours (spontaneously arising and plutonium-induced) of which the epidermoid carcinomas predominated (Gillett et al., 1992). This study demonstrated that EGFR may be a suitable biological marker for distinguishing bronchioalveolar carcinoma from other canine lung adenocarcinomas (Gillett et al., 1992). It also raised the possibility that EGFR overexpression may be a late event in the development of lung tumours in dogs and that EGFR may be a potential therapeutic target for subsets of canine lung cancer.

1.6 Nucleic acid-based gene silencing

The three major nucleic acid-based gene silencing molecules currently in use are antisense oligodeoxyribonucleic acids (ODNs), ribozymes and

small interfering RNAs (Dorsett and Tuschl, 2004). ODNs are single stranded DNA molecules of approximately 20 nucleotides in length which cause gene silencing through hybridization to mRNA to produce a substrate for ribonuclease H (RNase H) which specifically degrades RNA strands of DNA-RNA duplexes (Dorsett and Tuschl, 2004). Ribozymes bind to RNA and act to degrade target RNA by catalysing the hydrolysis of the phosphodiester backbone (Dorsett and Tuschl, 2004). Both these technologies are used in current drug developments, but RNAi-based gene silencing using small interfering RNAs (siRNAs) have in most instances superseded these technologies mainly because RNAi requires much lower nucleic acid concentrations and produces more specific gene silencing (Dorsett and Tuschl, 2004, Kurreck, 2006, Pai et al., 2006).

1.6.1 RNA interference

RNAi is a relatively new technology first described in the nematode *Caenorhabditis elegans* in 1998 (Fire et al., 1998). Three years later RNAi was described in mammalian cells by Dr. Tuschl and colleagues (Elbashir et al., 2001a). RNAi induces gene silencing at the post-transcriptional level by targeting mRNA for degradation (Hannon, 2002, Dorsett and Tuschl, 2004, Pai et al., 2006), through chromatin remodelling and by inhibition of protein translation (Pai et al., 2006).

1.6.1.1 Mechanisms of RNA interference

RNAi is a ubiquitous regulatory process found in all eukaryotic cells and is thought to be important in normal regulation of genes (Dorsett and Tuschl, 2004, Pai et al., 2006). When it was first described the mechanisms of action were still unknown, but Fire et al. (1998) reported two important observations. Firstly, the technique did not work if the sequence used

corresponded to intron or promoter regions of the gene in question. Secondly, they noted decreased mRNA levels following application, both suggesting interference at a post-transcriptional level (Fire et al., 1998). Later it was confirmed that siRNAs work by post transcriptional gene silencing (Scherer and Rossi, 2003, Dorsett and Tuschl, 2004). In plants and invertebrates, long double stranded RNA (dsRNA) are recognised by Dicer, an RNase III like endoribonucleotide, and cleaved into shorter 20-25 nucleotides siRNAs (Kittler and Buchholz, 2003) (Figure 1.5). The siRNA double helix is then unwound in an ATP-dependent manner, one strand is incorporated into the RNA-induced silencing complex (RISC), and the complementary siRNA sense strand is degraded (Hannon, 2002, Scherer and Rossi, 2003). The antisense siRNA-RISC complex then binds to complementary mRNA sequences. The mRNA is either cleaved by Argonaut family proteins (Dorsett and Tuschl, 2004) or the complex promotes translational inhibition effectively blocking subsequent gene expression (Hannon, 2002, Dorsett and Tuschl, 2004). The siRNA may be recycled to interact with further mRNA molecules (Kurreck, 2006). In invertebrates and plants siRNA molecules can function as primers for RNA-dependent RNA polymerase that synthesises additional dsRNA which in turn are processed into siRNA (Yu et al., 2002). It is not known whether this occurs in mammalian cells (Yu et al., 2002). In plants, siRNA also induces genomic methylation, but this has not been reported in mammalian cells (Dorsett and Tuschl, 2004). The net effect of the siRNA is a reduction in specific mRNA levels and the protein it encodes, inducing gene silencing (Scherer and Rossi, 2003).

Although the same mechanism exists in mammalian cells, initially it proved difficult to induce gene silencing experimentally due to apparent

non-selective cell death in response to long dsRNA (Dorsett and Tuschl, 2004). It has subsequently been established that dsRNA over 30 nucleotides in length trigger a strong interferon response in mammalian cells (Elbashir et al., 2001a). The interferon response activates Protein Kinase R (PKR) autophosphorylation and subsequent activation. PKR inhibits cell growth by phosphorylation of the essential protein-synthesis initiation factor eIF-2 and will often result in cell death (Williams, 1999, Yang et al., 2002). When dsRNA molecules of less than 30 nucleotides were used, gene silencing was achieved effectively without the concurrent non-selective interferon response (Elbashir et al., 2001a).

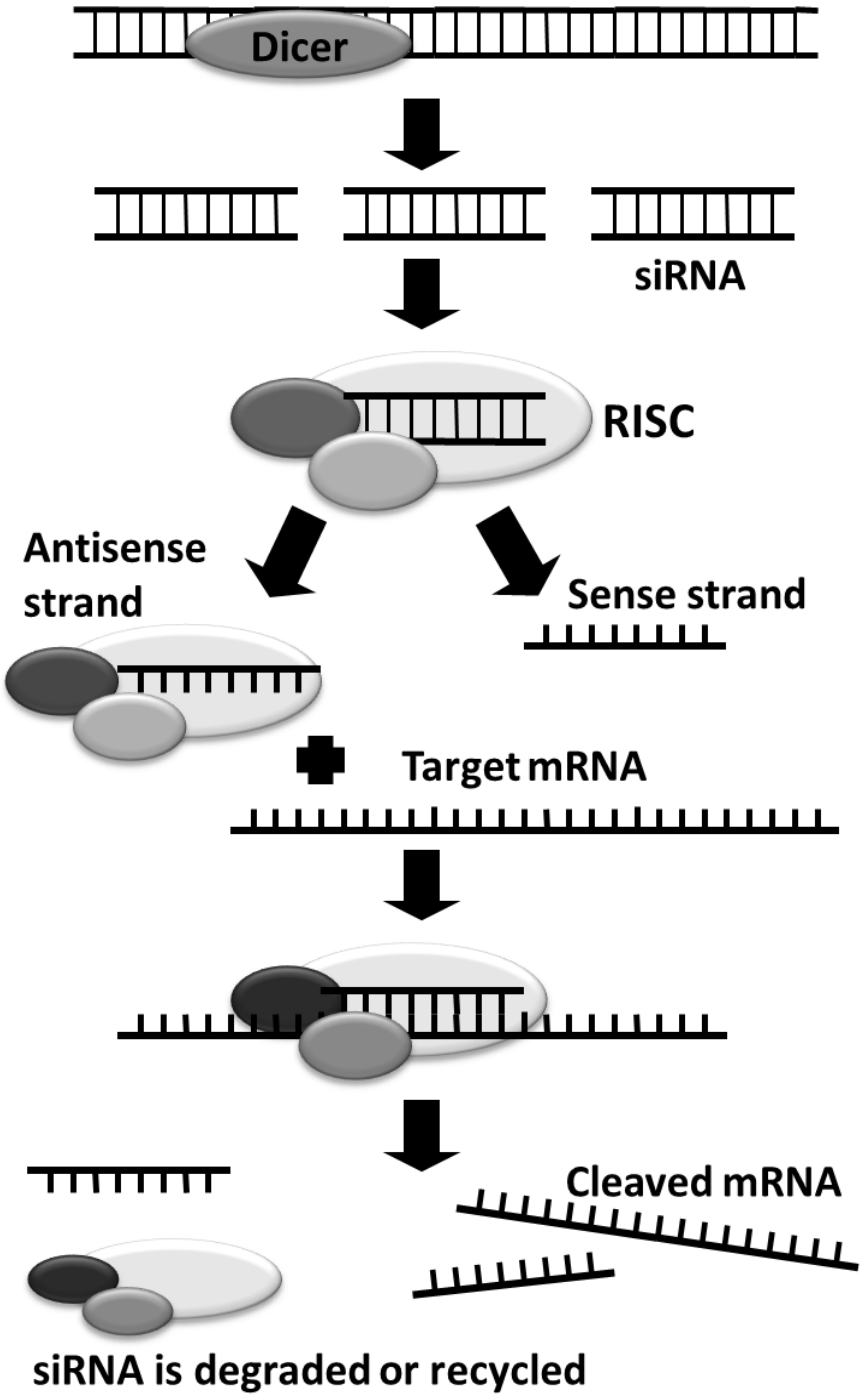

Figure 1.5: Schematic diagram to show the RNA interference pathway. Long dsRNA molecules are recognised and processed into shorter siRNAs by Dicer, and the antisense strand is then incorporated into RISC. The antisense siRNA-RISC complex binds complementary mRNA sequences, facilitating cleavage of the mRNA by Argonaut family proteins or the complex promotes translational inhibition effectively blocking subsequent gene expression.The siRNA may be recycled to interact with further mRNA molecules Modified from Scherer and Rossi (2003).

1.6.1.2 Synthesis of siRNA

The siRNA molecules used in mammalian cells usually consist of two complementary annealed single strands of 21-28 nucleotides in length with 3′ ends containing two nucleotide overhangs with hydroxyl termini (Scherer and Rossi, 2003, Dorsett and Tuschl, 2004). Alternatively, the siRNA may be in the form of a single stem-loop of 19-27 nucleotides in the stem, often referred to as hairpin RNA (shRNA) (Scherer and Rossi, 2003). Both types of molecules become incorporated into RISC in a similar manner.

Identifying an optimal target sequence is a crucial step in RNAi. Different siRNAs targeting different parts of the target mRNA sequence have sometimes vast differences in their silencing efficiency (Kurreck, 2006). So far it has not been possible to predict the optimal siRNA sequence for a target, so multiple siRNAs will usually have to be screened for their efficiency (Kittler and Buchholz, 2003). However, three factors have been identified that aid in the design of efficient siRNA (Kurreck, 2006). As discussed previously, low thermodynamic stability of the antisense strand 5′ end helps to preferentially incorporate the antisense strand into the RISC complex (Dorsett and Tuschl, 2004, Patzel et al., 2005, Kurreck, 2006). Secondly, the accessibility of the target site on the mRNA influences silencing efficiency. Some mRNA molecules have a very tight secondary structure leading to the inability of the RISC-siRNA complex to interact with its mRNA target site (Patzel et al., 2005, Kurreck, 2006). The third suggested factor is the potential for the siRNA antisense strand to form secondary structures (Patzel et al., 2005). It was found that antisense strands with base–paired termini were inactive, even when the first two criteria were fulfilled (Patzel et al., 2005, Kurreck, 2006). Active structures were comprised of free terminal nucleotides especially at the 3′end (Patzel et al., 2005).

Several methods have been used to produce siRNAs, each of which has its drawbacks (Kittler and Buchholz, 2003). The first publications used chemically synthesised RNA, and this method is still one of the most commonly used techniques (Elbashir et al., 2001a, Kittler and Buchholz, 2003). The main advantages of this technique are that large quantities can be made and base modifications are possible. They are, however, expensive to produce and require screening for an effective molecule (Kittler and Buchholz, 2003). *In vitro* transcription of siRNA and shRNA is cheaper, but screening of molecules is still required (Yu et al., 2002, Kittler and Buchholz, 2003).

SiRNA can also be produced in cells by transfection of an expression vector containing the hairpin sequence and a promoter (Yu et al., 2002, Kittler and Buchholz, 2003). This approach was found to be highly effective in gene silencing, but again the molecules require screening (Yu et al., 2002). Finally, a method of producing siRNA by enzymatic digestion of long dsRNA by *Escherichia coli* RNase III has been described (Yang et al., 2002). This technique produces several endoribonuclease-prepared siRNA (esiRNA) molecules with complementary sequences to the target mRNA, removing the need for screening (Yang et al., 2002, Kittler and Buchholz, 2003).

Despite these recent advances both in the design and the synthesis of siRNA, the potency of individual siRNA molecules can still not be accurately predicted. Additional research is required in this rapidly moving area.

1.6.1.3 Applications for RNA interference

RNAi is a powerful research tool as it is capable of specific gene silencing, and is extensively used in gene function analysis and genetic

screening (Kittler and Buchholz, 2003, Dorsett and Tuschl, 2004). Long term RNAi has been predicted to contribute extensively in drug development (Scherer and Rossi, 2003, Dorsett and Tuschl, 2004, Pai et al., 2006). Recently the first phase one trial using RNAi based systemically administered therapeutics was reported (Davis et al., 2010), marking another milestone in RNAi development.

The main challenges for the effective application of these technologies include overcoming problems with delivery, stability in tissues, minimisation of off-target effects and identification of effective siRNAs (Kittler and Buchholz, 2003, Scherer and Rossi, 2003, Dorsett and Tuschl, 2004, Pai et al., 2006).

Their stability in tissues may be overcome by chemical modifications rendering them more resistant to RNases (Dorsett and Tuschl, 2004, Pai et al., 2006). One potential way of making them more stable and aiding their delivery into tissues would be to link them to antibodies targeted towards cell surface receptors (Pai et al., 2006). This could be a feasible approach for targeting tumour cells in HNSCC known to overexpress EGFR.

A second approach used for delivery is using viral vector delivery systems. Viral vectors that have been used to date include retroviral, lentiviral, adenoviral and adeno-associated viral vectors (Pai et al., 2006). Major drawbacks of the viral vectors are lack of specificity, low efficiency of gene delivery as well as potential concerns regarding safety of the use of the vectors themselves (Pai et al., 2006).

Off target interference is a concern when developing therapeutics. Although siRNA are very specific in their effect, if they are not carefully selected they could be partially complementary to unintended targets (Pai et al., 2006). This off target effect increases with higher concentrations, so

highly specific siRNAs used at low concentrations should hopefully circumvent any potential side effects (Scherer and Rossi, 2003, Dorsett and Tuschl, 2004).

There are many challenges ahead before siRNA molecules can achieve their full potential as therapeutics. It is however, a rapidly moving field and hopefully these obstacles can be overcome, paving the way for a new generation of therapeutics.

1.7 Aims of PhD thesis

The aims of this study were to investigate the role of EGFR in feline oral SCCs and its potential as a therapeutic target. The first part of the study was an immunohistochemical study of EGFR expression in 67 feline oral SCC biopsy samples. In addition, these biopsy samples were labelled for Ki67, a proliferation marker, and their potentials as prognostic indicators were assessed.

The aim of the second part of the study was to clone the tyrosine kinase domain of the feline *Egfr*, and using this sequence as a basis, to design and construct siRNAs against the receptor. These siRNAs were screened using a vector based screening system and the most efficient siRNA was then selected for further knockdown studies in a feline SCC cell line.

The effective knockdown of feline *Egfr* in the cell line was verified by Real-Time PCR and western blot analysis. The siRNA sequence was also cloned into a hairpin expression vector system to investigate the effect of long term *Egfr* knockdown on the cell line. In parallel, treatment of the cell line with gefitinib, an EGFR specific tyrosine kinase inhibitor was evaluated. The effect of EGFR targeting on cell proliferation, migration and colony formation ability was determined.

A gefitinib resistant sub-line of the cell line was developed by long term treatment with sub lethal drug concentrations, and the effect of *Egfr* knockdown in the drug-resistant cell line was assessed. In addition, the effect of *Egfr* knockdown in combination with radiotherapy was investigated in the cell line.

The last part of the study investigated potential mechanisms of resistance to EGFR targeting therapies and conventional treatments, focusing on two potential mechanisms of resistance: cells undergoing an epithelial to mesenchymal transition and the presence of a putative cancer stem cell population within the cell line. The thesis is divided into an introduction with a review of the literature, a comprehensive materials and methods section and four individual result chapters with separate introductions, methods and discussions. In the final discussion chapter, the findings from the study are brought together and critically appraised and future areas of research are discussed.

Chapter 2:
Materials and methods

2.1 Miscellaneous

The microscope used for all fluorescence and phase contrast images was a Zeiss Axiovert40 CFL (Carl Zeiss Ltd., UK) microscope fitted with digital Axiocam monochrome or colour cameras respectively (Carl Zeiss Ltd.). Carl Zeiss Imaging systems Axiovision Software (Release 4.27.2) was used for image capture and image processing.

2.2 Immunohistochemistry

Biopsy samples were routinely fixed, processed and embedded in paraffin wax before being cut, mounted onto slides and stained. In short, the principle of tissue processing for histology follows five stages. Biological tissues are fixed by forming irreversible cross linking of amino acid groups, for example formaldehyde causes the formation of methylene linkage of proteins. Following preservation, all water has to be removed from the tissues. This is achieved through several dehydration steps where the tissues are transferred through progressively more concentrated ethanol baths to remove all water from the tissues. The next step is then to clear the alcohol from the tissues using a hydrophobic clearing agent (e.g. xylene). Following clearing, the samples are infiltrated with the embedding material; in most cases paraffin wax is used. The samples are then placed into moulds for external embedding in liquid embedding material and allowed to harden by cooling in the case of paraffin wax.

2.2.1 Tissue processing

Biopsy samples were fixed by immersion in 10% neutral buffered formalin for 48 hours before being processed. The samples were processed using an automated processor (Pathcentre, Thermo Fischer Scientific, UK) by dehydration in alcohol, clearing of alcohol with xylene and infiltration by immersion in liquid paraffin wax using the schedule described in Table 2.1. At the end of the processing programme, samples were placed in moulds filled with liquid paraffin at 60°C and allowed to set for a minimum of 24 hours before being cut and mounted onto slides (Superfrost Plus, Thermo Fisher Scientific).

Processing Stage	Agent	Time
Fixation	10% neutral buffered formalin	1 hour
Dehydration	70% Industrial methylated spirit (IMS)	1 hour
Dehydration	95% IMS	1 hour
Dehydration	IMS	3 x 1 hour
Dehydration	Absolute alcohol	1 hour
Clearing	50% Absolute ethanol and 50% Xylene	1 hour
Clearing	Xylene	2 x1 hour
Infiltration	Paraffin wax 60℃	4 x 1 hour

Table 2.1: Overview of tissue sample processing schedule used at the Easter Bush Veterinary Centre Pathology Unit.

2.2.2 Immunohistochemical markers

Two commercially available primary antibodies were used in the study. The EGFR antibody (Ab-10, clone 111.6, Thermo Fisher Scientific) had been previously used on feline oral squamous cell carcinomas and a range of normal feline tissues (Looper et al., 2006). It was further validated for use in the cat in this study by western blotting (Chapter 3.3.2). The antibody is a monoclonal antibody raised in mouse against human recombinant EGFR

protein. It binds to the extracellular domain of the receptor specifically at the EGF binding site, blocking EGF binding.

The Ki67 antibody (MIB-1, Dako UK Ltd, UK) is a mouse monoclonal antibody raised in mouse against human recombinant Ki67 peptide corresponding to a 1002 bp cDNA fragment. It recognises a 66 bp repetitive element in the Ki67 gene (Key et al., 1993). The antibody was known to cross-react with the Ki67 equivalent protein in various mammals, including cow, dog, horse, sheep and swine according to the manufacturer. A number of published studies have also used the MIB-1 clone in feline tumour tissues (Castagnaro et al., 1998, Melzer et al., 2006, Roels et al., 2000). The same horseradish peroxidase (HRP) conjugated secondary antibodies (Envision Kit, Dako UK Ltd.) were used with both primary antibodies.

For both antibodies, the optimum dilutions were determined by testing the dilution ranges recommended by the manufacturers on positive control tissues as indicated. For the EGFR antibody, additional optimisation of incubation times was performed. Incubation times ranging from 1-24 hours were tested, and 24 hours incubations yielded superior results.

2.2.3 Immunohistochemical labelling

Following formalin-fixation and paraffin wax embedding as described in Chapter 2.2.1, the samples were sectioned. Four micron sections were cut, mounted onto electrostatically charged slides (Superfrost plus, Thermo Fisher Scientific), dried at 60°C for 1 hour, dewaxed and rehydrated. Antigen retrieval was performed in 0.1M citrate buffer pH 6.0 for 15 minutes at 110°C (Ki67) or with Proteinase K (Dako UK Ltd.) for 3 minutes at 37°C (EGFR). Endogenous peroxidase was blocked using REAL Solution (Dako UK Ltd.) for 10 minutes at room temperature (RT). Primary antibodies were incubated

at 1:100 dilution for 1 hour at 37°C (Ki67) and for 24 hours at 4°C (EGFR). Primary antibodies were substituted for normal mouse serum as a negative control on representative samples from each batch. Horseradish Peroxidase labelled secondary antibodies (Envision Kit, Dako UK Ltd.) were added to the sections and incubated for 40 minutes at RT. Sections were washed 3 times between each step with 0.5 M tris buffered saline containing 0.1% Tween 20 at pH 7.5. Labelling was developed using ImmPACT DAB (Vector Labs Ltd., UK) at RT for 10 minutes producing a brown colour in positive sections. All samples were counterstained with Harris' haematoxylin prior to dehydrating, clearing and mounting under DPX (Sigma-Aldrich®, UK). Positive control tissues used included feline lymph nodes for the Ki67 antibody and feline skin tissue for EGFR antibody.

2.3 Cell Tissue Culture

2.3.1 Cell lines

The SCCF1 cell line is a previously characterised feline cell line derived from a laryngeal squamous cell carcinoma gratefully received from Professor T.J. Rosol, College of Veterinary Medicine, The Ohio State University, USA.

The 293FT cell line was obtained from Invitrogen, UK. It is derived from human embryonic kidney epithelial cells and is a commercially available and well-characterised cell line commonly used for transfections. The MDA-MB-468 cell line was obtained from MD Anderson Cancer Centre (USA). It is a fully characterised, commercially available human breast carcinoma cell line that overexpresses EGFR and was used as a positive control for EGFR expression within a cell line.

2.3.1.1 SCCF1 cell line characterisation

The SCCF1 cell line is a previously characterised cell line (Tannehill-Gregg et al., 2001). A brief summary of the derivation of the cell line and previously published findings is given here.

The cell line was derived from a small piece of laryngeal SCC removed from a recently euthanised cat with alligator forceps. The tissue was minced and washed in William's E medium containing gentamicin (0.05 mg per ml) and amphotericin B (0.25 μg per ml). The tissue was digested with collagenase by incubation with agitation at 37°C for 2 hours, washed and plated in 10 cm plates and maintained in William's E medium supplemented with 10% Foetal Bovine Serum (FBS), 0.05 mg/ml gentamicin, 2mM L-glutamine, 10 ng/ml EGF, and 0.1 nM cholera toxin as described by Tannehill-Gregg et al., (2001). The medium was changed every 3-5 days and the cells were passaged every 7-10 days.

A growth curve showed the cell line to reach confluence after approximately 10 days of logarithmic growth. It grew in an anchorage dependent manner showing an epithelial pattern typical of keratinocytes. The dominant cell morphology observed was polyhedral cells with a small amount of cytoplasm. Single cells formed small colonies that coalesced with time and exhibited limited contact inhibition with eventual layering of cells. A number of stellate shaped cells were also present, but these became less apparent as the cells reached confluence, mainly localising to the edge of the expanding cell colonies (Tannehill-Gregg et al., 2001).

Immunohistochemical labelling of the cell line revealed strong expression of cytokeratins and no expression of p53 and vimentin at the earlier passages, consistent with cells of epithelial origin. Some vimentin labelling did start to appear in scattered cells and the number of positively

labelled cells increased with passage number. The authors speculated that there was a degree of EMT taking place in the cells, especially in response to TGFβ (Tannehill-Gregg et al., 2001).

Karyotype analysis of the cell line was also compared to normal feline peripheral blood mononuclear cells. The SCCF1 cell line was found to be aneuploid with a stem line number of 34 chromosomes. Normal diploid feline cells have 38 chromosomes (Tannehill-Gregg et al., 2001).

2.3.2 Cell culture reagents and equipment

All cell culture reagents were obtained from Gibco® Invitrogen, UK unless otherwise specified. The SCCF1 cell line was grown in William's E medium with GlutaMAX I supplemented with 10% FBS, 10 ng per ml EGF and 0.05 mg per ml gentamicin sulphate. For selection of SCCF1 cells having taken up vectors following some transfections, 0.4 mg/ml Geneticin (G418) was added to the medium.

The 293FT cell line was initially grown in Dulbecco's Modified Eagle Medium (DMEM) supplemented with 10% FBS, 0.1 M non-essential amino acids, 6 mM L-glutamine, 1 mM sodium pyruvate, 1% penicillin-streptomycin (DMEM start up media). After 24 hours cells could be passaged in DMEM medium as above with added 0.5 mg/ml geneticin (G418) (DMEM growth medium). During transfections, cells were grown in DMEM medium as above without antibiotics (DMEM growth medium 2) and, immediately following electroporation, cells were resuspended in RPMI medium containing 10% FBS before being plated in DMEM growth medium 2.

For sphere assays the cells were grown in N2 medium with methylcellulose prepared in house (Appendix A). All the constituents for the N2 medium was obtained from Sigma-Aldrich®, except the recombinant

human EGF and the recombinant human basic fibroblast growth factor (bFGF) which were obtained from Pepro Tech EC Ltd., UK. In short, the N2 medium was prepared in a laminar hood using basic protective clothing by making up a two times solution of DMEM/F12 base medium with distilled water. To that, 1.2 g of sodium bicarbonate was added and pH was adjusted to 7.0 with 1M sodium hydroxide (NaOH). The solution was then filter-sterilised through a 0.22 μm filter, which raises the pH to 7.2. To the 2x base medium 20 nM progesterone, 100 μM putrescine, 30 nM sodium selenite, 25 μg per ml transferrin, 3.48 μM insulin, 10 ng per ml EGF and 10 ng per ml bFGF were added. The base medium was protected from light and stored at 4°C. Equal amounts of 1.6% methylcellulose were prepared by adding 1.6 g of methylcellulose per 100 ml of distilled water. To dissolve the methylcellulose the water was heated to 80-100°C before adding the methylcellulose which was then stirred until cooled to RT. The solution was stirred overnight at 4°C before being autoclaved the following day. The solution was again cooled to 4°C before an equal volume of 2x N2 base medium was added and stirred at 4°C overnight. The 1x N2 medium was aliquoted into 100 ml sterile bottles and stored at -20°C until use. Thawed medium stored at 4°C were used for up to 4 weeks.

All other media were made up freshly and stored at 2-8°C and used within 4 weeks. To detach cells, 0.25% (SCCF1 cell line) or 0.05% (293FT cell line) trypsin-EDTA was used. Cells were frozen down in freezing medium containing 10% dimethyl sulphoxide in FBS.

Tissue culture plastics were obtained from Becton Dickinson-Biosciences, UK (Falcon tubes and flow cytometer tubes), Sigma-Aldrich® (Corning® low adhesion tissue culture plates and pipette tips), Techno Plastic Products® AG, Switzerland (routine cell culture plates and flasks)

and Thermo-Fischer Scientific (NUNC™ white 96 well plates). Eppendorf tubes were supplied by Axygene from VWR, USA and freezing containers (Nalgene freezing container "Mr Frosty Control Freeze") and cryogenic vials were obtained from Scientific Laboratory Supplies Ltd., UK and Starlab (UK) Ltd. respectively. Pipettes (2-1000 μl Nichipets) were obtained from Nichiryo, Japan and Integra, Switzerland (Pipetteboy 1-50 ml).

2.3.3 Cells from liquid nitrogen

The SSCF1 cell line was donated as frozen vials stored in liquid nitrogen at passage 52. The 293FT cell line was purchased as frozen vials stored in liquid nitrogen at unknown passage number. Cells were quickly defrosted in a 37°C water bath and by rubbing between fingers before being transferred into Falcon tubes containing 5 ml phosphate buffered saline (PBS) (Appendix B) and being centrifuged at 200 x *g* for 5 minutes. The supernatant was discarded and the cell pellets were resuspended in 8 ml of their respective media, transferred to T25 flasks, and incubated at 37°C/5% CO_2 overnight.

2.3.4 Passaging cells

At first passage, the cell lines were transferred to T75 flasks. Cells were routinely passaged at 80-95% confluency every 3-4 days (293FT cell line) and at 95-100% confluency every 5-10 days (SCCF1 cell line).

To passage cells, medium was removed by pipetting, and the cells were washed twice in 8 ml of PBS before incubation at 37°C in 0.25% trypsin-EDTA (Table 2.2) until detached. Trypsinization was terminated by adding at least twice the trypsin volume of FBS-containing media to the cells. Cells were split as required (1:2 to 1:20) and seeded directly into new culture vessels with fresh media.

Cell Culture Vessel	Cell number seeded	Approx. surface area	Total Volume of Media	Volume of 0.25% Trypsin-EDTA
T25	0.1-1 x 10^6	25 cm^2	8 ml	2 ml
T75	1-3 x 10^6	75 cm^2	10-13 ml	3 ml
T150	1-5 x 10^6	150 cm^2	18-30 ml	3-5 ml
10 cm plates	1-3 x 10^6	60 cm^2	10 ml	3 ml
6 well plates	1-5 x 10^5	9 cm^2	2-2.5 ml	1-2 ml
24 well plates	1-20 x 10^4	2 cm^2	1 ml	0.5 ml
96 well plates	1-10 x 10^3	0.3 cm^2	0.05-0.2 ml	N/A

Table 2.2: Summary of cell culture vessels used during the project and their surface area, total volume of media and 0.25% trypsin-EDTA.

2.3.5 Determining cell density and viability

Following trypsinization as described in 2.3.4, 100 µl of cell suspension were transferred to an Eppendorf tube, gently mixed with 10 µl of trypan blue stain, and incubated for two minutes. Ten µl of cell suspension were then added to the counting chamber of a haemocytometer and the cells were counted. Cell viability and cell density were then determined using formulas in Table 2.3 and cell culture vessels were seeded accordingly (Table 2.2).

DF= (Volume of cell suspension + Volume of stain)/Volume of cell suspension
Cell density (cells per ml) = Total cell count / 0.1µl x DF x 10^4
Total number of cells = cells/ml x volume of cell suspension
Cell Viability (%) = [1-(# of stained cells/total # of cells)] x 100

Table 2.3: Formulas used when determining cell viability and density. DF= dilution factor, # stands for number and 0.1 µl is the volume of the haemocytometer counting chamber.

2.3.6 Sphere assay protocol

2.3.7 Setting up spheres from adherent cells

The SCCF1 cells were trypsinated as described in Chapter 2.3.4, and 1 ml of cell suspension was removed and centrifuged at 80 x *g* for 5 minutes

and resuspended in 1 ml PBS. Cells were then counted as described in Chapter 2.3.5. Six-well low adherence plates were seeded with 8-10 $x10^6$ cells in 2 ml of N2 media per well. Cells were incubated at 37°C/5% CO_2 and fed with 500μg per ml of EGF and bFGF each every 48 hours until spheres formed.

2.3.7.1 Passaging spheres

To passage spheres, cells were collected by pipetting and the wells were washed in PBS to maximise collection. The cells were then spun down at 200 x *g* for 5 minutes and the N2 medium was discarded. Five ml of 0.25% trypsin-EDTA was added to the cells and incubated at RT for 10 minutes. Three ml of FBS-containing media were added to terminate trypsinization and cells were collected by centrifugation at 200 x *g* for 5 minutes. The cell pellet was resuspended in 1 ml of PBS and counted as previously described in Chapter 2.3.5 and a six-well low adherence plate was seeded with 8-10 $x10^6$cells per well in 2 ml of N2 media.

2.3.8 Cells into liquid nitrogen

Cells were grown to near confluency and trypsinated and the total number of cells were determined as previously described (2.3.5). The SCCF1 cell line was frozen down at approximately $3x10^6$ cells in 0.5 ml of freezing medium (Appendix B). The cell suspension was centrifuged at 200 x *g* for 5 minutes and resuspended in the appropriate volume of freezing medium, aliquoted into cryovials, transferred to freezing vehicle and frozen down in a minus 80°C freezer. Using a freezing vehicle containing 100% isopropyl alcohol allowed for a steady freezing rate of 1°C per minute which ensures successful cryopreservation of cells and decreases overall cell death. After a

minimum of 3 hours, cells were transferred to liquid nitrogen for long term storage.

2.3.9 Gefitinib treatment of SCCF1 cell line

Gefitinib (Astra Zeneca, UK) is an EGFR-specific small molecule tyrosine kinase inhibitor and was purchased from Tocris Bioscience (UK). Ten mg of the drug was supplied in powdered form, and was made up to a 10 mM stock solution in DMSO and stored in 50 μl aliquots at minus 20°C.

The SCCF1 cell line was treated with a range of concentrations from 1 nM to 100 μM in William's E media for up to 72 hours. Before use, the drug was further diluted in William's E medium to twice the desired concentration, before being added to the same volume of medium in each well. DMSO control treated cells were treated with DMSO concentrations corresponding to the highest drug concentration used in the experiment. Untreated control cells were always also included in each experiment.

2.3.10 Creating a gefitinib resistant SCCF1 cell line

In order to create a gefitinib resistant SCCF1 cell line, the cells were passaged as described in Chapter 2.3.4 for six months in gefitinib containing medium. William's E media was made up as described in Chapter 2.3.2. Gefitinib containing medium was made up freshly every week in 100 ml aliquots containing 5 μM gefitinib.

2.3.11 Harvesting adherent cells

To harvest, cells were washed with chilled PBS, scraped in 5 ml ice-cold PBS and pelleted by centrifugation at 2500 x *g* for 4 minutes at 4°C. Supernatant was discarded and cell pellets were snap frozen on dry ice and stored at minus 70°C.

2.3.12 G418 titration kill curve for SCCF1 cell line

In order to select for cells carrying the neomycin-resistance gene following DNA plasmid transfections, the cells were grown in William's E medium containing the antibiotic geneticin (G418), an analogue of neomycin. G418 is an aminoglycoside antibiotic produced from *Micromonospora rhodorangea*, and its mode of action is to block polypeptide synthesis by inhibiting the elongation step in both prokaryotes and eukaryotes (Haynes et al., 1995). The resistance gene confers resistance by encoding an aminoglycoside 3' phosphotransferase enzyme (Ambion, 2008b). To determine the optimal G418 concentration in the media, a titration kill curve was performed to determine the concentration of drug that would cause massive cell death in seven days.

Cells were seeded at $2x10^4$ cells per well in 24 well plates in 1 ml media containing no antibiotics and incubated overnight at 37°C/5% CO_2. The following day, 0.5 ml of medium containing G418 at different concentrations was added to each well according to diagram in Figure 2.1, and then changed completely to G418 containing medium every 48 hours. The cells were checked and photographed 3 times weekly for cell death.

2.3.13 Optimal plating density for SCCF1 cell line

To determine the cell plating density that allowed cells to reach 80% confluence in selective media before undergoing massive cell death an optimal plating density titration was performed. Cells were plated into 24 well plates at $1.2\text{-}6x10^4$ cells per well and incubated at 37°C/5% CO_2 in 1 ml William's E medium without antibiotics. The following day one ml of G418-containing medium containing the optimum concentration obtained from the kill curve described in Chapter 2.3.12 was added to each well

according to Figure 2.2. This produced wells containing half the optimum G418-concentration determined by the kill curve, and the cells were incubated in this for 24 hours. The following day the medium was then changed to medium containing the optimum concentration of G418. The cells were washed in PBS and fresh G418-containing medium was added every 48 hours until the experiment was complete. The cell confluence was noted and the cells photographed three times weekly until massive cell death occurred.

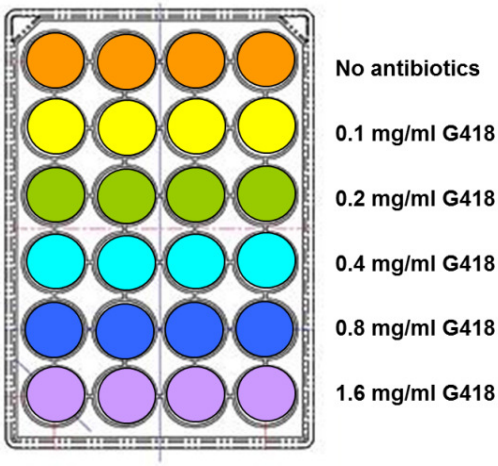

Figure 2.1: 24 well plate set up for G418 titration kill curve for SCCF1 cell line

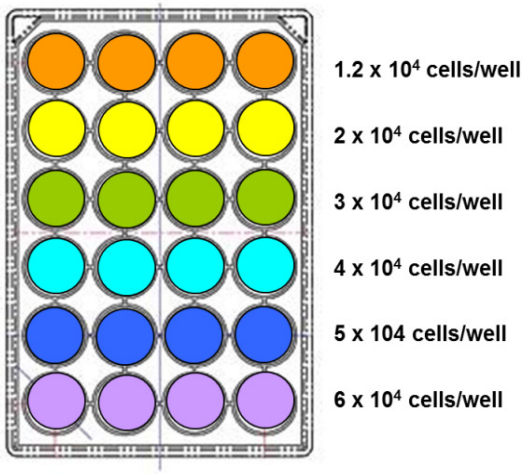

Figure 2.2: Diagram to show set up of optimal plating density curve for SCCF1 cell line.

2.4 Isolation and quantification of nucleic acids

2.4.1 RNA extraction

Total RNA was isolated from the cells utilising the RNeasy Mini Kit with QIAshredder (UK Qiagen Ltd.) according to the manufacturer's Animal Cells Spin protocol including a DNase on-column digestion step utilising the RNase-free DNase Free Set (Qiagen). This commercial kit extracts RNA from cells utilising the spin column-based nucleic acid extraction principle.

Cells were counted as described in Chapter 2.3.5. Up to $1x10^7$ of cells were centrifuged at 300x *g* for 5 minutes and resuspended in 350-600 µl RLT lysis buffer. Alternatively, the cell monolayer was directly lysed in the culture vessel by adding 350-600 µl of RLT lysis buffer directly to the well. Samples were then mixed thoroughly by pipetting or vortexing. RLT is a highly denaturing buffer containing guanidine thiocyanate which inactivates RNases.

The cell lysate was then passed through a QIAshredder homogeniser by centrifugation at full speed for 2 minutes to reduce the viscosity of the lysate and to shear high molecular weight genomic DNA and other cellular components which may reduce RNA binding to the silica-gel membrane. Seventy percent ethanol was then added and the lysate was transferred to the spin column.

Ethanol in the presence of chaotropic salts from the RLT buffer promotes adsorption of RNA to the silica-gel membrane allowing selective binding of RNA. The spin column was spun at 8000 x *g* for 15 seconds and the flow through containing denatured protein and cellular debris was discarded. A further wash step in 350 µl of buffer RW1 at 8000 x *g* for 15 seconds removed further contaminants.

To ensure no DNA contamination of RNA sample an on-column DNase digestion was performed with the RNase-Free DNase Set. Ten μl of stock DNase were added to 70 μl of RDD buffer from the kit and added to the spin column membrane. After 15 minutes of incubation at RT a further wash step with 350 μl RW1 buffer was performed.

A further two wash steps with 500 μl RPE buffer containing 80% ethanol was then performed, first at 8000 x *g* for 15 seconds and then a further 2 minute centrifugation step at 8000 x *g*. To ensure no carryover of ethanol a one minute centrifugation step at full speed was performed to ensure the membrane dried completely. RNA was eluted in 30-50 μl of RNase-free water by centrifugation at 8000 x *g* for 1 minute.

2.4.2 DNA plasmid purification

Plasmid purification was performed using the QIAfilter Plasmid Maxi Kit from Qiagen following the manufacturer's protocol with some modifications. The kit protocol is based on a modified alkaline lysis procedure followed by filtration. Plasmid DNA is then bound to an anion-exchange resin under low-salt and pH conditions, and impurities are removed by medium-salt washes. Plasmid DNA is eluted in a high-salt buffer, concentrated by isopropanol precipitation, before desalted with ethanol, dried and dissolved in TE buffer (Appendix B).

2.4.2.1 Transformation reaction

The transformation reactions were performed using One Shot Chemically Competent *E. coli* (Invitrogen). Either 2 μg of plasmid or 1-3 μl of ligation reactions were used directly in the transformation reaction. To prove absence of antibiotic resistance in the competent cells, a cells only control reaction was always included.

One vial of competent cells per sample was slowly defrosted on ice. The plasmid or the ligation mixtures were added directly to the cells, incubated on ice for 30 minutes before being heat shocked at 42°C in water bath for 30 seconds. Cells were immediately transferred to ice, 250 µl of S.O.C. media was added, and the vials were shaken horizontally at 225 rpm at 37°C for 1 hour. Ten µl from each transformation reaction in 20 µl of S.O.C. media (growth media provided with the competent cells) were plated out on separate LB agar plates containing Ampicillin (imMedia™ Amp Blue sachets, Invitrogen, Appendix B) and incubated overnight at 37°C. Following incubation, plates were checked for growth and colonies were counted.

2.4.2.2 Bacterial culture

Single colonies were picked and used to inoculate 250 ml of sterile LB broth containing 100 mg/ml Ampicillin (Appendix B). The cultures were grown overnight at 37°C at 220 rpm in a shaking incubator.

2.4.2.3 Bacterial lysis and DNA extraction

Bacterial cell cultures were harvested by centrifugation at 3000 x *g* for 30 minutes at 4°C. The bacterial pellet was then resuspended in 10 ml lysis buffer P1 containing RNase A until completely dissolved. An equal volume of buffer P2 containing sodium hydroxide was then added, thoroughly mixed, and incubated at RT for 5 minutes. The alkaline lysate was then neutralised by adding 10 ml of acetic acid containing chilled buffer P3. The cell lysate was then incubated at RT for 10 minutes in the QIAfilter cartridge before gently inserting the plunger and filtering the lysate directly into a QIAGEN-tip previously equilibrated with QBT buffer containing isopropanol. The cleared lysate was allowed to enter the anion exchange

resin by gravity flow before being washed twice in 30 ml of medium-salt QBC buffer. Finally, the DNA was eluted in 15 ml of high-salt QF buffer.

2.4.2.4 Alcohol precipitation of DNA

Alcohol precipitation (ethanol, isopropanol) is a commonly used technique for concentrating and de-salting nucleic acid preparations in aqueous solutions. The basic principle involves adding salt and alcohol to an aqueous solution causing the nucleic acids to precipitate. The nucleic acids can then be separated out by centrifugation and de-salted by ethanol washes.

Isopropanol was added to the DNA high-salt eluate at RT and centrifuged at 15,000 x *g* for 30 minutes at 4°C. The supernatant was decanted, and 5 ml of 70% ethanol was added followed by a centrifugation step at 15,000 x g for 10 minutes. The supernatant was removed, and the DNA pellet was air dried for 10 minutes before redissolved in 400 µl of TE buffer.

2.4.3 Quantification and quality assessment of nucleic acids

RNA and DNA samples were quantified using the NanoDrop™ ND1000 (Thermo Fischer Scientific) by measuring absorbance at 230, 260 and 280 nm (A_{230}, A_{260}, and A_{280} respectively). Purity of RNA was determined using the A_{260}/A_{280} ratio. Only good quality RNA with a ratio of 1.9-2.1 was used in further applications.

2.4.4 DNA electrophoresis

Routine analysis of DNA was performed on 1-2% agarose gels in TAE buffer (Appendix B). Gels were made from electrophoresis grade agarose (Appendix B, Sigma-Aldrich®) melted in TAE buffer. The solution was allowed to cool down, and ethidium bromide (Sigma-Aldrich®, from stock solution of 0.5 mg per ml) was added to give a final concentration of 0.5 µg

per ml. After January 2009 ethidium bromide was replaced with GelRed™ Nucleic Acid Gel Stain (10,000 x in water, Biotium, UK). GelRed™ was diluted to 1x concentration in the gels. Samples were loaded with Blue/Orange 6x loading dye (Promega, UK) and sizes were compared to 1kb or 100 bp DNA ladders (Promega). TAE buffer was used as the electrophoresis buffer.

2.4.5 Gel imaging and image capture

Gels were visualised using the Dual Intensity Transilluminator (UVP Ltd., UK prior to January 2009) and the Molecular Imager® Gel Doc™ XR Imaging System (Bio-Rad, UK since January 2009) and recorded using the CCD digital camera with an Amber emission filter (Bio-Rad). Files were analysed using the Quantity One® 1-D Analysis Software (Bio-Rad) and stored in a jpeg or tiff format and printed using the Mitsubishi P93D thermal printer.

2.5 DNA sequencing

All sequencing was performed by The University of Edinburgh sequencing service (The Gene Pool, Ashworth Laboratories, King's Buildings, Edinburgh). Samples were prepared in clearly labelled thin walled PCR strip tubes. Five μl of nuclease free water containing approximately 5-20 ng (PCR products) or 200-500 ng (plasmid vectors) of DNA together with 1 μl of primer at 3.2 pmol per μl were prepared. All samples were sequenced in both directions using the BigDye® Terminator v3.1 (Applied Biosystems, UK) sequencing reaction followed by capillary analysis using the ABI3730 DNA analyzer (Applied Biosystems).

2.6 Reverse Transcriptase Polymerase Chain Reaction (RT-PCR)

The RT-PCR reactions were performed using commercially available kits and the optimum conditions had to be established in optimisation reactions.

2.6.1 First strand cDNA synthesis

Three commercially available first strand cDNA synthesis kits were used during the study according to the manufacturers' protocols. Details of the different kits and the protocol used for first strand cDNA synthesis are given below. The cDNA synthesis reactions were used immediately for PCR or stored at -20°C.

2.6.1.1 Invitrogen Cloned AMV First-Strand cDNA Synthesis Kit

The kit contains purified cloned Avian Myeloblastosis Virus (AMV) Reverse Transcriptase (AMV-RT). One and a half μg of total cellular RNA, 0.5 mM dNTP mix and 2.5 μM of oligoT in diethyl pyrocarbonate (DEPC) water was denatured at 65°C for 5 minutes and then placed on ice. The first strand synthesis reaction was performed in a reaction mix containing the denatured nucleotides and RNA, 15 U of AMV-RT, 50 mM dithiothreitol (DTT), 40 U RNase OUT™, and DEPC water to a total volume of 20 μl in the manufacturer's buffer. The reaction mixture was incubated at 50°C for 50 minutes and terminated by a 5 minute incubation step at 85°C in the Bio-Rad iCycler thermal cycler.

2.6.1.2 Qiagen Omniscript® Reverse Transcriptase Kit

The Omniscript Reverse Transcriptase (O-RT) enzyme, unlike the AMV-RT, is not derived from a RNA-containing retrovirus but is derived from a different, unnamed source (Qiagen Omniscript® Reverse

Transcription Handbook). An aliquot of 2 μg of total cellular RNA in RNase free water was heat denatured at 65°C for 5 minutes and quenched on ice. A master mix was prepared on ice consisting of 0.5 μM of each dNTP, 1 μM oligoT primers (Invitrogen), 10 U of rRNasin® RNase inhibitor (Promega), RNase free water, and 4 U of O-RT in the manufacturer's buffer and then aliquoted into PCR tubes (Bio-Rad) containing the denatured RNA. The solution was then incubated at 37°C for 1 hour using the Bio-Rad iCycler thermal cycler.

2.6.1.3 Roche Transcriptor High Fidelity cDNA Synthesis Kit

The Roche Transcriptor High Fidelity cDNA Synthesis Kit was used to produce cDNA for downstream Real-Time PCR applications. It contains a blend of a recombinant reverse transcriptase (rRT) and an enzyme conferring proofreading activity for high accuracy RNA transcription (Roche handbook).

Template-primer mixes were prepared on ice by adding 1 μg total cellular RNA and random hexamers to a final concentration of 60 μM into PCR-grade water and denaturing at 65°C for 10 minutes in the iCycler thermal cycler (Bio-Rad) before being quenched on ice. A master mix containing 20 U of Protector RNase Inhibitor, 1 mM of each dNTP, 5 mM of DTT and 10 U of rRT in manufacturer's buffer was aliquoted into the template-primer mixes and incubated at 50°C for 30 minutes. The enzyme was inactivated by an incubation step at 85°C for 5 minutes. The cDNA synthesis reactions were diluted 1:10 for use in subsequent Real-Time PCR reactions or stored at minus 20°C.

2.6.2 Polymerase Chain Reactions (PCR)

PCR reactions were set up using two commercially available PCR kits. To ensure consistency all experiments were performed on the same thermal cycler (iCycler, Bio-Rad) using the optimised conditions for the respective primers. To assess consistency of sample loading and PCR conditions between separate experiments, primers that amplified cDNA of transcripts from the ubiquitously expressed housekeeping gene feline β-actin or feline glyceraldehyde 3-phosphate dehydrogenase (GAPDH) were included in separate reactions. The thermal conditions used with both kits are summarised in Table 2.4.

PCR Kits	**GoTaq® PCR Core Systems (Promega)**			**HotStarTaq® DNA polymerase kit (Qiagen)**		
Cycle stage	# of cycles	Temp °C	Time (minutes)	# of cycles	Temp °C	Time (minutes)
Initial denaturation	1	95	2	1	95	15
Denaturation		95	1		94	1
Annealing	35	59	1	25	52-62	1
Extension		72	1		72	1
Final extension	1	72	5	1	72	10
Holding step	1	4	∞	1	4	∞

Table 2.4: Summary of PCR reaction cycling conditions used with the two commercial kits.

2.6.2.1 Primer design

All DNA oligonucleotides were purchased from Eurofins MWG Operon (eurofinsdna.com). As the feline *Egfr* sequence has not been published, three intron spanning primer sets were designed to span the putative tyrosine kinase region of the feline *Egfr* gene using areas with a high degree of homology between the human, murine and canine published

sequences (NCBI, 2010c) and predicted feline sequences (EMBL-EBI, 2010b) (Table 2.5).

The feline housekeeping genes GAPDH and β-actin were designed from published sequences (accession numbers AB038241 and AB051104 respectively (NCBI, 2010c)). To produce intron spanning primers (GAPDH only) the published sequence was aligned with the predicted sequence (EMBL-EBI, 2010b) using needle alignment tool (EMBL-EBI, 2010a) (Table 2.5). Primers were designed using the online PCR primer design tool on eurofinsdna.com.

2.6.2.2 GoTaq® PCR Core Systems (Promega)

Each reaction contained primers at a final concentration of 0.5 μM each, dNTP at 0.2 mM each, MgCl at 1.5 mM, 1.25 U of a proprietary formulation of *Taq* DNA polymerase (GoTaq® DNA Polymerase) and nuclease free water (Qiagen) in manufacturer's buffer. Master mixes were prepared on ice and aliquoted into thin walled PCR tubes (Bio-Rad) with 2 μl of cDNA synthesis reaction described in Chapter 2.6.1.1 as template in 50 μl reaction volumes.

2.6.2.3 HotStarTaq® DNA polymerase kit (Qiagen)

Each reaction contained primers at a final concentration of 0.25 μM each, dNTP at 0.2 mM each, $MgCl_2$ at 1.5 mM, 1.25 U of modified recombinant DNA polymerase originated from *Thermus aquaticus* (HotStarTaq® DNA polymerase) and nuclease free water in manufacturer's buffer. Master mixes were prepared on ice and aliquoted into PCR tubes with 3 μl cDNA synthesis reaction described in Chapter 2.6.1.2 as template in 50 μl reaction volumes.

Primer Set			Restriction enzyme	Sequence 5'-3'
A	Feline EGFR TK1	Forward	-	GAATATCACCTGCACAGGAC
		Reverse	-	GCCATCACGTAAGCTTCATC
B	Feline EGFR TK2	Forward	-	GGAGAAGCTCCCAACCAGGCT
		Reverse	-	GATAGGCACTTTGCCTCCTTC
C	Feline EGFR TK2	Forward	Xho1	TTACTCGAGGGAGAAGCTCCCAACCAGGCT
		Reverse	Not1	AAGCGGCCGCGATAGGCACTTTGCCTCCTTC
D	Feline EGFR TK3	Forward	-	TGCGAAGGGCATGAACTAC
		Reverse	-	ACTCATCGGCATCTACGAC
E	Feline GAPDH 1	Forward		AGCTGCCAAATACGATGAC
		Reverse		CATACCAGGAAATGAGCTTGAC
F	Feline GAPDH 2	Forward		GATTGTCAGCAATGCCTCC
		Reverse		CCAGTGAGCTTCCCATTCAG
G	Feline GAPDH 3	Forward		GATTGTCAGCAATGCCTCC
		Reverse		CATACCAGGAAATGAGCTTGAC
H	Feline β-actin 1	Forward		GCACCACACCTTCTACAAC
		Reverse		ATGCCACAGGACTCCATAC
I	Feline β-actin 2	Forward		TTCGAGACCTTCAACACCCC
		Reverse		GCCATCTCCTGCTCAAAATCC
J	Feline β-actin 3	Forward		GCACCACACCTTCTACAAC
		Reverse		GCCATCTCCTGCTCAAAATCC
K	Feline β-actin 4	Forward		TTCGAGACCTTCAACACCCC
		Reverse		ATGCCACAGGACTCCATAC

Table 2.5: Primer sequences for feline cells. EGFR primers were constructed using the tyrosine kinase region of human, murine, and canine EGFR sequences. The tyrosine kinase region has the greatest sequence homology between species. The control primers were produced from published and predicted feline sequences.

2.7 Vector Cloning Experiments

Vectors psiCHECK™-2 (Promega) and p*Silencer*™ neo Kit (Ambion, UK) were used in the experiments (Figure 2.3). The psiCHECK-2 vector system is designed to optimise RNA interference experiments by the rapid

and quantitative screening of small interfering RNAs (siRNAs). The p*Silencer*™ neo Kit is a hairpin expression vector system capable of generating short hairpin RNA (shRNA) transcripts that can induce long term gene silencing in cells.

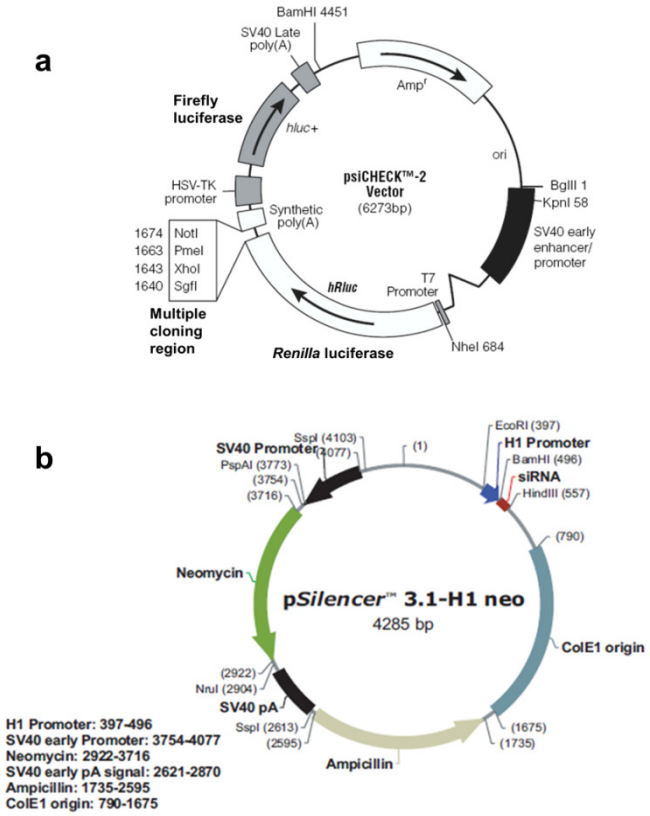

Figure 2.3 a) Vector map of psiCHECK™-2 vector (from Promega TB 329) and b) pSilencer™ 3.1-H1 neo (from p*Silencer™* handbook, Ambion) showing antibiotic resistance genes, promoters and multiple cloning regions present.

2.7.1 Gel and PCR product clean up

Prior to cloning, DNA from PCR reactions and DNA plasmids were purified using Wizard® SV Gel and PCR Clean-Up System (Promega) according to manufacturer's protocol. The kit is based on the principle of selective DNA binding to a silica membrane in the presence of chaotropic salts. During subsequent wash steps the salt is removed with ethanol and the DNA is eluted under low salt conditions in nuclease free water.

An aliquot of the PCR product was assessed by gel electrophoresis as described in Chapter 2.4.4 to verify minimal primer-dimer formation and that only a single product of expected size was present. The remaining PCR products were then purified directly. Alternatively, following restriction enzyme digestion, the PCR products and plasmid DNA were separated by gel electrophoresis and visualised as previously described in Chapters 2.4.4 and 2.4.5, and the band excised using a scalpel blade. The gel slices were then weighed and Membrane Binding Solution (MBS) was added at a ratio of 10 µl of solution per 10 mg of gel slice. The gel slices were dissolved by incubating them in a heat block at 65°C. For direct purification of PCR products, an equal volume of MBS was added to the PCR reaction.

The volumes were transferred to SV Minicolumns and incubated for 1 minute at RT before centrifugation at 10,000 x *g* for 1 minute. The column was washed with Membrane Wash Solution in two subsequent wash steps and spun at 10,000 x *g* for 1 minute and 5 minutes respectively. The column was centrifuged again for 1 minute with the lid off to allow evaporation of ethanol. DNA was eluted by incubation of 50 µl of nuclease free water on the column membrane for 1 minute before centrifugation at 10,000 x *g* for 1 minute to draw down the DNA. DNA quantity and quality were assessed as described in Chapter 2.4.3.

2.7.2 Restriction enzyme digestion

The psiCHECK™-2 vector and the PCR product were digested using *Xho*I and *Not*I restriction enzymes (Promega) in separate reactions. One µg aliquots of vector or PCR product were digested by 5 U of each restriction enzyme in manufacturer's buffer D containing 0.1 µg per µl acetylated bovine serum albumin (BSA) for 2 hours in a 37°C water bath. Acetylated BSA provides additional protein to the reaction which stabilises the enzymes

and counteracts any negative effects arising as a result of enzyme interaction with solid surfaces and/or the air-liquid interface (Williams et al., 1996). The entire reaction volumes were run on a 1.2 % agarose gel for gel purification as described in Chapter 2.7.1.

2.7.3 Ligation

Gel purified PCR reactions (psi-CHECK™-2 vector) or annealed DNA oligonucleotides (p*Silencer*™ neo Kit, Chapter 5) were ligated into their respective vectors using T4 DNA ligase (Bioline, UK) following the manufacturer's protocol. Inserts and vectors were quantified as described in Chapter 2.4.3 and used in the ligation reaction at a ratio of 3:1 (psi-CHECK™-2 vector) or 5:1 (p*Silencer*™ neo Kit). The ratios were calculated using the formula in Table 2.6. Control reactions included no insert and no enzyme controls. Vectors and inserts were incubated at 4°C overnight in manufacturer's buffer solution containing 1 mM ATP, 66 mM Tris-HCl (pH 7.6), 5 mM $MgCl_2$, 10 mM DTT, and 10 U of T4 DNA ligase. The ligation reactions were then used directly in One Shot Chemically Competent *E.coli* (Invitrogen) transformation reactions and plated out overnight. Colonies were selected the next day and expanded overnight before performing plasmid purification as previously described in Chapter 2.4.2. A restriction enzyme digest of the purified plasmids was then performed as described in Chapter 2.7.2 and the presence of inserts was then confirmed by gel electrophoresis as described in Chapter 2.4.4. In addition, each clone was then sequenced as described in Chapter 2.5 to ensure only plasmids containing the correct sequences were used in subsequent experiments.

Amount of vector (ng) / length of vector (bp)	=	Amount of insert (ng) / length of insert (bp)

Table 2.6: Formula used to determine the insert to vector ratio for ligation reactions.

2.8 RNA interference

2.8.1 Small interfering RNA (siRNA) design

Potential siRNA sequences against the feline *Egfr* were designed using a combination of online design tools including the siRNA finder (Ambion, 2008b), the siRNA design tool (MWG, 2008) and the siRNA selection server at (Yuan et al., 2004). Potential 21 nucleotide sequences that began with an adenine dinucleotide (AA) were recorded (Elbashir et al., 2001a). Any sequences with four or more guanine or cytosine nucleotides in a row or with more than 60% or less than 30% GC content were removed (Reynolds et al., 2004). Lastly, BLAST searches against the feline whole genome shotgun sequence and nucleotide collection were performed (NCBI, 2010a). Any sequences with more than 17 contiguous base pairs of homology to other coding sequences were eliminated. Control siRNAs were also designed. A negative control was produced by scrambling target sequences siRNA3. The sequence was then checked against the feline genome shotgun sequence (NCBI, 2010a) for lack of homology. Positive control sequences against *Renilla Luciferase* included a published sequence (Betz, 2005) as well as a newly designed sequence. The chosen sequences were the constructed and screened for efficiency (Table 2.7).

siRNA	siRNA sequence antisense strand 5'-3'	Target	GC content	BLAST homology
1	UUGUGGGAUCCAGAGUCCCUU	feline *Egfr*	52.4%	17/21
2	UGUGGCUUCUCGAUACUCCUU	feline *Egfr*	47.6%	15/21
3	CGUAAGCUUCAUCAAGGAUUU	feline *Egfr*	38.1%	16/21
4	CUGGGAGCCAAUGUUGUCCUU	feline *Egfr*	52.4%	16/21
5	CUUGACAUGCUGUGGCGUCUU	feline *Egfr*	52.4%	16/21
6	AAGCUAGAAUUAUCGGCUCUU	scrambled	38.1%	15/21
7	GUUGAUGAAGGAGUCCAGCAC	Renilla 1	52.4%	15/21
8	AGUUCAUCAAGGAUUUCCUU	feline *Egfr*	38.1%	17/21
9	GUUGAUGAAGGAGUCCAGCCC	Renilla 2	57.1%	15/21
10	CUUCUCGGAAUCAUAGUAGCC	Renilla 3	47.6%	15/21

Table 2.7: Overview of the siRNA sequences designed against the feline *Egfr, Renilla* and the scrambled control sequence used in the screening process.

2.8.2 Construction of siRNA sequences

All siRNAs were constructed using *Silencer*® siRNA Construction Kit (Ambion) using DNA oligonucleotide templates purchased from Eurofins MWG Operon (eurofinsdna.com). DNA oligonucleotide templates were designed by adding the T7 Promoter primer sequence 5′ CCTGTCTC 3′ to the 3′ end of both the sense and the antisense templates producing 29-mer oligonucleotides. This was done manually or by using the online siRNA Template Design Tool for *Silencer*® siRNA Construction Kit (Ambion, 2008a). The control DNA oligonucleotide templates supplied with the kit was used in parallel when constructing the siRNAs as an internal control of the efficiency of the kit.

2.8.2.1 Transcription template preparation

The DNA oligonucleotide templates were resuspended to a concentration of approximately 200 μM in nuclease free water and then

quantified as described in Chapter 2.4.3. Each DNA oligonucleotide template was then diluted to 100 μM and 2 μl aliquots were hybridised in separate reactions with 2 μl T7 Promoter primer supplied with the kit in manufacturer's DNA hybridisation buffer at 70°C for 5 minutes. This step anneals the eight nucleotide leader sequence added to the DNA oligonucleotide template with the T7 Promoter primer which contains a promoter sequence for the T7 RNA polymerase used subsequently to produce the RNA (Figure 2.4). In the next step dNTP, manufacturer's reaction buffer and nuclease free water were added to each hybridisation reaction and incubated at 37°C for 30 minutes. This step allows the Exo-Klenow DNA polymerase enzyme to fill in the gaps and produce double stranded DNA transcription template containing 21 nucleotides encoding the siRNA sequence and the full length T7 promoter site separated by an eight nucleotide leader sequence.

2.8.2.2 Double stranded RNA synthesis

To synthesise double stranded RNA, the DNA templates were first transcribed in separate reactions to eliminate any potential competition between templates for transcription reagents that might limit the synthesis of one of the two strands (Figure 2.4). Two μl of sense or antisense template was mixed with NTPs, T7 RNA Polymerase enzyme and nuclease free water in manufacturer's reaction buffer and incubated at 37°C for 2 hours. The antisense and sense siRNA template reactions were then mixed and incubated overnight.

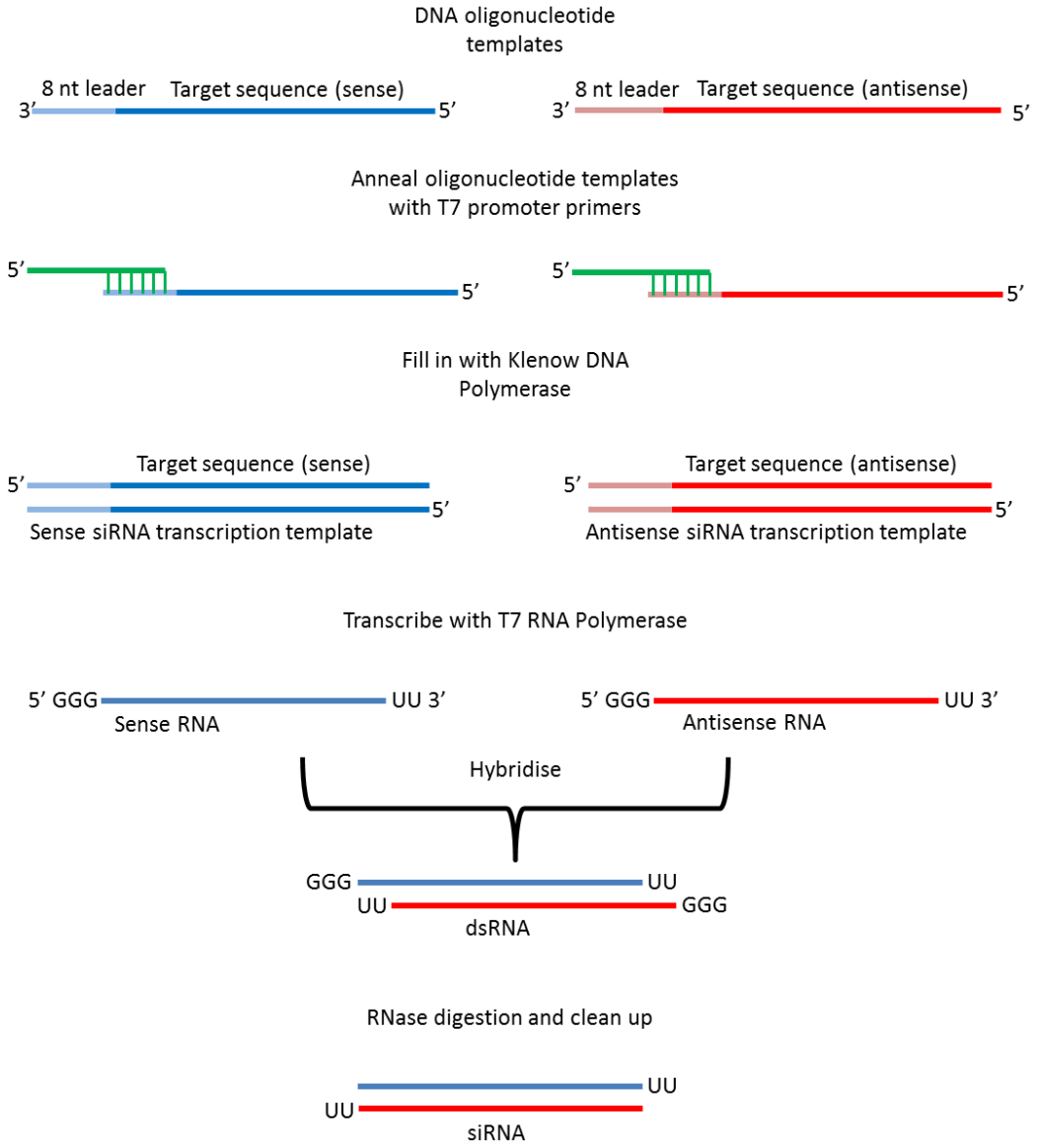

Figure 2.4: Schematic diagram showing the siRNA construction steps using the *Silencer*® siRNA Construction Kit (Ambion).

2.8.2.3 Purification of siRNA

Double stranded RNA (dsRNA) 5′ overhanging leader sequences produced by the *in vitro* transcription were removed in a digestion step using RNase which cleaves single stranded guanine residues (Figure 2.4). In the same step, DNase digestion eliminates remaining DNA templates. Three

µl of RNase and 2.5 µl of DNase were diluted in 48.5 µl of nuclease free water and added to the dsRNA together with manufacturer's digestion buffer and incubated for 2 hours at 37°C.

The dsRNA was then column purified by adding 400 µl of siRNA binding buffer containing ethanol and incubated for 5 minutes at RT. Filter cartridges were pre-wet with 100 µl of Binding buffer, the dsRNA solutions were transferred to the cartridge, and centrifuged at 4,500 x *g* for 1 minute. The column was washed twice in 500 µl siRNA Wash Buffer by centrifugation at 4,500 x *g* for 1 minute. The RNA was then eluted by adding 100 µl of nuclease free water pre-heated to 75°C to the cartridge filter and incubated at RT for 2 minutes before being centrifuged at 6,500 x *g* for 2 minutes. The purified siRNA was quantified as described in Chapter 2.4.3 and stored in aliquots at minus 20°C.

2.9 Transfections

The 293FT and SCCF1 cell lines were transfected using electroporation and liposome-mediated transfections respectively. All transfection reactions were optimised for the cell lines to achieve maximum knockdown while maintaining high cell viability and transfection efficiencies.

2.9.1 Electroporation optimisation

Transfections by electroporation were performed using the Nucleofector® 96-well shuttle (Amaxa, Lonza, Switzerland) and Cell Line 96-well Nucleofector® Solution SF Kit (Amaxa). The protocol was optimised for cell numbers, DNA plasmid and siRNA concentrations as well as for different programs on the Nucleofector® 96-well shuttle using negative scrambled and positive *Renilla* control siRNAs. Transfection efficiency and cell viability were determined by flow cytometry (Chapter 2.10) using green

fluorescent protein (GFP) expressing vector pmaxGFP™ (Amaxa) and propidium iodide (PI, Sigma-Aldrich®).

2.9.2 Electroporation protocol

Recently passaged 293FT cells were trypsinized and counted as previously described (2.3.4 and 2.3.5) and a total of $7.6x10^6$ cells were spun down at 90 x *g* for 10 minutes. The supernatant was discarded and the cell pellet was resuspended in 760 µl of Nucleofector™ Solution SF. Five hundred µl of the SF solution were added to 25 µl of psiCHECK™-2.EGFR at a concentration of 1 µg/µl to produce master mix A (Table 2.8). The remaining cell suspension was used as master mix B. The Nucleocuvette™ 96 well plate was prepared by adding the required amount of each substrate to the corresponding wells according to Figure 2.5. Twenty µl of master mix A or B was then added to the wells according to Table 2.8. The Nucleocuvette™ 96 well plate was electroporated in the Nucleofector® 96 well shuttle using program DS-150. Immediately after electroporation the cells were resuspended in 80 µl of RPMI media pre-warmed to 37°C. Twenty-five µl of each samples were seeded in triplicate into an opaque 96 well plate containing 175 µl of DMEM growth 2 media per well. The entire volume of the pmaxGFP™ transfected samples were used to seed wells of a 24 well plate and grown for 24 hours before being analysed by flow cytometry as described in Chapter 2.10 to determine cell viability and transfection efficiency.

The pGL3 basic vector (Promega, UK) contains a Firefly luciferase gene, and it was used to monitor the performance of the Dual-Glo™ Stop & Glo® reagent in quenching the Firefly reaction. The 'no program' control was used as a cells only control to allow for background subtraction from all luminescence readings. Two siRNA controls were used, one targeting the

Renilla part of the mRNA constructs (positive control siRNA10), and one scrambled control sequence (negative control siRNA6) made up by scrambling sequence siRNA3. To determine the effect of the scrambled control siRNA, a vector only transfection was performed. The effect on the scrambled control on the luciferase readings could then be compared to the vector only control to investigate if the scrambled control caused any reduction in luciferase readings.

Column	DNA	siRNA	Cell #	Program	siRNA target
1	psiCHECK™-2.EGFR	siRNA1	$2x10^5$	DS-150	feline *Egfr*
2	psiCHECK™-2.EGFR	siRNA2	$2x10^5$	DS-150	feline *Egfr*
3	psiCHECK™-2.EGFR	siRNA3	$2x10^5$	DS-150	feline *Egfr*
4	psiCHECK™-2.EGFR	siRNA4	$2x10^5$	DS-150	feline *Egfr*
5	psiCHECK™-2.EGFR	siRNA5	$2x10^5$	DS-150	feline *Egfr*
6	psiCHECK™-2.EGFR	siRNA6	$2x10^5$	DS-150	scrambled
7	psiCHECK™-2.EGFR	siRNA8	$2x10^5$	DS-150	feline *Egfr*
8	psiCHECK™-2.EGFR	siRNA10	$2x10^5$	DS-150	Renilla
9	pmaxGFP™	-	$2x10^5$	DS-150	n/a
10	pGL3 plasmid	-	$2x10^5$	DS-150	n/a
11	psiCHECK™-2.EGFR	-	$2x10^5$	DS-150	No siRNA control
12	psiCHECK™-2.EGFR	-	$2x10^5$		No program control
Master mix A				**Master mix B**	
Cell suspension 500 µl (i.e. 25 wells @ 20 µl containing $2x10^5$ cells).				Cell suspension 260 µl (i.e. 13 wells @ 20 µl containing $2x10^5$ cells).	
Add 25 µl of psiCHECK™-2.EGFR vector @ 1µg/µl to produce 1 µg DNA plasmid per well.				Add 20 µl to wells A,B&C 9-12 containing the respective controls according to diagram	
Add 20 µl to wells A,B&C 1-8 containing the respective siRNA according to diagram					

Table 2.8: Overview of the setup of the siRNA screening process using the psiCHECK-2 vector system (Promega) and the Nucleofector® 96 well shuttle (Amaxa).

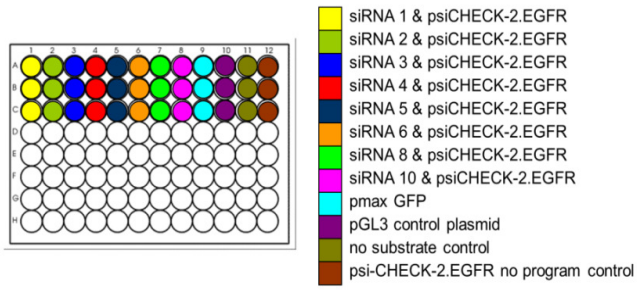

Figure 2.5: Schematic diagram to show setup of the siRNA screening process.

2.9.3 Liposome-mediated transient transfections

2.9.3.1 Naked siRNA transient transfection optimisation

The SCCF1 cell line was optimised for naked siRNA transfections using *Silencer*® FAM™-Labeled Negative Control #1 siRNA (Ambion), and transfection efficiency was determined by fluorescence microscopy and flow cytometry as described in Chapter 2.10. Transfections were performed in triplicate in a 24 well format at three different confluences (30, 50 and 80%), three different siRNA concentrations (20, 50 and 100 nM), and with two different amounts of Lipofectamine 2000™ reagent (Invitrogen) (1.0 and 1.5 µl per well in 24 well plate) and assessed by fluorescence microscopy using the FAM/FITC filters on a Zeiss Axiovert40 CFL microscope.

To further assess transfection efficiency and cell viability by flow cytometry the transfections were repeated in a six well format with 50nM and 100nM of siRNA and 7.5 µl of Lipofectamine 2000™ reagent on cells grown to 30% confluence.

2.9.3.2 Naked siRNA transient transfection protocol

The SCCF1 cell line was cultivated, trypsinized, and counted as previously described (2.3.4, 2.3.5) and seeded into culture vessels in William's E medium without antibiotics to achieve 30% confluence the following day.

Lipofectamine 2000™ was diluted in OptiMEM® I Reduced-Serum medium and incubated at RT for 5 to 25 minutes and the required amounts of RNA were similarly diluted in OptiMEM® I Reduced-Serum medium to achieve an end concentration of 50 nM RNA in the wells (Table 2.9). The solutions were mixed and incubated for 20 minutes at RT to allow RNA-Lipofectamine 2000™ complexes to form. The complexes were then added

dropwise to the wells and the plates were incubated at 37°C/5%CO_2 for 72 hours. The medium was changed to William's E medium with antibiotics 6 hours following transfection, and the cells were analysed at 24, 48, and 72 hours following transfection.

Constituent	96 well plates	6 well plates	10 cm plates
siRNA	50 nM	50 nM	50 nM
Lipofectamine 2000™	0.4 µl	7.5 µl	45 µl
Opti MEM® I Reduced serum media			
Dilution of RNA	25 µl	250 µl	1.5 ml
Dilution of Lipofectamine 2000™	25 µl	250 µl	1.5 ml
End volume of media per well	100 µl	2.5 ml	13 ml

Table 2.9: Naked siRNA transfections using Lipofectamine 2000™ setup.

2.9.3.3 DNA plasmid transfections optimisation

The SCCF1 cell line was optimised for two transfection agents following the manufacturer's protocol for Lipofectamine 2000™ and siPORT™ *XP-1* (Ambion) and their transfection efficiencies were compared. The GFP expressing plasmid pmaxGFP™ (Amaxa) was used for the optimisations, and assessed by fluorescence microscopy and flow cytometry as described in Chapter 2.10.

To compare transfection reagents, SCCF1 cells were seeded to achieve between 30 to 60% and >90% confluency the next day for siPORT™ *XP-1* and Lipofectamine 2000™ transfections respectively. The transfections were performed at four different ratios for both reagents (Table 2.10) following the manufacturers' protocols. In brief, DNA and transfection agents were diluted in OptiMEM® I Reduced-Serum media before mixed and incubated for 20 minutes at RT to form complexes. The complexes were then added to the culture wells dropwise, and the plates were incubated at 37°C/5%CO_2 for 72

hours. Transfection efficiencies were compared by fluorescent microscopy using a FAM/FITC filter at 24, 48, and 72 hours following transfections.

Transfection agent					
siPORT™ *XP-1*			**Lipofectamine 2000™**		
Ideal confluence to reach for cells at transfection: 30-60 %			Ideal confluence to reach for cells at transfection: >90 %		
Ratio	Reagent (µl)	DNA (µg)	Ratio	Reagent (µl)	DNA (µg)
2:1	0.4	0.2	1:2	0.4	0.8
3:1	0.6	0.2	5:2	2.0	0.8
4:1	0.8	0.2	4:1	3.2	0.8
3:2	0.6	0.2	5:1	4.0	0.8

Table 2.10: Comparison of the two transfection reagents used for naked siRNA transfections of the SCCF1 cell line.

The Lipofectamine 2000™ transfections were then further optimised by repeating the transfections with pmaxGFP™ plasmid DNA: Lipofectamine 2000™ ratios of 1:4 and 1:5 in 96 and 6 well plates. The cells were assessed after 48 hours by flow cytometry for transfection efficiency as described in Chapter 2.10 and for cell viability using CellTiter-Glo® Luminescent Cell Viability Assay as described in Chapter 2.11.2.

2.9.3.4 Plasmid DNA stable transfection protocol

The SCCF1 cell line was cultivated, trypsinized and counted as described in Chapter 2.3 and seeded into 6 well plates in William's E medium without antibiotics to achieve >90% confluence the following day. Each transfection was performed in triplicate and the transfections were performed at a ratio of 1:5 DNA: Lipofectamine 2000™. In brief, 20 µl of Lipofectamine 2000™ was diluted in 250 µl OptiMEM® I Reduced-Serum medium per sample and incubated at RT for 5 to 25 minutes. Similarly, 4 µg of DNA was diluted in 250 µl of OptiMEM® I Reduced-Serum medium for

each sample. The dilution mixes were combined and incubated for 20 minutes at RT. Five hundred µl of DNA-reagent complexes were then added dropwise to each well, and the plates were incubated at 37°C/5%CO_2 for 24 hours.

The cells were then trypsinated and counted as described in Chapter 2.3 and seeded into 6 well plates at their optimal plating density as determined in Chapter 2.3.13. After 24 hours of incubation at 37°C/5%CO_2 cells containing the plasmid was selected for using G418 containing William's E medium as described in 2.3.12. Cells were grown for approximately 20 days until confluent, when they were passaged as previously described in Chapter 2.3.4.

2.10 Flow Cytometry

Flow cytometry was performed following transfections with *Silencer*® FAM™-Labeled Negative Control #1 siRNA (2.9.3.1) or with pmaxGFP™ plasmid (2.9.1 and 2.9.3.3) to determine transfection efficiency and cell viability.

In brief, cells were washed and detached by adding 1 ml of 0.25% trypsin-EDTA to each well. The trypsinization was terminated by addition of 2 ml of PBS/0.5% BSA (Appendix B) and cell suspensions were transferred to Falcon tubes. The cells were centrifuged at 90 x *g*, 4°C for 10 minutes and the cell pellets were resuspended in 1-5 ml of PBS/0.5% BSA. The cell suspensions were then put through a BD Falcon cell strainer with 40 µm pore size to stop cells from clumping before transferring to flow cytometer tubes and stored on ice until analysed. Flow cytometer analysis was performed using a BD FACSCalibur (Becton Dickinson-Biosciences, USA) instrument using the FITC and PI channels. For each sample 10,000 events

were counted, then 0.2 mg/ml PI (Appendix B) to a final concentration of 0.5 μg/ml was added to the cell suspensions to stain dead cells before a further 10,000 events were counted. The data were analysed using Cell Quest Pro software (Becton Dickinson-Biosciences, USA) and transfection efficiency and cell viability were determined for each sample.

2.11 Luminescence assay systems

Two luciferase based assay systems were used following transfection experiments; both purchased from Promega, UK. The Dual-Glo™ Luciferase System was used with the psiCHECK™-2 vector system and the CellTiter-Glo® Luminescent Cell Viability Assay was used to assess cell viability following transfection experiments.

2.11.1 Dual-Glo™ Luciferase System

The Dual-Glo™ Luciferase System (Promega) allows for sequential measurements from a single sample of luminescence signals from the two reporter genes present in the psiCHECK™-2 vector. The control reporter Firefly (*Photinus pyralis)* luciferase is a 61 kDa protein that does not require post translational processing for enzymatic activity. Similarly, *Renilla* luciferase purified from *Renilla reniformis*, a 36 kDa protein functions as an enzyme immediately after translation. The Firefly luciferase substrates are beetle luciferin, ATP, magnesium, and oxygen while *Renilla* luciferase requires only coelenterazine and oxygen. Both Firefly and *Renilla* undergo spontaneous inactivation after generating luminescence. The Dual-Glo™ Luciferase System allows for effective cell lysis and activation of Firefly luciferase directly in the sample well. Following Firefly luminescence measurements the signal is then quenched and *Renilla* luciferase is activated and measured in the same sample well.

To perform the assay the 96 well plates and all the reagents were equilibrated to RT and 125 µl of media was removed from each sample well. An equal volume of Dual-Glo™ Luciferase Reagent (75µl) was added to each sample well and mixed well. After 10 minutes incubation at RT the plate was inserted into the 1420 Multilabel Counter Victor^{3TM} (Perkin Elmer, Germany) using the Wallac 1420 Manager program (Perkin Elmer) and luminescence was measured for 30 seconds per well. Seventy-five µl of Dual-Glo™ Stop & Glo® Reagent was then added to each well and incubated for a further 10 minutes before luminescence was measured for 30 seconds per well. Background readings were subtracted and *Renilla* readings were normalised to Firefly readings by dividing the *Renilla* readings by the Firefly readings for each well.

2.11.2 CellTiter-Glo® Luminescent Cell Viability Assay

The CellTiter-Glo® Luminescent Cell Viability assay determines the relative number of metabolically active cells present in culture based on quantification of the ATP present. The assay utilises a thermostable recombinant luciferase which catalyses the same reaction with the same substrates as described in 2.11.1. The luminescence signal is proportional to the amount ATP present which again is directly proportional to the number of metabolically active cells present in culture.

Reagents and culture plates were equilibrated to RT before assaying. The cell culture medium in the 96 well plate was adjusted to 100 µl per well before 100 µl of CellTiter-Glo® reagent was added to each well. The solutions were thoroughly mixed on an orbital shaker for 2 minutes to induce cell lysis before being incubated at RT for 10 minutes to stabilise the luminescent signal. The luminescence was then recorded for 1 second per well using the Perkin Elmer 1420 Multilabel Counter Victor^{3TM} plate reader.

2.12 Real-Time Polymerase Chain Reaction (Real-Time PCR)

All Real-Time PCR reactions were performed on the Roche LightCycler® 480 Instrument using LightCycler® 480 Multiwell Plate 96 following manufacturer's recommendations. To compare relative mRNA levels in transfected samples the samples analysed were transfected in triplicate and each triplicate was run as three technical replicates in the Real-Time PCR analysis. Two negative controls were included in all assays; no template control (replace cDNA template with PCR grade water which reveals possible contamination problems) and no reverse transcriptase control (omit addition of reverse transcriptase to the cDNA synthesis reaction which indicates possible genomic DNA contamination of RNA samples).

2.12.1 Real-Time PCR primers and probes

The cloned feline *Egfr* sequence and the published feline β-actin sequence (accession number AB051104) (NCBI, 2010c) were used in conjunction with their predicted sequences (EMBL-EBI, 2010b) to design intron spanning primers and probes utilising the Roche Universal Probe Library Assay Design Centre (Roche, 2009). Primers and probes were selected and HPLC purified primers were ordered from Eurofins MWG Operon (eurofinsdna.com). FAM labelled probes number 147 (cat # 04694333001) for the feline *Egfr* sequence and number 11 (cat # 046851105001) for the feline β-actin sequence were ordered from Roche Applied Science. The primer sequences can be seen in Table 2.11. For relative quantification Eukaryotic 18S rRNA Endogenous Control Set (Applied Biosystems) was used as internal calibrator. The control set contained VIC labelled minor groove binder (MGB) probes to allow for multiplexing and was supplied in a primer limiting ready to use solution.

Primer set		Sequence
RT-F.EGFR	Forward	GGAGCATTTGGCACAGTGTA
	Reverse	TGGAGATGTGGCTTCTCGTA
RT-F.B-ACTIN	Forward	ATCACCATCGGCAACGAG
	Reverse	GGATGCCACAGGACTCCATA

Table 2.11: Real-Time PCR primer sequences

2.12.2 Real-Time PCR reactions

The Real-Time PCR reactions were performed using LightCycler® 480 Probes Master (Roche) master mixes with a reaction volume of 20 µl in a 96 well plate format. Real-Time PCR reactions contained 0.5 µM of each primer, 0.1 µM of each probe in manufacturer's reaction buffer and 2 µl of a one in ten dilution of cDNA synthesis reaction described in Chapter 2.6.1.3 as template. The cycling conditions used are summarised in Table 2.12.

2.12.3 Data Analysis of Real-Time results

All data analysis was performed and all graphs were generated using Microsoft Office Excel 2003 program (Microsoft Corporation, USA). Statistical analyses of data were performed using Minitab© 15 Statistical Software (Minitab Ltd., UK).

2.12.3.1 Primer efficiency

To determine primer efficiency cDNA from untreated SCCF1 cell line was used as template. Serial dilutions of cDNA reaction mixtures from 1:10 to 1:10,000 were made and Real-Time PCR reactions were performed in three technical replicates with each primer set individually (EGFR, 18S rRNA and β-actin primers) as well as multiplexed (EGFR and 18S rRNA primers).

The primer efficiency was calculated according to the Pfaffl method (Table 2.13) (Pfaffl, 2001). The cycling threshold (Ct) or Crossing point (Cp)

values of each of the dilutions were plotted against the cDNA concentrations and the slopes were calculated from the graphs. High primer efficiency produces graphs with a high correlation coefficient (Pearson's correlation coefficient r>0.99) and with high linearity in the investigative range. E values of approximately 2 for primer pairs are required as that equates to a doubling of transcript in each PCR cycle. This is a prerequisite in order to use the comparative delta-delta method, which is based on the assumption of 100% primer efficiency (Pfaffl, 2001).

Real-Time PCR Setup			
Detection Format		Block type	Reaction volume
Mono or Dual Colour Hydrolysis Probes		96 well	20 µl
Programs			
Program Name	Cycles	Analysis method	
Pre-Incubation	1	None	
Amplification	45	Quantification	
Cooling	1	None	
Temperature targets			
Target (°C)	Acquisition Mode	Hold	Ramp rate (°C/s)
Pre-Incubation			
95	None	10 minutes	4.4
Amplification			
95	None	10 seconds	4.4
54	None	30 seconds	2.2
72	Single	1 second	4.4
Cooling			
40	None	10 seconds	1.5

Table 2.12: Real-Time PCR cycling conditions for mono- and dual-colour hydrolysis probes.

2.12.3.2 Relative Expression Analysis

All analyses of relative gene expression levels were performed using the comparative delta-delta method (Pfaffl, 2001). The equations used are shown in Table 2.13. The method assumes 100% primer efficiencies for both reference and target genes. Following primer efficiency estimations, Real-Time PCR reactions are performed in triplicate on transfected samples and negative scrambled control transfected samples. The reference gene and the target gene primers were either added to separate wells (EGFR and β-actin primer sets) or in the same well (multiplexing EGFR and 18S rRNA primer sets). The delta Cp value (ΔCp= mean Cp target gene- mean Cp reference gene) for each sample was calculated, and the negative control samples were then averaged to produce negative control ΔCp_{NC} value. The delta-delta Cp value (ΔΔCp) was the difference between the ΔCp value for the transfected cells and the negative control sample. The relative expression level of the target gene was then calculated from the formula in Table 2.13b where 2 represents 100% primer efficiencies of both primer pairs resulting in doubling of product in each PCR cycle to the power of negative ΔΔCp. Relative knockdown was then calculated from formula c (Table 2.13).

a) $E=10^{[-1/\text{-slope}]}$

b) $RE= 2^{-\Delta\Delta Cp}$

c) Percentage knockdown= $(1-2^{-\Delta\Delta Cp}) \times 100$

Table 2.13: Calculation of a) primer efficiency, b) relative expression (RE) and c) percentage knockdown of target gene using equations from Pfaffl (2001). E= efficiency of primers, slope is taken from the linear graph produced when plotting cDNA concentrations against Cp values. RE= Relative expression, $\Delta\Delta Cp=\Delta Cp_{\text{treated sample}}-\Delta Cp_{\text{negative control}}$. ΔCp=Cp for target gene-Cp reference gene.

2.13 Recovery and detection of protein

2.13.1 Reagents and antibodies

All reagents used were purchased from Sigma-Aldrich unless otherwise specified. The primary antibodies used were mouse monoclonal EGFR (MS-400-P0, Thermo-Scientific, UK) at a 1:100 dilution, rabbit monoclonal phospho-MAPK (Erk1/2) (D13.14.4E, Cell Signalling Technologies, USA) at 1:2,000 dilution, rabbit monoclonal phospho-Akt (4060S, Cell Signalling Technologies, USA) at 1:1,000 dilution, mouse monoclonal phospho-STAT-3 (SC-81523, Santa Cruz, USA) at 1:200 dilution, and mouse monoclonal β-actin at 1:40,000 dilution (ab6276-100, Abcam, UK). The secondary antibodies used were polyclonal swine anti-rabbit (SAR) HRP conjugated immunoglobulins (P0217) and polyclonal rabbit anti-mouse (RAM) HRP conjugated immunoglobulins (P0260), both purchased from Dako Cytomation, Denmark. Optimum dilutions were determined for each antibody by testing a range of dilutions on feline cell lysates before using the antibodies for the experiments.

2.13.2 Cell lysis

All manipulations were performed on ice. Cells were harvested as described (2.3.11) and twice the pellet volume of chilled urea buffer (Appendix B) was added to the frozen cell pellet, and allowed to thaw on ice. The pellet was then mixed by pipetting until no cell clumps were visible and incubated for 15 minutes on ice. The cell lysates were cleared by centrifugation at 4°C at 15,000 x *g* for 15 minutes, snap frozen on dry ice, and stored at minus 70°C.

2.13.3 Bradford assay

Two µl of cell lysates or 5 µl of known BSA protein standards were mixed with 200 µl of Quick Start™ Bradford Dye Reagent (BioRad) and added to a clear 96 well plate. The absorbance at 595 nm was measured and the protein concentrations were determined from a standard curve generated from the known BSA concentrations.

2.13.4 SDS polyacrylamide gel electrophoresis (SDS PAGE)

Protein samples were resolved on denaturing SDS-polyacrylamide gels by electrophoresis. Different percentage SDS-polyacrylamide gels were poured according to size of protein of interest with low percentage gels used to separate high molecular weight proteins (e.g. EGFR: 176 kDa) and higher percentage gels for lower molecular weight proteins (e.g. MAPK: 42 and 44 kDa).

The SDS-polyacrylamide gels were prepared and assembled using Bio-Rad Protean II minigel system. The resolving gel (Appendix B) was poured and overlaid with isopropanol to remove air bubbles. The gel was allowed to set at RT, and the isopropanol was removed. The stacking gel (Appendix B) was poured and ten well loading combs were inserted and the gel was allowed to set at RT.

Protein samples were prepared into 60 µg aliquots in 2 x Laemmli Sample buffer (Appendix B) and boiled in a heat block for 2 minutes at 100°C to denature the proteins. The gel was immersed in running buffer (Appendix B), and the samples were loaded into wells in the stacking gel and subjected to electrophoresis at 150 V until the gel front had run off the bottom of the resolving gel. Five µl of pre stained Full Range Rainbow Marker (Amersham

Pharmacia Biotech) was run in parallel with the protein samples to allow size comparison of protein bands.

2.13.5 Immunoblotting

The resolved proteins were electrophoretically transferred onto nitrocellulose membranes (Hybond™-C, Amersham Biosciences, UK) in transfer buffer (Appendix B) at 75 V for 90 minutes. Nitrocellulose membranes were ink stained (0.4% ink (Pelikan, UK) in PBS) for 15 minutes to visualise protein bands and ensure equal loading. The membranes were blocked for 1 hour at RT in PBST/5% Milk (Appendix B) or TBST/5% BSA (Appendix B) before being incubated overnight with primary antibodies at 4°C in blocking solution.

After three 15 minutes washes in PBST or TBST the membranes were incubated for 1 hour at RT with HRP-conjugated secondary antibodies diluted 1:2,000 in blocking solution. After a further three 15 minutes washes with TBST or PBST the blots were developed using Immun-Star™ WesternC™ Kit (Bio-Rad) and protein bands were visualised by exposure to X-ray film (Hybond™-ECL™ Film, Amersham Biosciences).

2.14 Cell proliferation assays

Cells were seeded into 96 well plates at 1,500-3,000 cells/well and allowed to attach overnight at 37°C/5% CO_2 before being exposed to different drug concentrations or being transfected. Cellular proliferation was measured using the CellTiter 96® AQ_{ueous} One Solution Cell Proliferation Assay (Promega) at different time points. Controls were untreated cells and DMSO vehicle treated cells for the drug assays. For transfection experiments scrambled control siRNA transfected, mock transfected and untransfected cells were used as controls. The assay is a colorimetric assay based on the

addition of a tetrazolium compound [3-(4,5-dimethylthiazol-2-yl)-5-(3-carboxymethoxyphenyl)-2-(4-sulfophenyl)-2H-tetrazolium, inner salt; MTS] and an electron coupling reagent (phenazine ethosulfate; PES) which forms a stable solution (AQueous One Solution), in culture medium. The tetrazolium compound (MTS) is then bioreduced by the viable cells to formazan, a coloured substance which is soluble in culture medium. Absorbance at 490 nm is then measured and is directly proportional to the number of living cells in culture.

To perform the assay, 20 µl of AQueous One Solution was added to each well containing 100 µl medium and incubated at 37°C/5%CO_2 for 3 hours. Absorbance at 490 nm was then determined on a plate reader (Perkin Elmer 1420 Multilabel Counter Victor^{3TM}) using the Wallac 1420 Manager program (Perkin Elmer).

2.15 Colony Formation Assays

Cells were counted as described in Chapter 2.3.5 and seeded at a density of 300 to 500 cells per 10 cm plate containing 10 ml of normal or selective medium. The medium was changed and the plates were checked for colony formation twice weekly. When visible colonies had formed after 10 to 20 days the colonies were fixed. The medium was removed from each plate, and the cells were washed twice in PBS. Five ml of cold methanol were then added to each plate and left to stand at RT for 30 minutes to fix the cells. The methanol was removed and 5 ml of 10% Giemsa stain (Sigma-Aldrich®, Appendix B) was used to stain the colonies for 15 minutes. The plates were rinsed thoroughly in tap water before allowed to dry. The colonies were then either counted manually or counted using the colony counting program from Quantity One® 1-D Analysis Software (Bio-Rad) on the Molecular Imager® Gel Doc™ XR Imaging System (Bio-Rad). Colonies were photographed using

the CCD digital camera (Bio-Rad) and files were stored in a jpeg or tiff format and printed using the Mitsubishi P93D thermal printer.

2.16 *In vitro* scratch assay

Cells were passaged and counted as previously described (Chapter 2.3). The cells were seeded at high density into 6 well plates and allowed to reach confluency (usually after 24 hours). A scratch was then created with a 1 ml pipette tip in the monolayer as described by (Liang et al., 2007). Following the creation of the scratch, the medium was removed and the wells were washed with 2 ml PBS per well until all floating cells were removed and a clean, sharp edge of cells could be visualised in all wells by phase contrast light microscopy. The cells were then treated with drugs at different concentrations as described in Chapter 2.3.9 and photographed using the 10x objective at 0, 12, and 24 hours following drug treatments. The area photographed was marked by permanent marker on the lid for each well so that the same area could be photographed at every time point. The gap width was then measured at ten different points for each photograph and the mean was determined for each time point. The mean was then expressed as percentage of gap width at 0 hours and compared between treatment groups to compare migratory ability between treatment groups and cells.

2.17 Irradiation treatment of SCCF1 cell line

All cells were irradiated in William's E culture medium using a Faxitron® cabinet X-ray system 43855D (Faxitron X-ray Corporation, Lincolnshire, IL, USA) at a central dose rate of 2 Gray (Gy)/min. All irradiation was given as a single fraction at room temperature at doses of 0.5, 1, 3, 4 and 5 Gy and incubated at 37°C/5% CO_2.

2.18 Magnetic cell sorting (MACS sorting)

The separation columns, magnetic separator and the CD133 MicroBead Kit were all purchased from Miltenyi Biotec Inc., Germany. Cells were harvested and counted as described in Chapter 2.3. A maximum of $1x10^8$ cells per sample were pelleted by centrifugation at 80 x *g* for 5 minutes and resuspended in 300 μl of chilled separation buffer (Appendix B). One hundred μl of FcR blocking reagent and 100 μl of CD133 MicroBeads were added and the solution was incubated for 30 minutes at 4°C with rotation.

The cells were washed by adding 5 ml of cold separation buffer and centrifuged at 300 x *g* for 10 minutes at 4°C before resuspended in 1 ml of separation buffer and transferred to a pre-wet separation column mounted on the magnetic separator. The column was washed three times with 3 ml of separation buffer and the flow through containing the negative fraction was collected. The column was then removed from the magnetic separator and the labelled fraction was flushed out in 5 ml of separation buffer using the plunger. The labelled and unlabelled fractions were counted and seeded at required density for cell culture or pelleted and snap frozen for RNA or protein analysis.

2.19 Statistical analysis

All experiments with the exception of the radiosensitivity assay were repeated at least on two separate occasions with similar results. All quantitative analysis was based on a minimum of three replicates for 6 well plates and 10 cm plates or a minimum of four wells for 96 well plates.

Data were analysed using Minitab® 15 Statistical Software (Minitab Ltd., UK) and all graphs and diagrams were generated using Microsoft

Office 2003 software (Microsoft Corporation). *P* values < 0.05 were considered statistically significant.

When data followed a normal distribution, parametric tests were performed. If parametric tests could not be used, non-parametric testing was performed. One-way ANOVA was used to compare differences between more than two samples. Two sample *t*-tests or Mann Whitney *U*-tests were used to compare differences between two samples. Correlations between two groups were assessed using Pearson's correlation coefficient. Survival analysis was performed using Kaplan-Meier survival curves and the survival plots were compared using the Log Rank test. To assess combined treatment effects on the SCCF1 cell line, the Bliss additivism model was used (Buck et al., 2006).

Chapter 3:

Expression of EGFR and Ki67 in Feline Oral Squamous Cell Carcinomas

3.1 Abstract

The aims of this study were to establish the level of expression of EGFR and Ki67 in feline oral squamous cell carcinomas (FOSCCs) and to establish if the expression of either marker was predictive of survival. Scoring systems were developed for each marker from immunolabelling of biopsy samples. Sixty seven archived biopsy samples of FOSCC were scored. Statistical analyses of data, including Kaplan Meier survival curves, were performed. All samples expressed both markers although levels differed between samples. Median overall survival was 46 days and one year survival was five percent. There was no correlation between Ki67 and EGFR scores (Pearson's correlation coefficient, p=0.861). Low cellular proliferation (low Ki67 score) was positively correlated with an overall longer survival (Log Rank, p=0.02) and a trend towards better survival for the high EGFR group was observed (Log Rank, p=0.076). Ki67 and EGFR immunolabelling in FOSCC may be of value as biochemical markers for screening of biopsies from cases of FOSCC.

3.2 Introduction

Traditionally, the methods used in oncology to aid the clinician in providing a prognosis in both the human and veterinary field are based on an histological evaluation of the tumour sometimes in combination with labelling for specific immunohistochemical markers (Partridge et al., 2005, Pircher et al., 2010). In some instances, the predictive value of these parameters can be limited (Pircher et al., 2010). With the advent of targeted therapies in oncology, the ability to screen tumours for different markers that can predict prognosis, response to therapy and potentially resistance to therapy (Pircher et al., 2010, Wheeler et al., 2010a) is an attractive possibility. In veterinary medicine, currently few such markers are routinely used. The most widely used marker to date is Ki67, a nuclear protein expressed only during G1 to M phase of the cell cycle (Partridge et al., 2005). It has been reported to have prognostic value in HNSCC (Partridge et al., 2005), and has been extensively used as a tumour proliferation marker (Brown and Gatter, 2002). Ki67 is already an established immunohistochemical marker in feline tumours (Melzer et al., 2006, Morris et al., 2008).

A small immunohistochemical study recently reported that FOSCCs expressed EGFR (Looper et al., 2006). A subset of HNSCC has been found to commonly overexpress EGFR (Grandis and Tweardy, 1993, Mrhalova et al., 2005), and the prognostic value of EGFR expression in HNSCC has been widely reported in the literature. Several studies have demonstrated that high EGFR expression correlates with poor overall survival (Bankfalvi et al., 2002, Hitt et al., 2005, Ma et al., 2003) although others have contradicted this (Gupta et al., 2002). High EGFR expression has also been shown to predict a better response to accelerated radiotherapy compared to longer overall treatment times (Bentzen et al., 2005, Eriksen et al., 2004).

The central aims of this study were to establish whether EGFR and Ki67 were expressed in feline squamous carcinoma and whether they could be used as predictors of survival. The expression of EGFR in feline tumours would support the investigation of EGFR targeted therapy in the cat and would also indicate that the natural disease in cats might be a good model for human HNSCC.

3.3 Materials and Methods

3.3.1 Samples and clinical data

Biopsy samples from cats diagnosed with oral squamous cell carcinomas submitted to the Animal Health Trust (AHT), Newmarket (54 samples) and the Veterinary Pathology Unit, Royal (Dick) School of Veterinary Studies, Edinburgh (18 samples) were collected. The original histopathological diagnosis of each case was re-evaluated and validated by a veterinary pathologist (Mrs Linda Morrison). Samples that were not confirmed to be FOSCC or lacked sufficient tissue for processing were excluded. Clinical histories were collected by means of a questionnaire as previously described (Hayes et al., 2007) (Appendix C), by telephone to submitting veterinary surgeons and from the clinical records in the Hospital for Small Animals at the R(D)SVS using the questionnaire as a template.

3.3.2 Validation of antibodies

The EGFR antibody has previously been used on FOSCC biopsy samples and on a range of normal feline tissues (Looper et al., 2006), and on feline cutaneous squamous cell carcinomas (Sabattini et al., 2010). To further validate the EGFR antibody for use in the cat the same antibody clone was used for western blotting (EGFR antibody Ab-12, Thermo Fisher Scientific, UK) on cell lysates from human EGFR overexpressing breast cancer cell line

MDA-MB-468 (MD Anderson Cancer Centre, Texas, USA) and the SCCF1 cell line (Tannehill-Gregg et al., 2001). In addition, feline skin was used as positive control tissue for immunohistochemical labelling.

The Ki67 antibody has been used for immunolabelling of biopsy samples in previous feline studies (Castagnaro et al., 1998, Eckstein et al., 2009, Melzer et al., 2006, Morris et al., 2008, Roels et al., 2000). To validate the antibody for use in the set-up for this study, feline lymph nodes were used as positive control tissues.

3.3.3 Immunohistochemical labelling

Immunolabelling was performed on paraffin wax embedded FOSCC biopsy samples. The biopsy samples were sectioned, mounted, processed and stained using the protocols described in Chapter 2.2.

3.3.4 Immunohistochemical Scoring

All scoring was carried out blinded by two independent observers. Separate scoring systems were developed for Ki67 and EGFR due to the different labelling patterns produced by the two antigens.

3.3.4.1 Ki67 Scoring

Three representative high power fields (x40 microscope objective) of each Ki67 slide were photographed and the areas containing tumour nests were outlined using Image-Pro Plus Software (Media Cybernetics, Inc., USA) to remove stromal cells from the count. All positive and negative cells were counted and each photograph was counted twice. The mean of the two counts was calculated and expressed as the percentage of cells that expressed Ki67.

3.3.4.2 EGFR Scoring

Labelling criteria were reviewed in a random subset of samples before scoring all cases. EGFR slides were scored independently three times in random order by each assessor. Overall percentage of EGFR positive cells and the pattern of labelling (membranous, cytoplasmic and nuclear) were subjectively assessed. The overlying epithelium if present was excluded from the EGFR scoring area as keratinized epithelial cells cause artifactual EGFR immunolabelling (Gupta et al., 2002). All membranous labelling was considered significant. Cytoplasmic labelling was also considered significant unless only fine, pale brown stippling was present as this was considered non-specific background and was disregarded. Approximately 30% of the samples had some discrepancy between one of the six scores. These samples were scored again and the scorers came to a consensus agreement. The EGFR score was expressed as a percentage EGFR positive cells obtained from the mean of the six readings.

3.3.5 Statistical analysis

Data were analysed using Minitab® 15 Statistical Software (Minitab Ltd., UK). *P* values < 0.05 were considered statistically significant. When data followed a normal distribution, parametric tests were performed. If parametric tests could not be used, non-parametric testing was performed. Correlation between the Ki67 and EGFR scores was assessed using Pearson's correlation coefficient.

Survival according to Ki67 scores, EGFR scores, and tumour sites was assessed using Kaplan-Meier survival curves and the survival plots were compared using the Log Rank test. The influences of age (less than vs. greater than/ equal to median age,) and gender (female vs. male) on survival

and EGFR scores were assessed using the Mann Whitney *U*-test while their influences on Ki67 scores were assessed using the two sample *t*-test.

Cats that were lost to follow up (n=6), euthanised for reasons other than complications arising from oral cancer (n=1, due to progression of pre-existing, chronic renal failure) or alive at end of study period (n=1) were right censored. All but one of the remaining cases were euthanised for reasons relating to the disease and were classified as having died of the disease for the purposes of this study (Table 3.1).

In this study, survival data may have been skewed by the premature euthanasia of some cats due to the widely reported poor prognosis associated with this diagnosis (Hayes et al., 2007) rather than due to progression of disease. To account for this effect, survival data from patients that were euthanised within the first seven days of diagnosis were separated into an early euthanasia group and the remainder of the data were grouped into a late euthanasia group (Table 3.1). Analyses of the influence of Ki67 expression and EGFR scores on survival were performed on the entire data set and separately on data from both the early and the late euthanasia groups. Ki67 levels and EGFR scores were compared between the early and late euthanasia groups using two sample *t*-test and Mann Whitney *U*-test respectively.

	All cases		Early euthanasia group		Late euthanasia group	
Descriptive Statistics	**N**	**Value (%)**	**N**	**Value (%)**	**N**	**Value (%)**
Age	57*		9		47	
Mean		12.9 years		13.0 years		13.0 years
Median		13.9 years		13.1years		13.6 years
Range		5-20 years		7-20 years		5-20 years
Breed	59*		9		49	
Non pedigree		56 (95)		7 (78)		48 (98)
Gender	60		9		51	
Female neutered		30 (50)		5 (56)		25 (49)
Male neutered		26 (43)		3 (33)		23 (45)
Male entire		4 (7)		1 (11)		3 (6)
Reason for presentation	59		9		50	
Routine health check		7 (12)		1 (11)		6 (12)
General health concerns		14 (24)		1 (11)		13 (26)
Oral health concerns		38 (64)		7 (78)		31 (62)
Therapy	59		9		50	
Medical therapy only		46 (78)		6 (67)		40 (80)
Definitive treatment		5 (8)		1 (11)		4 (8)
No treatment		8 (14)		2 (22)		6 (12)
Tumour location	59		9		50	
Sublingual		23 (39)		5 (56)		18 (36)
Tongue		3 (5)		0		3 (6)
Mandible		16 (27)		2 (22)		14 (28)
Maxilla		7 (12)		1 (11)		6 (12)
Palate		2 (3)		0		2 (4)
Cheek		4 (7)		0		4 (8)
Unknown site oral cavity		1 (2)		0		1 (2)
Larynx/pharynx		3 (5)		1 (11)		2 (4)
Median survival according to tumour location						
Sublingual	23	64 days	5	N/A	18	98 days
Mandible	16	35 days	2	N/A	14	41 days
Other sites	20	44.5 days	2	N/A	18	49 days
Survival	60		10		50	
One year survival		3 (5)		N/A		3 (6)
Median survival		46 days		6 days		59 days
Ki67 score	67*		10		50	
mean		52.1		52.1		52.9
median		54.6		49.4		53.9
range		4.8-91		22.0-81.0		4.8-91.0
EGFR score	67*		10		50	
mean		31.2		28.2		33.9
median		20.0		9.0		22.5
range		5.0-93.0		5.0-93.0		5.0-91.0

Table 3.1: (Table previous page). Summary of data from the study divided into three groups: all cases, the early, and the late euthanasia groups. * Whole group includes cases with incomplete clinical data which could not be allocated to the early or late euthanasia groups.

3.4 Results

3.4.1 Samples and descriptive data

A total of 72 biopsies where evaluated for inclusion in the study. Two samples were excluded as they were classified on re-evaluation as squamous cell carcinoma *in situ* and three were excluded due to there being insufficient tissue. Clinical histories were available for 60 cases. These are summarised in Table 3.1.

Age did not influence the Ki67 expression level assessed by two sample *t*-test (p=0.613), the EGFR score or survival assessed by Mann-Whitney *U*-test (p=0.081 and p=0.588 respectively). Gender did not influence the EGFR score or survival as assessed by Mann-Whitney *U*-test (p=0.156 and p=0.779 respectively) nor did it influence the level of Ki67 expression as assessed by the two sample *t*-test (p=0.251).

Presenting signs included ptyalism, halitosis, swellings, dysphagia, anorexia, weight loss, mouth pain, and reduced grooming and/or poor coat condition. Approximately two thirds of the cases were presented to the veterinary surgeon because of owner concerns regarding the oral health of the animal, while one quarter of cases was presented due to concerns about general health. In the remaining 14% of cases, the tumour was an incidental finding during a routine health check (Table 3.1). Reported signs had been present for a few days to over six months prior to presentation.

Therapy was recorded for 59 cases. Only five cases had treatment with curative intent (surgery in all cases), eight cases had no treatment at all while the remaining 46 cases had some form of palliative treatments (non-steroidal anti-inflammatory drug therapy, antibiotic therapy and steroid therapy)

including two cats which received palliative tracheostomy tube placements (Table 3.1).

The most commonly affected sites were the sublingual region and the mandible (Table 3.1). Tumour location correlated with survival. When compared to all other locations, cases with sublingual tumours had the best survival and mandibular tumours had the worst survival in the late euthanasia group (Figure 3.1, p=0.026 and Table 3.1).

3.4.2 Immunohistochemistry

The EGFR mouse monoclonal antibody was validated by western blotting (Figure 3.2). Human and feline cell line lysates produced similar bands of expected size when analysed in parallel by western blotting, validating the use of the antibody on feline tissues. Paraffin wax embedded samples of feline skin were used as positive control tissue, and showed strong membranous labelling of keratinocytes. The Ki67 antibody has already been validated for use in feline tissues (Castagnaro et al., 1998, Eckstein et al., 2009, Melzer et al., 2006, Morris et al., 2008, Roels et al., 2000). In this study, paraffin wax embedded sections of feline lymph node were used as positive control tissues and showed strong nuclear labelling.

All biopsy samples showed both Ki67 and EGFR positive immunolabelling, but there was a large variation between samples with Ki67 expression in 4.8 to 91% of cells and EGFR expression in 5 to 93% of cells. There was no correlation between the two scores by Pearson's correlation coefficient (r=0.022, p=0.861).

3.4.2.1 High Ki67 proliferation index is associated with decreased overall survival

An average of 1307 cells (range 262-2312) was counted for each biopsy sample. Samples with positive Ki67 labelling exhibited strong nuclear labelling. In tumours with low level of Ki67 labelling (Figure 3.3a) the positive cells were located mainly at the periphery of the tumour cell nests. As the percentage of positive cells increased the labelling became more diffuse and included cells in the centre of the nests (Figure 3.3b& c). The mean Ki67 score was 52.7% (95% CI 46.7-57.5%) and the median score was 54.6% (95% CI 45.4-62.2%). More than half of the samples showed Ki67 positive labelling in more than 50% of cells (39/67).

Samples were separated into two groups on the basis of Ki67 expression. Low Ki67 expression was defined as expression below the median level (54.6%). High Ki67 expression was defined as expression at or above the median level. In the late euthanasia group the Kaplan Meier Survival Plots, (Figure 3.4), showed statistically significant difference between the low and high Ki67 expression groups by Log Rank test (p=0.02). The Ki67 scores of the early euthanasia group (≤ 7 days post presentation) and the late euthanasia group (> 7 days post presentation) did not differ significantly (p=0.835).

3.4.2.2 High EGFR score shows a trend towards better overall survival

Tumours exhibited membranous or cytoplasmic labelling, or a mixture of both (Figure 3.5). No nuclear labelling was seen. Approximately 94% of the samples showed membranous labelling and just over half (54%) showed cytoplasmic labelling. The labelling varied markedly in intensity as well as in area covered. The mean EGFR score (percentage of positive cells) was 32.9%

(95% CI 24.4-38.1%) and the median score was 20.0% (95% CI 13.0-30.0%). Just over a quarter of the cases showed positive EGFR immunolabelling in more than 50% of cells (19/67). The EGFR scores separated into two distinct groups when plotted as a histogram giving high EGFR scores >50% (15/49) and low scores ≤50% (34/49). A trend towards a better survival for the high EGFR group was observed by Log Rank Test (p=0.076) in the late euthanasia group (Figure 3.6). The EGFR scores of the early euthanasia group (≤ 7 days post presentation) and the late euthanasia group (> 7 days post presentation) (p=0.320) did not differ significantly.

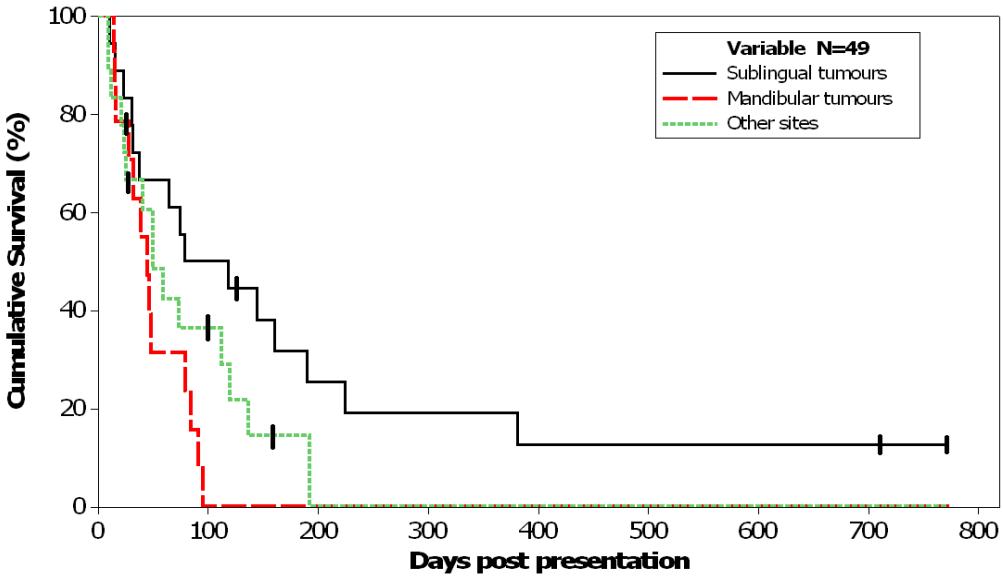

Figure 3.1: Kaplan Meier Survival Plot according to tumour location. Sublingual tumours had a statistically significantly better survival than mandibular tumours and tumours of other sites, p=0.026 by Log Rank test, N=49. Ticks on graph represent censored observations.

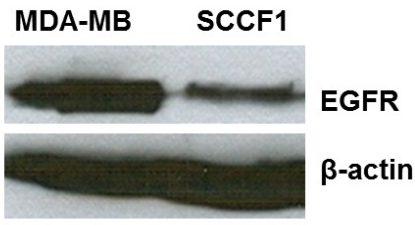

Figure 3.2: Western blot showing EGFR protein labelling in cell lysates from human and feline cell lines. MDA-MB (lane 1) contains lysate from the MDA-MB-468 cell line, a human breast cancer cell line that overexpresses EGFR. It was used as positive control to validate the antibody for the use on feline protein lysates. Lane 2 shows lysate from SCCF1 cell line. Protein loaded: 30 µg MDA-MB, 60 µg SCCF1.

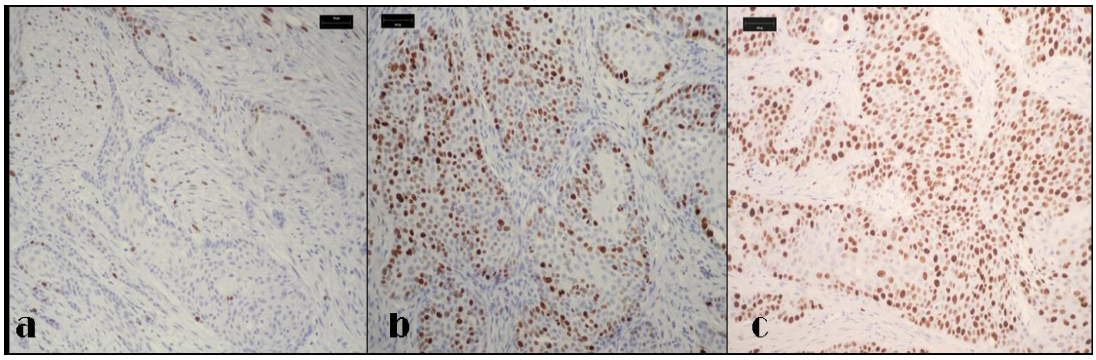

Figure 3.3: Example of low (a), medium (b), and high (c) Ki67 scoring FOSCCs. Positive cells are predominantly present in the periphery of the tumour nests in the lower scoring tumours (a). In the higher scoring tumours increasingly more cells towards the centre of the tumour nests exhibit positive labelling (b & c). Bars 100 µm.

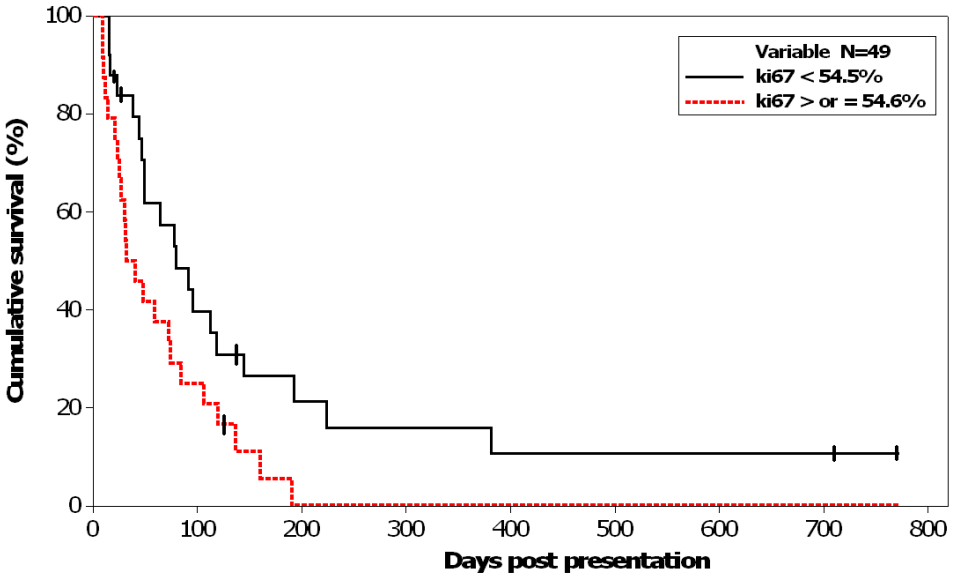

Figure 3.4: Kaplan Meier Survival Plot according to Ki67 score. The low Ki67 scoring tumours had a statistically significantly better survival *p*=0.02 by Log Rank test, N=49. Ticks on graph represent censored observations.

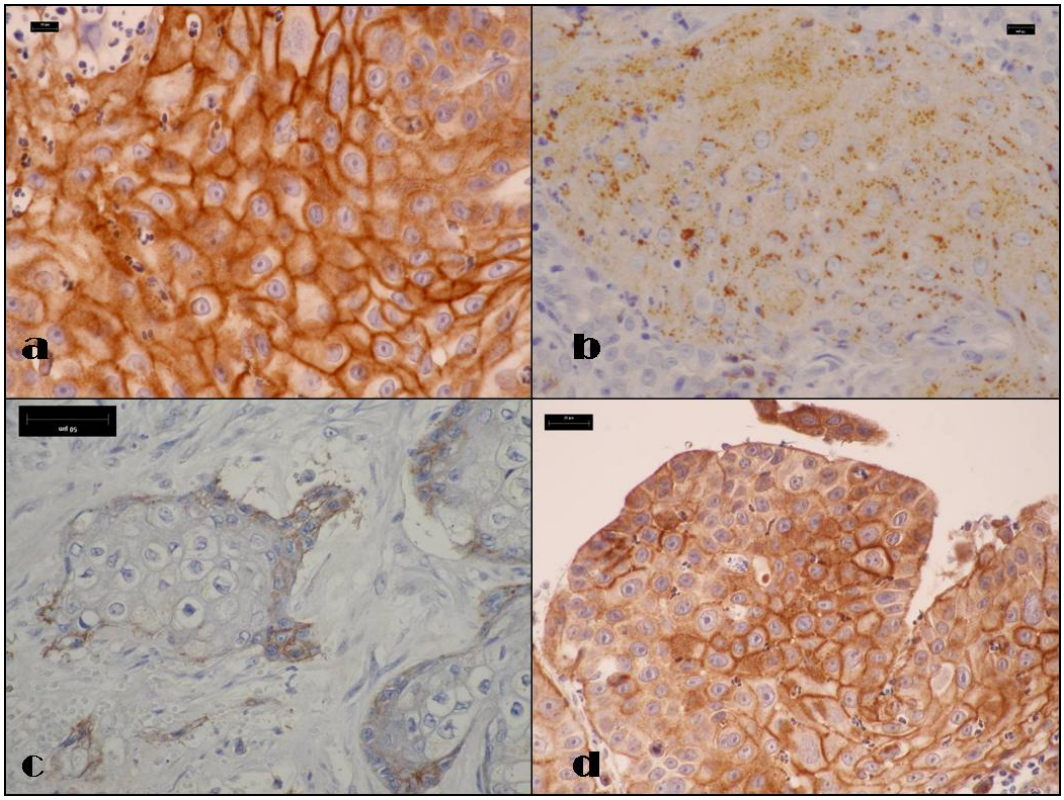

Figure 3.5: EGFR immunohistochemistry of FOSCCs (a) Example of high intensity membranous labelling combined with cytoplasmic labelling, bar 10 µm, (b) cytoplasmic labelling of high intensity with marked granularity, bar 10 µm, (c) low intensity membranous labelling, bar 50 µm, (d) medium and high intensity membranous labelling, bar 25 µm.

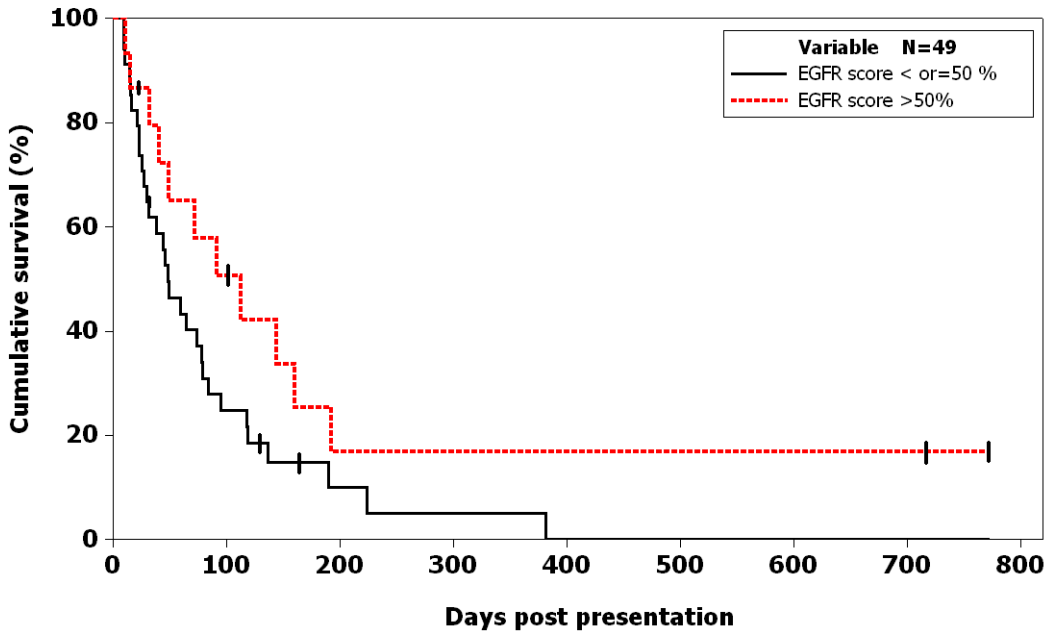

Figure 3.6: Kaplan Meier Survival Curve according to EGFR score. The tumours with high EGFR score had a trend towards better survival compared to the low scoring tumours, p=0.076 by Log Rank Test, N=49. Ticks on graph indicate censored observations.

3.5 Discussion

3.5.1 Study Population

The breed, sex, and age of cats in this study were similar to what has been previously reported (Bregazzi et al., 2001, Fidel et al., 2007, Postorino-Reeves et al., 1993). Patients were predominantly non-pedigree and this is representative of the overall cat population in the UK (pfma.org.uk, 2010). FOSCC occurred in older cats in agreement with previous studies (Gardner, 1996, Stebbins et al., 1989).

This study showed no sex predisposition associated with development of FOSCC. This is also in agreement with previous studies (Gardner, 1996, Stebbins et al., 1989). This differs from HNSCC where gender has a marked influence on incidence and men are affected more frequently than women (cancerresearchuk.org, 2005). The higher incidence of HNSCC seen in men can be partly explained by a higher alcohol consumption combined with tobacco use, but a gender factor cannot be ruled out (Dobrossy, 2005). Gender is unlikely to influence the exposure to environmental toxins in neutered cats. In this study gender did not influence survival in FOSCC. In HNSCC, women have a significantly higher survival rate than men (Dobrossy, 2005). It is tempting to speculate that as animals in this study (and other veterinary reports) are predominantly neutered at an early age, this may remove any effect of gender on survival.

The range of presenting signs reported in this study was mainly associated with oral health and included salivation and difficulty eating. These were similar to clinical signs reported in previous studies (Bertone et al., 2003, Kapatkin et al., 1991).

Only five cases in this study received any treatment with curative intent after diagnosis. This may be because a large proportion of the samples in this study were collected as part of a previous study looking at survival in FOSCC in general practice in the UK (Hayes et al., 2007) skewing the population away from referral cases that are more likely to have further specific treatments performed. Disappointingly, nine cases received no treatment including pain relief at any time and 40% of cases received no pain relief at the time of biopsy even though oral pain was one of the presenting signs recognised by the owners. This may reflect the historical nature of the data set used representing a time when analgesia for cats was not as widely used or as readily available in easy-to-use formulations. Definitive treatments were only attempted in a very small number of cases in this study (Table 3.1) so meaningful analysis could not be performed on the influence of treatment on survival.

The sublingual area was the most commonly affected site followed by the mandible and the maxilla consistent with previous reports (Dorn and Priester, 1976, Postorino-Reeves et al., 1993, Stebbins et al., 1989). Sublingual tumours have been reported to have a worse prognosis than other oral tumours (Evans et al., 1991), and were excluded from surgical treatments in one study (Hutson et al., 1992). In the study reported here the sublingual tumours did significantly better than tumours of other sites, indicating that exclusion of sublingual FOSCC cases from treatment may be unwarranted if they are not inoperable.

3.5.2 Statistical Analysis of Survival Data

Analysing survival data in veterinary epidemiological studies is frequently problematic because companion animals are likely to be euthanised and do not die naturally from progression of the disease leading

to possible bias of survival data. Euthanasia was used as the end point criterion for inclusion in this study but this practice has been criticised as the decision to euthanise animals is affected by many factors other than disease progression such as financial constraints on treatment, predicted prognosis, age at presentation and concurrent disease (Hosgood and Scholl, 2001, Johnson et al., 2004). In addition, individual owner and veterinarian attitudes towards euthanasia and treatment vary, influencing the timing of euthanasia. It has been suggested that all euthanised animals should be right censored for Kaplan Meier survival analysis (Hosgood and Scholl, 2001) but, when this is done in studies such as this one where 53 out of 54 cases were euthanised, censoring becomes too restrictive. Johnson and colleagues (2004) demonstrated that when euthanised client-owned animals were treated as having reached the end point and were included in survival analyses a more complete analysis was possible.

In order to account for the possible influence of anticipated poor prognosis of FOSCC on the survival data (Hayes et al., 2007, Looper et al., 2006), animals were divided into early and late euthanasia groups and animals from the early euthanasia group were excluded from subsequent survival analyses. The EGFR scores and Ki67 expression levels of the early euthanised groups did not differ significantly from the scores of the remainder of the population indicating that early euthanasia could not be linked to either EGFR score or Ki67 expression. This supports the decision to divide these observations into two separate groups as the euthanasia of these cases may have been driven by other factors than the severity of their disease.

The overall survival in this study, in which cases largely received only palliative care, was very poor with one year survival of only 5%. In

comparison, in other studies in which patients received radical surgery or radical surgery with radiotherapy, one year survivals of 43% (Northrup et al., 2006) and 57% (Hutson et al., 1992) have been reported. These latter studies were of limited size and excluded some patients, but do demonstrate that, with treatment, some cats survive for longer.

3.5.3 Immunohistochemical labelling

The tumours in this study exhibited irregular nests and cords of stratified squamous epithelial cells which crossed the basement membrane and invaded the underlying lamina propria and submucosa, the characteristic appearance of oral squamous cell carcinomas (Van Kruiningen, 1995). Depending on aggressiveness, the tumours on occasions also invaded underlying bone and muscle.

These irregular nests of cells resembled to a varying degree the normal architecture of stratified squamous epithelia. The equivalent of the cuboidal basal cells responsible for cell division which rest on the basement membrane in normal stratified squamous epithelia (Young and Heath, 2002a) were observed occupying the periphery of the tumour nests. In normal oral epithelium, cells become more flattened with pyknotic nuclei as they move away from the basal layer towards the surface (Young and Heath, 2002a). In the tumours, flattening of cells could be observed in the cells towards the centre of the tumour nests.

Normal oral stratified squamous epithelium can become keratinised in exposed areas if subjected to excessive desiccation or abrasion like, for example, in the palatal regions (Young and Heath, 2002b). In neoplastic tissues, the amount of keratin present varies depending on the degree of differentiation present, with poorly differentiated tumours containing few keratinized cells and numerous mitotic figures (Van Kruiningen, 1995). Most

tumour samples in this study contained few keratinized cells, but numerous keratin pearls were observed in a small number of specimens, which is a marker of well differentiated tumours (Van Kruiningen, 1995).

No correlation was seen between the two labelling patterns of Ki67 and EGFR. Since EGFR can be a driver of proliferation (Yarden and Sliwkowski, 2001) it would be reasonable to assume that high EGFR scores would correlate with a high proliferation index. This was not the case, which may indicate the heterogeneity of the underlying molecular pathways driving these tumours (Yarden and Sliwkowski, 2001). Similar results have been reported in HNSCC (Bentzen et al., 2005).

3.5.3.1 Ki67 immunolabelling

The high number of Ki67 positive labelling cells in the majority of tumours seen here supports the suspected fast growth rate of squamous cell carcinomas (Melzer et al., 2006). The Ki67 labelling pattern observed in these tumours, with the low grading tumours only exhibiting positive cells in the periphery of the tumour nests and the higher grades showing positive nuclear labelling towards the centre of the tumour nests, reflects the remnants of the normal epithelial architecture (Young and Heath, 2002a). These labelling patterns with high scoring tumours exhibiting more heterogeneous labelling were similar to what has been previously reported in HNSCC (Rittà et al., 2009) and in feline mammary carcinomas (Castagnaro et al., 1998).

In this study the median Ki67 score was chosen as a cut-off point to differentiate the high and low scoring groups as has been described for other feline tumours (Castagnaro et al., 1998, Eckstein et al., 2009). The Ki67 data did follow a normal distribution, hence the median and mean scores were approximately equal (Table 3.1) (Petrie and Watson, 2006b). However, when

a data set includes censored observations, the mean score should not be used (Castagnaro et al., 1998, Petrie and Watson, 2006b). The median Ki67 score was therefore considered to be an appropriate cut-off point for the purpose of this study.

The Ki67 antibody clone used in this study (MIB-1) is raised against human Ki67 recombinant protein, but it has been shown to cross-react with cow, dog, sheep, horse and swine. It has also been used in previously published feline tumour studies (Castagnaro et al., 1998, Melzer et al., 2006, Roels et al., 2000). No further validation of the antibody was performed in this study other than the use of feline lymph nodes as positive control tissues to aid in optimisation of the labelling protocol.

The Ki67 proliferation index was found to correlate with worse outcome in FOSCC in this study mirroring the findings of some reports on the evaluation of Ki67 in HNSCC where it has been found to be associated with a poor prognosis (Partridge et al., 2005, Rittà et al., 2009). However, other reports have found no association between Ki67 proliferation index and prognosis in HNSCC (Ma et al., 2003, Quon et al., 2001). While Ki67 expression is a well-established marker of proliferation in a range of human tumours, its role as a prognostic indicator is more controversial (Partridge et al., 2005, Pich et al., 2004). Similarly, Ki67 is an established proliferation marker in cats (Castagnaro et al., 1998, Eckstein et al., 2009) but in addition has shown value as a prognostic indicator in feline mammary carcinoma (Castagnaro et al., 1998). High Ki67 expression has also been associated with an increased response to accelerated radiation therapy in cats with cutaneous SCC (Melzer et al., 2006). It also correlates strongly with histological differentiation (Lörz et al., 1994) and provides an indication of the aggressiveness of the tumour. This study indicates that Ki67 labelling of

FOSCCs may function as a useful guide for clinicians to assess the potential prognosis of patients.

3.5.3.2 EGFR immunolabelling

In this study, all tumours showed some degree of EGFR labelling, with 25% of samples showing labelling in over half of the cells. The majority of tumours showed membranous labelling with or without cytoplasmic labelling. This is in agreement with previously published results in FOSCC (Looper et al., 2006). Membranous labelling demonstrates receptor at the plasma membrane while cytoplasmic labelling is caused by either newly synthesized receptors located in the Golgi apparatus (Damjanov et al., 1986) or internalised receptors (Wiley, 2003). Some authors disregard cytoplasmic labelling when scoring tumours and only take the membranous labelling into account (Agulnik et al., 2007, Hitt et al., 2005) while others include it (Grandis et al., 1996, Looper et al., 2006). In this study we included both cytoplasmic and membrane labelling as receptor located in the cytoplasm is part of the normal receptor life cycle (Wiley, 2003), and dysregulation of receptor processing may be involved in tumorigenesis (Wheeler et al., 2008). No nuclear labelling was seen in these samples. Translocation of EGFR to the nucleus has been reported as a mechanism of resistance to therapy by cancer cells (Li et al., 2009). All the biopsy samples used in this study were taken prior to treatments. Further studies investigating the pattern of EGFR labelling in tumours following therapy, in particular with EGFR targeting drugs if they became available, could reveal if nuclear translocation of EGFR plays a role in acquired resistance in FOSCC.

Immunohistochemistry is a commonly used technique for evaluation of EGFR expression in HNSCC tumour samples, and a high EGFR score is extensively reported to be inversely correlated to overall survival (Grandis et

al., 1996, Hitt et al., 2005, Kumar et al., 2007, Ma et al., 2003). All these studies used different scoring systems with arbitrary cut off values. Extrapolation from published EGFR scoring systems used in HNSCC for use in this study was problematic as these were based on much larger sample sizes allowing for division into multiple groups. In this study the EGFR scores separated into two distinct groups when plotted on a histogram and this was used to select the cut-off point between low and high scores. Lack of a properly validated cut off point is a major limitation in this and similar studies.

A trend towards a better survival in the high scoring EGFR group was observed although statistical significance was not reached. This could be due to a number of factors including the small sample size of the study, the considerable heterogeneity in the patients with regard to early and late stage disease and potentially due to an inappropriate cut off point (Kumar et al., 2007).

This study has established that FOSCC frequently express EGFR and that patients with high EGFR expression may have a better prognosis. Recent advances in treatment of HNSCC have included therapies targeting EGFR with radiotherapy, surgery, and/or chemotherapy (Baselga et al., 2005, Bonner et al., 2006). HNSCC with high EGFR expression responded better to an overall shortened treatment time for radiotherapy (Bentzen et al., 2005, Eriksen et al., 2004). In FOSCC, targeting EGFR in combination with established treatment protocols such as radiotherapy or surgery may offer patients an improved survival and warrants further investigations. Evaluation of EGFR expression in FOSCC for selecting patients for radiotherapy may also prove of value.

3.6 Summary

In summary, FOSCC is a disease with a very poor prognosis but better selection of patients may enable more targeted treatments and improve survival. This study demonstrates that Ki67and EGFR labelling of biopsy samples have potential in this selection process. A low Ki67 score showed correlation with better survival in this cohort, while cases with high EGFR labelling showed a trend towards better survival times. In addition, we have established that EGFR expression is a feature of FOSCC with a subset of tumours showing high expression levels similarly to what has been reported in HNSCC. Further studies are indicated to establish the role of EGFR in FOSCC, in particular the effect of potential EGFR targeting as a treatment strategy especially in combination with established treatment strategies like radiotherapy.

Chapter 4:

Development of RNA interference targeting strategies against feline EGFR

4.1 Abstract

Feline squamous cell carcinomas exhibit similarities to human head and neck cancer with a subset of tumours overexpressing EGFR. In order to investigate the potential role of EGFR in the feline tumour, targeting strategies have to be developed. In this study, the feline *Egfr* tyrosine kinase domain was sequenced and showed high degree of homology to the human EGFR sequence and a conserved ATP binding region. Six small interfering RNAs targeting the feline *Egfr* were developed and screened using an *in vitro* vector system, and the most effective siRNAs against the feline *Egfr* was determined. These results pave the way for further gene silencing studies to determine the effect of EGFR knockdown in feline squamous cell carcinomas. In addition, conservation of the ATP binding pocket between the human and feline receptors suggests EGFR targeting with human small molecule receptor tyrosine kinase inhibitors may be effective in feline cells.

4.2 Introduction

In man, targeting EGFR using a range of strategies has been widely evaluated for treating HNSCC. RNA interference is a highly specific method of gene silencing which utilises small interfering RNA molecules (siRNAs) complementary to the target sequence (Pai et al., 2006). These bind to gene transcripts targeting them for early destruction before translation can occur (Pai et al., 2006). RNA interference techniques are extensively used in research in gene function studies, but also carry promise for the development of drugs capable of targeting specific proteins (Scherer and Rossi, 2003, Dorsett and Tuschl, 2004, Davis et al., 2010) including EGFR (Nozawa et al., 2006). RNA interference allows for rapid and highly specific gene targeting allowing for the effect of silencing a particular gene to be assessed in both *in vitro* and *in vivo* systems (Scherer and Rossi, 2003, Dorsett and Tuschl, 2004). It is a particularly powerful tool when assaying gene function in mammalian cancer cell lines for potential drivers of oncogenic pathways (Kittler and Buchholz, 2003).

Although EGFR is widely expressed in feline oral SCC (Looper et al., 2006, Bergkvist et al., 2010) no studies have investigated the effect of EGFR targeting in the veterinary species (Bergkvist and Yool, 2010). The full human *EGFR* cDNA sequence was first published in 1984 by Ullrich and colleagues (Ullrich et al., 1984). Since then, the *Egfr* cDNA sequences for a range of mammals have been published, and a high degree of homology between species, particularly in the tyrosine kinase region (NCBI, 2010b) is present. Although the cat genome is now available (Pontius et al., 2007, NCBI, 2010a), no annotations to the feline *Egfr* sequence have been made.

The aims of this study were to sequence the tyrosine kinase region of the feline *Egfr* receptor and design and screen a set of siRNAs sequences

against it to evaluate the potential of using RNA interference as a targeting strategy in feline squamous cell carcinomas. In addition, sequence homology between the human and the feline receptors were investigated to assess the potential of using currently available human EGFR targeting drugs in cats.

4.3 Materials and Methods

4.3.1 Cloning and sequencing of feline EGFR tyrosine kinase region

Total cellular RNA was isolated from the SCCF1 cell line as described in Chapter 2.4.1, and first strand cDNA was synthesised as described in Chapter 2.6.1.2 and 2.6.1.2. Since the feline *Egfr* sequence has not been published, three primer sets were designed to span the putative tyrosine kinase region of the feline *Egfr* gene using areas with a high degree of homology between the human, murine and canine published sequences (EMBL-EBI, 2010b, NCBI, 2010c) (primer pairs A, B & D, Table 4.1). Primers were designed (Chapter 2.6.2.1) and PCR reactions were performed as described in Chapter 2.6.2.2 and 2.6.2.3.

Samples were sequenced in both directions as previously described in Chapter 2.5. The sequences were then checked against the feline genome (NCBI, 2010a) using a Basic Local Alignment Search Tool (BLAST) nucleotide search, and sequence homology to other species were compared (NCBI, 2010b).

4.3.2 Vector cloning

The psiCHECK™-2 vector from Promega was used in the experiments. The psiCHECK-2 vector has two reporter genes. The primary reporter gene is fused with the target gene allowing monitoring of target gene expression. The secondary reporter gene acts as an internal control for normalisation of

data to correct for variations due to different transfection efficiency between samples. The principle of the psiCHECK™-2 vector system is summarised in Figure 4.1.

Restriction enzyme sites XhoI and NotI were added to the 5′ end of the upstream and downstream primer sequences respectively to allow for directional cloning (primer set C, Table 4.1), and PCR reactions were repeated as described in Chapter 2.6.2.2. The psiCHECK-2 vector and the PCR product were then digested using Xho1 and Not1 restriction enzymes in separate reactions as described in Chapter 2.7.2 before being gel purified as described in Chapter 2.7.1. The digested plasmid and PCR products were combined using the ligation protocol (Chapter 2.7.3).

Primer Set			Restriction enzyme	Sequence 5'-3'
A	Feline EGFR TK1	Forward	-	GAATATCACCTGCACAGGAC
		Reverse	-	GCCATCACGTAAGCTTCATC
B	Feline EGFR TK2	Forward	-	GGAGAAGCTCCCAACCAGGCT
		Reverse	-	GATAGGCACTTTGCCTCCTTC
C	Feline EGFR TK2	Forward	Xho1	TTACTCGAGGGAGAAGCTCCCAACCAGGCT
		Reverse	Not1	AAGCGGCCGCGATAGGCACTTTGCCTCCTTC
D	Feline EGFR TK3	Forward	-	TGCGAAGGGCATGAACTAC
		Reverse	-	ACTCATCGGCATCTACGAC

Table 4.1: *Egfr* primers were constructed using the tyrosine kinase region of human, murine, and canine *EGFR* sequences. The tyrosine kinase region has the greatest sequence homology between species.

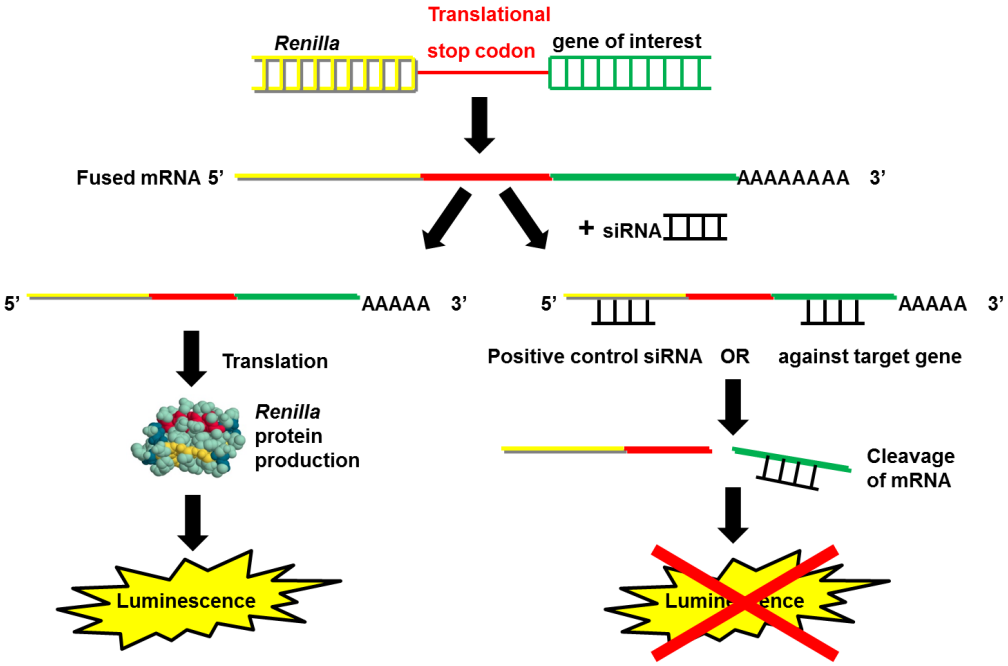

Figure 4.1: Schematic diagram to illustrate the principle of psiCHECK™-2 vector system. The gene of interest is cloned into the vector by directional cloning downstream of the *Renilla* luciferase translational stop codon resulting in a fused mRNA being transcribed. Cells are co-transfected with vector and siRNAs against the *Renilla* sequence (positive control siRNA) or the gene of interest, which leads to targeting of the mRNA sequence for degradation and no luminescence signal. No siRNA or scrambled negative control siRNAs allows *Renilla* protein translation which leads to a luminescence signal. Based on a diagram from Promega Technical Bulletin #329.

The ligation reactions were used directly in the transformation reactions as described in Chapter 2.4.2.1, see Figure 4.2. Colonies were selected and expanded overnight before performing plasmid preparations as described in Chapters 2.4.2.2 to 2.4.2.4. The vector was then sequenced as described in Chapter 2.5 to ensure insertion of the correct sequence.

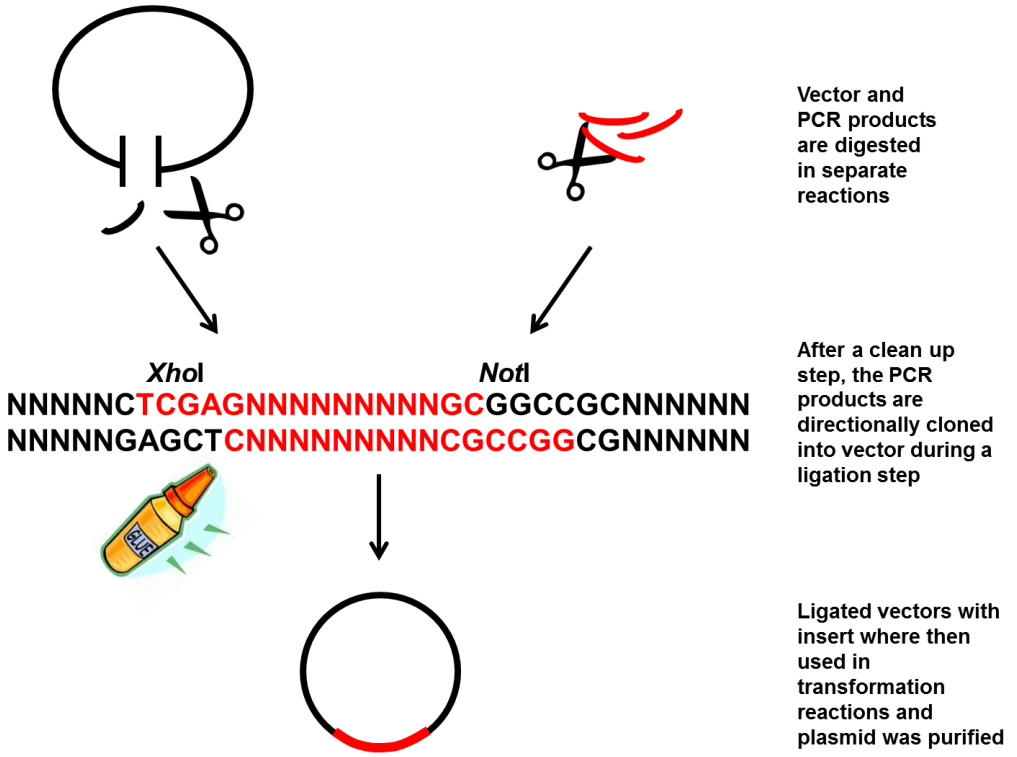

Figure 4.2: Schematic diagram illustrating the restriction enzyme digestions and the ligation process.

4.3.3 Design, production and screening of siRNAs

4.3.3.1 Design and production of siRNAs

Six siRNAs (Table 2.7) against the feline *Egfr* tyrosine kinase region sequenced using primer pair B (Table 4.1) were designed. In addition one scrambled sequence negative control siRNA and three positive control siRNAs against the vector's *Renilla* sequence were designed as described in Chapter 2.8.1. All ten siRNAs were produced by *in vitro* transcription using the *Silencer*® siRNA Construction Kit (Ambion) following manufacturer's recommendations as described in Chapter 2.8.2.

4.3.3.2 Optimisation of electroporation of 293FT cell line

Several optimisation experiments were performed to optimise an electroporation protocol for the 293FT cell line as described in Chapter 2.9.1. A more detailed description complementary to Chapter 2.9.1 is given below.

Firstly, optimum cell numbers per well were determined by transfecting the 293FT cells at a range of cell numbers with 1 μg psiCHECK™-2 vector. The normalised *Renilla* readings as measured by the Dual-Glo™ Luciferase System (Promega, Chapter 2.11.1) were compared after 24 hours to establish the optimum cell number per well.

The cell line was then co-transfected with the psiCHECK™-2 vector containing the insert (psiCHECK™-2.EGFR) and one of the three positive control siRNAs designed against the *Renilla* sequence or the scrambled control siRNA6 sequence. The efficiencies of the three *Renilla* siRNA sequences in reducing normalised *Renilla* luminescence as percentage of scrambled control were compared.

To determine if DNA vector concentrations influenced knockdown efficiency, 200nM positive control *Renilla* siRNA and 1, 3 and 5 μg of psiCHECK™-2.EGFR vector was co-transfected into the cell line, and the impact on normalised *Renilla* luminescence was assessed.

Next, the optimum electroporation program was evaluated. The positive control *Renilla* siRNA was co-transfected with the psiCHECK™-2.EGFR vector using three of the pre-programmed electroporation programs on the Nucleofector® 96-well shuttle (Amaxa). The pmaxGFP™ control plasmid was also transfected into the cell line using all four programs to determine transfection efficiency and cell viability by flow cytometry (Chapter 2.10). The optimal program was then selected based on a

combination of transfection efficiency achieved with pmaxGFP™ control plasmid and cell viability following transfections as assessed by flow cytometry (Chapter 2.10) and relative reduction in normalised *Renilla* readings achieved following siRNA control transfections.

Finally, optimum siRNA concentrations were determined comparing 250 nM and 500 nM final concentrations of control siRNAs in wells.

4.3.3.3 Electroporation protocol

The electroporation protocol is described in detail in Chapter 2.9.2. In short, 293FT cells were trypsinated and counted as described in Chapter 2.3.4 and 2.3.5 and $2x10^5$ cells were seeded into a Nucleocuvette™ 96 well plate. Control plasmid pmaxGFP™ or 1 μg psiCHECK-2.EGFR vector was co-transfected with 250 nM siRNAs in triplicate by electroporation as described in Chapter 2.9.2. *Renilla* luminescence was read 24 hours after transfection and normalised against Firefly luminescence of the secondary reporter as previously described (Chapter 2.11.1). The experiments were repeated on two different occasions with similar results.

4.4 Results

4.4.1 The feline *Egfr* tyrosine kinase region is highly conserved between species

The sequences obtained with the primers designed from the known human, canine, and murine *EGFR* sequences had a 100% sequence homology with the feline genome as assessed by performing a BLAST search (GenBank accession number Felis HQ185236) (Appendix D). The feline DNA sequence has 92% sequence homology to the canine *Egfr* sequence and 89% sequence homology with the human *EGFR* sequence. The feline *Egfr* tyrosine kinase region amino acid sequence has 97% and 95% homology with the canine and

human EGFR protein sequences respectively. The amino acid sequence of the ATP binding pocket in the human EGFR was conserved in the feline EGFR. Table 4.2 shows an overview of the degree of homology between EGFR tyrosine kinase regions in a range of species.

Species		**% homology to feline *Egfr***	
Latin name	**Common name**	**DNA**	**Amino acid**
Homo sapiens	Man	89%	95%
Callithrix jacchus	Marmoset	89%	96%
Canis familiaris	Dog	92%	97%
Sus scrofa	Wild boar	88%	95%
Bos taurus	Ox	88%	95%
Equus caballus	Horse	92%	97%
Monodelphis domestica	Opossum	83%	93%
Rattus norvegicus	Rat	87%	94%
Mus musculus	Mouse	87%	95%
Gallus gallus	Chicken	81%	90%
Felis catus	Cat	100%	100%

Table 4.2: Overview of degree of homology between species in the tyrosine kinase region of *Egfr* sequences.

4.4.2 Synthesis of siRNAs by *in vitro* transcription yielded adequate amounts of good quality siRNAs

Ten siRNA sequences were designed and synthesised; six against the feline *Egfr*, three positive control sequences against the *Renilla* sequence in the psiCHECK™-2 vector and one scrambled control sequence. The manufacturers provided a DNA control to assess yield of siRNA construction, and a yield of 68 μg of RNA was produced in this study using the control DNA (the manufacturer recommended that a minimum yield of

10 μg RNA using the control DNA indicated satisfactory siRNA construction). Five of the siRNA templates designed in this study yielded satisfactory amounts of RNA of 10 μg or more, while two yielded less. These yields were however, adequate for the screening process, and the quality of all siRNA samples was satisfactory with A_{260}/A_{280} ratios between 1.9 and 2.1.

4.4.3 Optimisation of the electroporation protocol resulted in a threefold increase in positive control siRNA efficiency

A total of $2x10^5$ cells per well in a 96 well format gave the highest normalised *Renilla* reading following transfection of psiCHECK-2 vector (data not shown). This cell density was used for all further experiments.

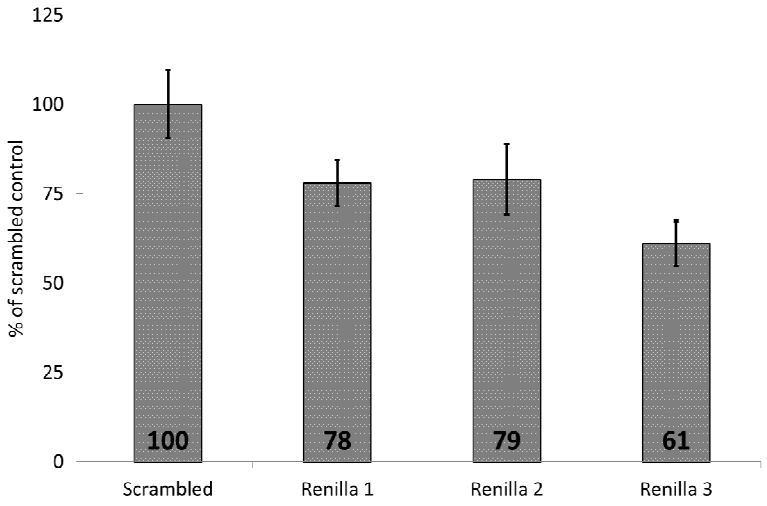

Figure 4.3: Results of electroporation screening of the three positive control *Renilla* sequences showed variable reduction in normalised luminescence, with Renilla 3 (siRNA10) producing the overall largest reduction in luminescence readings.

The three positive control sequences targeting the *Renilla* sequence in the psiCHECK-2 vector produced 22-39% reduction in normalised *Renilla* luminescence readings (Figure 4.3). The most effective siRNA (siRNA10, Table 2.7) was then used for the remaining optimisation. Further optimisation for DNA vector concentrations showed no increase in siRNA

control knockdown efficiency or in transfection efficiency with increasing DNA concentrations, so 1 μg of DNA template per reaction was used for subsequent experiments (data not shown).

Four pre-programmed electroporation programs were compared for transfection efficiency, post-transfection cell viability and reduction in normalised *Renilla* luminescence (Table 4.3). Program DS-150 produced the maximum reduction in *Renilla* luminescence (Figure 4.4) and an approximately equal transfection efficiency and post electroporation cell viability when compared to the other programs, and was therefore chosen for further experiments.

Program	% *Renilla* knockdown	Transfection efficiency		Cell viability	
		Overall	Viable cells only	Transfected cells	Untransfected cells
DS-130	50%	62%	44%	61%	84%
DG-130	28%	70%	60%	83%	84%
CM-130	20%	54%	48%	78%	84%
DS-150	59%	60%	43%	59%	84%

Table 4.3: Results of electroporation screening using siRNA10 *Renilla* showing effect of four different pre-programmed programs on Renilla knockdown, transfection efficiency and cell viability.

Finally, the effect of increasing the siRNA concentration from 250 to 500 nM was investigated, and the higher siRNA concentration of 500nM produced a 71% reduction of *Renilla* luminescence compared to scrambled control (Figure 4.5). Overall, optimisation of transfection conditions resulted in a threefold increase in the relative efficiency of the positive control siRNA.

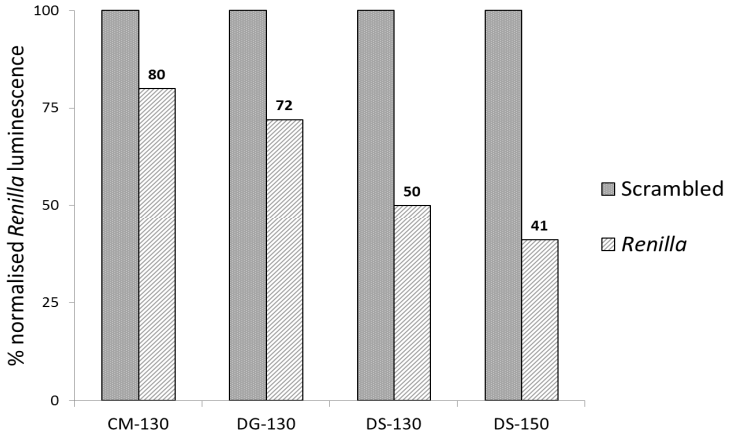

Figure 4.4: Percentage of scrambled control *Renilla* luminescence achieved using the four different programs. An almost doubling in efficiency was seen between the worst and the best performing programs. All readings shown were normalised against the Firefly luminescence.

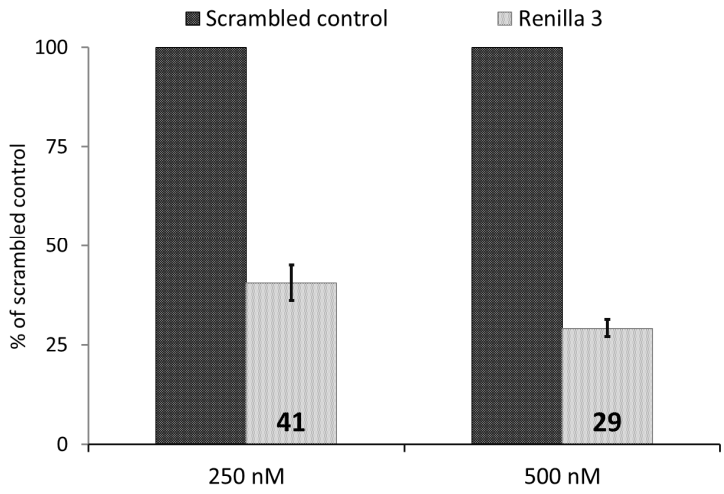

Figure 4.5: Result of screening using two different siRNA concentrations of 250 and 500 nM siRNA. The higher siRNA concentration yielded a greater reduction in *Renilla* luminescence readings. Bars are average of six luminescence readings with +/- standard deviations

4.4.4 The siRNA screening produced three efficient siRNAs targeting the feline *Egfr*

Both siRNA screening experiments had transfection efficiencies of between 40-65% as measured by flow cytometry on pmaxGFP™ transfected

cells. Residual background Firefly activity as determined with plasmid pGL3 was < 0.06%. Scrambled control siRNA transfected cells exhibited a 12% reduction in normalised Renilla levels when compared to vector only controls. *Renilla* positive controls produced an average 40% reduction in *Renilla* luminescence when compared to scrambled control transfected cells (Figure 4.6).

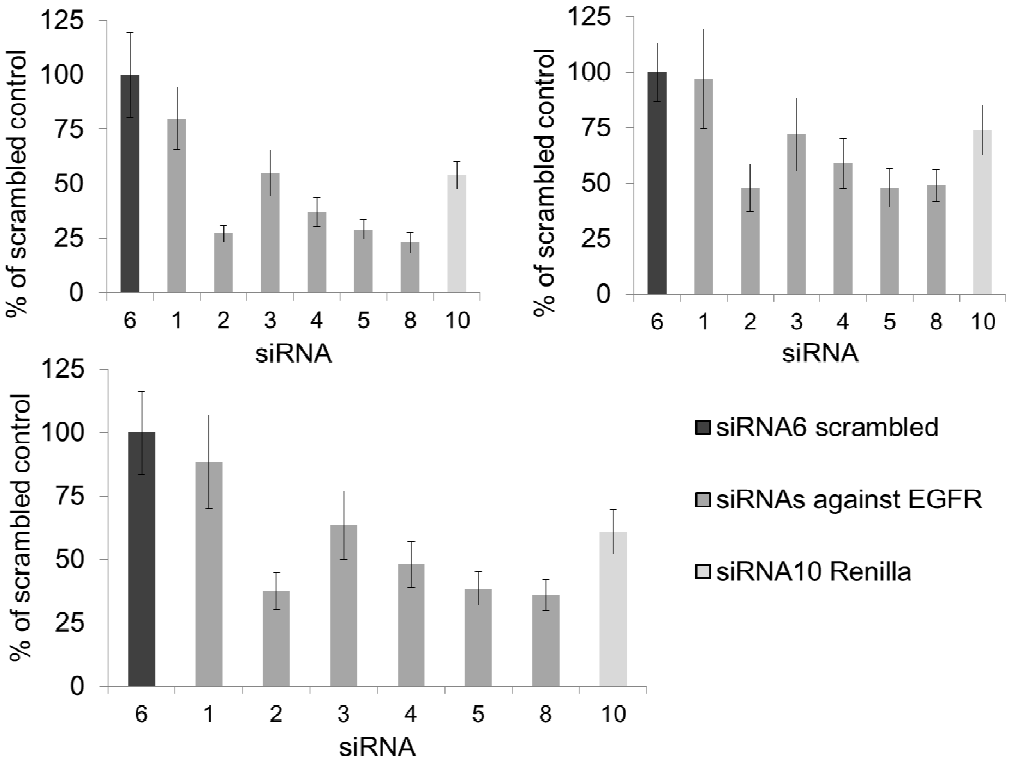

Figure 4.6: Result of siRNA screening using psiCHECK™-2 vector system and Nucleofector® 96-well shuttle. Upper left and right panels show results of individual experiments, where each bar represents an average of nine replicates +/- standard deviations. The lower panel show an average of all experiments where each bar represents an average of 18 replicates +/- standard deviations.

siRNA	Target	% of scrambled control		
		Screen 1	Screen 2	Average
6	Scrambled	100	100	100
1	Egfr	80	97	89
2	Egfr	27	48	38
3	Egfr	55	72	64
4	Egfr	37	59	48
5	Egfr	29	48	39
8	Egfr	23	49	36
10	Renilla	48	74	61

Table 4.4: Summary of results from siRNA screens using psiCHECK™-2 vector system and Nucleofector® 96-well shuttle.

The results of the siRNA screening are summarised in Table 4.4 and Figure 4.6. The most effective siRNAs overall were siRNAs 2, 5 & 8 when compared to scrambled control cells. These siRNAs were consistently more effective than the positive control in reducing *Renilla* luminescence. Two siRNAs (siRNA1 & 3) were consistently less efficient than the positive control siRNA, while the remaining siRNA, (siRNA4) exhibited an intermediate level of efficiency. The overall most efficient siRNA was siRNA8, which on average caused a 64% reduction in luminescence, so this siRNA sequence was therefore used for all further *Egfr* knockdown experiments in this study.

4.5 Discussion

This study demonstrated that the tyrosine kinase region of the feline *Egfr* gene has a high degree of homology with the human gene and other mammals (NCBI, 2010b) as well as a conserved ATP binding pocket. The ATP binding pocket has been shown to be essential for receptor tyrosine

kinase activity as point mutations in the binding pocket severely affects receptor activity (Redemann et al., 1992). A favoured therapeutic approach for EGFR blockade is the use of small molecule competitive inhibitors that bind to the ATP binding pocket (Arteaga, 2003). A number of EGFR specific tyrosine kinase inhibitors are currently in use in human medicine (Lurje and Lenz, 2009). The high degree of homology of this key domain between man and cat indicates that small molecule tyrosine kinase inhibitors targeting this domain in man may be effective in inhibiting feline *Egfr* activity.

This study has also demonstrated that a commercially available monoclonal antibody produced against the EGF binding region of the human protein (EGFR Ab-12, Thermo-Scientific) also binds specifically to feline EGFR epitopes showing species cross reactivity (Chapter 3.3.2). In addition to TKIs, specific therapeutic monoclonal antibodies (mAbs) have been approved for clinical use in a range of solid tumours including HNSCC (Lurje and Lenz, 2009). The mAbs block the ligand binding region of the receptor preventing activation of the receptor and target it for antibody dependent cell-mediated cytotoxicity (Lurje and Lenz, 2009).

This study aimed to investigate means of targeting the feline EGFR. According to these results both drug classes may potentially have activity in feline cells; TKIs by binding to the ATP binding pocket and mAbs via interactions with the ligand binding domain of the receptor. However, mAbs used in human medicine are either humanised or chimeric antibodies. If used in veterinary species they are likely to cause anti-human antibody responses similar to the human anti-mouse antibody responses seen in man to murine antibodies (Nissim and Chernajovsky, 2008, Bergkvist and Yool, 2010). TKIs on the other hand, have no such known complications, and these

results suggest that TKIs used in human medicine may be effective in feline patients.

In this study siRNAs were developed to target the feline *Egfr*. When RNA interference techniques were in their infancy, it was thought that all siRNAs produced were equally efficient in producing gene silencing (Kurreck, 2006). It soon became apparent that this was not the case, as different siRNAs against a particular target gene caused widely differing effects (Scherer and Rossi, 2003, Reynolds et al., 2004). A number of design rules and algorithms have been suggested for the design of efficient siRNAs.

Early on the optimum siRNA length was suggested to be 21 base pairs (Elbashir et al., 2001a). When RNA interference was first described in *Caenorhabditis elegans* (Fire et al., 1998), long double stranded RNA (dsRNA) was used. In mammalian cells, long dsRNA induces an interferon response which activates a ubiquitously expressed serine/threonine protein kinase (PKR) (Williams, 1999). PKR is a member of the antiviral arm of the mammalian stress response which is activated by dsRNA, cytokines, growth factors and other stress signals (Williams, 1999). If triggered, PKR initiates overall inhibition of gene expression and cell death (Kittler and Buchholz, 2003). The exact length at which dsRNA triggers the interferon response is not known, but dsRNA shorter than 30 base pairs long does not trigger cell death in most cell lines (Kittler and Buchholz, 2003). In this study 21mere siRNAs were used, as most design tools are designed to produce siRNAs of this length. However, later evidence suggested that 27meres may be the optimum length for siRNA efficiency (Kurreck, 2006).

An early criterion used for selection of potential sequences was the Tuschl rule (Elbashir et al., 2001b). According to this rule, sequences starting with an AA dinucleotide which produces siRNAs with 3' overhanging UU

dinucleotides are more efficient (Elbashir et al., 2001b). This is in agreement with several other authors (Khvorova et al., 2003, Schwarz et al., 2003). However, some authors claim that this is unnecessarily limiting and risks exclusion of effective siRNAs (Naito et al., 2004), while others suggest that the 3′ UU overhang need not match the target sequence (Yu et al., 2002, Schwarz et al., 2003), avoiding exclusion of sequences that do not start with an AA dinucleotide.

All siRNAs in this study complied with the Tuschl rule, except the positive control siRNAs targeting the *Renilla* gene. Positive controls *Renilla* 1 and 2 were based on a published sequence (Betz, 2005) and had previously been used in the psiCHECK-2 vector system. The third *Renilla* sequence was designed using online siRNA design programs as previously described (Chapter 2.8.1). In this study, the positive control siRNAs were not as efficient in gene silencing as the best siRNAs against the *Egfr*, all of which were designed according to the Tuschl rule indicating that it may be relevant in siRNA design.

A further design criterion is that there should be no G residues in the 3′-overhangs of the siRNA molecule. RNases used in the clean-up step in the Ambion *Silencer*® siRNA Construction Kit cleave single stranded RNA containing G residues (Ambion, 2008b), and would truncate the siRNA if it contained this residue. Free nucleotide overhangs have been shown to be crucial for siRNA activity (Patzel et al., 2005), so this criterion was critical in the design of these nucleotides.

The proportion of functional siRNAs increases when their GC content is between 36 and 52% (Elbashir et al., 2002, Reynolds et al., 2004, Kurreck, 2006) or 30 and 70% (Kumar et al., 2003). All but one (*Renilla* 2/siRNA9) of

the siRNAs used in this study achieved the more stringent criteria set by Reynolds and colleagues (Reynolds et al., 2004).

RISC preferentially incorporates antisense strands with relatively lower 5'- end thermodynamic stability (Khvorova et al., 2003, Schwarz et al., 2003). It has been proposed that a lower internal stability at one end of the duplex aids duplex unwinding and increases efficient entry into the silencing complex (Khvorova et al., 2003, Schwarz et al., 2003). A relatively simple way of achieving a lower thermodynamic stability at one end is to increase the A or U base pair content of one end. According to the second criteria of Reynolds et al. (2004) there should be at least one, or preferably more than three A or U base pairs at positions 1-5 of the antisense strand. Eight of the siRNAs in this study had three A or U base pairs at this position; one had two U's and one had only one U. The three most effective siRNAs in this study had two or three A or U base pairs at this position.

To minimise off target effects of the siRNAs the sequences should have no more than 16-17 contiguous base pairs homology when performing a BLAST search (Reynolds et al., 2004, Kurreck, 2006, NCBI, 2010a). Some authors suggest that as little as eleven contiguous base pairs may cause off target effects (Naito et al., 2004), and that BLAST searches are not stringent enough to predict all possible off target effects (Naito et al., 2004, Zhou et al., 2006). All our sequences had between 15 and 17 base pairs sequence homology with other genes according to a BLAST search of the feline genome. Although adhering to the criteria set by Reynolds and colleagues (Reynolds et al., 2004), ideally the homology to other sequences should have been less in this study. However, the choice of sequences was restricted due to the constraints of only having a 500 base pairs long sequence to design the siRNAs from.

In order to achieve maximal efficiency of knockdown, an optimal transfection protocol has to be established for each cell line, as efficiency of siRNA knockdown is directly related to the delivery of siRNA into cells (Kittler and Buchholz, 2003). The results of the optimisation performed in this study illustrated this with a threefold increase in knockdown efficiency achieved for the positive control siRNA following optimisation. The amount of siRNA used is of particular importance. A dose dependent increase in efficiency is observed with increasing siRNA concentrations (Kumar et al., 2003), but the effect does eventually tail off, and too high concentrations are undesirable for several reasons. Higher siRNA concentrations can lead to increased off target effects and increased toxicity (Scherer and Rossi, 2003, Dorsett and Tuschl, 2004). In addition, the cost of producing siRNAs is significant (Takasaki, 2010), so finding the lowest effective siRNA concentration is highly desirable.

As discussed, there are currently a number of design rules and algorithms published on how to design a highly effective siRNAs (Takasaki, 2010), as well as statistically based computer software designed to aid in this process (Naito et al., 2004, Takasaki, 2010). Despite all these available tools, the consensus is that siRNA sequences produced by *in vitro* transcription or chemical synthesis all require screening in order to establish their efficiency (Kittler and Buchholz, 2003, Scherer and Rossi, 2003). Endoribonuclease prepared siRNAs (esiRNAs), on the other hand produce multiple siRNAs against a given mRNA and do not require screening (Yang et al., 2002, Kurreck, 2006). This approach produces a mix of siRNAs that can be transfected together into cells to cause gene silencing. This approach was not appropriate for this study, however, as we required a known effective siRNA sequence that we could use in further studies. The siRNAs in this study were

therefore produced by *in vitro* transcription using T7 RNA polymerase necessitating a screening process.

The maximum effect obtained by the siRNA in this study was 77% reduction in target gene expression. The reports in the literature vary in what constitutes an efficient siRNA. In general highly effective siRNAs are defined as producing more than 95% (Reynolds et al., 2004) or more than 90% (Khvorova et al., 2003) gene silencing and functional siRNAs are defined as producing more than 70% gene silencing (Khvorova et al., 2003). According to these criteria the siRNAs in this study can only be classified as functional siRNAs. The vector based screening method used here has been shown to produce a relatively larger reduction in target gene protein levels compared to the normalised reduction in luminescence seen from control gene expression during screening (Kumar et al., 2003). For example, a siRNA which produced a 50% reduction in normalised fluorescence during screening achieved an 80% reduction in protein levels expressed as a relative reduction in band intensity by western blotting. The study also confirmed that siRNAs chosen using vector based screening also suppressed endogenous gene product *in vitro* (Kumar et al., 2003), which suggests that the siRNAs screened in this study should be efficient in suppressing endogenous feline EGFR levels as well.

Three of the siRNAs screened in this study showed that they could efficiently reduce the level of feline *Egfr* mRNA in the psiCHECK-2 vector system, while the remaining siRNAs showed poor efficiency. The probability of designing a high potency siRNA is low, so screening of potential candidates is essential (Yang et al., 2002, Scherer and Rossi, 2003). Reynolds and colleagues (2004) suggest that on average only one in ten to one in four siRNAs designed produce over 95% gene suppression, while others report

that one in five achieve this level (Kumar et al., 2003). In this study six siRNAs were screened, and three of these showed acceptable to moderate efficiency, which would be as expected according to the reports in the literature.

The reasons why siRNAs differ so widely in their efficiency can largely be explained by different sequence properties of the individual siRNAs. In addition to the rules discussed above, five different studies have produced specific recommendations for preferred nucleotides at specific positions within the siRNA sequence (Takasaki, 2010). The recommendations from these studies do correlate well (Takasaki, 2010), but they can severely limit the number of available sequences in studies were the target sequence is relatively short, as was the case in this study.

Internal repeats or palindromes within the siRNA can also limit the effectiveness of a siRNA (Reynolds et al., 2004). These can lead to increased internal stability and secondary structure of the siRNAs, causing reduced uptake into the RISC complex (Reynolds et al., 2004, Patzel et al., 2005). Some authors propose that secondary structures of the target mRNA also affect siRNA efficiency (Kurreck, 2006, Takasaki, 2010), while others propose that target mRNA secondary structure has little effect on siRNA efficiency (Elbashir et al., 2002). The consensus is now that a combination of the thermodynamic properties of the siRNA which affects the asymmetric strand incorporation into RISC as well as accessibility to the target site all contribute towards silencing efficiency (Kurreck, 2006). In this study the structure of the mRNA could not be taken into account when designing the siRNAs as the full length feline *Egfr* mRNA sequence is not known. The screening process allowed for a selection of the potentially most efficient siRNA. The chosen sequence can now be used to assess the effect of *Egfr* gene silencing in a

feline model system, the feline squamous cell carcinoma cell line SCCF1 (Tannehill-Gregg et al., 2001).

4.6 Summary

These findings facilitate further investigation of *Egfr* targeting in feline oral SCC suggesting two potential mechanisms for EGFR targeting. A specific siRNA against the feline *Egfr* sequence have been developed, and the efficiency of this siRNA against the feline *Egfr* and the effect of *Egfr* gene silencing on the SCCF1 cell line can now be further elucidated.

This study also discovered that the ATP binding pocket was conserved between the feline and human EGF receptors, suggesting that TKIs designed to target the human EGFR may be effective in feline cells. These results support a trial of a small molecule TKIs in the feline SCCF1 cell line.

Chapter 5:

Targeting the feline EGFR in a feline SCC cell line and rescue of gefitinib resistance by RNA interference

5.1 Abstract

This study investigated different methods of EGFR targeting in a feline squamous cell carcinoma cell line. Both RNA interference techniques and a small molecule tyrosine kinase inhibitor reduced cell proliferation and migration in the cell line. The use of hairpin expression vectors was explored to evaluate the potential for long term EGFR suppression, and they produced sustained knockdown of EGFR in the cell line. EGFR targeting with RNAi also reversed acquired gefitinib resistance in the cell line, and produced an additive effect when used in combination with radiotherapy. These results support the use of EGFR targeting as a viable therapeutic strategy for the management of feline oral SCC.

5.2 Introduction

In feline oral SCC, current treatment options include surgery (Northrup et al., 2006), radiotherapy (Fidel et al., 2007), chemotherapy (Fox et al., 2000), or a combination of these (LeBlanc et al., 2004), but overall survival remains poor (Hayes et al., 2007). Treatment is often hampered by the locally aggressive nature of these tumours (Hayes et al., 2007) and the high morbidity that may be seen with treatment (Northrup et al., 2006). New approaches to the treatment of feline SCC would be beneficial, and are likely to include combination therapies with current established treatment protocols.

Since the early nineties when the first reports on the potential involvement of EGFR in the carcinogenesis of HNSCC were published (Weichselbaum et al., 1989, Grandis and Tweardy, 1993), developing strategies to target EGFR in HNSCC has been the main focus of research in this area. Several EGFR targeting drugs are now available which belong to two drug classes, the small molecule tyrosine kinase inhibitors (TKIs) and the therapeutic monoclonal antibodies (mAbs) (Chen et al., 2010). The response to TKIs have been modest in HNSCC (Ratushny et al., 2009, Chen et al., 2010) due to tumour cells either exhibiting an inherent resistance to the drugs or through acquiring resistance over time (Li et al., 2009, Chen et al., 2010). The search is on to find molecular markers that can predict response to therapy by identifying tumours that possess intrinsic resistance to therapy (Wheeler et al., 2010a). Some success has already been achieved in some tumour types, for example the identification of activating mutations located in the tyrosine kinase domain which predicts response to gefitinib in non-small-cell lung cancer (NSCLC) (Pircher et al., 2010, Wheeler et al., 2010a). By selecting individuals more likely to respond these trials have achieved

response rates of 50 to 70% (Wheeler et al., 2010a) compared to 12 to 18% reported in earlier trials (Pircher et al., 2010). However, identifying the molecular mechanisms utilised by cells to acquire resistance is equally important. In NSCLC such a mutation has been identified in the tyrosine kinase region, and it is thought that with the advent of irreversible TKIs these cells will become sensitised again (Wheeler et al., 2010a). Although mutations conferring oncogene addiction have been identified in other solid tumours, in HNSCC similar tyrosine kinase mutations seem to be rare events (Chen et al., 2010).

The aim of this study was to investigate the role of EGFR in feline SCCs by using two mechanisms to inhibit receptor signalling. RNAi was used to investigate the effect of *Egfr* specific gene silencing on the cell line by evaluating cell proliferation, cell migration and downstream targets of the EGFR signalling pathways. In addition, the observation that the feline ATP binding pocket was conserved (Chapter 4) paved the way for investigating the use of TKIs in a feline cell line SCCF1. The ability of the SCCF1 cell line to develop resistance to TKI after prolonged exposure, a common treatment failure in man (Chen et al., 2010, Wheeler et al., 2010a), was assessed by chronic exposure of the cell line to sub-lethal doses of TKIs. The ability of feline *Egfr* RNAi to rescue TKI resistance in the cell line was then assessed. Finally, the effect of combining EGFR targeting with conventional therapies was investigated in the cell line.

5.3 Materials and Methods

5.3.1 Gefitinib treatment of SCCF1 cell line

The SCCF1 cell line was cultured as previously described in Chapter 2.3. The cell line was treated with different concentrations of gefitinib and

SCCF1G, the gefitinib resistant cell line, was developed as described in Chapter 2.3.8 and 2.3.9 respectively. To investigate the acquisition of point mutations as a potential mechanism of acquiring resistance in the cell line, the tyrosine kinase domain of the SCCF1G cell line was sequenced using the same primer sets as described in Chapter 4.2.1. Following gefitinib treatments, cell proliferation assays (Chapter 2.14) and *in vitro* scratch assays (Chapter 2.16) were performed.

5.3.2 Liposome-mediated transfections of SCCF1 cell line

The SCCF1 cell line was optimised for both transient siRNA and plasmid DNA transfections as described in Chapters 2.9.3.1 and 2.9.3.3, and the optimised Lipofectamine 2000™ protocols (Chapters 2.9.3.2 and 2.9.3.4) were used in the study. Real Time PCR primer efficiencies were determined for the primer sets as described in Chapter 2.12.3.1. Following transient siRNA and hairpin expression vector transfections, Real-Time PCR analysis, western blot analysis and cell proliferation assays were performed as described in Chapters 2.12, 2.13 and 2.14 respectively. In addition, following plasmid transfections colony formation assays (CFAs) as described in Chapter 2.15 were performed. CFAs were performed during G418 selection as well as after 20 days of G418 selection.

Cells were transfected with siRNAs against the feline *Egfr*, scrambled sequence *Silencer*® Negative Control #1 siRNA (Ambion), or with p*Silencer*™ neo Kit hairpin expression vectors containing the sequence directed against the feline *Egfr* or a scrambled control sequence. Cells transfected with the hairpin expression vectors were trypsinated and counted 24 hours following transfection, seeded at their optimal cell density into six well plates before adding selective G418 containing media for 20 days.

5.3.3 Hairpin expression vector

The 3.1p*Silencer*™ neo Kit (Ambion) is a hairpin expression vector system capable of generating short hairpin RNA (shRNA) transcripts that can induce long term gene silencing in cells (Figure 2.3). The vector contains an H1 RNA polymerase III promoter which provides high levels of constitutive expression across a variety of cell types. The terminator sequence is a short stretch of uridines, which is compatible with the most commonly used siRNA design consisting of two 3' uridine overhangs (Elbashir et al., 2001b). In order to facilitate selection of transfected cells following transfections the vector also harbours a neomycin resistance gene. To select cells a neomycin analogue, G418 was used after establishing the optimum concentration (Chapter 2.3.11) and cell plating density (Chapter 2.3.12) for the SCCF1 cell line.

To design shRNA DNA oligonucleotide templates for the hairpin expression vector the sequence of siRNA8, the most effective sequence against the feline *Egfr* (Chapter 4), was entered into the online p*Silencer* converter tool (Ambion, 2008a). The DNA oligonucleotides templates were ordered from eurofinsdna.com and used directly in the ligation reaction as described in Chapter 2.7.3. The DNA oligonucleotide sequences can be seen in Table 5.1.

Strand	DNA template sequence 5' to 3' direction
Top	GATCCGGAAATCCTTGATGAAGCTTTCAAGAGAAGCTTCATCAAGGATTTCC TTTTTTGGAAA
Bottom	AGCTTTTCCAAAAAAGGAAATCCTTGATGAAGCTTCTCTTGAAAGCTTCATC AAGGATTTCCG

Table 5.1: DNA oligonucleotide template sequences contained the target sense and antisense sequences as well as a hairpin loop sequence allowing the formation of hairpins following expression.

5.3.4 Radiosensitivity assay

SCCF1 cells were transfected (with siRNA8 and scrambled control) or treated with 5 μM gefitinib in six and 96 well plates and incubated for 24 hours before being irradiated. All cells were irradiated in culture medium using a Faxitron® cabinet X-ray system 43855D (Faxitron X-ray Corporation, Lincolnshire, IL, USA) at a central dose rate of 2 Gray (Gy)/min. All irradiation was given as a single fraction at room temperature. The 96 well plates were irradiated at 0, 0.5, 3, and 5 Gy and incubated for 72 hours prior to performing cell proliferation assays. Cells from the six well plates were trypsinated and counted 24 hours after transfections and 300 cells were seeded in triplicate into ten cm plates and irradiated in suspension at 0, 0.5, and 3 Gy prior to performing CFAs as previously described (Chapter 2.15).

5.3.5 Statistical analyses

All statistical analyses were performed as described in Chapter 2.19. To assess the effect of combining radiation with EGFR knockdown in the SCCF1 cell line the Bliss additivism model was used as previously described (Buck et al., 2006). A theoretical curve was calculated for combined inhibition using the equation $E_{bliss} = E_A + E_B – (E_A \times E_B)$, where E_A and E_B is the fractional inhibition obtained by siRNA alone and radiation alone at different doses respectively. Combined treatments with experimental values equal to the theoretical E_{bliss} value show an additive effect, while experimental values displaying a larger inhibition compared to E_{bliss} represent synergism. Conversely, combined treatments with experimental values below the E_{bliss} value display antagonistic effects.

5.4 Results

5.4.1 Inhibition of EGFR signalling causes reduced cellular proliferation and migration in the SCCF1 cell line

Following 72 hours of continuous exposure to gefitinib in the cell line, a reproducible reduction in cell proliferation was observed (Figure 5.1). The effect was dose-dependent and approximately linear through the range of 1 to 10 μM. Doses in the nanomolar range had no effect on proliferation of the cell line when compared to untreated and DMSO treated controls. Average inhibitory concentration causing 50% reduction of proliferation in the SCCF1 cell line was approximately 5 μM (Figure 5.1).

To investigate the effect of inhibition of EGFR signalling on cellular migration, scratch assays were performed on cells treated with gefitinib. The SCCF1 cell line showed a dose-dependent reduction in migration following gefitinib treatment (Figure 5.2).

In contrast, using proliferation assays following gefitinib treatment the SCCF1G cell line showed no significant inhibition of proliferation at the 5 μM drug dose (Figure 5.1), and was consistently more resistant at concentrations of 1-15 μM gefitinib. Scratch assays performed on the gefitinib resistant cell line showed a comparatively faster migration in the resistant cell line when compared to the parent cell line (Figure 5.3). Gefitinib had no effect on migration in the resistant cell line at 24 hours.

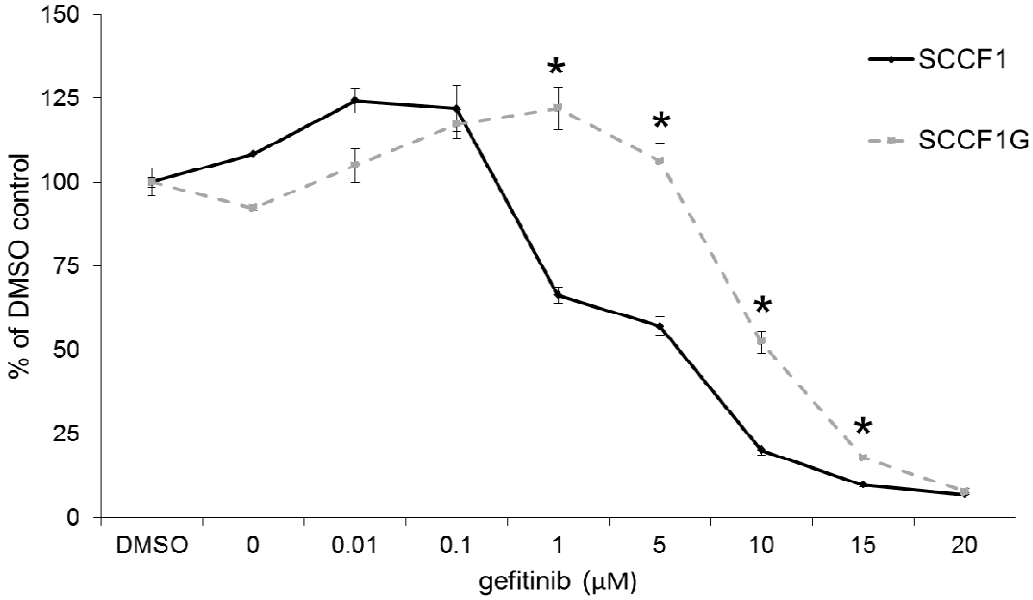

Figure 5.1: Cell proliferation assay showing proliferation of SCCF1 and SCCF1G after 72 hours of gefitinib treatment at variable concentrations. X axis represents gefitinib concentrations in μM and Y axis represents % of proliferation as compared to DMSO control treated cells. Error bars show standard deviations, and * denotes $p<0.05$ with two sample *t*-test showing statistically significant difference in proliferation ability.

To investigate the acquisition of point mutations as a potential mechanism of acquiring resistance in the cell line, the tyrosine kinase domain of the SCCF1G cell line was sequenced. No mutations were found in the tyrosine kinase domain of the receptor in the SCCF1G gefitinib resistant cell line.

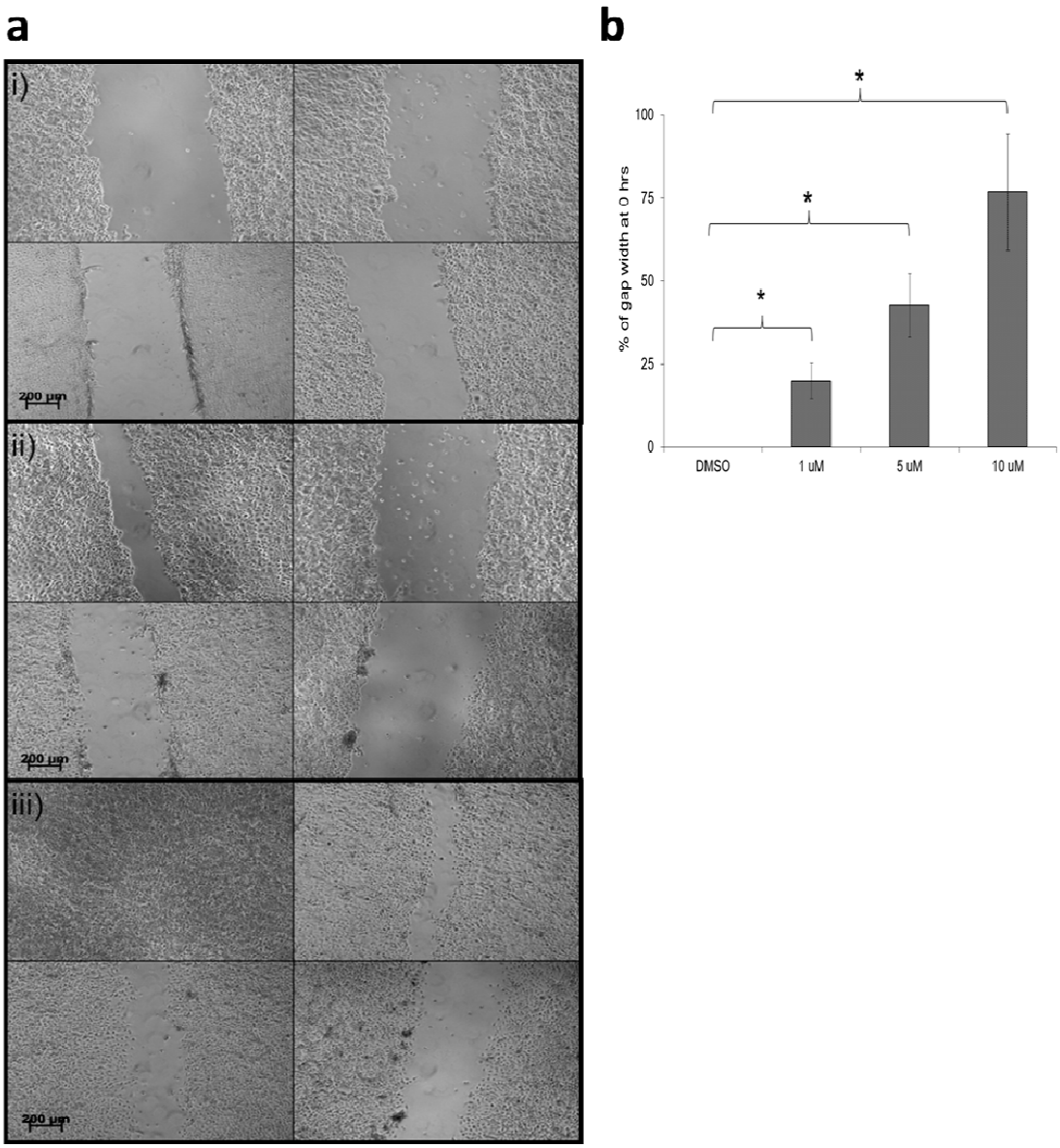

Figure 5.2 a) *In vitro* scratch assay of SCCF1 cell line showing effect of EGFR specific tyrosine kinase inhibitor gefitinib on cellular migration. Each box shows top left DMSO control, top right 1 µM gefitinib, bottom left 5 µM gefitinib, bottom right 10 µM gefitinib at i) 0 hrs, ii) 12 hrs and iii) 24 hrs. b) Histogram showing relative migration of the SCCF1 cell line after 24 hrs of gefitinib treatment compared to DMSO control treated cells. The 10µM gefitinib dose produced a 23% reduction in gap width after 24 hours compared with the 100% reduction observed in DMSO treated cells (* $p<0.001$ by One-way ANOVA).

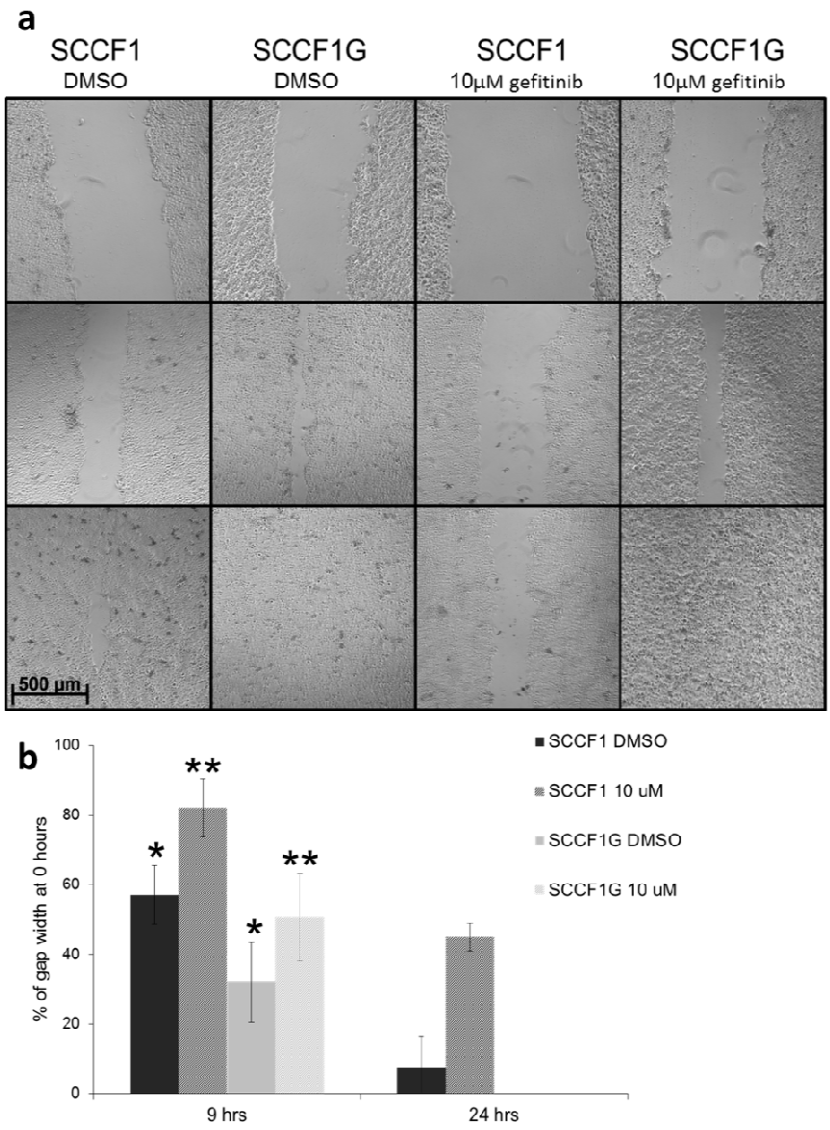

Figure 5.3 a) *In vitro* scratch assays comparing migratory ability of the two cell lines. Top row 0 hours, middle row 9 hours and bottom row 24 hours following gefitinib treatment. b) Histogram showing relative migration of cell lines after 9 and 24 hours. After nine hours, the DMSO control treated SCCF1 had closed the gap created for the assay by less than half while the SCCF1G cell line had reduced the width with over two thirds (*p<0.001, two sample *t*-test). Similarly, a dose of 10 μM gefitinib had different effect on the cell lines. At 9 hours the resistant cell line had reduced the gap width with approximately half compared to only a fifth in the parent cell line (**p<0.001, two sample *t*-test), and at 24 hours the resistant cell line had migrated and filled the gap completely while the parent cell line had only migrated approximately half way across the gap.

5.4.2 Optimisation of liposome mediated transfections increased the transfection efficiency in the SCCF1 cell line

The use of the *Silencer*® FAM™-Labelled Negative Control #1 siRNA allowed for direct visualisation and assessment of transfection efficiency using fluorescent microscopy. This method was used for the initial screening performed in a 24 well format where the SCCF1 cell line was transfected at three different confluences, two different concentrations of transfection agent and three different siRNA concentrations (Figure 5.4). The cells were assessed at 24, 48 and 72 hours after transfection. However, by 72 hours the wells where the cells had been transfected at 75% confluence became over-confluent and significant cell death started to occur making comparison between wells unfeasible. For that reason only the 24 and 48 hour time points were used to assess relative transfection efficiency. Best transfection efficiency was achieved with the higher amount of transfection agent using a concentration of 50 nM or 100 nM siRNA in the wells transfecting cells at low confluence. To further optimise the protocol, the transfections were repeated in a six well format on low confluence cells using the higher Lipofectamine: RNA ratio (Table 2.9) with 50 nM and 100 nM siRNA for flow cytometry assessment of cell viability and transfection efficiency. The cells were photographed again before being analysed (Figure 5.5).

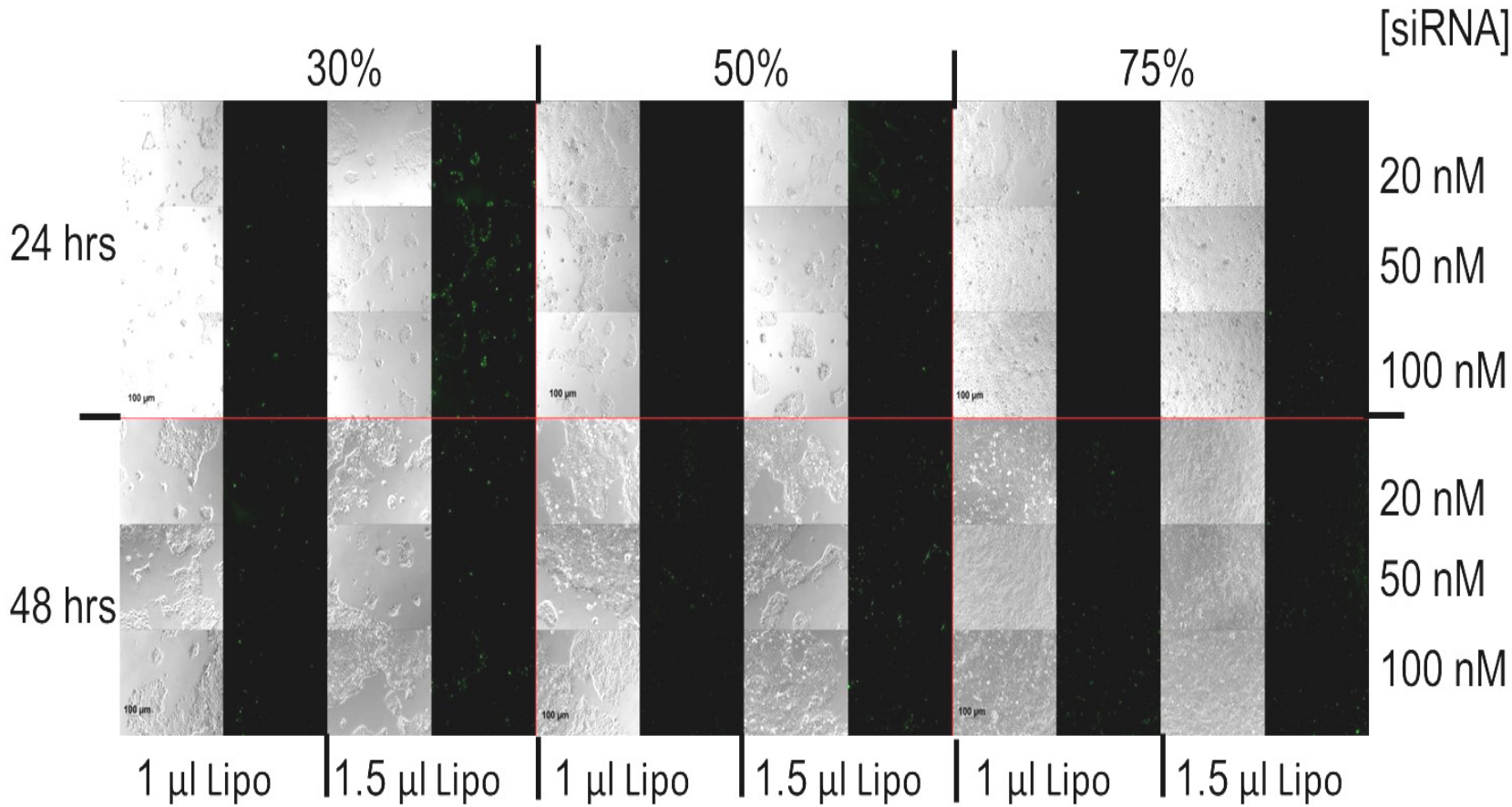
[siRNA]
30%
50%
75%
24 hrs
48 hrs
20 nM
50 nM
100 nM
20 nM
50 nM
100 nM
100 µm
1 µl Lipo
1.5 µl Lipo
1 µl Lipo
1.5 µl Lipo
1 µl Lipo
1.5 µl Lipo

Figure 5.4 (Figure on previous page): Fluorescent microscopy of the SCCF1 cell line using a FITC filter showed increased transfection efficiency seen as increased green fluorescence from cells. The cells were transfected in a 24 well format and photographed at 24 and 48 hours following transfections. The result of this screen showed that the cells exhibited maximum fluorescence at 24 hours after transfection. The cells transfected at confluency of less than 30% and with the higher siRNA concentrations and the higher Lipofectamine: RNA ratios showed the highest transfection efficiency.

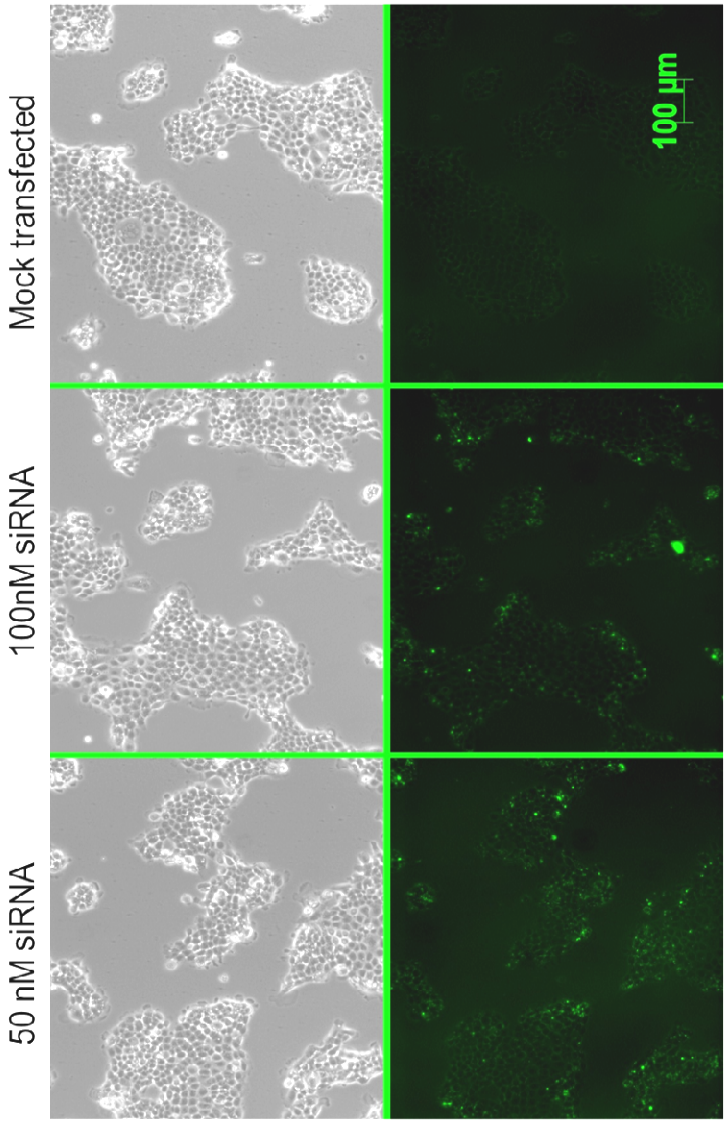

Figure 5.5: Fluorescent microscopy of SCCF1 cell line using a FITC filter. Photographs were taken 24 hours following transfection with two different siRNA concentrations using the higher Lipofectamine: RNA ratio and compared to mock transfected cells. Green fluorescence was observed in the siRNA transfected cells but not in the mock transfected control cells. No significant difference between the two siRNA concentrations was observed.

Flow cytometry showed that both 50nM and 100nM of siRNA produced approximately 69% transfection efficiency for both, but cells transfected with the lower siRNA concentration had better cell viability. The mock transfected cells had cell viability of 99% compared to 95% and 89% for the 50 and 100 nM siRNA concentrations respectively (Figure 5.6).

SCCF1 cell line DNA plasmid transfection optimisation was performed using the pmaxGFP™ plasmid in a similar manner with an initial screening using two transfection agents at different ratios between DNA and transfection reagent (Figure 5.7). Lipofectamine 2000™ gave far superior transfection efficiencies at all four ratios when assessed by fluorescence microscopy. The two highest DNA: Lipofectamine 2000™ ratios gave the best results, so these transfections were repeated in six and 96 well format. Transfection efficiency was estimated by flow cytometry to be 40% and 53% for the 1:4 and 1:5 ratios respectively. Cell viabilities for the two ratios were similar at 96% and 94% of untransfected cell viability respectively as assessed by CellTiter-Glo® Luminescent Cell Viability Assay. Increasing the transfection agent amount increased the transfection efficiency without a detrimental effect on cell viability, so the higher Lipofectamine 2000™ amount was used for all hairpin expression vector experiments.

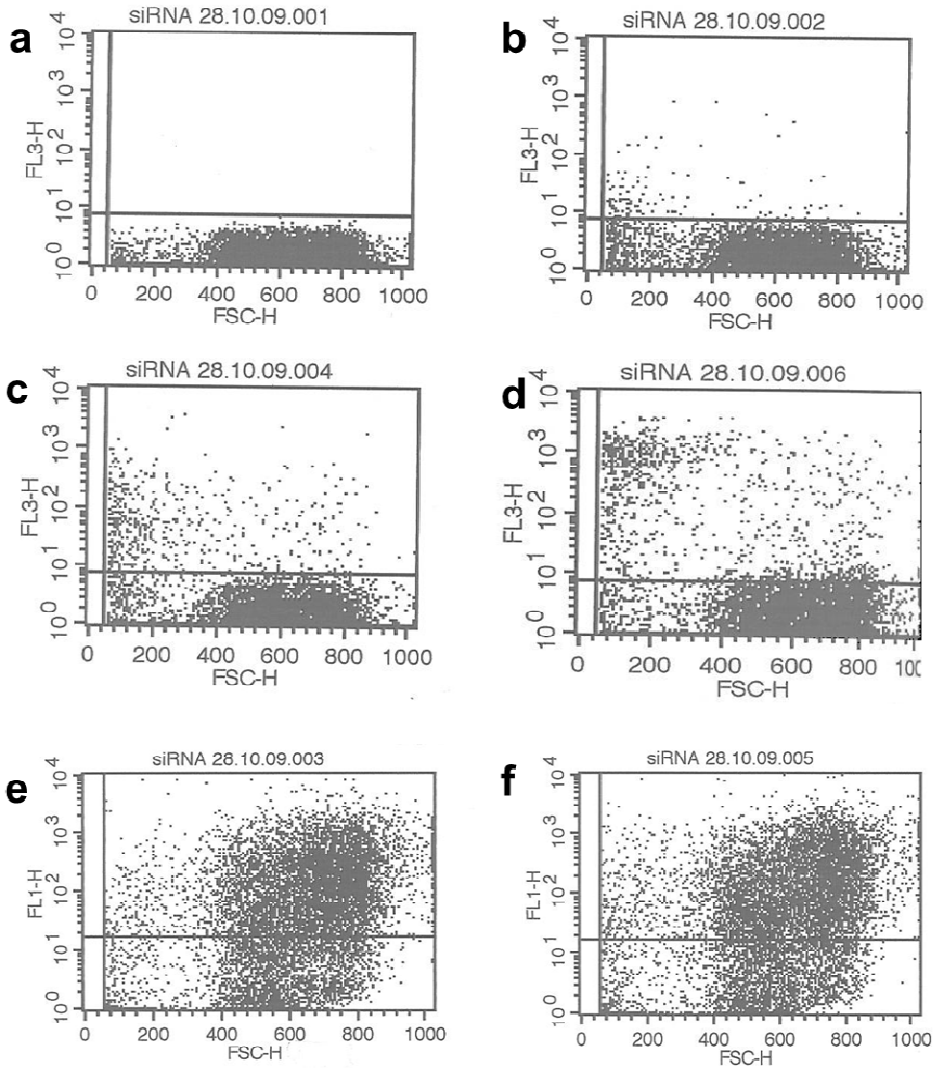

Figure 5.6: Flow cytometry results of siRNA optimisation. X-axis shows forward scatter (proportional to cell size) (a-f), plotted against FL3-H channel (detects GFP fluorescence) (a-d) and FL1-H channel (detects PI fluorescence) (e, f) on y-axis. Mock transfected SCCF1 cells with (a) no added PI allows for a cut off line to be set, and after adding PI (b) mock transfected SCCF1 cells are shown to exhibit 99% cell viability. SCCF1 cells transfected with 50nM siRNA (c) and 100nM siRNA (d), revealed cell survival of 95% and 89% respectively when adding PI. GFP fluorescence were positive in 68.5% (e) and 68.7% (f) of SCCF1 cells transfected with 50nM and 100nM pmaxGFP™ plasmid respectively.

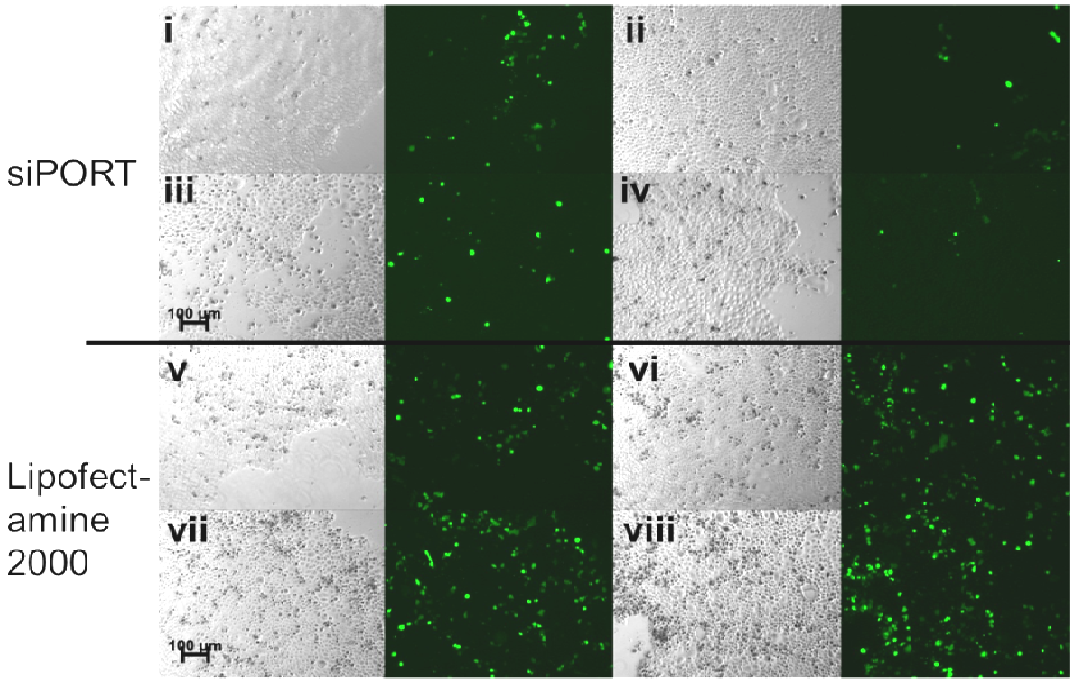

Figure 5.7: Transfection optimisation of SCCF1 cell line comparing two transfection agents (siPORT and Lipofectamine 2000™) at four different ratios assessed by fluorescent microscopy using a FITC filter. **i-iv:** siPORT: DNA ratios of 2:1, 3:1, 4:1 and, 3:2 respectively, **v-viii:** DNA: Lipofectamine ratios of 1:0.5, 1:2.5, 1:4 and, 1:5 respectively. Magnification: bottom left bar shows 100µm.

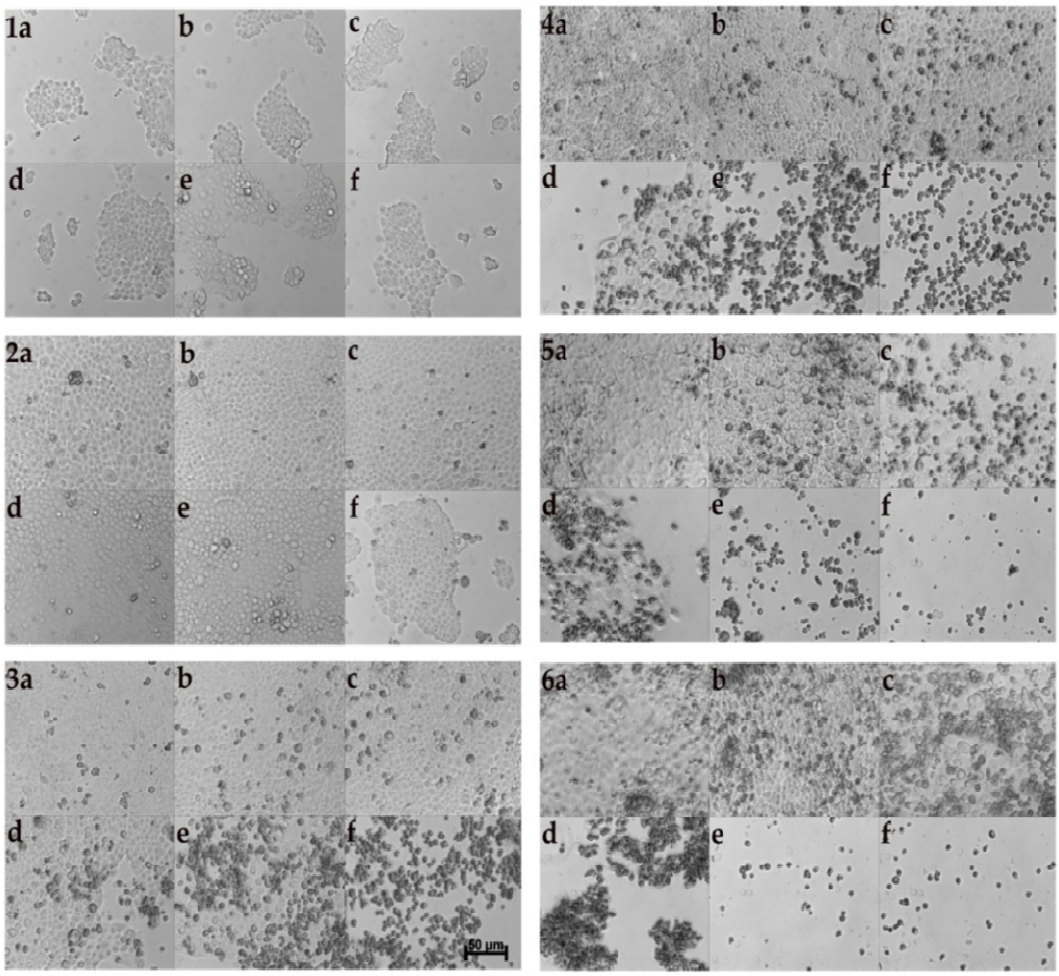

Figure 5.8: Kill Curve performed on SCCF1 cell line to determine G418 sensitivity a) no antibiotic added, b) 100 µg/ml, c) 200 µg/ml, d) 400 µg/ml, e) 800 µg/ml, f) 1600 µg/ml G418 added to media respectively. 1) 24 hours following seeding of cells when 1 ml of corresponding media a-f was added to each well already containing 1 ml of media without antibiotics, 2) 48 hours later after having been in G418-containing media only for 24 hours, no cell death was noted, 3) 96 hours in G418 containing media, cell death starting to appear in wells e & f, 4) 1 week of antibiotics and wells a & b are fully confluent, well c was 90% confluent, and wells d-f marked and massive cell death, 5) after 9 days a-c are all fully confluent while all cells are dead in e & f, while massive cell death was observed in well d, 6) wells a-c were now over-confluent while wells d-f all showed complete cell death.

5.4.3 G418 titration curve and optimal plating density results for SCCF1 cell line

The G418 titration curve of the SCCF1 cell line determined that a concentration of 0.4mg/ml G418 added to the normal William's E growth medium produced massive cell death in the SCCF1 cell line after seven days of culture (Figure 5.8). This G418 concentration was then used to determine an optimal cell density for seeding the SCCF1 cells 24 hours after transfection. Cells seeded at $6x10^4$ cells into a 24 well plate achieved 80% confluency before massive cell death occurred. This cell density was scaled up for a six well plate format giving an optimal cell density of $3x10^5$ cells seeded per well 24 hours following hairpin expression vector transfections. The optimal G418 concentration and the optimal cell density determined in these assays were used for all technical replicates in all the hairpin expression vector transfections.

5.4.4 The Real Time PCR primer pairs showed adequate primer efficiencies in the investigative range

All Real-Time PCR reactions used cDNA of at least 1:10 dilutions because, when using lower dilutions, an inhibitory action had been observed previously by colleagues in the lab (data not shown). After investigations by the Roche technical support team it was presumed to have been caused by an unidentified ingredient in the Roche Transcriptor High Fidelity cDNA Synthesis Kit reaction mixture (Dr Karen Tan, personal communications). This effect was also seen in the SCCF1 samples at cDNA reaction mixture dilutions of 1:5 (Figure 5.9), so all cDNA samples were diluted 1:10 before Real Time PCR reactions were performed.

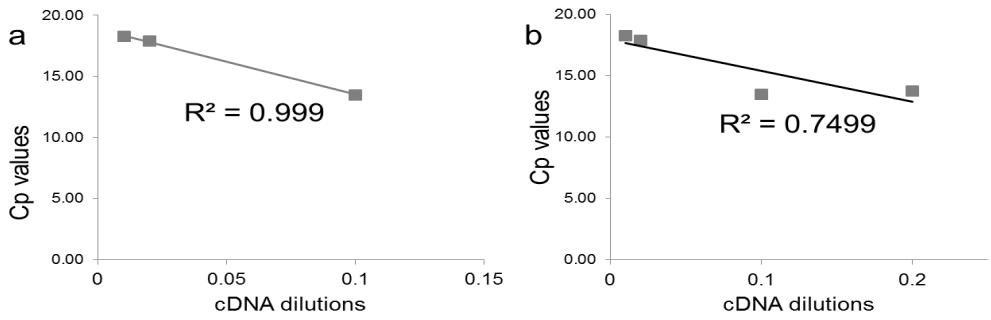

Figure 5.9: Graphs showing the inhibitory effect observed with higher cDNA dilutions using the 18s rRNA primers. Graph a) shows an example of a graph plotted to assess primer efficiency with the cDNA dilutions shown on the x-axis and the Cp values plotted on the y-axis. The R squared value is approximately one, b) shows when the 1:5 dilution Cp value is included, the R squared value is approximately 0.75. A marked inhibitory effect can be seen when the lower dilution is included.

Results of the evaluation of the efficiencies of the primer sets used for Real Time PCR reactions are summarised in Table 5.2. All primer sets used showed acceptable primer efficiencies in the investigative range, allowing for the delta-delta method to be used to assess relative mRNA levels.

Primer Set	E value	R^2 value	Pearson's correlation coefficient, (*p* value)
EGFR primers	2.07	1.00	0.991 (0.0001)
18 s rRNA primers	2.00	1.00	0.991 (0.0001)
β-actin primers	1.96	0.99	0.989 (0.0001)

Table 5.2: Table showing the results of the evaluation of primer efficiencies for Real Time PCR reactions.

5.4.5 Feline *Egfr* siRNA transfections cause reduced cell proliferation and EGFR knockdown in SCCF1 cell line

SCCF1 cells transfected with siRNA8 against the feline *Egfr* exhibited reduced proliferation ability compared to mock and scrambled transfected cells as well as untreated cells for up to 72 hours following transfection

(Figure 5.10a). Transfecting the cells with siRNA8 reduced cell proliferation to a level equivalent to that achieved with a 10 μM dose of gefitinib in the SCCF1 cell line (Figure 5.10b).

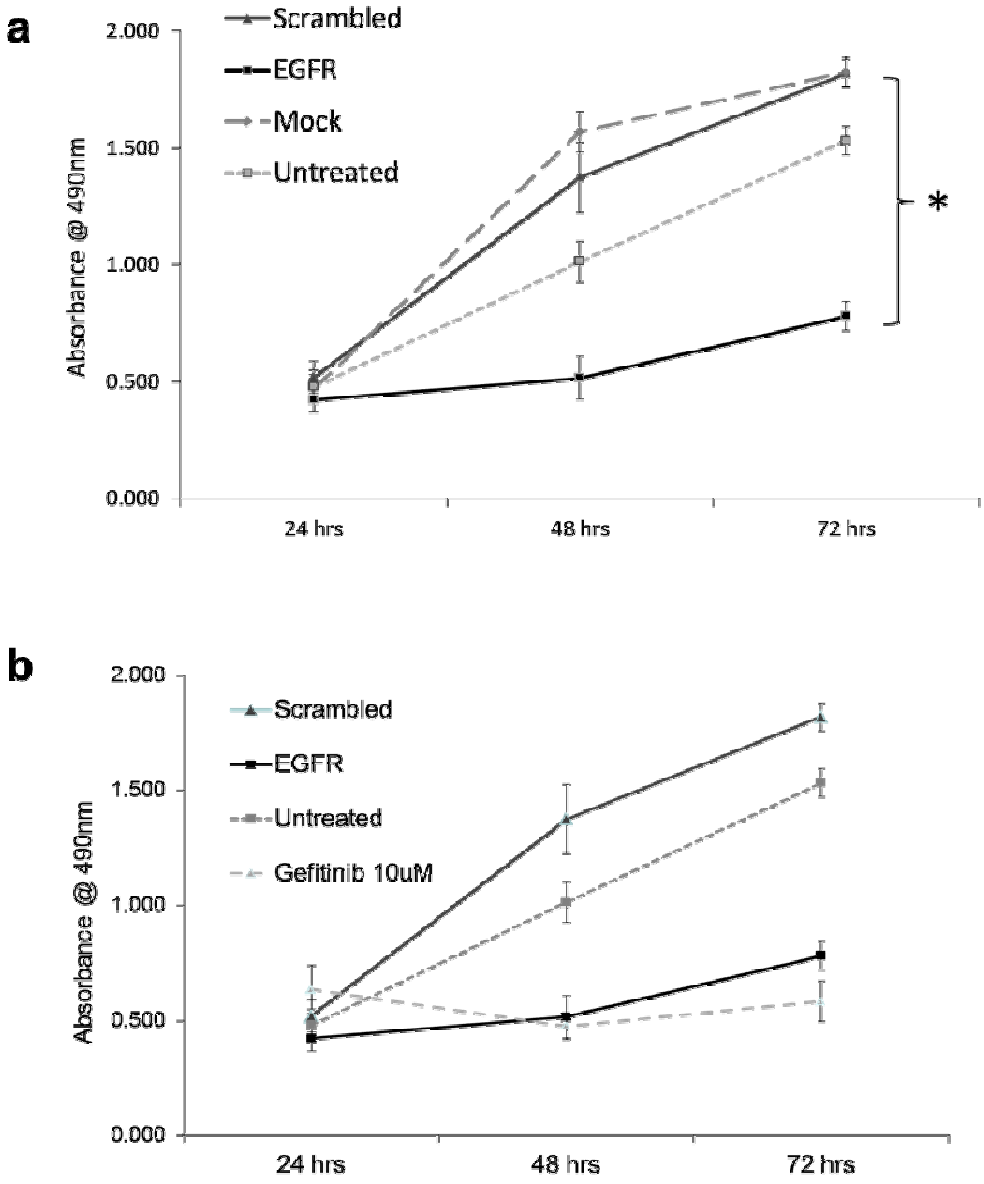

Figure 5.10: a) Cell proliferation assay showing proliferation of SCCF1 cells up to 72 hrs following siRNA8 transfections compared to untreated SCCF1 cells, mock and scrambled control transfected cells (* $p<0.0001$, at 48 and 72 hrs by One-Way ANOVA). b) Cell proliferation assay comparing the effect on proliferation of siRNA transfection against *Egfr* and gefitinib at 72 hours. A single transfection of cells with siRNA produced an equivalent effect to a 10 μM dose of gefitinib.

Real Time PCR revealed a 55% relative reduction in *Egfr* mRNA levels as compared to scrambled control transfected SCCF1 cells at 24 hours following transfection (Figure 5.11). Western blot analysis showed reduction in EGFR protein levels at 72 hours following transfection when compared to untreated cells and scrambled control transfected cells (Figure 5.12). To investigate the effect of *Egfr* knockdown on signalling pathways downstream of EGFR, western blot analyses were performed on markers of the major downstream elements of the EGFR signalling pathway in transfected cells. Reduction in phosphorylated Erk1/2 and phosphorylated STAT-3 were seen following *Egfr* knockdown, but phosphorylated Akt protein levels remained unchanged (Figure 5.13).

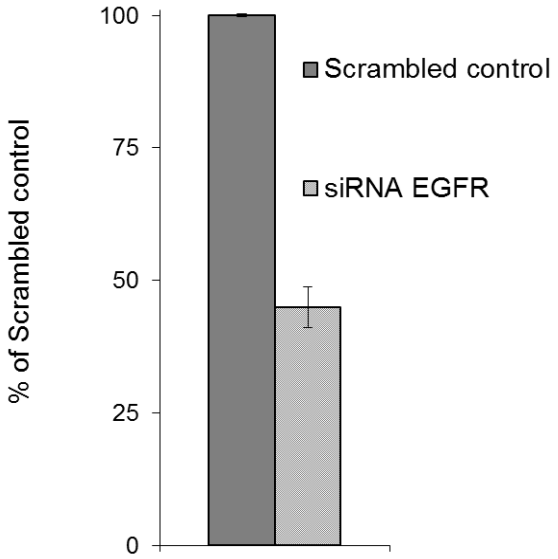

Figure 5.11: Histogram showing Real Time PCR result of EGFR mRNA levels in SCCF1 cells transfected with siRNA8 against the feline EGFR expressed as percentage of scrambled control levels. EGFR results shown are an average of triplicate transfections and each transfection was run in three technical replicates for the Real Time PCR analysis. Similar results were obtained in separate experiments. Bars show +/- standard deviation.

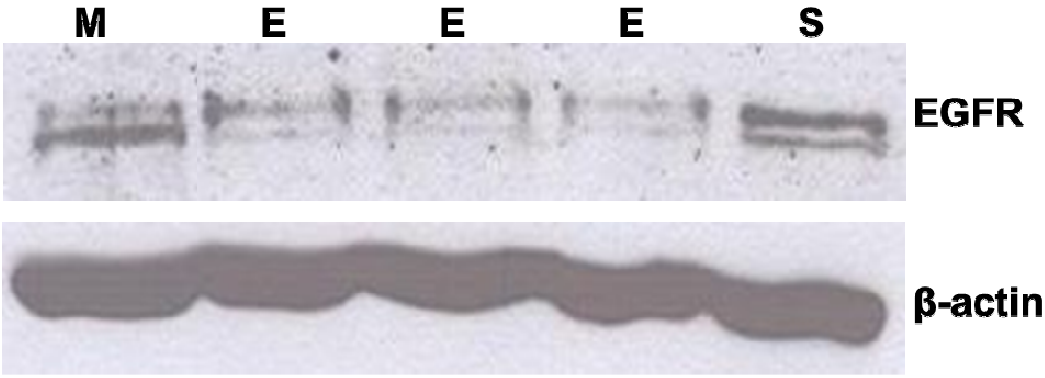

Figure 5.12: Western blot showing reduction in EGFR protein levels 72 hours post siRNA transfection of SCCF1 cell line. Lysates from mock transfected (M) and scrambled control transfected cells (S) are show next to lysates from SCCF1 cells transfected with siRNA8 against the feline EGFR in triplicate (E). The lower band on gel show β-actin protein levels as a loading control. Similar results were obtained in separate experiments.

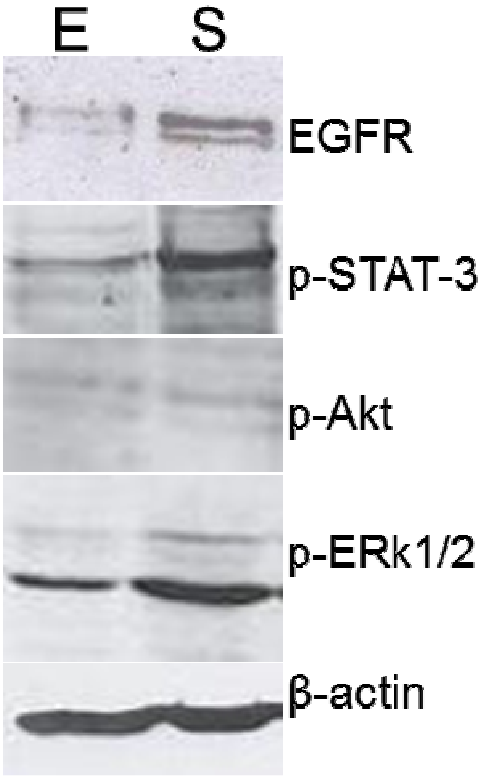

Figure 5.13: Western blot showing levels of phosphorylated downstream targets of EGFR in siRNA8 transfected SCCF1 cells (E) compared to scrambled control transfected cells (S). A reduction was seen in phosphorylated STAT-3 and Erk1/2 levels but not in Akt phosphorylation levels.

5.4.6 siRNA transfections rescue gefitinib resistance in cell line

Transfection of the resistant SCCF1G cell line with siRNA8 rescued the gefitinib resistance in the cell line and produced a marked reduction in cellular proliferation at 72 hours following transfections when compared to mock transfected cells. In comparison, gefitinib treatment at 5 μM of the resistant cell line caused no significant reduction in proliferation when compared to DMSO control (p=0.898, two sample t-test), and 10 μM of gefitinib only had a modest effect on proliferation (Figure 5.14).

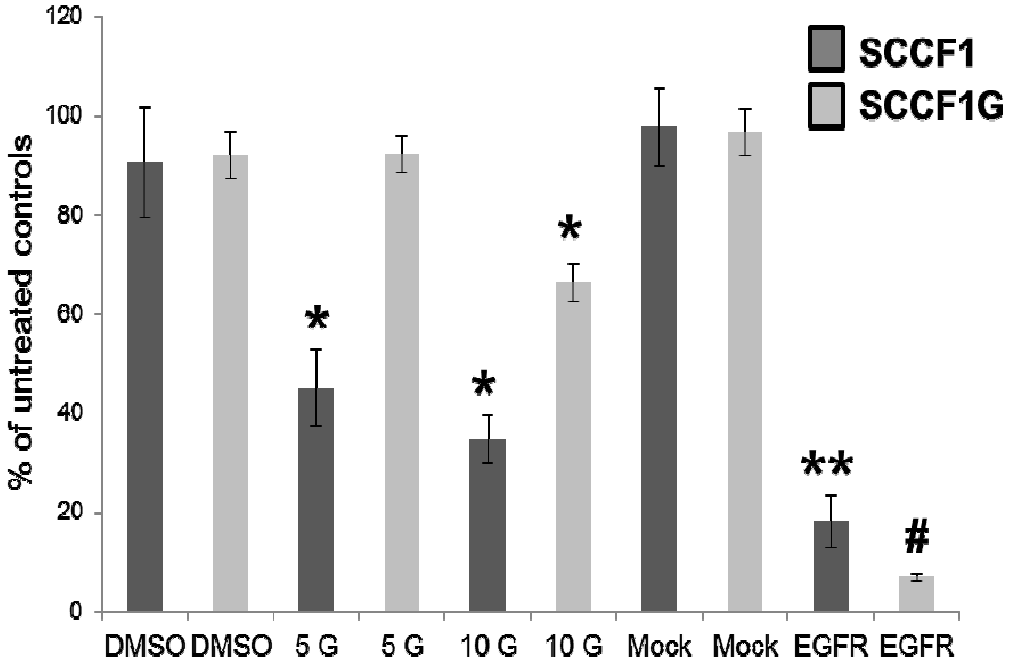

Figure 5.14: Mock transfections and DMSO treatments of both cell lines had minimal effect on proliferation, while gefitinib treatment and EGFR siRNA transfections caused marked effects on the SCCF1 cell line. The SCCF1G cell line exhibited resistance to doses of gefitinib of up to 10 μM while siRNA transfections against the feline EGFR still caused reduction in proliferation in the cell line. Bars show standard deviations, * p<0.001, ** p<0.001 compared to DMSO control and mock transfected respectively by two sample t-test, # p= 0.005 compared to mock transfected cells by Mann Whitney U test.

5.4.7 Hairpin expression vectors cause long term knockdown of EGFR and reduced proliferating ability and colony formation in the SCCF1 cell line

Real Time PCR analysis (Figure 5.15) showed variable reduction in *Egfr* mRNA levels in sh*Egfr* transfected cells compared to scrambled control transfected cells with an average reduction of 35% (SD 18%, range 10-53%). Similarly, western blot analysis (Figure 5.16) of cell lysates produced three weeks after transfection showed variable reduction in EGFR protein levels when compared to scrambled controls.

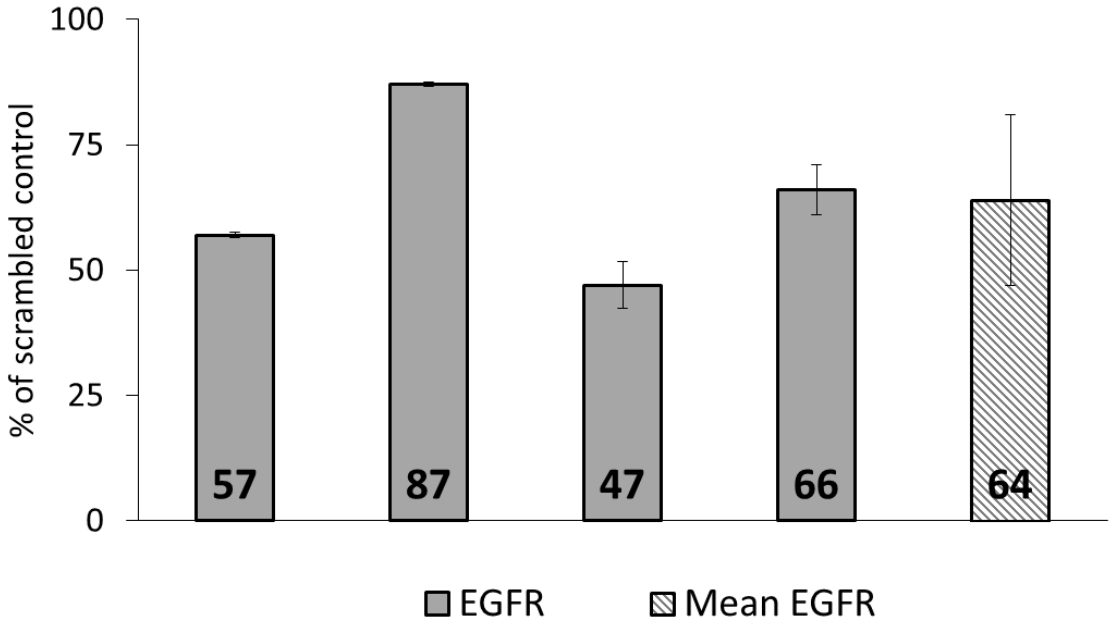

Figure 5.15: Real Time PCR results showing EGFR mRNA levels as percentage of scrambled control in hairpin expression vector transfected SCCF1 cells after 3 weeks culture in selective G418 containing media. Each individual result is representative of three technical replicates run from separate transfection experiments, bars shows +/- standard deviations.

Figure 5.16: Western blot showing variable reduction in EGFR protein levels in two lysates from different hairpin vector transfections. MDA-MB (lane 1) contain lysate from the MDA-MB-468 cell line (MD Anderson Cancer Centre, Texas, USA), a human breast cancer cell line that overexpresses EGFR. It was used as positive control to validate the antibody for the use on feline protein lysates. Lanes 2-5 contains lysates from SCCF1 cell line: EGFR: transfected with vector expressing shRNA against EGFR, Scram: transfected with vector with scrambled control sequence, SCCF1: untransfected cells. Protein loaded: 30 µg MDA-MB, 60 µg remaining samples. Lower bands show β-actin for loading control.

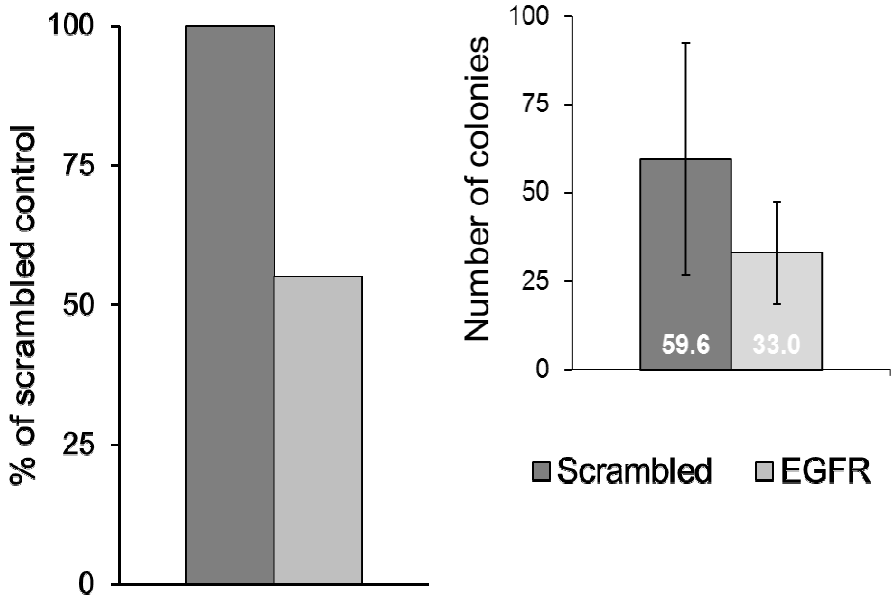

Figure 5.17: Colony formation assay performed during 3 weeks of G418 selection post hairpin expression vector transfection. A 45% reduction in colony formation ability was seen in the sh*Egfr* transfected cells when compared to scrambled control transfected cells. Inset shows average number of colonies counted with bar showing standard deviation. Bars are average of 8 (sh*Egfr*) and 9 (Scrambled) 10 cm plates for each sample and represent transfections performed in triplicate. The difference in colonies showed a trend towards statistical significance (p=0.06, Mann Whitney U-test).

Colony formation assays were performed during antibiotic selection (Figure 5.17) and after 20 days of antibiotic selection of cells (Figure 5.18). The ability of the cell lines to form colonies was reduced on average by 45% and 22% compared to scrambled control transfected cells during and after antibiotic selection, respectively.

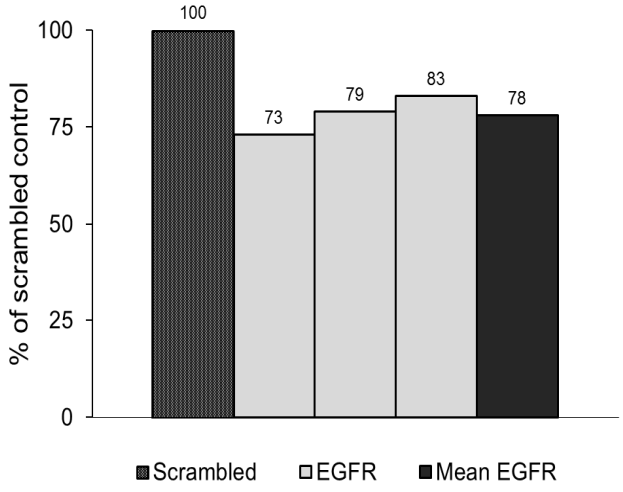

Figure 5.18: Histogram showing average number of colonies formed (light grey bars show individual counts, while the dark grey bar shows the average of the three counts) when CFA were set up after 20 days of G418 selection of SCCF1 cells following transfections. EGFR knockdown still had some effect on colony formation ability (on average 22% reduction compared to scrambled control transfected cells) for up to 5 weeks after transfections, but the effect was reduced compared to during the first three weeks (Figure 5.16).

Cell proliferation assays performed on the cell line after 20 days of antibiotic selection (Figure 5.19) showed a statistically significant difference between the cell proliferation rates at all three time points. The effect on cell proliferation observed after the G418 selection period was less pronounced compared to the effect observed in transiently transfected cells (Figure 5.10).

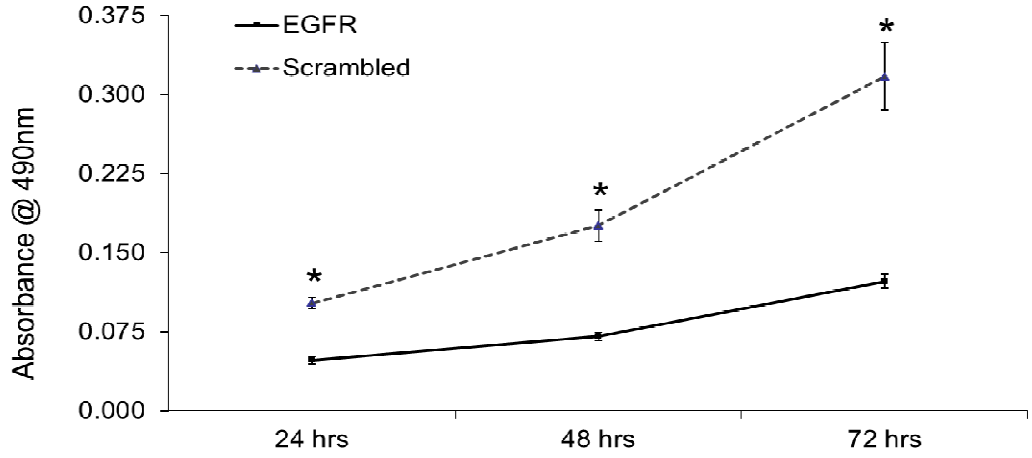

Figure 5.19: Cell proliferation assay showing SCCF1 cell lines proliferating ability after 20 days of selection with G418 containing media. EGFR transfected cells showed a statistically significant lower proliferation rate when compared to scrambled transfected cells at 24, 48 and 72 hours following seeding into 96 well plates (* p=0.001, p=0.003 and p<0.001 respectively, two sample t-test). Each point shows an average absorbance value of four wells with the background subtracted, bars show standard deviation. Similar results were obtained in two separate experiments.

5.4.8 Radiation and EGFR knockdown show an additive effect in the SCCF1 cell line

To investigate the effect of *Egfr* targeting in combination with conventional therapies a radiosensitivity assay was performed. Radiation doses of up to 5 Gy had no effect on SCCF1 cell line proliferation ability 72 hours following irradiation (Figure 5.20). The modest effects seen of *Egfr* knockdown by siRNA or treatment with gefitinib were not enhanced by any of the radiation doses used (Figure 5.20).

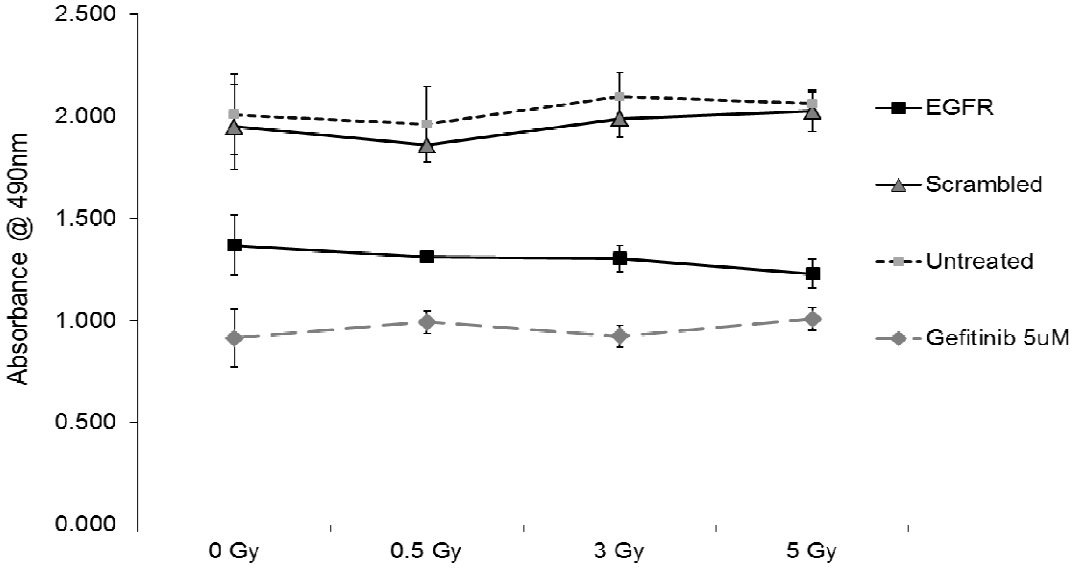

Figure 5.20: Cell proliferation assays performed 72 hours following radiation treatment and 96 hours after transfection and gefitinib treatment. The radiation treatments had minimal effect on cell proliferating ability at this early stage following therapy. The EGFR targeting has had some effect on cell proliferation when compared to scrambled and untreated controls, but no enhancement is seen at any of the radiation doses. Each point on the chart represents an average of absorbance readings from six wells with bars showing standard deviations.

However, ten days after radiation exposure, colony formation assays showed a dose dependent reduction in colony formation ability in the irradiated cells which was enhanced in the siRNA8 but not the scrambled-control transfected or gefitinib treated cells (Figure 5.21). An additive but not a synergistic effect was seen when siRNA8 transfections were combined with irradiation according to the Bliss Additivism model (Figure 5.22).

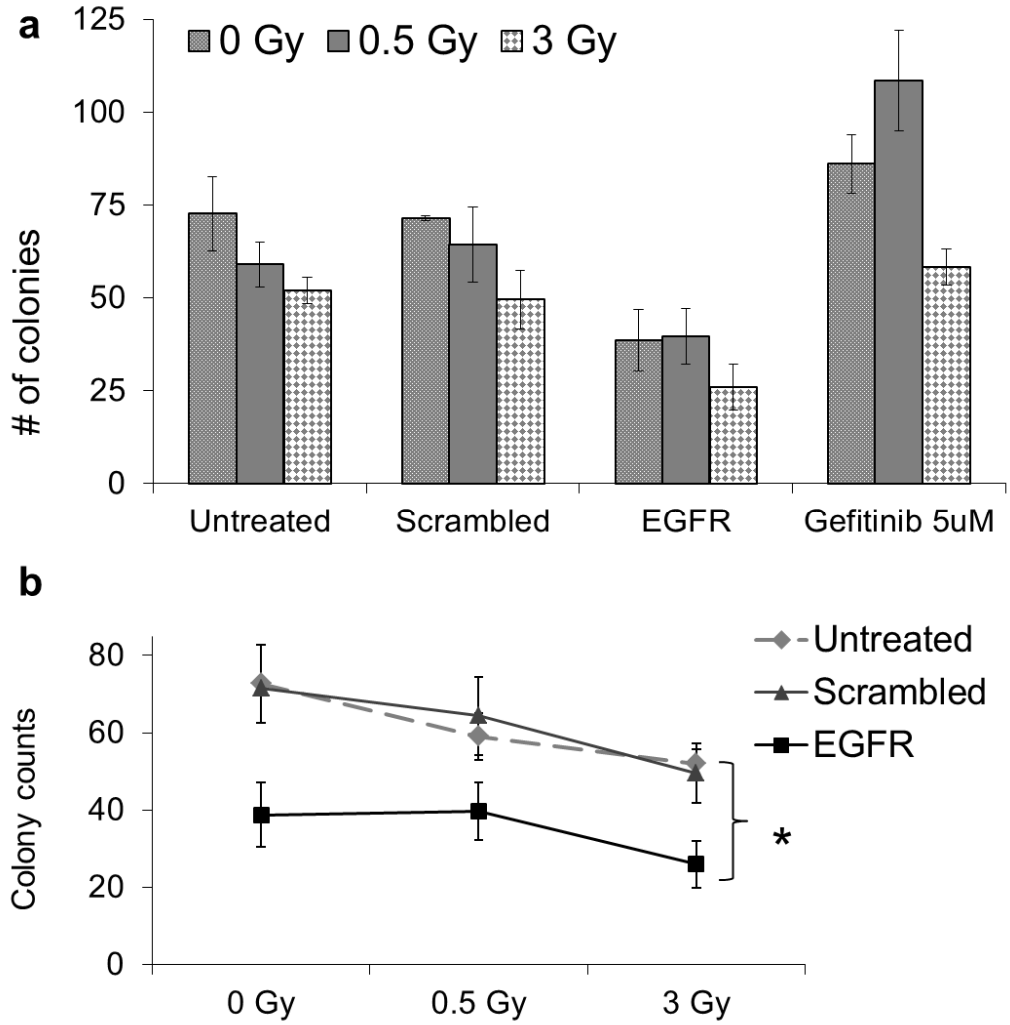

Figure 5.21: a) Histogram showing colony formation assay following EGFR targeting by either siRNA or with gefitinib in combination with radiation doses of 0, 0.5 and 3 Gy compared to untreated and scrambled control transfected cells. Gefitinib at a dose of 5 μM had no effect on colony formation ability compared to *Egfr* targeting by siRNA. b) Graph comparing colony formation ability of untreated cells and cells transfected with scrambled control and siRNA8 against *Egfr* over the range of radiation doses, * $p<0.05$ by two sample *t*-test.

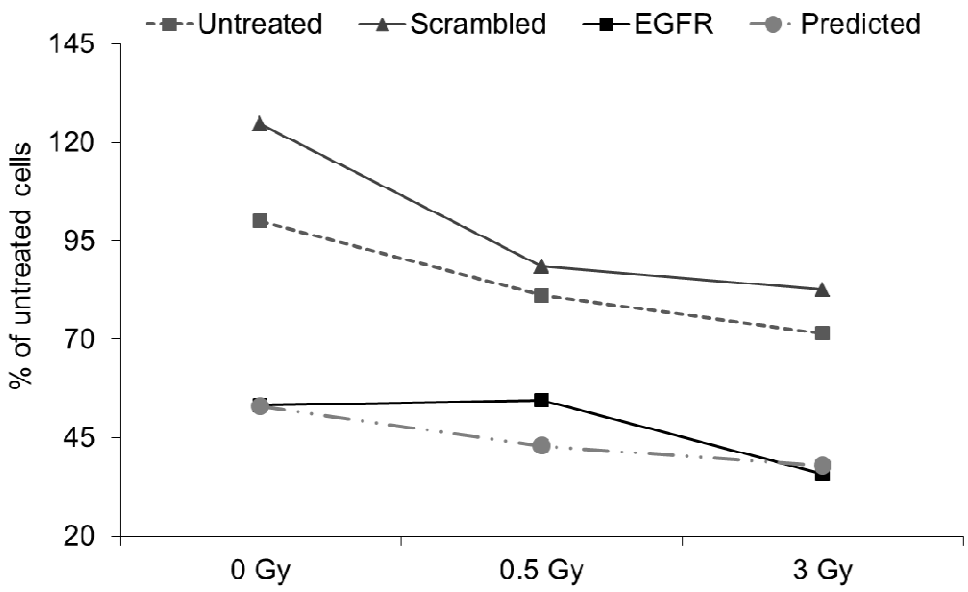

Figure 5.22: Graph showing additive effect of combining EGFR siRNA8 knockdown and radiation. The predicted graph show the calculated E_{bliss} values expected if radiation treatment and EGFR inhibition were causing an additive effect according to the Bliss Additivism Model. The graph showing the effect of combined siRNA8 EGFR transfection and radiation treatment from the experiment runs roughly parallel to the predicted graph.

5.5 Discussion

Small molecule TKIs like gefitinib bind to the ATP binding pocket in the tyrosine kinase domain of the receptor and block phosphorylation (Arteaga, 2003). Since the ATP binding pocket was conserved in the feline cell line (Chapter 4), we hypothesised that human drugs like gefitinib would be effective against the feline receptor. As RNAi targeting feline *Egfr* was an unproven approach to EGFR inhibition, gefitinib was assessed in tandem with the RNAi strategies.

In this study gefitinib did effectively reduce cellular migration and proliferation in the feline cell line, but at the relatively high dose rate of 10μM. An *in vitro* dose of gefitinib of 1 μM is equivalent to a clinical dose of

250 mg per day used in NSCLC (Sharma et al., 2007). In NSCLC *in vitro* studies doses of gefitinib above 2 μM would class the cell line as insensitive to the drug (Sharma et al., 2007). Early studies on HNSCC cell lines used much higher doses than this (Huang et al., 2002) while more recent studies all have used doses below 2 μM gefitinib (Huang et al., 2004, Erjala et al., 2007). In conclusion, the SCCF1 cell line can therefore be classed as being relatively insensitive to gefitinib, requiring a relatively high dose (when compared to therapeutic doses of gefitinib currently used in man) in order to show a significant effect on proliferation and migration. Following chronic exposure to gefitinib the cell line became resistant to the drug, further reducing its effect on the ability of the cell line to proliferate and migrate.

Development of resistance to TKIs during treatment is well documented in human cancers, and mutations in the tyrosine kinase domain of the receptor are one of the mechanisms involved. In NSCLC in man, the T790M mutation in the tyrosine kinase domain has been associated with the development of resistance to gefitinib (Wheeler et al., 2010a). It results in a substitution of methionine for threonine in the ATP binding site increasing the receptor affinity for ATP (Wheeler et al., 2010a). To evaluate if a similar mechanism was responsible for development of resistance in this cell line, the ATP binding pocket of *Egfr* in the resistant cell line was sequenced but, as no mutations were found, this was not the mechanism of resistance in these cells. This is similar to the development of resistance to TKIs in HNSCC in which tyrosine kinase mutations of *Egfr* are rare events (Chen et al., 2010). The mechanism of the development of acquired gefitinib resistance in the SCCF1G cell line in this study is not known, but some of the previously reported mechanisms of resistance could be consistent with an apparent resistance to tyrosine kinase inhibition but not to siRNA. Nuclear

translocation has been implicated in resistance to the monoclonal antibody cetuximab (Li et al., 2009). Although it has been suggested that small molecule TKIs affect nuclear EGFR (Li et al., 2009), their relative efficiencies in the nucleus are unknown. siRNAs exert their effect mainly in the cytoplasm of cells (Kittler and Buchholz, 2003), but if efficient will reduce nuclear as well as membranous and cytoplasmic receptor levels. Increased expression of receptor ligands (Li et al., 2009) would have limited effect on transfected cells as the receptor levels would be markedly reduced. If the cells upregulated other members of the receptor family like for example ErbB3 (Wheeler et al., 2008), the siRNA would not be expected to be effective. A novel resistance pathway relies on transactivation of EGFR by the cytosolic tyrosine kinase Src (Chaturvedi et al., 2009). siRNAs targeting *Egfr* would still be effective in this scenario as the reduction in receptor protein levels would counteract the increased phosphorylation. Likewise, if the receptor ubiquitination and degradation pathways were dysregulated (Shtiegman et al., 2007), siRNAs targeting *Egfr* would still be effective. Regardless of the mechanism used by the cells in this study, the net effect was that resistance to gefitinib could be reversed by using siRNA to target *Egfr*. As discussed, the vast majority of the resistance mechanisms reported in the literature would be less effective against RNAi targeting. RNAi works on the mRNA level, while the majority of the resistance mechanisms are modifications affecting the cell at the protein level. This study illustrated how the resistant cancer cells were still dependent on EGFR for proliferation, despite acquiring resistance to an EGFR targeting drug. This suggests that the resistance mechanism used by the cell line in this study circumvented the effect of the drug not by relying on other pathways but by a mechanism that rendered the drug ineffective against EGFR.

RNAi was used in this study as it is a highly selective method of evaluating the effect of gene silencing of a target gene (Pai et al., 2006). We demonstrated that our siRNA8 *Egfr* reduced both *Egfr* transcripts and EGFR protein in the SCCF1 cell line. The relatively poor reduction of *Egfr* mRNA levels seen in this study with a reduction in mRNA levels of on average 55% (siRNA) and 35% (shRNA) would class the siRNA8 sequence as an non-functional siRNA by some authors (Khvorova et al., 2003). The SCCF1 cell line was found to have a relatively low basal level of *Egfr* mRNA with Cp values in the mid-twenties as seen when testing primer efficiencies for Real Time PCR reactions using untreated SCCF1 cDNA. Similarly, when comparing protein levels of EGFR with the human EGFR overexpressing cell line MD-MBA-468 by western blot analysis, the SCCF1 cell line had a low basal level of receptor expression (Figure 5.16). It is tempting to speculate that when starting from such a low level of transcript, the relative reduction achieved is likely to be less pronounced. The net effect in the cell line did nonetheless translate into a measurable reduction in protein level and a profound effect on cell proliferation and colony formation ability and this effect could be sustained over time. This study supports the observation that the level of EGFR expression in tumours does not necessary directly correlate with tumour EGFR dependency and response to EGFR targeting therapy as was first anticipated (Wheeler et al., 2010a). These results demonstrated that EGFR is an important oncogenic driver in this model of feline oral SCC despite the relatively low receptor level present in the cell line, and that targeting EGFR in feline oral SCC has potential as a therapeutic strategy. It also does, however, show that not all EGFR targeting strategies are equally effective.

This study also investigated the effect of EGFR targeting on the pathways downstream of the receptor and demonstrated that the MAPK and STAT3 pathways involved in cell proliferation and angiogenesis were downregulated while the PI3K pathway was not. A marked reduction in proliferation seen following EGFR knockdown is consistent with a reduction in phosphorylation in these two pathways. Although EGFR has been shown to directly activate the PI3K pathway mediated by growth factor receptor binding 2 (Grb-2)-associated binding protein 1 (Gab1) (Cao et al., 2009), ErbB3, a closely related member of the *Egfr* gene family, is the major activator of the PI3K pathway with six separate phosphorylation sites for the p85 subunit of PI3K (Baselga and Swain, 2009). EGFR targeting may be less likely to cause a major reduction in PI3K pathway activation if ErbB3 receptor remains active. The clinical responses to EGFR targeting therapies in human trials have so far been modest (Ratushny et al., 2009) and this may be because tumours have an intrinsic resistance to EGFR-targeted therapy (Li et al., 2009, Ratushny et al., 2009). These problems may be overcome by using combination therapies that target these alternative resistance pathways and by improved selection of patients that are more likely to respond to EGFR targeting (Ratushny et al., 2009). The results of this study suggest that inhibiting Akt concurrently may improve the response to EGFR targeting.

Part of effective clinical application of *Egfr* RNAi is likely to include inducing prolonged EGFR inhibition to have a sustained effect in tissues. Direct transfection of siRNA molecules produces only transient inhibition of *Egfr* gene expression as siRNA molecules become depleted or destroyed (Pai et al., 2006). To evaluate the effect of sustained *Egfr* gene knockdown, a plasmid that expressed short-hairpin RNA molecules was developed. This study demonstrated that a hairpin expression vector can be effectively taken

up by cells and lead to sustained production of shRNAs. The short hairpin expression vector transfection efficiency was lower than the naked siRNA transfection efficiency (53% vs. 69% for plasmid and siRNA transfections respectively). To counter this effect, antibiotic selection was used to enrich for cells incorporating the expression vector. Despite selection, the efficacy of gene knockdown and the variability between transfection replicates were greater when using hairpin expression vectors compared to naked siRNAs. Possible explanations for this include that some clones may have developed resistance to the shRNAs by acquiring mutations rendering them insensitive to interference by the shRNA. Alternatively, as experiments have shown, between 1-10% of vectors integrated into the genome during stable transfection experiments are not intact (Recillas-Targa, 2006). These clones may have acquired the antibiotic resistance gene without acquiring functionally intact shRNA expression. Considering that EGFR knockdown is deleterious to cell proliferation, these clones would have a growth advantage over the cells expressing shRNAs against the feline *Egfr*. Whichever mechanism was at play in this study is unknown. It highlights however, the limitations of RNAi techniques for therapeutic use; achieving efficient and reliable tissue delivery remains a major obstacle for the development of RNAi therapeutics.

In HNSCC the role of chemoradiation is well established (Ratushny et al., 2009), and a monoclonal antibody targeting EGFR, cetuximab, has been given FDA approval for use in combination with radiotherapy for HNSCC (Lurje and Lenz, 2009, Ratushny et al., 2009). Combination of EGFR targeted therapy and radiotherapy for management of feline oral squamous cell carcinoma is attractive as EGFR-mediated therapy may be able to augment the efficacy of radiotherapy, an established treatment option (Fidel et al.,

2007). Combined therapy with radiation and RNAi against feline *Egfr* produced an additive effect similar to that observed in human HNSCC cell lines (Huang et al., 2002, Zhang et al., 2009) and xenograft models (Huang et al., 2002). A study investigating the effect of cetuximab in combination with cisplatin and irradiation in HNSCC cell lines reported an additive effect in five cell lines while two cancer cell lines exhibited a synergistic effect (Zhang et al., 2009). When comparing EGFR basal and phosphorylated levels between the cell lines exhibiting additive versus synergistic effects, they found that the cell line that exhibited synergy had a much higher basal level of EGFR and that the receptor became phosphorylated upon irradiation (Zhang et al., 2009). This supports the theory that overexpressing EGFR cell lines are more likely to respond to EGFR targeting therapy (Erjala et al., 2006), although as previously discussed, not all tumour types exhibit a direct correlation between EGFR expression levels and response to therapy (Wheeler et al., 2010a). In these responsive cell lines combination treatments are thought to act synergistically because the cell lines utilise EGFR pathways like the PI3K and MAPK pathways to counteract the effect of radiation (Thariat et al., 2007). When these pathways are blocked, the cells become more sensitive to radiation (Thariat et al., 2007).

As previously discussed, the SCCF1 cell line has a relatively low basal level of EGFR. HNSCC cell lines with low basal levels of EGFR showed additive rather than synergistic effects when cetuximab was combined with radiation (Zhang et al., 2009), which is similar to the findings in this study. EGFR-targeted therapy may be of clinical value in augmenting radiotherapy in feline oral SCC but tumours expressing higher EGFR levels may be more sensitive to combined treatment.

In contrast to the *Egfr* transfected cells, the gefitinib treatment of cells in combination with irradiation had no effect on colony formation in the cell line. As previously discussed, a 10 μM dose of gefitinib was required to produce an equivalent effect on cell proliferation as transfection with siRNA8 against the feline *Egfr*. A 5 μM dose was chosen for the combined treatment in order to use a sub-lethal dose that should still produce a significant reduction of proliferation in the cell line, but that would be closer to the therapeutic dose of the drug used in patients (Sharma et al., 2007). Gefitinib at this dose did not produce any beneficial effect when used in combination with radiotherapy, suggesting that therapeutic use of this drug in feline patients would necessitate a relatively higher daily dose than that currently used in man.

In this study RNAi was used for EGFR targeting, and it proved to efficiently reduce the target protein levels and cell proliferation in the cell line. RNAi techniques have wide research applications and are now showing promise for therapeutic use (Pai et al., 2006). RNA interference may prove to be a powerful tool for the new generation of targeting therapies where acquired resistance to drugs has developed over time. In a recent study, transfection of cetuximab resistant HNSCC cell lines with siRNA against EGFR reversed the acquired resistance in the cell lines (Wheeler et al., 2008). This is similar to the findings in this study, where transfection of the gefitinib resistant cell line caused similar reduction in cell proliferation as in the non-resistant parent cell line SCCF1. The major obstacle to wider clinical use of RNAi-based drugs is the lack of a good *in vivo* delivery system (Pai et al., 2006) but this area is advancing and the first siRNA-based clinical trial using a nanoparticle delivery system has recently been reported (Davis

et al., 2010). If a suitable delivery vector can be found, RNAi may become an attractive option for achieving EGFR-targeted therapy.

Feline SCCs are naturally occurring tumours that have developed in pet animals which possess an intact immune system and which share their environment with man. The aetiopathogenesis of the disease in cats is not fully characterised, but environmental factors similar to those in human patients have been postulated as risk factors (Tannehill-Gregg et al., 2006). Evaluating drug strategies in naturally occurring disease in pets may help bridge the gap between *in vitro* research and clinical application in man (Paoloni and Khanna, 2008). This study supports the use of feline SCC as a model for HNSCC, an approach that could potentially benefit both felines and humans alike. During the development of a TKI against KIT (SU11654, toceranib) (London et al., 2009) the human field benefitted greatly from the canine studies (Paoloni and Khanna, 2008), and the development of acquired resistance to single-agent TKIs in dogs with mast cell tumours is of particular interest (Paoloni and Khanna, 2008). Further studies in cats with SCCs using EGFR targeting siRNA based therapies in combination with radiotherapy would potentially advance the treatment of the disease in both species.

5.6 Summary

Two methods of EGFR targeting were investigated in a feline SCC cell line. Following extensive optimisation of all the methods used, this study showed that both RNA interference techniques and a TKI, gefitinib, reduced cell proliferation and migration in the cell line. Targeting of EGFR using RNA interference caused a reduction in *Egfr* mRNA and protein levels, and the effect could be sustained over time when using hairpin expression vectors. EGFR targeting with RNAi also reversed acquired gefitinib resistance in the cell line, and produced an additive effect when used in

combination with radiotherapy. These results support the use of EGFR targeting as a viable therapeutic strategy for the management of feline oral SCC. Further studies in cats with SCCs using EGFR targeting siRNA based therapies in combination with radiotherapy would potentially advance the treatment of the disease.

Chapter 6:

Mechanisms of resistance to cancer therapies in the SCCF1 cell line

6.1 Abstract

Tumours consist of heterogeneous populations of cells that exhibit different sensitivities to cytotoxic therapies and irradiation. These subpopulations of cells utilise a range of mechanisms to evade apoptosis, and are effectively selected for when using current cancer treatment strategies causing development of resistance from previously sensitive tumours over time. Two mechanisms that have been implicated in tumour progression are cells undergoing an epithelial to mesenchymal transition (EMT) and the presence of a subpopulation of stem cell-like cells with inherent drug resistance in tumours.

In this study the gefitinib resistant SCCF1G cell line underwent morphological changes consistent with an EMT. Both SCCF1G and the parent cell line SCCF1 were investigated for markers of EMT and for their ability to form tumour spheres in non-adherent conditions. The presence of CD133 positive stem cell-like cells was investigated in the cell lines and the subpopulations were tested for inherent resistance to radiotherapy as well as to cytotoxic drugs.

The SCCF1G cell line had increased levels of fibronectin, vimentin and Slug consistent with an EMT but unchanged levels of E-cadherin and β-catenin. Both cell lines formed spheres in non-adherent conditions and contained a CD133 positive subpopulation. Resistance to gefitinib and to irradiation were increased in the SCCF1 CD133 positive population and overall in the SCCF1G cell line. The SCCF1G cell line had an increased CD133 positive subpopulation compared to the parent cell line, similar to an epithelial-mesenchymal to stem-like transition.

6.2 Introduction

Tumours of epithelial origin are by far the most commonly diagnosed group of cancers in man accounting for 80% of tumours (Visvader and Lindeman, 2008). Despite recent advances in the treatment of these tumours, they are still a major cause of death worldwide (Visvader and Lindeman, 2008, Harper et al., 2010). Death is usually due to tumour recurrence following treatment caused by resistance to therapies including EGFR targeting drugs developing in initially responsive tumours (Harper et al., 2010). Several mechanisms including epithelial to mesenchymal transition (EMT) (Wheeler et al., 2010a) and the presence of a subpopulation of stem cell-like cells with inherent drug resistance (Visvader and Lindeman, 2008) have been implicated in tumour progression and the development of resistance to therapy.

EMT is a fundamentally important, reversible cellular mechanism that occurs during development and wound healing. It allows tightly anchored epithelial cells to break down their cellular adhesions and acquire migratory and invasive properties (Barr et al., 2008, Thiery et al., 2009). During development cells undergo cycles of primary, secondary and tertiary EMT where they also undergo the reverse process, a mesenchymal to epithelial

transition (MET) (Thiery et al., 2009). These subsequent rounds of EMT and MET allow the normally tightly anchored epithelial cells to break down their adhesions and migrate to different niches in different areas of the developing embryo. When reaching their respective niches the cells then undergo MET and then differentiate into specialised cells. These cycles of EMT and MET are crucial for the development of the complex three-dimensional structures of organs present in the body (Thiery et al., 2009). Primary EMT takes place during gastrulation when, for example, parietal endodermal cells migrate from the inner cell mass to form the primitive endoderm. Secondary EMT takes place in the transient epithelial tissues of the notochord, the somites, the somatopleure and the splanchnopleure (Thiery et al., 2009). Upon undergoing EMT these structures generate mesenchymal cells that will differentiate into specialised cell types of the different organs like, for example, the pancreas and liver (Thiery et al., 2009). Tertiary EMT is a crucial step in the formation of the cushion mesenchyme in the heart from the atrioventricular canal which gives rise to the cardiac valves (Thiery et al., 2009). Similarly, during tissue healing, keratinocytes undergo a partial EMT which allows cells to migrate across a wound as a sheet while maintaining loose connections (Thiery et al., 2009).

During EMT, cells undergo distinct morphological changes. Both squamous cell carcinoma cells and normal keratinocytes form three inherent cellular colony morphologies when grown in culture, the holoclones, the meroclones and the paraclones (Costea et al., 2006). The holoclones exhibit the typical epithelial morphology of tightly packed cells with small cytoplasm giving rise to a cobblestone pattern (Oda and Watson, 1990, Costea et al., 2006, Barr et al., 2008). Meroclones and paraclones contain more loosely packed ovoid cells, but these cells are still of a predominantly

epithelial morphology (Costea et al., 2006). Mesenchymal cells in contrast have larger cytoplasm and a more spindle shaped morphology (Barr et al., 2008, Rho et al., 2009). They also exhibit reduced polarity and increased pseudopodia formation compared to epithelial cells (Rho et al., 2009, Thiery et al., 2009). On the molecular level these changes are associated with the downregulation of E-cadherin and β-catenin (Barr et al., 2008) and the upregulation of fibronectin, vimentin, Twist, Slug, Snail and Zeb1 (Barr et al., 2008, Eyzaguirre et al., 2008, Thiery et al., 2009).

Markers of EMT	Description	Expected changes during EMT
E-cadherin	Cell adhesion molecule	Decreased expression
β-catenin	Adherens junction	Decreased membranous expression
Fibronectin	Binds extracellular matrix components, important in cell migration	Increased expression
Vimentin	Component of cytoskeleton	Increased expression
Twist	bHLH transcription factor, represses E-cadherin	Increased expression
Slug	Zn-finger transcription factor, represses E-cadherin	Increased expression
Snail	Zn-finger transcription factor, represses E-cadherin	Increased expression
Zeb1	Zn-finger transcription factor, represses E-cadherin	Increased expression

Table 6.1: Summary of markers involved in EMT

Recently, EMT has been shown to be a necessary step to enable metastasis although it is insufficient to induce metastasis in isolation. EMT has also been reported to have an important role in the acquisition of resistance to therapy in a range of epithelial tumours (Barr et al., 2008, Thiery et al., 2009).

The cancer stem cell (CSC) hypothesis is a separate model put forward to account for the heterogeneity and inherent differences in tumour regenerating capacity that exist between individual cells within tumours (Prince et al., 2007, Visvader and Lindeman, 2008). It proposes a hierarchical tumour organisation containing subpopulations of stem-cell like cells responsible for sustaining tumour growth (Visvader and Lindeman, 2008). These putative CSCs have been shown to be more resistant to current treatment modalities (Visvader and Lindeman, 2008). Several putative stem cell markers have been used in oral squamous cell carcinomas to isolate a subset of cells enriched for CSCs, including CD133 (Harper et al., 2007, Xia et al., 2010), CD44 (Harper et al., 2007, Prince et al., 2007, Okamoto et al., 2009, Harper et al., 2010), CD29 (β-integrin) (Harper et al., 2007), CD34 (Locke et al., 2005), Aldehyde dehydrogenase 1 (ALDH 1) (Chen et al., 2009) and podoplanin (Atsumi et al., 2008). Another favoured assay for the identification of CSCs is the non-adherent sphere assay. It is an *in vitro* assay based on the assumption that only individual cancer stem cells present will survive serial passages under non-adherent conditions. Following serial passages, the cells should give rise to the full range of morphologies observed in the original cell line when returned to adherent conditions; in the cases of oral squamous carcinoma cells this would be the three clonal morphologies previously described (Costea et al., 2006, Visvader and Lindeman, 2008). For solid tumours, the most widely reported successful sphere assays are the neurosphere and the mammosphere (Visvader and Lindeman, 2008).

The mechanisms behind the apparent inherent resistance to therapy harboured by CSCs are unknown, but it is likely that several mechanisms are responsible. Current cancer treatment modalities are based on the classic

assumption that all tumour cells proliferate at a high rate and cancer drugs and irradiation preferentially kill rapidly dividing cells (Costea et al., 2006, Harper et al., 2010). CSCs, however, have been shown to rarely divide, and often exist in a quiescent state (Costea et al., 2006, Visvader and Lindeman, 2008). This is likely to contribute to their inherent resistance to treatment. However, most CSCs also appear to use active mechanisms to evade cytotoxic drugs or radiation treatment (Visvader and Lindeman, 2008, Xia et al., 2010). For example, in glioma tumour xenographs CD133 positive cells showed increased resistance to radiotherapy due to a more efficient DNA damage repair (Visvader and Lindeman, 2008). In one study of head and neck, breast and prostate carcinoma cell lines and HNSCC tumour biopsies, the CD44-high cell population spent an increased time in the G2 phase of the cell cycle allowing for DNA repair to take place following UV and cytotoxic insults (Harper et al., 2010). In HNSCC, the EGFR signalling pathway has been implicated as one of the pathways used by cancer cells to escape the effects of radiation through activation of the PI3K and MAPK pathways (Thariat et al., 2007). The PI3K pathway was preferentially activated in CSCs conferring resistance to radiotherapy in medulloblastomas (Visvader and Lindeman, 2008). CSCs also express high levels of drug transporters which enable the cells to expel noxious substances effectively and rapidly (Costea et al., 2006, Visvader and Lindeman, 2008). Lastly, solid tumours often contain hypoxic areas which contribute to resistance to cytotoxic drugs and irradiation (Wheeler et al., 2010b). It is thought that hypoxia may promote CSC maintenance and augment the CSC populations in solid tumours (Visvader and Lindeman, 2008).

Recent studies have linked the mechanism of EMT and cancer stem cell-like subpopulation of cells. For example, in nasopharyngeal carcinomas

EMT was reported to induce stem cell-like traits in the epithelial cells, including increasing the CD133-positive cell fraction, sphere formation ability and *in vivo* tumourigenicity (Xia et al., 2010). Similar changes were seen in breast cancer cells undergoing EMT, with an increase in the stem cell-like CD44-positive, CD24-low population (Santisteban et al., 2009).

In this study we investigated if the morphological changes observed in the SCCF1 cell line during chronic gefitinib exposure were associated with an EMT by comparing the molecular signatures of the parent and resistant cell lines. The presence of CD133-positive subpopulations in the cell lines was also explored, and the response of the two cell lines to different therapies was further elucidated.

6.3 Materials and methods

6.3.1 Cell culture

Both the parent cell line SCCF1 and the gefitinib resistant sub-line SCCF1G were cultured as previously described in chapter 2.3. During development of the SCCF1G cell line (chapter 2.3.9), the cells were monitored for cell death and morphological changes by light microscopy and photographed at regular intervals. Initially, the cells were treated with both 5 and 10 μM gefitinib.

Sphere assays were set up from both cell lines and passaged after 7-14 days (chapter 2.3.6). Cells were monitored by light microscopy and photographed at regular intervals.

6.3.2 Western blot analysis of EMT markers

The SCCF1 and SCCF1G cell lines were harvested as described in chapter 2.3.10. Cell lysates were prepared and their protein content was

determined according to protocols described in chapter 2.13.2 and 2.13.3 respectively. Aliquots of cell lysates containing 20 μg of protein were prepared and SDS-polyacrylamide gel electrophoresis and immunoblotting were performed on the cell lysates as described in chapter 2.13.4 and 2.13.5 respectively. The primary antibodies used were mouse monoclonal E-cadherin at 1:5,000 dilution, mouse monoclonal β-catenin at 1:1,000 dilution, and mouse monoclonal fibronectin at 1:1,000 dilution (all from Becton Dickinson Biosciences Ltd., UK), mouse monoclonal vimentin at 1:1,000 dilution and Slug at 1:500 dilution (both from Abcam, UK), and finally rabbit polyclonal Twist at 1:100 dilution (Santa Cruz Biotechnology Inc., USA). For loading control, mouse monoclonal β-actin at 1:4,000 dilution (Abcam, UK) was used. All primary antibodies were incubated in PBST/5% Milk at 4°C overnight, and the protocols described in chapter 2.13.5 were followed for secondary antibody incubations, development and visualisation of the blot.

6.3.3 MACS sorting

The SCCF1 cell line was MACS sorted for CD133 as described in chapter 2.18. The two different cell fractions were counted (chapter 2.3.5) and the overall percentage of CD133 positive cells was determined. Following MACS sorting, the cell fractions were then assayed for sphere forming ability and sensitivity to gefitinib, mitoxantrone, doxirubicin and irradiation. In addition, both cell fractions were expanded and MACS sorted again for CD133. The SCCF1G cell line was similarly MACS sorted for CD133 and the two cell fractions were counted and assayed for radiation sensitivity.

6.3.3.1 Sphere formation ability assay

Following MACS sorting of the SCCF1 cell line, both cell fractions were seeded into low adherence 24 well plates in N2 medium. Each cell fraction was seeded at 2, 1, 0.5 and 0.2 $x10^4$ cells per well into six wells for each cell density, giving a total of 24 wells for each cell fraction at four different cell densities. Cells were incubated at 37°C/5%CO_2, and fed with 500 μg per ml EGF and bFGF every 48 hours as described in chapter 2.3.6.1. After one week, all spheres seen in ten high power fields (x20 objective) were counted for each well and the total numbers of spheres per well were calculated. Each sample (i.e. each cell density for each cell fraction) was then averaged between six wells, and statistical analysis was performed as described in chapter 2.19. In addition, spheres were trypsinized and harvested and the total number of cells from each cell fraction was determined as previously described (chapters 2.3.6.2 and 2.3.5 respectively).

6.3.3.2 Gefitinib sensitivity assay

Following MACS sorting and counting, cells from each fraction were seeded at $3x10^3$ cells per well into three 96 well plates in 50 μl normal medium. Media aliquots containing gefitinib at twice the final concentrations were prepared, and 50 μl were added to each well to produce gefitinib concentrations in the wells of 1,3,5,7 and 10 μM respectively. Six wells on each 96 well plate were used per drug concentration. Controls included on each 96 well plate were DMSO control (cells treated with a DMSO dose equivalent to the DMSO concentration present in the wells with the highest gefitinib dose) and untreated cells. Medium-only containing wells were included on each plate to subtract assay background absorbance. The plates were incubated at 37°C/5%CO_2, and cell proliferation assays were performed as described in chapter 2.14 at 24, 48, 72 and 96 hours following treatment.

6.3.3.3 Chemosensitivity assays

Cells were MACs sorted (chapter 2.18) and the two cell fractions were resuspended at $1x10^4$ cells per ml and seeded at 500 cells per well (50µl) into 96 well plates and incubated overnight at 37°C/5%CO_2. The following day the cells were treated by addition of media containing the drugs (etoposide, doxirubicin and mitoxantrone) at a range of concentrations from 1 nM to 100 µM. Each drug concentration was performed in triplicate for each cell fraction. Controls included on each plate were one medium-only control for each drug concentration and four untreated cells controls for each cell fraction. Cells were incubated for 72 hours before cell viability was assessed with CellTiter-Glo® Luminescent Cell Viability Assay (Chapter 2.11.2). An ATP standard curve was performed to confirm the kit was working correctly.

6.3.3.4 Radiation sensitivity assay

Both cell lines were maintained in their respective media as described in chapter 2.3.2 and 2.3.9. The SCCF1G cell line was maintained in 5 µM of gefitinib during the entire assay.

Following MACS sorting, the negative and the positive cell fractions were counted and 300 cells were added to 10 ml media in 10 cm plates in triplicate for each cell line, each cell fraction and each radiation dose (36 plates in total). The cells were then irradiated in suspension at 0, 1, and 4 Gy prior to performing CFAs. After 10 days the cells were fixed, stained and counted as described in chapter 2.15.

6.3.3.5 Evaluation of CD133 positive and negative cells ability to generate CD133 positive cells

Both cell fractions were seeded at $4x10^5$ cells into T75 flasks and expanded for two weeks to produce three near confluent T150 flasks. The cells were trypsinated and counted as described in chapters 2.3.4 and 2.3.5 before MACS sorted as previously described (chapter 2.18). Each cell fraction was counted, and the overall percentage of CD133 positive cells present was determined.

6.4 Results

6.4.1 Chronic gefitinib treatment induces morphological changes suggestive of an epithelial to mesenchymal transition

During gefitinib treatment of the SCCF1 cell line marked morphological changes were observed in the cell line. These changes were apparent after one day of gefitinib treatment. Cells became much larger with spindle shaped morphology, abundant cytoplasm, loss of polarity and with increased pseudopodia formation (Figure 6.1). After first passage, two distinct morphologies were present in the cells treated with 5 μM of gefitinib. All cells treated with 10 μM gefitinib died when passaged, so no further analyses were performed of these cells. In the 5 μM gefitinib treated wells some cells reverted to their epithelial morphology with tightly packed colonies of cells with a small amount of cytoplasm producing a cobblestone effect, while others retained their mesenchymal morphology (Figure 6.2). Clear demarcations between the two morphologies were seen in culture where two colonies of different cell morphologies had coalesced. After ten or more passages the SCCF1G cell line became more homogenous and two distinct populations were no longer so clearly visible. The morphology became more epithelial-like with more tightly packed cells forming

cobblestone-like monolayers containing cells with a smaller amount of cytoplasm, although the cells were still larger and more loosely packed when compared to the parent cell line. The relative difference in cell size was illustrated by the relative difference in cell numbers obtained from confluent flasks from both cell lines (Figure 6.2 and Table 6.2). A comparison between the two cell lines' proliferation rates and colony formation ability is summarised in Table 6.2.

The parent cell line, SCCF1, exhibited a typical epithelial morphology when grown as an adherent monolayer, except for occasional colonies consisting of cells with a larger amount of cytoplasm and increased pseudopodia formation. Larger cells were also found at the edge of colonies, or when confluence was reached, occasional cells with a large amount of cytoplasm and scatter morphology were present throughout the monolayer (Figure 6.3).

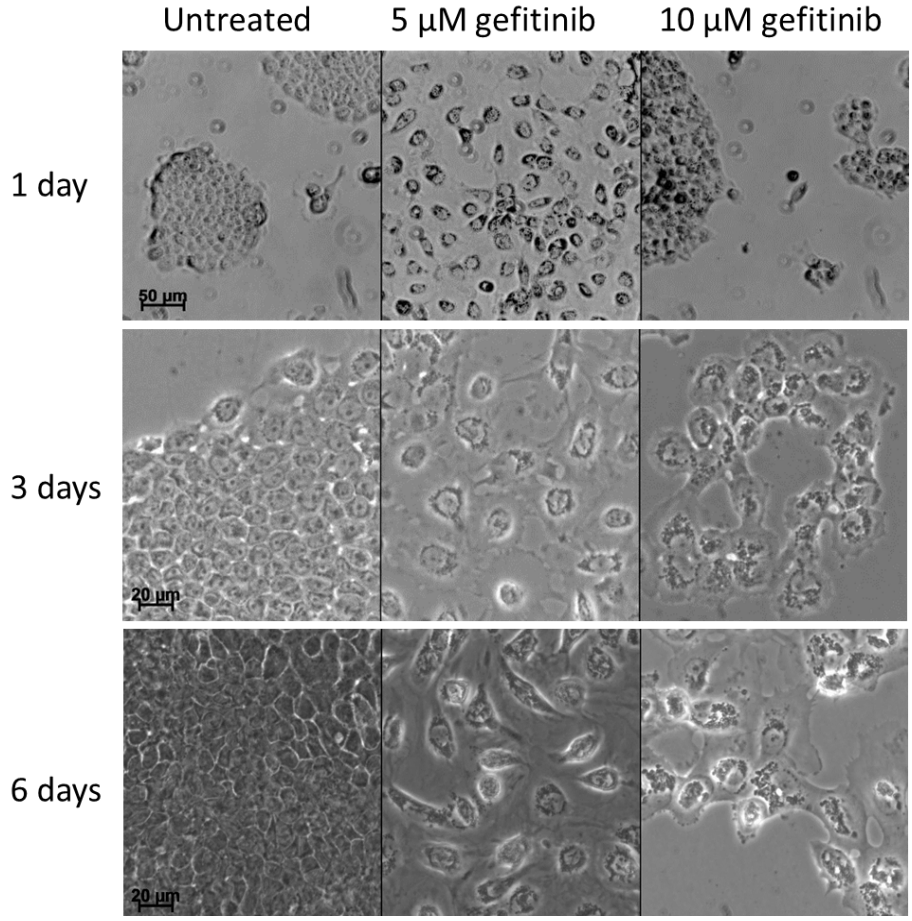

Figure 6.1: The morphology changes observed in the SCCF1 cell line during the first week of gefitinib treatment. The untreated cells became confluent during the first six days with densely packed cells creating the typical cobblestone appearance typical of epithelial cells (left column). The wells treated with 5 µM gefitinib (middle column) had marked cell death in the well, and did not reach confluence in the six days. However, large colonies of much larger spindle shaped cells with extensive cytoplasm were formed in the wells. These cells exhibited loss of polarity and increased pseudopodia formation. In the wells treated with 10 µM gefitinib massive cell death occurred, but some sparse colonies of spindle shaped cells formed in the wells (right column).

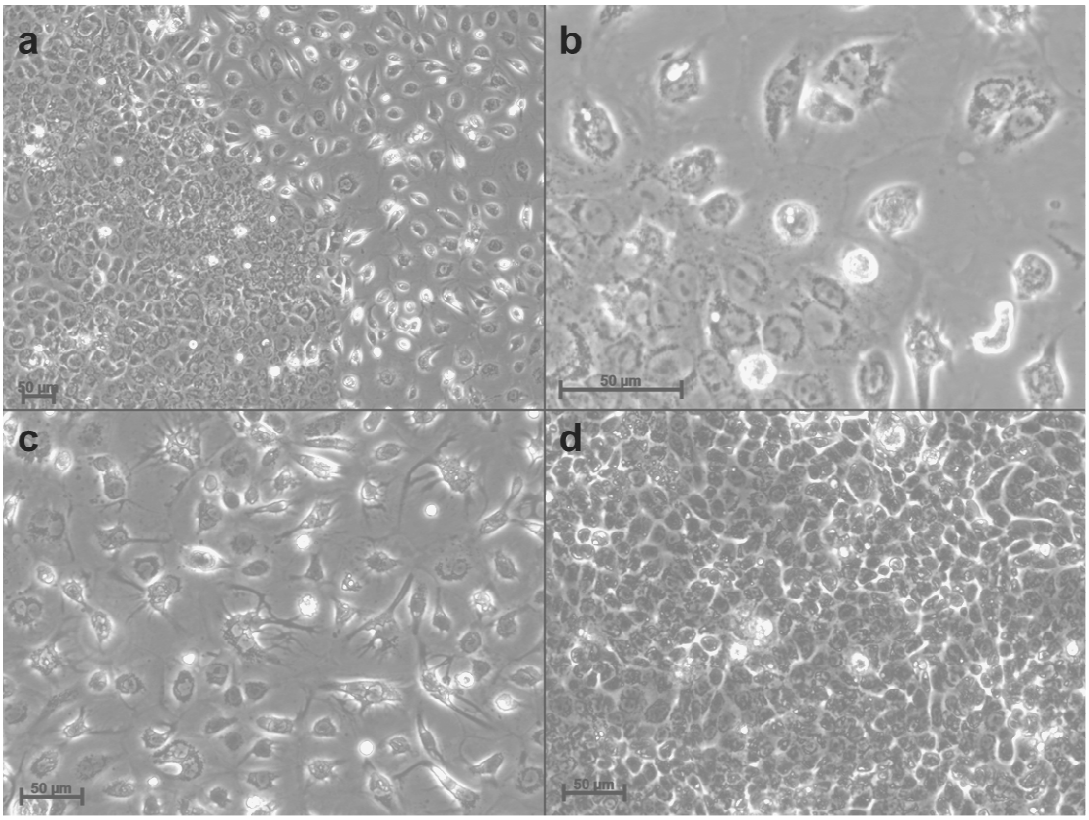

Figure 6.2: The cells from Figure 6.1 were all passaged and monitored while being expanded in gefitinib containing medium. This figure shows cells treated with 5 µM gefitinib as all cells treated with 10 µM died following passage.
a) During expansion following the first passage two distinct morphologies were observed. Some cells reverted to their epithelial type morphology while other retained their spindle-shaped morphology. Distinct colonies of the two cell types formed, and as the cells reached confluence, cells from the two distinct groups merged forming clear demarcations between the two cell types.
b) High power view of the demarcation line between the two cell types.
c) High power view of spindle shaped cells.
d) High power view showing the cells that had reverted to a typical epithelial-like morphology exhibiting the cobblestone appearance.

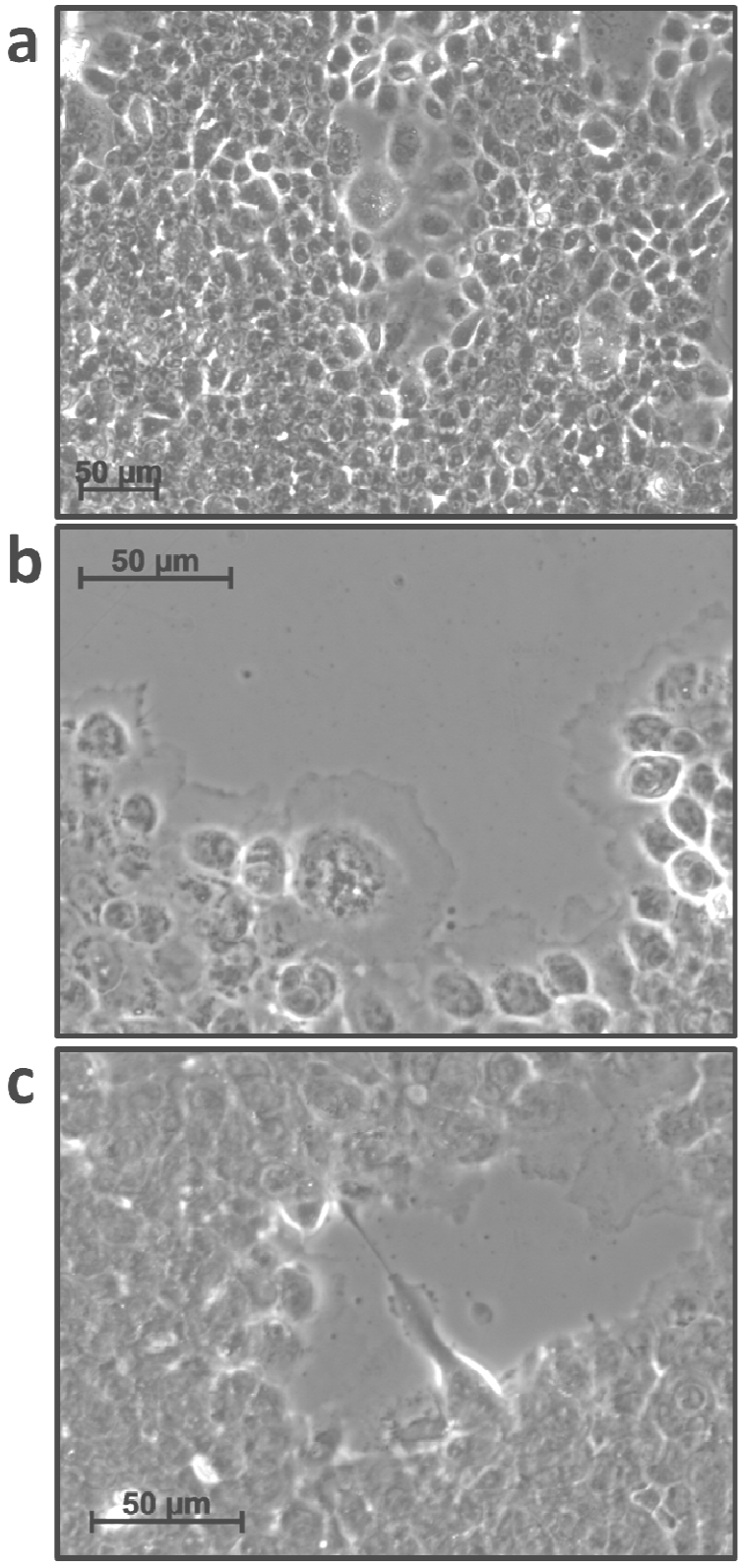

Figure 6.3: Normal untreated SCCF1 cell line showing the presence of occasional cells in the monolayer with a larger amount of cytoplasm (a). Similar cells with pseudopodia formation and abundant cytoplasm were observed at the invasive edges (b, c).

Parameter	Cell line		Passage	Comments
	SCCF1	SCCF1G		
Average total cell numbers per confluent flask				A confluent flask of the SCCF1 cell line yielded ~3-5 fold more cells
T150 flasks	~8 x 10^7	1.2-1.9 x 10^7	P64 (3)	
T75 flasks	~4 x 10^7	1.4 x 10^7	P73(13)	
Relative proliferation rate of cell lines measured by proliferation assays	1	0.34	P65 (4)	Proliferation rate of SCCF1G increased with passage numbers before plateauing
	1	0.59	P73(12)	
	1	0.66	P74(13)	
Relative colony formation ability				
	1	0.27	P85(14)	
	1	0.23		

Table 6.2: Comparison between SCCF1 and SCCF1G cell lines comparing average number of cells in a confluent flask for each cell line, relative proliferation rates and colony formation abilities .The passage number P shows total passages of cell line with passages of cell line in gefitinib containing media in parenthesis.

6.4.2 Chronic gefitinib treatment causes upregulation of mesenchymal markers

Western blot analysis of cell lysates from both cell lines showed no change in the epithelial markers E-cadherin and β-catenin, while mesenchymal markers fibronectin and vimentin were increased in the SCCF1G cell line when compared to the parent cell line SCCF1 (Figure 6.4). E-cadherin and β-catenin were present in relatively high levels in both cell lines, while fibronectin and vimentin were not detectable in the parent cell line and had become upregulated in the gefitinib treated cells.

The transcriptional regulators of E-cadherin, Slug and Twist, showed a mixed picture; Twist protein levels remained unchanged while Slug was upregulated. Their basal levels in the SCCF1 cell line differed, with Twist being expressed in the parent cell line while Slug protein levels were not detectable.

6.4.3 The SCCF1 and SCCF1G cell lines forms spheres which senesce in early passages

Both the SCCF1 and SCCF1G cell lines grew in non-adherent sphere assay conditions for up to two passages. The first week following transfer into non-adherent media the cells grew rapidly and formed large tight cell clusters (Figure 6.5). After one week the spheres were passaged, and they continued to grow for a further week forming tighter spheres where individual cells were difficult to visualise (Figure 6.6). At the end of this two week period, the cells would then senesce, and no further growth would occur eventually leading to complete cell death.

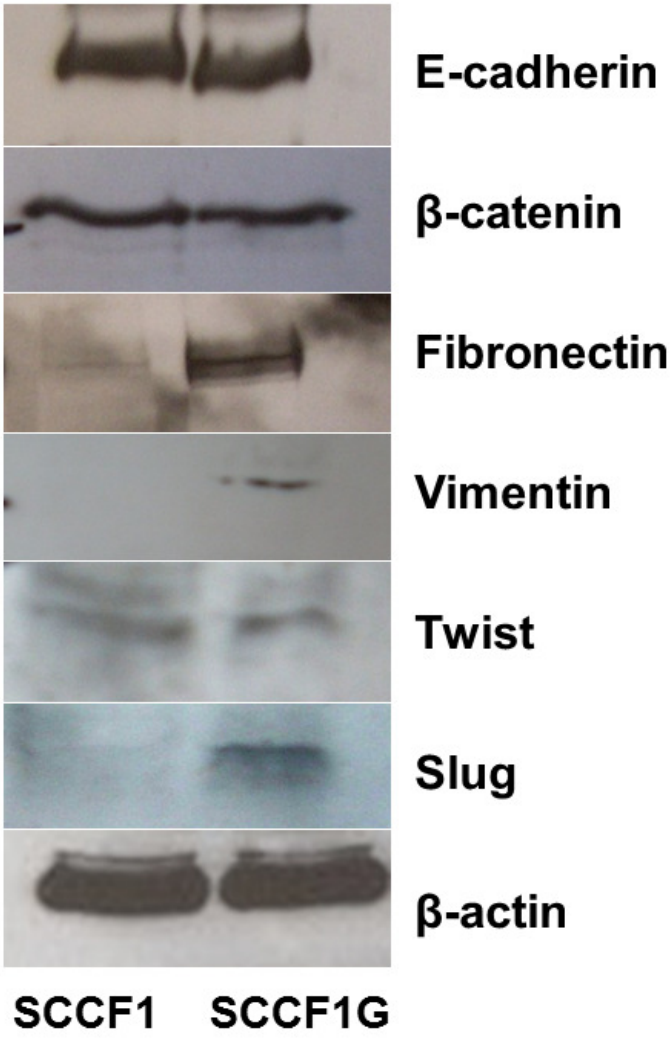

Figure 6.4: Western blot analysis of protein levels comparing the gefitinib resistant cell line (SCCF1G, right) to the parent cell line (SCCF1, left). E-cadherin, β-catenin and Twist protein levels remained unchanged as assessed by western blot analysis between the two cells lines. Fibronectin, vimentin and Slug were upregulated in the resistant cell line. Results courtesy of Alejandro Cervantes.

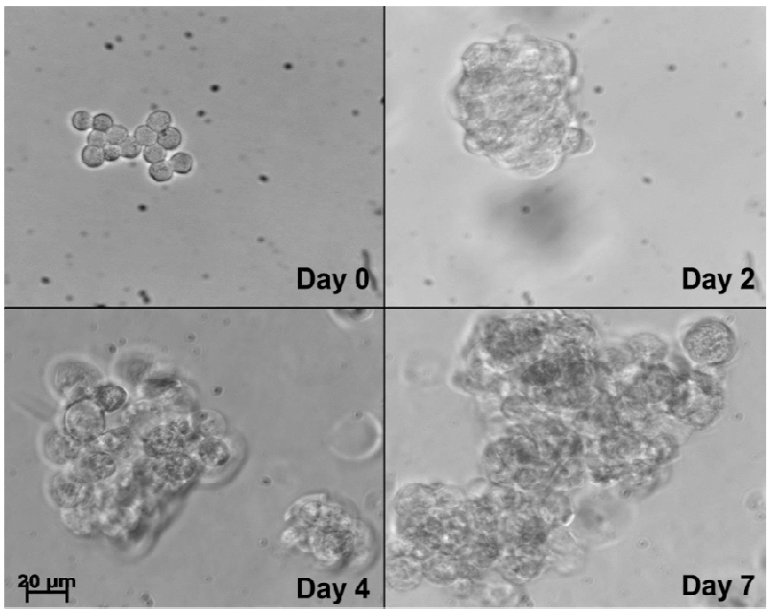

Figure 6.5: First week of SCCF1 cell line in non-adherent medium. Cells were seeded at low density into N2 medium. Individual cells were easily distinguished. After 2 days spheres could be seen forming in the medium which rapidly grew over the next five days.

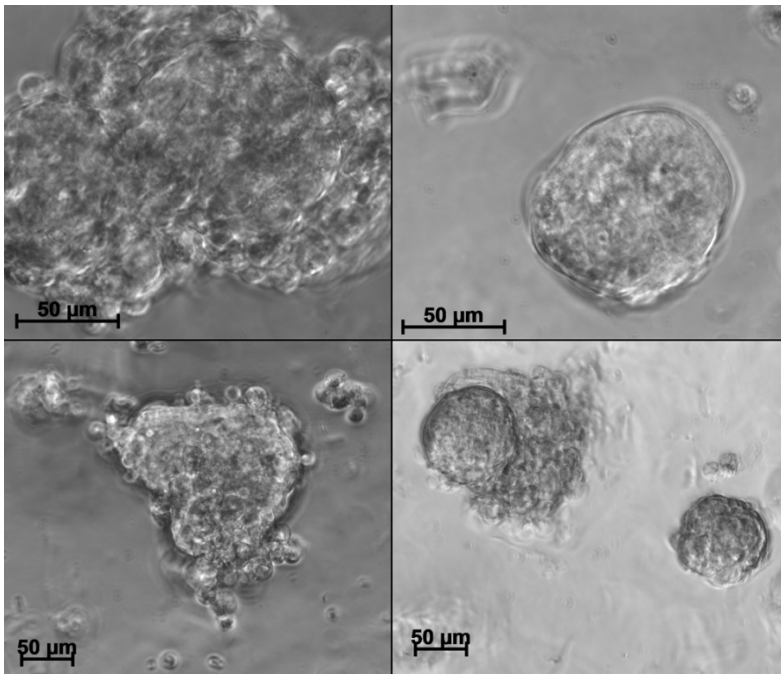

Figure 6.6: SCCF1 cell lines after first passage. Spheres of different sizes formed following passage, and grew rapidly for seven days following passage. Cells then became senescent and no further growth occurred regardless of whether the cells were passaged or left in the media. All images taken five days following first passage.

6.4.4 MACS sorting the SCCF1 cell line for CD133 produces a small population of labelled cells

MACS sorting the SCCF1 cell line for CD133 expression produced a small population of on average 1% (+/-0.7% standard deviation) of the total cell population (Table 6.3). Both CD133 positive and negative cell fractions gave rise to both cell populations when expanded for 10 days before being MACS sorted again, but on average the CD133 positive cell fractions gave rise to almost twice as many CD133 positive cells as the CD133 negative population (Table 6.3). The SCCF1G cell line gave rise to a much larger CD133 positive population of 7%.

Cells	Average CD133+ve fraction	SD	Number of counts
SCCF1	1.0 %	+/- 0.7 %	9
Re-sorted SCCF1			
CD133 –ve	1.1 %	+/- 0.7 %	2
CD133 +ve	1.9 %	+/- 0.1 %	2
SCCF1G	7 %	N/A	1

Table 6.3: Average cell fractions positive for CD133 labelling when MACS sorting the SCCF1 and SCCF1G cell lines. The CD133 –ve and +ve cells were MACS sorted, expanded for approximately 10 days and then re-sorted to see if the different fractions could give rise to both cell fractions.

6.4.5 CD133 positive SCCF1 cells show increased sphere forming ability and increased resistance to drug and radiation therapies

The CD133 positive cells formed on average more spheres than the CD133 negative cell fraction at all four cell densities (Figure 6.7). The assay was repeated on two separate occasions with similar results. The difference in sphere numbers was statistically significant for all four cell densities by two sample *t*-test or Mann Whitney *U* test.

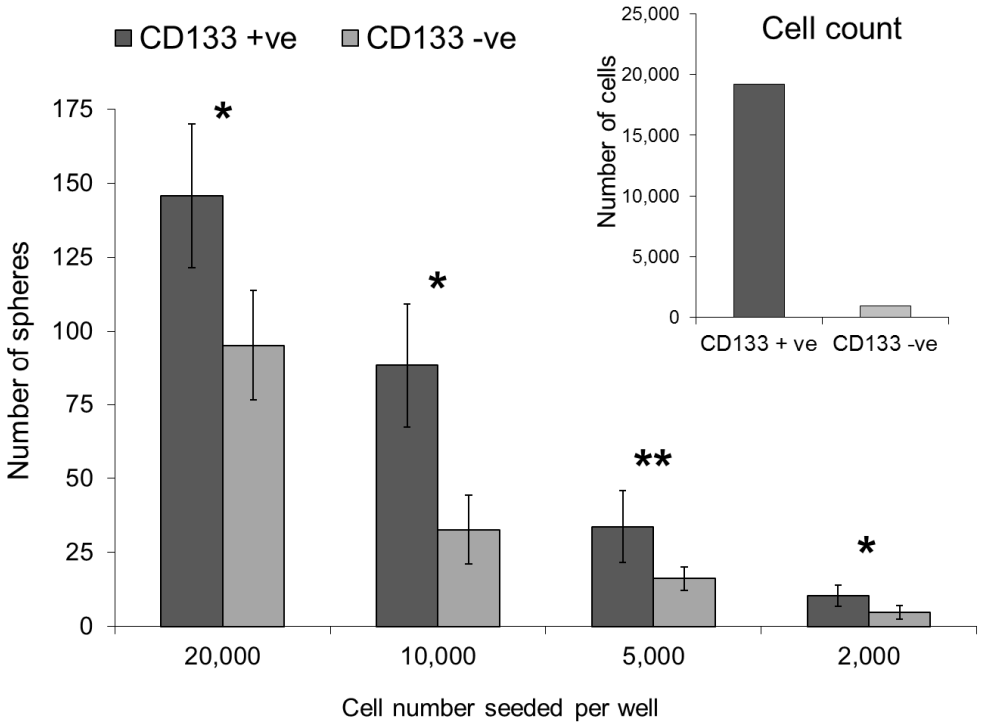

Figure 6.7: Sphere forming ability one week after seeding into non-adherent media at four different cell densities, all showing statistically significant difference in sphere-forming ability. ** p=0.01 by Mann Whitney U test, *p=0.002, p<0.001, p=0.009 by two sample t-test left to right respectively, bars show +/- standard deviations. Top right insert shows actual live cell count following trypsin treatment of spheres and counting using Trypan blue exclusion and a haemocytometer chamber.

The spheres were then harvested from all wells, trypsinated and counted. The total numbers of viable cells from all wells from each cell fraction were determined, and there were 20-fold more viable cells in the CD133 positive fraction (Figure 6.7). However, when CD133 positive cells only were seeded in non-adherent media, they became senescent after the second passage similar to the unsorted SCCF1 cell line.

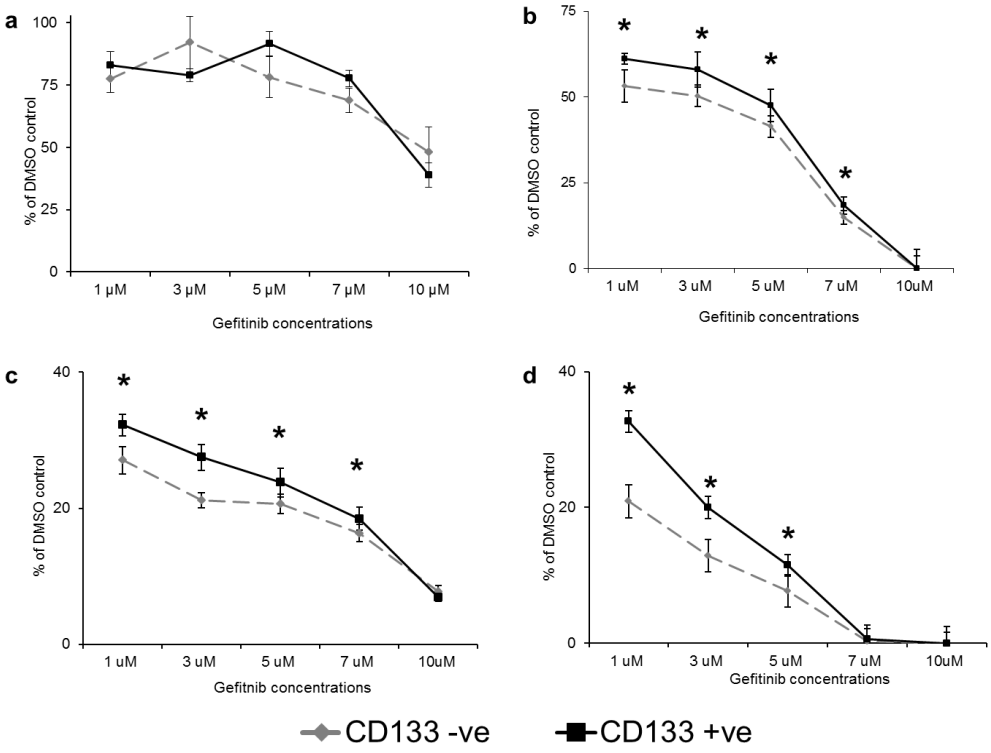

Figure 6.8: The SCCF1 cell line was MACS sorted for CD133 and the two cell fractions were seeded into 96 well plates and treated with different concentrations of gefitinib. At 24, 48, 72 and 96 hours (a, b, c & d) following gefitinib treatment cell proliferation assays were performed to assess level of viable cells present in each well. The CD133 positive cell fraction was consistently more resistant to gefitinib treatment over the drug concentration range after 48 hours (* $p<0.05$ by two sample *t*-test, bars show +/- standard deviations).

The CD133 positive cells were more resistant to gefitinib treatment than the unlabelled fraction at 48, 72 and 96 hours following treatment (Figure 6.8). There were relatively more viable CD133 positive cells left at gefitinib concentrations of 1, 3, 5 and 7 µM when compared to the CD133 negative cell fraction at 48 and 72 hours following treatment. At the 10 µM dose there were no differences between the two cell fractions as the dose was sufficiently high to kill the majority of the cells in all culture wells. At 96 hours, total cell death was also observed in the wells treated with 7 µM gefitinib. The experiment was performed on three different occasions with similar results. The CD133 positive fraction was also more resistant to the

chemotherapeutic agents etoposide, mitoxantrone and doxirubicin when compared to CD133 negative cells over a wide range of concentrations (Figure 6.9).

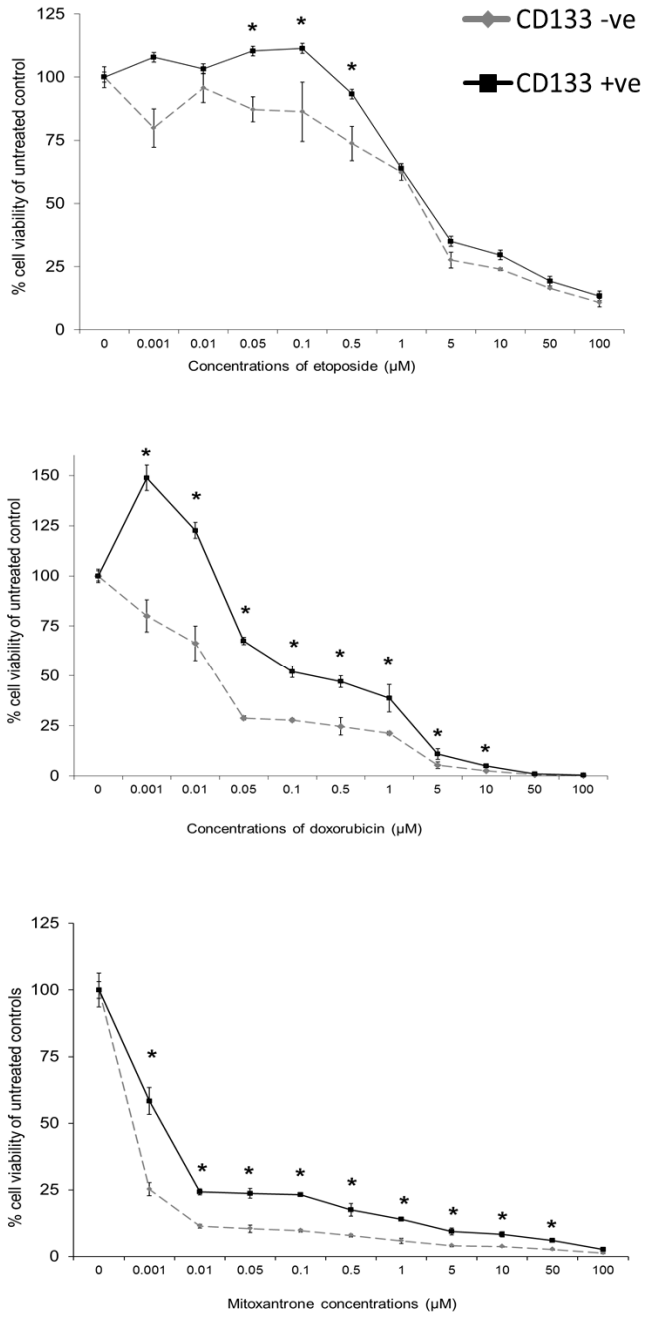

Figure 6.9: The SCCF1 cell line CD133 positive cell fractions were more resistant to chemotherapeutic agents over a wide range of concentrations. Top panel shows etoposide, middle panel shows doxirubicin and lower panel shows mitoxantrone treated cells. Bars show +/- standard deviation, each point is an average of three wells, * denotes $p<0.05$ by two sample *t*-test. All data courtesy of Dr. Lisa Pang.

Parameter	SCCF1		SCCF1G	
	CD133 +ve	**CD133 –ve**	**CD133 +ve**	**CD133 –ve**
Average number of untreated colonies formed (SD)	161 (+/-15.1)	208 (+/-12.7)	37 (+/-3.6)	56 (+/-6.1)
Radiosensitivity of cell lines at dose of:				
1 Gray	*p*=0.09	***p*<0.001**	*p*=0.6	*p*=0.71
4 Gray	***p*=0.003**	***p*<0.001**	***p*=0.004**	***p*=0.004**
*Comparison of radiosensitivity of CD133 positive vs. negative cell fractions at dose of:				
1 Gray		***p*=0.001**		*p*=0.99
4 Gray		***p*=0.004**		*p*=0.83
*Comparison of radiosensitivity of CD133 fractions between cell lines		**CD133 +ve fractions** 1 Gy *p*=0.1 4 Gy *p*=0.18 **CD133 –ve cell fractions** 1 Gy ***p*=0.009** 4 Gy *p*=0.09		

Table 6.4: Summary of data and statistical analysis performed on radiosensitivity assay of SCCF1 and SCCF1G cell lines, *p* values refers to the stars shown in Figures 6.10 and 6.11. Statistically significant *p* values from two sample *t*-tests marked in bold. Analyses were performed on non-normalised and *normalised data respectively.

The radiosensitivity of both cell fractions were analysed by colony formation assays following radiation in both cell lines. The basal colony formation ability of the SCCF1G cell line was significantly slower than that of the parent cell line ($p<0.001$, by two sample *t*-test) at approximately a quarter of colonies formed per 300 cells seeded for both cell fractions (Table 6.2).

Overall, the untreated CD133 negative cell fractions from both cell lines formed on average significantly more colonies than the untreated CD133

positive cell fractions (Table 6.4), (p=0.014 and p=0.009 by two sample t-test for SCCF1 and SCCF1G cell lines respectively).

Both CD133 positive and negative cells from both cell lines were sensitive to a radiation dose of 4 Gy, but only the CD133 negative fraction from the parent cell line showed statistically significant reduction in colony formation at the lower radiation dose of 1 Gy (Table 6.4, Figure 6.10).

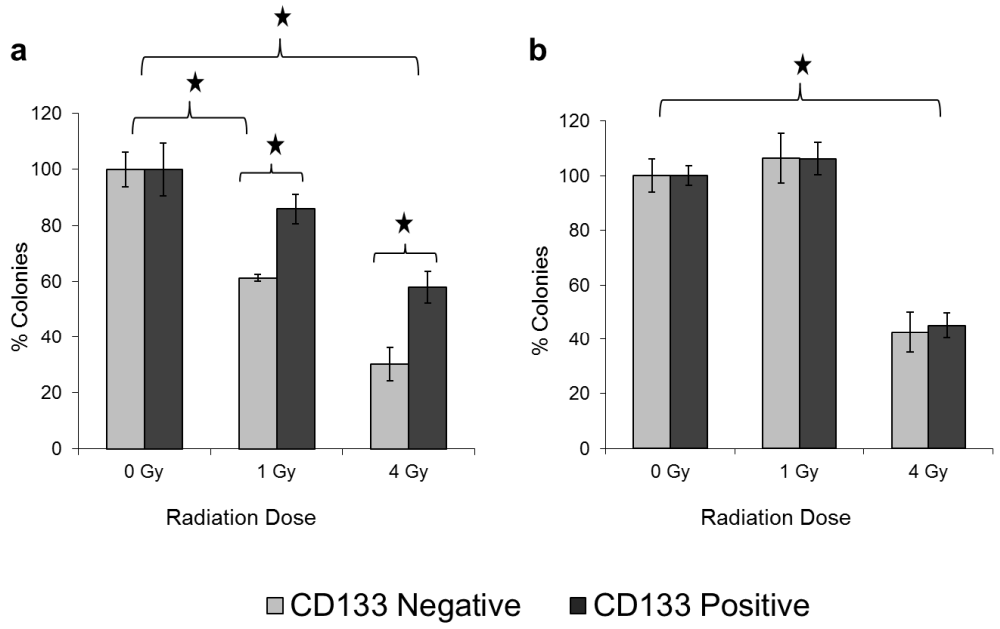

Figure 6.10: Colony formation assays following radiation treatment of CD133 sorted SCCF1 (a) and SCCF1G (b) cell lines shown as percentage of untreated control. The parent cell line (a) exhibited a dose dependent statistically significant reduction in colony formation ability in response to radiation. The CD133 negative cell fraction was significantly more sensitive to both radiation doses. The resistant cell line (b) required the higher radiation dose of 4 Gy before reduction in colony formation ability was observed. There were no difference in sensitivity to radiation between the CD133 positive and negative fractions in this cell line (* p values <0.05 by two sample t-test, bars show +/- standard deviations). All data courtesy of Dr. Lisa Pang, statistical analysis and graphical representation of data performed by GTB.

In the SCCF1 cell line the CD133 positive cells were consistently more resistant to radiation compared to the unlabelled fraction at both radiation doses, but in the gefitinib resistant sub-line SCCF1G there were no difference in radiosensitivity between the two cell fractions (Table 6.4, Figure 6.10). The

relative colony formation ability of the CD133 positive SCCF1G cells was similar to that of the CD133 positive SCCF1 cells at both radiation doses, while the CD133 negative fraction of the SCCF1G cell line was markedly more resistant to the lower radiation dose than its negative counterpart from the parent cell line (Figure 6.11, Table 6.4).

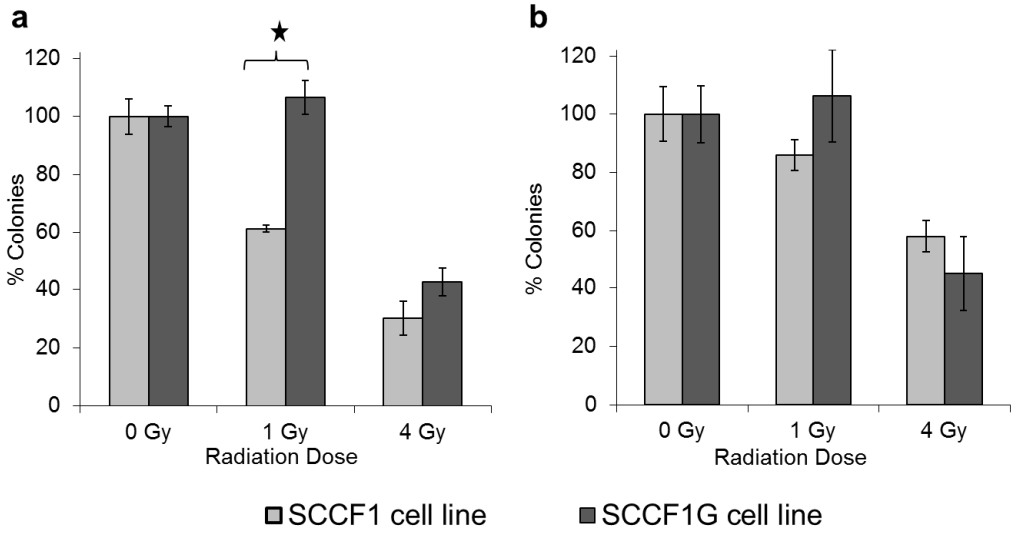

Figure 6.11: Comparison of radiation response of the two cell lines according to CD133 status shown as percentage of untreated control. a) Histograms compare the CD133 negative cell fractions from both cell lines. The SCCF1G cell line was statistically significantly more resistant at the lower dose of 1 Gy, while the difference was less pronounced at the higher radiation dose. b) Histograms comparing the CD133 positive cell fractions from both cell lines. There were no significant differences between the CD133 positive fractions of the two cell lines (* $p<0.05$ two sample *t*-test, bars show +/- standard deviations). All data courtesy of Dr. Lisa Pang, statistical analysis and graphical representation of data performed by GTB

6.5 Discussion

When cells undergo an EMT marked phenotypic changes occur, and these changes are accompanied by specific changes in molecular markers. The mesenchymal phenotype is associated with the downregulation of E-cadherin and β-catenin (Barr et al., 2008) and the upregulation of fibronectin, vimentin, Twist, Slug, Snail and Zeb1 among others (Barr et al.,

2008, Eyzaguirre et al., 2008, Thiery et al., 2009). In contrast, epithelial cells express high levels of E-cadherin and cytokeratins, and relatively low levels of vimentin and fibronectin (Barr et al., 2008, Thiery et al., 2009).

The SCCF1 cell line exhibited the typical morphology observed in cultured epithelial cells with cuboidal cells arranged in clusters during the exponential growth phase, and in a cobblestone pattern after confluence was reached (Oda and Watson, 1990, Barr et al., 2008). This was in contrast to the morphology observed in the cell line after chronic exposure to gefitinib, which was of a mesenchymal-like scattering or migratory morphology (Barr et al., 2008). Similar changes were described in a NSCLC cell line in response to chronic gefitinib exposure to produce a gefitinib resistant cell line (Rho et al., 2009). The NSCLC cell line showed cross-resistance against other TKIs including the new generation irreversible TKIs, while resistance to other conventional anti-cancer drugs such as cisplatin and paclitaxel developed to a lesser degree (Rho et al., 2009). The authors compared the relative expression of markers of EMT in the resistant and the parent NSCLC cell lines by western blot analysis and immunohistochemistry, and they found reduced levels of E-cadherin and cytokeratins and increased vimentin levels consistent with a mesenchymal phenotype supporting the development of an EMT in the resistant cell line (Rho et al., 2009).

In this study the rate of proliferation of the SCCF1G cell line was reduced compared to the parent cell line. It is possible that the doubling time of the two cell lines would have equalised with prolonged exposure of increasing concentrations of gefitinib as was the case in the NSCLC cell line used in the Rho et al. (2009) study. However, in a recent study by Basu and colleagues (2010) which investigated if the heterogeneity observed within ten SCC cell lines could be used as a basis for selection of drug resistant

subpopulations, all cell lines were reported to contain different proportions of E-cadherin-low, vimentin-high mesenchymal-like subpopulations. The two cell populations were isolated by flow cytometry, and the mesenchymal-like population had a lower proliferation rate than their epithelial-like counterparts (Basu et al., 2010). The mesenchymal subtype contained a greater proportion of cells in the G0 phase of the cell cycle as determined by Ki67 labelling (Basu et al., 2010). In addition, the SCC cell line turnover was assessed using dilution of the fluorescent membrane label, PKH-67 with ongoing cell division, and they reported that the E-cadherin low population had the highest label retention indicating a slower turnover of cells (Basu et al., 2010). Other studies have reported that cells that have undergone EMT were chemoresistant because of their slower proliferation rate (Nagane et al., 2001, Valcourt et al., 2005). It is possible that the differing proliferation rates observed in the cell lines in this study played a part in the apparent resistance to radiotherapy observed in the gefitinib resistant cell line. Further studies should investigate whether the increased resistance to radiotherapy observed here in the SCCF1G cell line would be lost if an increased proliferation rate could be achieved following longer exposure to gefitinib.

The parent cell line in this study may harbour a population of mesenchymal-like cells. During the original development of the cell line, positive vimentin labelling was observed in different proportions of the cells at different passages, and the authors believed this was due to epithelial to mesenchymal transdifferentiation occurring in the cell line consistent with their observations in feline SCCs (Tannehill-Gregg et al., 2001). During this study, however, the parent cell line was negative for vimentin and vimentin was only upregulated after chronic gefitinib exposure in the SCCF1G cell line. In contrast to the upregulation of vimentin observed that would

support an EMT in the SCCF1G cell line, E-cadherin and β-catenin levels seemed unchanged between the two cell lines contrary to what might be predicted with an EMT event. A possible explanation for the failure to demonstrate changes in E-cadherin and β-catenin levels could be the presence of a mixed population in the SCCF1G cell line with some cells having undergone EMT whilst others had not. Assessment of the cell morphologies present in the cell lines supports this explanation. If there were epithelial-like cells present in the cell line expressing high levels of E-cadherin and β-catenin, protein from these cells may mask a reduction of protein in EMT cells when the whole cell population was assessed by western blot analysis. The proteins which were expected to be low or absent in the parent cell line but upregulated in a cell line undergoing EMT (with the exception of Twist) were all increased in the SCCF1G cell line. In a truly mixed population of cells, these results would be expected. If a protein that was absent in the parent cell line became upregulated (even if it was only in a proportion of the cells), western blot analyses would reveal an upregulation of protein levels. Comparatively subtle reductions in expression of a heavily expressed protein could be masked due to the semi-quantitative nature of western blot analysis. These predications are in agreement with Basu and colleagues (2010) who stated that analysing cell lines as a total population for overall levels of markers may not reflect the levels within particular subsets of the tumour cell population. Studies using immunofluorescence labelling and flow cytometry to identify distinct subpopulations in the cell lines to determine if these subpopulations differ significantly in size and in the markers they express would help clarify this further.

There is an additional possible explanation of why β-catenin was not downregulated in the SCCF1G cell line as might be expected in cells undergoing EMT. In epithelial tissues cells form strong cell to cell adhesions, a crucial mechanism for the barrier function of epithelial cells (Wirtz-Peitz and Zallen, 2009, Harris and Tepass, 2010). The primary protein involved in these adhesions is E-cadherin which dimerizes in the intercellular space between adjacent cells at junctional complexes (Harris and Tepass, 2010). The intracellular domain of E-cadherin interacts with β-catenin, which in turn anchors the protein complex to the microtubules and the actin skeleton of the cell, providing stability and structure to the epithelial sheet (Harris and Tepass, 2010). In the SCCF1G cell line, β-catenin was predicted to be downregulated as it has been reported to be during EMT in other studies (Sahlgren et al., 2008). Despite this, overall levels of β-catenin did not appear reduced on western blot analysis following transdifferentiation of the cell line. This may be due to the presence of different subpopulations as discussed above. Alternatively, breakdown of adherens junction which occurs during EMT with loss of E-cadherin can lead to an increase in cytoplasmic β-catenin and translocation of β-catenin to the nucleus (Barr et al., 2008, Thiery et al., 2009). Translocation of β-catenin to the nucleus is a hallmark of active Wnt/β-catenin signalling, and has been shown to be involved in cutaneous cancer stem cell maintenance (Malanchi et al., 2008). In such an event, western blot analysis performed on whole cell lysates may not demonstrate reduction in β-catenin levels even though β-catenin had dissociated from E-cadherin and was undergoing different intracellular processing.

Based on the morphological change and increase in vimentin expression, the SCCF1G cell line did appear to undergo an epithelial to

mesenchymal transition upon chronic exposure to gefitinib despite the discordant results on western blot analysis. The role of EGFR and EGF in promoting EMT is well established (Barr et al., 2008, Thiery et al., 2009, Gan et al., 2010), so EGFR targeting might be expected to inhibit EMT, not induce it. However, there is an abundance of initiators of EMT reported in numerous cellular contexts (Thiery et al., 2009, Xia et al., 2010). It is possible that by blocking EGFR, we were selecting for or inducing an alternative pathway which drove the transition.

EGFR targeting has been shown to decrease migration and invasion of tumour cells through decreased STAT3 phosphorylation (Wheeler et al., 2010b) and Akt phosphorylation (Gan et al., 2010). We found decreased migration in response to EGFR blockade in the parent cell line as well as decreased levels of phosphorylated STAT3 supporting the hypothesis that this mechanism occurs in the SCCF1G cell line (Chapter 5.3.1). In one recent study hepatocytes that had undergone EMT were found to have increased levels of phosphorylated STAT3 and Akt (Wheeler et al., 2010a), both of which are downstream targets of EGFR (Yarden and Sliwkowski, 2001). The authors reported that the pathways were not, however, activated through EGFR, but by an alternative integrin-linked kinase (ILK) (Wheeler et al., 2010a). This again highlights the abundant receptor crosstalk present in cancer cells (Jorissen et al., 2003) which can come into play when one pathway is targeted. In this study, the gefitinib resistant cell line had an increased migration rate compared to the parent cell line. This was not due to increased proliferation, as the SCCF1G cell line proliferated at a lower rate than the parent cell line. EMT has been reported to induce a more invasive and migratory phenotype (Barr et al., 2008, Xia et al., 2010), and the resistant sub-line exhibited such increased migratory abilities. Further studies should

compare the phosphorylated STAT3 and Akt levels between the two cell lines to further elucidate the possible mechanisms behind the enhanced migratory ability of the SCCF1G cell line.

Whether the cells in this study actively underwent an EMT (Rho et al., 2009) or whether a more mesenchymal-like subpopulation already present in the cell line was selected for (Basu et al., 2010) by treating them with gefitinib is unknown. In HNSCC cell lines the presence of different morphological subpopulations (holoclones, paraclones and meroclones) with different proliferating abilities is well documented (Locke et al., 2005, Harper et al., 2007). Holoclones contain smaller, epithelial cuboidal shaped cells of a more proliferative nature which label strongly for E-cadherin and β-catenin (Locke et al., 2005, Harper et al., 2007). Paraclones consist of larger, flattened cells with a more scattered morphology, and have a much slower turnover by 5-bromo-2-deoxyuridine (BrdUrd) incorporation when compared to holoclones (Locke et al., 2005). They have also been reported to express vimentin (Harper et al., 2007). The third colony pattern described, the meroclones exhibit an intermediate phenotype. Similar features were observed in the SCCF1 cell line; although the dominant cell type observed by far were the small cuboidal, tightly packed cells so typical of epithelial monolayers, the morphology is suggestive of the presence of different cell populations . In one study comparing gene expression levels between holoclone and paraclone colonies of five different HNSCC cell lines by Real-Time PCR, it was reported that holoclones had relatively higher E-cadherin as well as ErbB3 gene expression when compared to paraclones (Locke et al., 2005). This indicates that E-cadherin-high, more epithelial-like cells express higher levels of EGFR family members, possibly indicating that the mesenchymal-like phenotype is less dependent on EGFR signalling,

providing an explanation why EGFR inhibition may be associated with the acquisition of an EMT phenotype. The presence of a mixed population containing mesenchymal-like cells that are less dependent on EGFR would result in selection for or induction of this cell type during chronic gefitinib treatment. In a recent study, EGFR expression levels were indeed seen to be reduced in the E-cadherin low subset of cells from HNSCC cell lines, and reduced levels corresponded with a decreased phosphorylation of the MAPK and PI3K pathways in response to EGF (Basu et al., 2010). Further studies investigating the potential existence of mesenchymal-like subpopulations in the SCCF1 and SCCF1G cell lines and their gene expression profiles are therefore warranted.

Non-adherent sphere assays are extensively used to evaluate the presence of putative CSC in cancer cell lines (Visvader and Lindeman, 2008). The assay can demonstrate extensive self-renewal if performed over more than five passages, but does not quantify CSC frequency (Visvader and Lindeman, 2008). The assay maintains CSCs in an undifferentiated state in serum-free medium, and then by the addition of growth factors the cells are stimulated to proliferate and form cell aggregates described as tumour spheres (Monroe et al., 2010). In addition, following serial passage in serum-free non-adherent medium these cells are able to recapitulate the original cellular morphologies (holoclones, paraclones and meroclones) observed in the parent cell line when returned to adherent conditions (Costea et al., 2006). It is these abilities of the cells selected for by sphere assays that have led to the use of this assay as a means to enrich for putative CSC (Costea et al., 2006, Visvader and Lindeman, 2008). Four studies have reported sphere formation in HNSCC cell lines (Harper et al., 2007, Okamoto et al., 2009, Harper et al., 2010, Xia et al., 2010), but none of the studies report

sphere formation beyond the second passage. This was consistent with our experience in this study, where the cells readily formed spheres in culture but they could not be cultured beyond the second passage. As spheres could not be passaged indefinitely they did not meet the criteria to be considered as CSC origin so this was not pursued further. Instead, the cell line was screened for markers of cells with stem-like traits as an alternative.

Magnetic cell sorting for the putative stem cell marker CD133 produced a subpopulation consisting of approximately 1% of the total cell population. This is similar to CD133 positive subpopulations reported in HNSCC cell lines of 0.1-0.2% (Harper et al., 2007) and 0.75% (Xia et al., 2010). Other markers used in human oral squamous cell carcinoma cell lines to enrich for CSCs produced highly variable and often much larger populations with CD44 positive cells constituting 10% (Prince et al., 2007), 3-12% (Harper et al., 2007), 3-5% or 2% (Okamoto et al., 2009) of the total cells, and podoplanin positive cells making up 38% of the total cell population (Atsumi et al., 2008). In one study, co-expression of CD44 and CD133 in HNSCC cell lines was evaluated by flow cytometry and was positive for 0.1% of the cells (Harper et al., 2007). The frequency of CSCs appears to be highly variable between tumours, and is often higher in solid tumours compared to haematological malignancies (Visvader and Lindeman, 2008). A definitive stem cell marker for oral SCC has not yet been determined (Costea et al., 2006). However, in human nasopharyngeal carcinomas, CD133 expression was associated with increased tumour sphere formation, increased tumourigenicity in mice xenografts as well as co-expression with stem cell markers Oct-4 and ALDH 1 (Xia et al., 2010). In our study, CD133 consistently selected a small but consistent population of cells. The CD133 positive population formed spheres more readily and was more resistant to gefitinib therapy, different

chemotherapeutic agents and irradiation. Two previous studies on oral squamous cell carcinomas investigated potential drug resistance in putative CSC enriched populations, and they both found a CD44 positive population to be more resistant to chemotherapeutic agents (Okamoto et al., 2009, Harper et al., 2010) and to UVB and tumour necrosis factor (TNF) (Harper et al., 2010).

Recently, it was reported that carcinoma cells can undergo a reversible process termed the epithelial-mesenchymal to stem-like transition (EMST) in which cells undergo an EMT and acquire stem cell-like properties concurrently (Xia et al., 2010). This was mediated through downregulation of microRNAs (miRNAs) belonging to the miR-200 family of miRNA tumour suppressors (Xia et al., 2010). Suppression of miR-200a was shown to induce Zeb2 and hence E-cadherin downregulation and promotion to a mesenchymal phenotype, as well as inducing a larger CD133 positive population (Xia et al., 2010). In this study two mechanisms were utilised to enrich for more treatment resistant cells in the SCCF1 cell line. The CD133 positive subpopulation was more resistant to the effects of irradiation as well as to cytotoxic drugs and EGFR targeting drugs. In addition, when a more mesenchymal-like signature was produced in the cell line, the end result was a cell line with an increased proportion of CD133 positive cells supporting EMST in the cell line following gefitinib treatment. However, radiation resistance in the gefitinib resistant cell line was acquired through a separate mechanism, as the CD133 positive and negative SCCF1G cells were equally resistant to irradiation.

6.6 Summary

This study has shown that through an EGFR-dependant mechanism a mesenchymal-like phenotype can be selected for or induced in the SCCF1

cell line. These cells were not only more resistant to EGFR targeted therapy, but also to irradiation. In addition, the study demonstrated that the SCCF1 cell line harbours a small CD133 positive population which showed increased sphere formation ability and increased resistance to cytotoxic drugs, EGFR targeted therapy and irradiation. Through induction of EMT, the CD133 positive population in the cell line increased, supporting the occurrence of EMST in the cell line. The radiation resistance observed in these two cell lines were probably achieved through distinct mechanisms, which support the theory that stem-like cancer cells use multiple mechanisms to achieve resistance to apoptosis (Xia et al., 2010).

Chapter 7:

Discussion

The central aims of this study were to investigate the role of EGFR in feline oral SCCs and its potential as a therapeutic target. The first step in this investigation was to establish whether feline oral SCCs expressed EGFR. An immunohistochemical study labelling 67 feline oral SCC biopsy samples for EGFR and Ki67 was performed, and it showed that EGFR expression was widely present in these tumours. The tumours exhibited two commonly reported labelling patterns (cytoplasmic and membranous), while no nuclear labelling was observed in any of the samples. Translocation of EGFR to the nucleus has been reported as a mechanism of resistance to therapy by cancer cells following treatment with the EGFR specific monoclonal antibody cetuximab (Li et al., 2009). Nuclear EGFR was first observed in hepatocytes during liver degeneration, but has now been reported to be involved in cell proliferation, transcriptional regulation, DNA replication, DNA repair and chemo- and radiotherapy resistance (Wang et al., 2010). All the samples used in this study were pre-treatment biopsy samples. Further studies investigating the pattern of EGFR labelling in tumours following therapy, in particular with EGFR targeting drugs if they became available, could reveal if EGFR nuclear translocation plays a role in acquired resistance in FOSCC. In addition, immunofluorescent labelling of EGFR of the gefitinib resistant SCCF1G cell line would reveal if this cell line exhibited any translocation of EGFR to the nucleus. This study also reported a trend towards a better survival in the high scoring EGFR group although statistical significance was

not reached. In HNSCC, patients with high EGFR scores responded favourably to an overall shortened treatment time with radiotherapy (Bentzen et al., 2005, Eriksen et al., 2004). The use of an accelerated radiotherapy protocol has been reported in FOSCCs (Fidel et al., 2007), and a future study investigating any relationship between response to this form of therapy and EGFR expression would further elucidate whether the feline tumour responds in a similar manner to HNSCC in man. If this was the case, EGFR labelling of pre-treatment biopsies could be a useful tool for patient selection for radiotherapy.

After establishing that a subset of FOSCCs expressed high levels of EGFR, the next aims of the study were to clone the tyrosine kinase domain of the feline *Egfr* and using this sequence as a basis, design and construct siRNAs against the receptor. The tyrosine kinase domain was found to be highly conserved between species, and crucially, the ATP binding pocket shared 100% homology with the human *EGFR* sequence.

The most efficient siRNA against the feline *Egfr* was selected following extensive vector based screening, and the effective knockdown of feline *Egfr* in the SCCF1 cell line was verified by Real-Time PCR and western blot analysis following both naked and hairpin expression vector transfections. In parallel, gefitinib treatment of the cell line was evaluated. The results of these studies demonstrated that targeting of the feline EGFR in the cell line produced marked effects on cellular proliferation, colony formation ability and migration, providing evidence that targeting EGFR in the feline tumour may be a viable therapeutic target.

According to published reports, the most effective siRNA in this study would be classified as a functional siRNA rather than a highly effective siRNA (Khvorova et al., 2003, Reynolds et al., 2004). To investigate this

further and improve on knockdown efficiency several more siRNAs could be designed against the feline *Egfr* using the entire sequence instead of the 500 base pairs sequence used as the basis for the siRNA design in this study. These could quickly and efficiently be screened against the evaluated siRNA8 for comparison using cell proliferation assays. If pursuing using siRNAs as a therapeutic strategy, the use of more than one highly effective sequence simultaneously would be beneficial. These siRNAs could target separate areas of the *Egfr* sequence producing an increased knockdown efficiency. Using such a cocktail of siRNAs together would mimic the effect achieved when using endoribonuclease-prepared siRNA (esiRNA) molecules where a long complementary dsRNA is digested by *Escherichia coli* RNase III producing several esiRNAs (Yang et al., 2002). This method produces highly effective gene knockdown, as any reduction of efficiency due to mRNA secondary structure is minimised as different areas of the mRNA are targeted. In addition, for long term therapeutic use, the potential for resistance developing through point mutations is highly unlikely to occur if more than one sequence is used simultaneously.

The results of this study suggest that TKIs designed to target the human EGFR may be effective in feline cells, however, the *in vitro* dose required to obtain an effect on the cell line was relatively high. If comparing the *in vitro* dose to clinical doses used in man for the treatment of NSCLC, cell lines requiring more than 2 μM gefitinib are classed as insensitive to the drug (Sharma et al., 2007). HNSCC has been reported to require higher dose rates of gefitinib than NSCLC. A British clinical trial investigating the use of gefitinib as monotherapy in recurrent HNSCC doubled the current dose used in NSCLC with little detrimental effects (Kirby et al., 2006). Although the siRNA produced superior effects compared to the TKI in the cell line

used in this study, further studies should investigate the potential use of EGFR specific TKIs in cats as the therapeutic use of siRNAs are still in its infancy. This study was based on one cell line; ideally a panel of feline SCC cell lines should be screened. It seems reasonable to hypothesise that a range of TKI sensitivities would be discovered in feline tumour cell lines similarly to what has been reported in HNSCC cell lines (Erjala et al., 2007). In conjunction with such further studies, this study provides evidence in support of a trial of a small molecule TKI to be performed in cats. EGFR targeted therapy has produced superior results in HNSCC when used in combination with radiotherapy (Bernier and Schneider, 2007). In the feline cell line an additive effect was observed when EGFR targeting and radiotherapy were combined, suggesting that this treatment combination may offer improved outcomes compared to currently available treatments.

Further work is required in the field of tumour resistance to EGFR targeted therapy. The final part of this study investigated potential mechanisms of resistance to EGFR targeting therapies and conventional treatments, focusing on two potential mechanisms of resistance: cells undergoing an epithelial to mesenchymal transition and the presence of a putative cancer stem cell population within the cell line. In response to chronic gefitinib treatment, morphological changes consistent with an EMT were observed in the cell line, but western blot analysis for markers of EMT produced a mixed picture suggestive of the presence of two cell populations. In order to investigate this, future studies using flow cytometry and immunofluorescence to establish whether the SCCF1 and SCCF1G cell lines indeed do harbour two such populations should be performed. If two such populations exist, isolation by flow cytometry using for example E-cadherin antibodies, or alternatively purely based on their size, is possible. The two

populations could then be fully characterised to further elucidate the mechanisms underlying their resistance to therapy. A microarray analysis to establish the expression patterns of genes known to be involved in EMT like E-cadherin, β-catenin, fibronectin, vimentin, Twist, Slug, Snail and Zeb1 would further elucidate which cellular markers are differentially expressed in the more resistant cell fraction. Identifying the mechanisms used by this cell line to acquire resistance to these therapies would reveal important information about resistance pathways utilised by cancer cells.

Non-adherent sphere assays were used in an effort to demonstrate putative cancer stem cells in these cell lines, but serial passaging of the spheres was unsuccessful. The use of non-adherent sphere assays to demonstrate the presence of a cancer stem cell population is controversial, and results from these assays have been criticised for being over-interpreted (Visvader and Lindeman, 2008). To date, convincing data demonstrating the successful *in vitro* serial passaging of spheres of HNSCC origin have not been reported (Prince and Ailles, 2008). Other methods that have been used to identify CSCs in HNSCCs include the use of specific surface antigens as stem cell markers and the presence of a side population (SP) based on excretion of Hoechst dye (Monroe et al., 2010). However, the gold standard for evaluating the presence of CSC is serial orthotopic transplantation studies of sorted tumour cell subpopulations into immunocompromised mice (Visvader and Lindeman, 2008, Monroe et al., 2010). This has been performed using CD44-positive (Prince et al., 2007) and CD133-high (Monroe et al., 2010) flow cytometer sorted HNSCC cells as well as after injection of a Hoechst-excreting SP from three HNSCC cell lines (Song et al., 2010). In order to further investigate the presence of a CSC population in the feline cell line a xenotransplantation study would have to be performed

using cell populations produced preferably by double sorting for a stem cell marker using both flow cytometry and MACS sorting. Initial results from this study suggest that CD133 could be used as a possible stem cell marker in feline oral SCCs, but further studies would have to be performed to confirm this.

The results from this study suggest that EGFR targeting in feline oral SCCs may be a feasible therapeutic option. The study supports the future investigation of EGFR targeting in combination with current treatment modalities like radiotherapy. Using RNA interference techniques, the crucial role of EGFR as an oncogenic driver in this tumour cell line was demonstrated. Targeted therapies rely on tumour addiction to an oncogene, and EGFR has been shown to be such an oncogene in a range of solid tumours in man. The therapeutics developed so far to block EGFR have proven less successful as monotherapies than was initially anticipated (Lai et al., 2009). Recent efforts have been directed towards understanding the relationships between the different pathways, their potential overlap and mechanisms of intrinsic and acquired resistance to therapy (Wheeler et al., 2010a). This study demonstrated superior activity and efficiency using siRNA when compared to the more conventional TKI used to target the receptor in man, in particular after some resistance to therapy had been allowed to build up over time. If the major obstacle to wider clinical use of reliable *in vivo* delivery of RNAi-based drugs could be overcome, results from this study indicate that these may have superior action compared to conventional drugs. Until such time, FOSCC is a tumour-type that potentially could be amenable to local delivery of siRNAs by injection of the tumour, as a number of these tumours are readily accessible in the oral cavity.

In summary, this study has demonstrated that feline EGFR has potential as a therapeutic target in oral SCCs by reporting widespread EGFR expression in feline SCC tumour biopsy samples and demonstrating the effect of EGFR targeting in a feline SCC cell line. Future work should investigate the different therapeutic approaches available to establish the most efficient way of targeting the receptor.

Reference list

AGULNIK, M., DA CUNHA SANTOS, G., HEDLEY, D., NICKLEE, T., DOS REIS, P. P., HO, J., POND, G. R., CHEN, H., CHEN, S., SHYR, Y., WINQUIST, E., SOULIERES, D., CHEN, E. X., SQUIRE, J. A., MARRANO, P., KAMEL-REID, S., DANCEY, J., SIU, L. L. & TSAO, M. S. 2007. Predictive and Pharmacodynamic Biomarker Studies in Tumor and Skin Tissue Samples of Patients With Recurrent or Metastatic Squamous Cell Carcinoma of the Head and Neck Treated With Erlotinib. *J Clin Oncol,* 25**,** 2184-2190.

ALBERTS, B., BRAY, D., LEWIS, J., RAFF, M., ROBERTS, K. & WATSON, J. D. 1994. Chapter 15, p 721-734: Cell Signaling. *In:* ROBERTSON, M. & ADAMS, R. (eds.) *Molecular Biology of the Cell.* 3rd ed. New York: Garland Publishing, Inc.

AMBION. 2008a. *siRNA construction kit template design tool* [Online]. Ambion, Inc., an Applied Biosystems Business. Available: www.ambion.com/techlib/misc/siRNA_design.html [Accessed 21.04.08 2008].

AMBION. 2008b. *siRNA finder* [Online]. Ambion, Inc., an Applied Biosystems Business. Available: www.ambion.com/techlib/misc/siRNA_design.html [Accessed 21.04.08 2008].

ANWAR, J., WRONE, D. A., KIMYAI-ASADI, A. & ALAM, M. 2004. The development of actinic keratosis into invasive squamous cell carcinoma: Evidence and evolving classification schemes. *Clin Dermatol,* 22**,** 189-196.

ARTEAGA, C. L. 2003. ErbB-targeted therapeutic approaches in human cancer. *Exp Cell Res,* 284**,** 122-130.

ATSUMI, N., ISHII, G., KOJIMA, M., SANADA, M., FUJII, S. & OCHIAI, A. 2008. Podoplanin, a novel marker of tumor-initiating cells in human squamous cell carcinoma A431. *Biochem Biophys Res Commun,* 373**,** 36-41.

BAER, K. E. & HELTON, K. E. 1993. Multicentric Squamous Cell Carcinoma in situ Resembling Bowen's disease in Cats. *Vet Path,* 30**,** 535-543.

BANKFALVI, A., KRASSORT, M., VEGH, A., FELSZEGHY, E. & PIFFKO, J. 2002. Deranged expression of the E-cadherin/β-catenin complex and the epidermal growth factor receptor in the clinical evolution and progression of oral squamous cell carcinomas. *J Oral Pathol Med,* 31**,** 450-457.

BARR, S., THOMSON, S., BUCK, E., RUSSO, S., PETTI, F., SUJKA-KWOK, I., EYZAGUIRRE, A., ROSENFELD-FRANKLIN, M., GIBSON, N. W., MIGLARESE, M., EPSTEIN, D., IWATA, K. K. & HALEY, J. D. 2008. Bypassing cellular EGF receptor dependence through epithelial-to-mesenchymal-like transitions. *Clin Exp Metastasis,* 25**,** 685-693.

BASELGA, J. 2006. Targeting Tyrosine Kinases in Cancer: The Second Wave. *Science,* 312**,** 1175-1178.

BASELGA, J. & SWAIN, S. M. 2009. Novel anticancer targets: revisiting ERBB2 and discovering ERBB3. *Nat Rev Cancer,* 9**,** 463-475.

BASELGA, J., TRIGO, J. M., BOURHIS, J., TORTOCHAUX, J., CORTES-FUNES, H., HITT, R., GASCON, P., AMELLAL, N., HARSTRICK, A. & ECKARDT, A. 2005. Phase II multicenter study of the antiepidermal growth factor receptor monoclonal antibody cetuximab in combination with platinum-based chemotherapy in patients with platinum-refractory metastatic and/or recurrent squamous cell carcinoma of the head and neck. *J Clin Oncol,* 23**,** 5568-5577.

BASU, D., NGUYEN, T. T. K., MONTONE, K. T., ZHANG, G., WANG, L. P., DIEHL, J. A., RUSTGI, A. K., LEE, J. T., WEINSTEIN, G. S. & HERLYN, M. 2010. Evidence for mesenchymal-like sub-populations within squamous cell carcinomas possessing chemoresistance and phenotypic plasticity. *Oncogene,* 29**,** 4170-4182.

BENTZEN, S. M., ATASOY, B. M., DALEY, F. M., DISCHE, S., RICHMAN, P. I., SAUNDERS, M. I., TROTT, K. R. & WILSON, G. D. 2005. Epidermal growth factor receptor expression in pretreatment biopsies from head and neck squamous cell carcinoma as a predictive factor for a benefit from accelerated radiation therapy in a randomized controlled trial. *J Clin Oncol,* 23**,** 5560-5567.

BERGKVIST, G. T., ARGYLE, D. J., MORRISON, L., MACINTYRE, N., HAYES, A. & YOOL, D. A. 2010. Expression of Epidermal Growth Factor Receptor (EGFR) and Ki67 in Feline Oral Squamous Cell Carcinomas (FOSCC). *Vet Comp Oncol,* In press.

BERGKVIST, G. T. & YOOL, D. A. 2010. Epidermal Growth Factor Receptor as a Therapeutic Target in Veterinary Oncology. *Vet Comp Oncol,* In press.

BERNIER, J. & SCHNEIDER, D. 2007. Cetuximab combined with radiotherapy: an alternative to chemoradiotherapy for patients with locally advanced squamous cell carcinomas of the head and neck? *Eur J Cancer,* 43**,** 35-45.

BERTONE, E. R., SNYDER, L. A. & MOORE, A. S. 2003. Environmental and lifestyle risk factors for oral squamous cell carcinoma in domestic cats. *J Vet Intern Med,* 17**,** 557-562.

BETZ, N. 2005. Using bioluminescent Reporter Genes to Optimize shRNA Target Sites for RNAi of the *bcr/abl* Gene. *Promega Notes* 90.

BIRCHARD, S. Year. Surgical Management of Neoplasms of the Oral Cavity in Dogs and Cats In Proceedings of the 20th Waltham/OSU Annual Symposium. *In:* The 20th Waltham/OSU Annual Symposium, 24/07/07 1996. Waltham/OSU, 51-8.

BONNER, J. A., HARARI, P. M., GIRALT, J., AZARNIA, N., SHIN, D. M., COHEN, R. B., JONES, C. U., SUR, R., RABEN, D., JASSEM, J., OVE, R., KIES, M. S., BASELGA, J., YOUSSOUFIAN, H., AMELLAL, N., ROWINSKY, E. K. & ANG, K. K. 2006. Radiotherapy plus cetuximab for squamous-cell carcinoma of the head and neck. *N Engl J Med,* 354**,** 567-578.

BOSTOCK, D. E. 1972. The prognosis in cats bearing squamous cell carcinoma. *J Small Anim Pract,* 13**,** 119-125.

BRADLEY, R. L., MACEWEN, E. G. & LOAR, A. S. 1984. Mandibular resection for removal of oral tumors in 30 dogs and 6 cats. *J Am Vet Med Assoc,* 184**,** 460-463.

BREGAZZI, V. S., LARUE, S. M., POWERS, B. E., FETTMAN, M. J., OGILVIE, G. K. & WITHROW, S. J. 2001. Response of feline oral squamous cell carcinoma to palliative radiation therapy. *Vet Radiol Ultrasound,* 42**,** 77-79.

BROWN, D. C. & GATTER, K. C. 2002. Ki67 protein: the immaculate deception? *Histopathology* 40**,** 2-11.

BUCHHOLZ, J., KASER-HOTZ, B., KHAN, T., ROHRER BLEY, C., MELZER, K., SCHWENDENER, R. A., ROOS, M. & WALT, H. 2005. Optimizing Photodynamic Therapy: In vivo Pharmacokinetics of Liposomal meta-(Tetrahydroxyphenyl) Chlorin in Feline Squamous Cell Carcinoma. *Clin Cancer Res,* 11**,** 7538-7544.

BUCK, E., EYZAGUIRRE, A., BROWN, E., PETTI, F., MCCORMACK, S., HALEY, J. D., IWATA, K. K., GIBSON, N. W. & GRIFFIN, G. 2006. Rapamycin synergizes with the epidermal growth factor receptor inhibitor erlotinib in non-small-cell lung, pancreatic, colon, and breast tumors. *Mol Cancer Ther,* 5**,** 2676-2684.

CANCER RESEARCH UK 2005. *UK Oral Cancer incidence statistics* [Online]. Available: http://info.cancerresearchuk.org/cancerstats/types/oral/incidence [Accessed 08.07.09 2009].

CAO, C., HUANG, X., HAN, Y., WAN, Y., BIRNBAUMER, L., FENG, G. S., MARSHALL, J., JIANG, M. & CHU, W. M. 2009. Galpha(i1) and Galpha(i3) are required for epidermal growth factor-mediated activation of the Akt-mTORC1 pathway. *Sci Signal,* 2**,** ra17.

CARLISLE, C. H. & GOULD, S. 1982. Response of Squamous Cell Carcinoma of the Nose of the Cat to Treatment with X-rays. *Vet Radiol* 23**,** 186-192.

CASTAGNARO, M., DE MARIA, R., BOZZETTA, E., RU, G., CASALONE, C., BIOLATTI, B. & CARAMELLI, M. 1998. Ki-67 index as indicator of the post-surgical prognosis in feline mammary carcinomas. *Res Vet Sci,* 65**,** 223-226.

CAVALOT, A., MARTONE, T., ROGGERO, N., BRONDINO, G., PAGANO, M. & CORTESINA, G. 2007. Prognostic impact of HER-2/neu expression on squamous head and neck carcinomas. *Head Neck,* 29**,** 655-664.

CHATURVEDI, D., GAO, X., COHEN, M. S., TAUNTON, J. & PATEL, T. B. 2009. Rapamycin induces transactivation of the EGFR and increases cell survival. *Oncogene,* 28**,** 1187-1196.

CHEN, L. F., COHEN, E. E. W. & GRANDIS, J. R. 2010. New Strategies in Head and Neck Cancer: Understanding Resistance to Epidermal Growth Factor Receptor Inhibitors. *Clin Cancer Res,* 16**,** 2489-2495.

CHEN, Y.-C., CHEN, Y.-W., HSU, H.-S., TSENG, L.-M., HUANG, P.-I., LU, K.-H., CHEN, D.-T., TAI, L.-K., YUNG, M.-C., CHANG, S.-C., KU, H.-H., CHIOU, S.-H. & LO, W.-L. 2009. Aldehyde dehydrogenase 1 is a putative marker for cancer stem cells in head and neck squamous cancer. *Biochem Biophys Res Commun,* 385**,** 307-313.

CITRI, A., SKARIA, K. B. & YARDEN, Y. 2003. The deaf and the dumb: the biology of ErbB-2 and ErbB-3. *Exp Cell Res,* 284**,** 54-65.

COSTEA, D. E., TSINKALOVSKY, O., VINTERMYR, O. K., JOHANNESSEN, A. C. & MACKENZIE, I. C. 2006. Cancer stem cells - new and potentially important targets for the therapy of oral squamous cell carcinoma. *Oral Dis,* 12**,** 443-454.

COX, N. R., BRAWNER, W. R., POWERS, R. D. & WRIGHT, J. C. 1991. Tumours of the Nose and Paranasal Sinuses in Cats: 32 Cases with Comparison to a National Database (1977-1987). *J Am Anim Hosp Assoc,* 27**,** 339-347.

DAMJANOV, I., MILDNER, B. & KNOWLES, B. B. 1986. Immunohistochemical localization of the epidermal growth factor receptor in normal human tissues. *Lab Invest,* 55**,** 588-592.

DAVIS, M. E., ZUCKERMAN, J. E., CHOI, C. H. J., SELIGSON, D., TOLCHER, A., ALABI, C. A., YEN, Y., HEIDEL, J. D. & RIBAS, A. 2010. Evidence of RNAi in humans from systemically administered siRNA via targeted nanoparticles. *Nature,* 464**,** 1067-1070.

DE MARIA, R., OLIVERO, M., IUSSICH, S., NAKAICHI, M., MURATA, T., BIOLATTI, B. & DI RENZO, M. F. 2005. Spontaneous Feline Mammary Carcinoma Is a Model of HER2 Overexpressing Poor Prognosis Human Breast Cancer. *Cancer Res,* 65**,** 907-912.

DEI TOS, A. P. & ELLIS, I. 2005. Assessing epidermal growth factor receptor expression in tumours: what is the value of current test methods? *Eur J Cancer,* 41**,** 1383-1392.

DICKINSON, P. J., ROBERTS, B. N., HIGGINS, R. J., LEUTENEGGER, C. M., BOLLEN, A. W., KASS, P. H. & LECOUTEUR, R. A. 2006. Expression of receptor tyrosine kinases VEGFR-1 (FLT-1), VEGFR-2 (KDR), EGFR-1, PDGFRalpha and c-Met in canine primary brain tumours. *Vet Comp Oncol,* 4**,** 132-140.

DOBROSSY, L. 2005. Epidemiology of head and neck cancer: magnitude of the problem. *Cancer Metastasis Rev,* 24**,** 9-17.

DONNAY, I., DEVLEESCHOUWER, N., WOUTERS-BALLMAN, P., LECLERCQ, G. & VERSTEGEN, J. 1996. Relationship between receptors for epidermal growth factor and steroid hormones in normal, dysplastic and neoplastic canine mammary tissues. *Res Vet Sci,* 60**,** 251-254.

DORN, C. R. & PRIESTER, W. A. 1976. Epidemiologic analysis of oral and pharyngeal cancer in dogs, cats, horses, and cattle. *J Am Vet Med Assoc,* 169**,** 1202-1206.

DORN, C. R., TAYLOR, D. O. & SCHNEIDER, R. 1971. Sunlight exposure and risk of developing cutaneous and oral squamous cell carcinomas in white cats. *J Natl Cancer Inst,* 46**,** 1073-1078.

DORSETT, Y. & TUSCHL, T. 2004. siRNAs: applications in functional genomics and potential as therapeutics. *Nat Rev Drug Discov,* 3**,** 318-329.

DUBIELZIEG, R. R. 1982. Proliferative Dental and Gingival Diseases of Dogs and Cats. *J Am Anim Hosp Assoc,* 18**,** 577-583.

ECKSTEIN, C., GUSCETTI, F., ROOS, M., MULAS, J. M. D. L., KASER-HOTZ, B. & BLEY, C. R. 2009. A retrospective analysis of radiation therapy for the treatment of feline vaccine-associated sarcoma. *Vet Comp Oncol,* 7**,** 54-68.

EGAN, S. E. & WEINBERG, R. A. 1993. The pathway to signal achievement. *Nature,* 365**,** 781-783.

ELBASHIR, S. M., HARBORTH, J., LENDECKEL, W., YALCIN, A., WEBER, K. & TUSCHL, T. 2001a. Duplexes of 21-nucleotide RNAs mediate RNA interference in cultured mammalian cells. *Nature,* 411**,** 494-498.

ELBASHIR, S. M., HARBORTH, J., WEBER, K. & TUSCHL, T. 2002. Analysis of gene function in somatic mammalian cells using small interfering RNAs. *Methods,* 26**,** 199-213.

ELBASHIR, S. M., MARTINEZ, J., PATKANIOWSKA, A., LENDECKEL, W. & TUSCHL, T. 2001b. Functional anatomy of siRNAs for mediating efficient RNAi in Drosophila melanogaster embryo lysate. *Embo J,* 20**,** 6877-6888.

EMBL-EBI. 2010a. *Emboss Pairwise Alignment Tool* [Online]. Available: www.ebi.ac.uk/Tools/emboss/align/index.html [Accessed 19.06. 2010].

EMBL-EBI, S. I. 2010b. *Predicted feline sequences* [Online]. Available: www.ensembl.org/index.html [Accessed 19.11. 2009].

ERIKSEN, J. G., STEINICHE, T., ASKAA, J., ALSNER, J. & OVERGAARD, J. 2004. The prognostic value of epidermal growth factor receptor is related to tumor differentiation and the overall treatment time of radiotherapy in squamous cell carcinomas of the head and neck. *Int J Radiat Oncol Biol Phys,* 58**,** 561-566.

ERJALA, K., RAITANEN, M., KULMALA, J. & GRÉNMAN, R. 2007. Concurrent use of vinorelbine and gefitinib induces supra-additive effect in head and neck squamous cell carcinoma cell lines. *J Cancer Res Clin Oncol,* 133**,** 169-176.

ERJALA, K., SUNDVALL, M., JUNTTILA, T. T., ZHANG, N., SAVISALO, M., MALI, P., KULMALA, J., PULKKINEN, J., GRENMAN, R. & ELENIUS, K. 2006. Signaling via ErbB2 and ErbB3 Associates with Resistance and Epidermal Growth Factor Receptor (EGFR) Amplification with Sensitivity to EGFR Inhibitor Gefitinib in Head and Neck Squamous Cell Carcinoma Cells. *Clin Cancer Res,* 12**,** 4103-4111.

EVANS, A. G., MADEWELL, B. R. & STANNARD, A. A. 1985. A trial of 13-cis-retinoic acid for treatment of squamous cell carcinoma and preneoplastic lesions of the head in cats. *Am J Vet Res,* 46**,** 2553-2557.

EVANS, S. M., LACRETA, F., HELFAND, S., VANWINKLE, T., CURRAN, W. J., JR., BROWN, D. Q. & HANKS, G. 1991. Technique, pharmacokinetics, toxicity, and efficacy of intratumoral etanidazole and radiotherapy for treatment of spontaneous feline oral squamous cell carcinoma. *Int J Radiat Oncol Biolo Phys,* 20**,** 703-708.

EYZAGUIRRE, A., BUCK, E., IWATA, K., HALEY, J. & MIGLARESE, M. 2008. Mechanisms of resistance to EGFR tyrosine kinase inhibitors: implications for patient selection and drug combination strategies. *Target Oncol,* 3**,** 235-243.

FAVROT, C., WELLE, M., HEIMANN, M., GODSON, D. L. & GUSCETTI, F. 2009. Clinical, Histologic, and Immunohistochemical Analyses of Feline Squamous Cell Carcinoma In Situ. *Vet Path,* 46**,** 25-33.

FIDEL, J. L., EGGER, E., BLATTMANN, H., OBERHANSLI, F. & KASER-HOTZ, B. 2001. Proton irradiation of feline nasal planum squamous cell carcinomas using an accelerated protocol. *Vet Radiol Ultrasound,* 42**,** 569-575.

FIDEL, J. L., SELLON, R. K., HOUSTON, R. K. & WHEELER, B. A. 2007. A nine-day accelerated radiation protocol for feline squamous cell carcinoma. *Vet Radiol Ultrasound,* 48**,** 482-485.

FIRE, A., XU, S., MONTGOMERY, M. K., KOSTAS, S. A., DRIVER, S. E. & MELLO, C. C. 1998. Potent and specific genetic interference by double-stranded RNA in Caenorhabditis elegans. *Nature,* 391**,** 806-811.

FORD, A. C. & GRANDIS, J. R. 2003. Targeting epidermal growth factor receptor in head and neck cancer. *Head Neck,* 25**,** 67-73.

FOX, L. E. 1995. Feline cutaneous and subcutaneous neoplasms. *Vet Clin North Am Small Anim Pract,* 25**,** 961-979.

FOX, L. E., ROSENTHAL, R. C., KING, R. R., LEVINE, P. B., VAIL, D. M., HELFAND, S. C., MACEWEN, E. G., PEREZ-SOLER, R., CALDERWOOD-MAYS, M. & KURZMAN, I. D. 2000. Use of cis-bis-neodecanoato-trans-R,R-1, 2-diaminocyclohexane platinum (II), a liposomal cisplatin analogue, in cats with oral squamous cell carcinoma. *Am J Vet Res,* 61**,** 791-795.

FRIMBERGER, A. E., MOORE, A. S., CINCOTTA, L., COTTER, S. M. & FOLEY, J. W. 1998. Photodynamic therapy of naturally occurring tumors in animals using a novel benzophenothiazine photosensitizer. *Clin Cancer Res,* 4**,** 2207-2218.

FRY, D. W. 2003. Mechanism of action of erbB tyrosine kinase inhibitors. *Exp Cell Res,* 284**,** 131-139.

GAMA, A., GARTNER, F., ALVES, A. & SCHMITT, F. 2009. Immunohistochemical expression of Epidermal Growth Factor Receptor (EGFR) in canine mammary tissues. *Res Vet Sci* 87**,** 432-437.

GAN, H. K., KAYE, A. H. & LUWOR, R. B. 2009. The EGFRvIII variant in glioblastoma multiforme. *J Clin Neurosci,* 16**,** 748-754.

GAN, Y., SHI, C., INGE, L., HIBNER, M., BALDUCCI, J. & HUANG, Y. 2010. Differential roles of ERK and Akt pathways in regulation of EGFR-mediated signaling and motility in prostate cancer cells. *Oncogene,* 29**,** 4947-4958.

GARDNER, D. G. 1996. Spontaneous squamous cell carcinomas of the oral region in domestic animals: a review and consideration of their relevance to human research. *Oral Dis,* 2**,** 148-154.

GILLETT, N. A., STEGELMEIER, B. L., KELLY, G., HALEY, P. J. & HAHN, F. F. 1992. Expression of epidermal growth factor receptor in plutonium-239-induced lung neoplasms in dogs. *Vet Path,* 29**,** 46-52.

GOODFELLOW, M., HAYES, A., MURPHY, S. & BREARLEY, M. 2006. A retrospective study of (90)Strontium plesiotherapy for feline squamous cell carcinoma of the nasal planum. *J Feline Med Surg,* 8**,** 169-176.

GRANDIS, J. R., MELHEM, M. F., BARNES, E. L. & TWEARDY, D. J. 1996. Quantitative immunohistochemical analysis of transforming growth factor-alpha and epidermal growth factor receptor in patients with squamous cell carcinoma of the head and neck. *Cancer,* 78**,** 1284-1292.

GRANDIS, J. R., MELHEM, M. F., GOODING, W. E., DAY, R., HOLST, V. A., WAGENER, M. M., DRENNING, S. D. & TWEARDY, D. J. 1998. Levels of TGF-alpha and EGFR protein in head and neck squamous cell carcinoma and patient survival. *J Natl Cancer Inst,* 90**,** 824-832.

GRANDIS, J. R. & TWEARDY, D. J. 1993. Elevated levels of transforming growth factor alpha and epidermal growth factor receptor messenger RNA are early markers of carcinogenesis in head and neck cancer. *Cancer Res,* 53**,** 3579-3584.

GRANDIS, J. R., ZENG, Q. & DRENNING, S. D. 2000. Epidermal growth factor receptor-mediated stat3 signaling blocks apoptosis in head and neck cancer. *Laryngoscope,* 110**,** 868-874.

GRAUS-PORTA, D., BEERLI, R. R., DALY, J. M. & HYNES, N. E. 1997. ErbB-2, the preferred heterodimerization partner of all ErbB receptors, is a mediator of lateral signaling. *EMBO J,* 16**,** 1647-1655.

GUPTA, A. K., MCKENNA, W. G., WEBER, C. N., FELDMAN, M. D., GOLDSMITH, J. D., MICK, R., MACHTAY, M., ROSENTHAL, D. I., BAKANAUSKAS, V. J., CERNIGLIA, G. J., BERNHARD, E. J., WEBER, R. S. & MUSCHEL, R. J. 2002. Local recurrence in head and neck cancer: relationship to radiation resistance and signal transduction. *Clin Cancer Res,* 8**,** 885-892.

HADDAD, Y., CHOI, W. & MCCONKEY, D. J. 2009. Delta-Crystallin Enhancer Binding Factor 1 Controls the Epithelial to Mesenchymal Transition Phenotype and Resistance to the Epidermal Growth Factor Receptor Inhibitor Erlotinib in Human Head and Neck Squamous Cell Carcinoma Lines. *Clin Cancer Res,* 15**,** 532-542.

HAHN, K. A., PANJEHPOUR, M. & LEGENDRE, A. M. 1998. Photodynamic therapy response in cats with cutaneous squamous cell carcinoma as a function of fluence. *Vet Dermatol,* 9**,** 3-7.

HANAHAN, D. & WEINBERG, R. A. 2000. The hallmarks of cancer. *Cell,* 100**,** 57-70.

HANNON, G. J. 2002. RNA interference. *Nature,* 418**,** 244-251.

HARPER, L. J., COSTEA, D. E., GAMMON, L., FAZIL, B., BIDDLE, A. & MACKENZIE, I. C. 2010. Normal and malignant epithelial cells with stem-like properties have an extended G2 cell cycle phase that is associated with apoptotic resistance. *BMC Cancer,* 10**,** 166.

HARPER, L. J., PIPER, K., COMMON, J., FORTUNE, F. & MACKENZIE, I. C. 2007. Stem cell patterns in cell lines derived from head and neck squamous cell carcinoma. *J Oral Pathol Med,* 36**,** 594-603.

HARRIS, T. J. C. & TEPASS, U. 2010. Adherens junctions: from molecules to morphogenesis. *Nat Rev Mol Cell Biol,* 11**,** 502-514.

HASHIBE, M., BRENNAN, P., BENHAMOU, S., CASTELLSAGUE, X., CHEN, C., CURADO, M. P., DAL MASO, L., DAUDT, A. W., FABIANOVA, E., WUNSCH-FILHO, V., FRANCESCHI, S., HAYES, R. B., HERRERO, R., KOIFMAN, S., LA VECCHIA, C., LAZARUS, P., LEVI, F., MATES, D., MATOS, E., MENEZES, A., MUSCAT, J., ELUF-NETO, J., OLSHAN, A. F., RUDNAI, P., SCHWARTZ, S. M., SMITH, E., STURGIS, E. M., SZESZENIA-DABROWSKA, N., TALAMINI, R., WEI, Q., WINN, D. M., ZARIDZE, D., ZATONSKI, W., ZHANG, Z. F., BERTHILLER, J. & BOFFETTA, P. 2007. Alcohol drinking in never users of tobacco, cigarette smoking in never drinkers, and the risk of head and neck cancer: pooled analysis in the International Head and Neck Cancer Epidemiology Consortium. *J Natl Cancer Inst,* 99**,** 777-789.

HAYES, A. M., ADAMS, V. J., SCASE, T. J. & MURPHY, S. 2007. Survival of 54 cats with oral squamous cell carcinoma in United Kingdom general practice. *J Small Anim Pract,* 48**,** 394-399.

HAYNES, W. J., LING, K. Y., SAIMI, Y. & KUNG, C. 1995. Induction of antibiotic resistance in Paramecium tertaurelia by the bacterial gene APH-3-II. *J Eukaryot Microbiol,* 42**,** 83-91.

HENSON, E. S. & GIBSON, S. B. 2006. Surviving cell death through epidermal growth factor (EGF) signal transduction pathways: Implications for cancer therapy. *Cell Signal,* 18**,** 2089-2097.

HIGGINS, R. J., DICKINSON, P. J., LECOUTEUR, R. A., BOLLEN, A. W., WANG, H., WANG, H., CORELY, L. J., MOORE, L. M., ZANG, W. & FULLER, G. N. 2010. Spontaneous canine gliomas: overexpression of EGFR, PDGFRalpha and IGFBP2 demonstrated by tissue microarray immunophenotyping. *J Neurooncol,* 98**,** 49-55.

HITT, R., CIRUELOS, E., AMADOR, M. L., BENITO, A., SANCHEZ, J. J., BALLESTIN, C. & CORTES-FUNES, H. 2005. Prognostic value of the epidermal growth factor receptor (EGRF) and p53 in advanced head and neck squamous cell carcinoma patients treated with induction chemotherapy. *Eur J Cancer,* 41**,** 453-460.

HOLBRO, T. & HYNES, N. E. 2004. ErbB Receptors: Directing Key Signaling Networks Throughout Life. *Annu Rev Pharmacol Toxicol,* 44**,** 195-217.

HOSGOOD, G. & SCHOLL, D. T. 2001. The effects of different methods of accounting for observations from euthanized animals in survival analysis. *Prev Vet Med,* 48**,** 143-154.

HUANG, S., ARMSTRONG, E. A., BENAVENTE, S., CHINNAIYAN, P. & HARARI, P. M. 2004. Dual-Agent Molecular Targeting of the Epidermal Growth Factor Receptor (EGFR): Combining Anti-EGFR Antibody with Tyrosine Kinase Inhibitor. *Cancer Res,* 64**,** 5355-5362.

HUANG, S. M., LI, J., ARMSTRONG, E. A. & HARARI, P. M. 2002. Modulation of radiation response and tumor-induced angiogenesis after epidermal growth factor receptor inhibition by ZD1839 (Iressa). *Cancer Res,* 62**,** 4300-4306.

HUTSON, C. A., WILLAUER, C. C., WALDER, E. J., STONE, J. L. & KLEIN, M. K. 1992. Treatment of mandibular squamous cell carcinoma in cats by use of mandibulectomy and radiotherapy: seven cases (1987-1989). *J Am Vet Med Assoc,* 201**,** 777-781.

HYNES, N. E. & LANE, H. A. 2005. ErbB receptors and cancer: the complexity of targeted inhibitors. *Nat Rev Cancer,* 5**,** 341-354.

JAKUBIAK, M. J., SIEDLECKI, C. T., ZENGER, E., MATTEUCCI, M. L., BRUSKIEWICZ, K. A., ROHN, D. A. & BERGMAN, P. J. 2005. Laryngeal, laryngotracheal, and tracheal masses in cats: 27 cases (1998-2003). *J Am Anim Hosp Assoc,* 41**,** 310-316.

JIMENO, A. & HIDALGO, M. 2005. Blockade of epidermal growth factor receptor (EGFR) activity. *Crit Rev Oncol Hematol,* 53**,** 179-192.

JOHNSON, M. S., MARTIN, M., BINNS, S. & DAY, M. J. 2004. A retrospective study of clinical findings, treatment and outcome in 143 dogs with pericardial effusion. *J Small Anim Pract,* 45**,** 546-552.

JONES, P. D., DE LORIMIER, L. P., KITCHELL, B. E. & LOSONSKY, J. M. 2003. Gemcitabine as a radiosensitizer for nonresectable feline oral squamous cell carcinoma. *J Am Anim Hosp Assoc,* 39**,** 463-467.

JORISSEN, R. N., WALKER, F., POULIOT, N., GARRETT, T. P., WARD, C. W. & BURGESS, A. W. 2003. Epidermal growth factor receptor: mechanisms of activation and signalling. *Exp Cell Res,* 284**,** 31-53.

KALYANKRISHNA, S. & GRANDIS, J. R. 2006. Epidermal growth factor receptor biology in head and neck cancer. *J Clin Oncol,* 24**,** 2666-2672.

KAPATKIN, A. S., MARETTA, S. M., PATNAIK, A. K., BURK, R. L. & MATUS, R. E. 1991. Mandibular Swelling In Cats: Prospective Study of 24 Cats. *J Am Anim Hosp Assoc,* 27**,** 575-580.

KEY, G., BECKER, M. H. G., BARON, B., DUCHROW, M., SCHLUTER, C., FLAD, H.-D. & GERDES, J. 1993. New Ki-67-equivalent murine monoclonal antibodies (MIB 1-3) generated against bacterially expressed parts of the Ki-67 cDNA containing three 62 base pair repetitive elements encoding for the Ki-67 epitope. *Lab Invest,* 68**,** 629-636.

KHVOROVA, A., REYNOLDS, A. & JAYASENA, S. D. 2003. Functional siRNAs and miRNAs Exhibit Strand Bias. *Cell,* 115**,** 209-216.

KIRBY, A. M., A'HERN, R. P., D'AMBROSIO, C., TANAY, M., SYRIGOS, K. N., ROGERS, S. J., BOX, C., ECCLES, S. A., NUTTING, C. M. & HARRINGTON, K. J. 2006. Gefitinib (ZD1839, Iressa™) as palliative treatment in recurrent or metastatic head and neck cancer. *Br J Cancer,* 94**,** 631-636.

KITTLER, R. & BUCHHOLZ, F. 2003. RNA interference: gene silencing in the fast lane. *Semin Cancer Biol,* 13**,** 259-265.

KRAMER, R. H., SHEN, X. & ZHOU, H. 2005. Tumor cell invasion and survival in head and neck cancer. *Cancer Metastasis Rev,* 24**,** 35-45.

KUMAR, B., CORDELL, K. G., LEE, J. S., PRINCE, M. E., TRAN, H. H., WOLF, G. T., URBA, S. G., WORDEN, F. P., CHEPEHA, D. B., TEKNOS, T. N., EISBRUCH, A., TSIEN, C. I., TAYLOR, J. M. G., D'SILVA, N. J., YANG, K., KURNIT, D. M., BRADFORD, C. R. & CAREY, T. E. 2007. Response to Therapy and Outcomes in Oropharyngeal Cancer Are Associated With Biomarkers Including Human Papillomavirus, Epidermal Growth Factor Receptor, Gender, and Smoking. *Int J Radiat Oncol Biolo Phys,* 69**,** S109-S111.

KUMAR, R., CONKLIN, D. S. & MITTAL, V. 2003. High-Throughput Selection of Effective RNAi Probes for Gene Silencing. *Genome Res* 13**,** 2333-2340.

KURRECK, J. 2006. siRNA Efficiency: Structure or Sequence-That Is the Question. *J Biomed Biotechnol,* 2006**,** 83757.

LAI, S. Y., KOPPIKAR, P., THOMAS, S. M., CHILDS, E. E., EGLOFF, A. M., SEETHALA, R. R., BRANSTETTER, B. F., GOODING, W. E., MUTHUKRISHNAN, A., MOUNTZ, J. M., LUI, V. W. Y., SHIN, D. M., AGARWALA, S. S., JOHNSON, R., COUTURE, L. A., MYERS, E. N., JOHNSON, J. T., MILLS, G., ARGIRIS, A. & GRANDIS, J. R. 2009. Intratumoral Epidermal Growth Factor Receptor Antisense DNA Therapy in Head and Neck Cancer: First Human Application and Potential Antitumor Mechanisms. *J Clin Oncol,* 27**,** 1235-1242.

LANA, S. E., OGILVIE, G. K., WITHROW, S. J., STRAW, R. C. & ROGERS, K. S. 1997. Feline cutaneous squamous cell carcinoma of the nasal planum and the pinnae: 61 cases. *J Am Anim Hosp Assoc,* 33**,** 329-332.

LANGO, M. N., SHIN, D. M. & GRANDIS, J. R. 2001. Targeting growth factor receptors: integration of novel therapeutics in the management of head and neck cancer. *Curr Opin Oncol,* 13**,** 168-175.

LEBLANC, A. K., LADUE, T. A., TURREL, J. M. & KLEIN, M. K. 2004. Unexpected toxicity following use of gemcitabine as a radiosensitizer in head and neck carcinomas: a veterinary radiation therapy oncology group pilot study. *Vet Radiol Ultrasound,* 45**,** 466-470.

LENFERINK, A. E., PINKAS-KRAMARSKI, R., VAN DE POLL, M. L., VAN VUGT, M. J., KLAPPER, L. N., TZAHAR, E., WATERMAN, H., SELA, M., VAN ZOELEN, E. J. & YARDEN, Y. 1998. Differential endocytic routing of homo- and hetero-dimeric ErbB tyrosine kinases confers signaling superiority to receptor heterodimers. *EMBO J* 17**,** 3385-3397.

LEVKOWITZ, G., WATERMAN, H., ZAMIR, E., KAM, Z., OVED, S., LANGDON, W. Y., BEGUINOT, L., GEIGER, B. & YARDEN, Y. 1998. c-Cbl/Sli-1 regulates endocytic sorting and ubiquitination of the epidermal growth factor receptor. *Genes Dev,* 12**,** 3663-3674.

LI, C., IIDA, M., DUNN, E. F., GHIA, A. J. & WHEELER, D. L. 2009. Nuclear EGFR contributes to acquired resistance to cetuximab. *Oncogene,* 28**,** 3801-3813.

LIANG, C.-C., PARK, A. Y. & GUAN, J.-L. 2007. In vitro scratch assay: a convenient and inexpensive method for analysis of cell migration in vitro. *Nat Protoc,* 2**,** 329-333.

LIPSITZ, D., HIGGINS, R. J., KORTZ, G. D., DICKINSON, P. J., BOLLEN, A. W., NAYDAN, D. K. & LECOUTEUR, R. A. 2003. Glioblastoma multiforme: clinical findings, magnetic resonance imaging, and pathology in five dogs. *Vet Path,* 40**,** 659-669.

LOCKE, M., HEYWOOD, M., FAWELL, S. & MACKENZIE, I. C. 2005. Retention of intrinsic stem cell hierarchies in carcinoma-derived cell lines. *Cancer Res,* 65**,** 8944-8950.

LONDON, C. A., MALPAS, P. B., WOOD-FOLLIS, S. L., BOUCHER, J. F., RUSK, A. W., ROSENBERG, M. P., HENRY, C. J., MITCHENER, K. L., KLEIN, M. K., HINTERMEISTER, J. G., BERGMAN, P. J.,

COUTO, G. C., MAULDIN, G. N. & MICHELS, G. M. 2009. Multi-center, placebo-controlled, double-blind, randomized study of oral toceranib phosphate (SU11654), a receptor tyrosine kinase inhibitor, for the treatment of dogs with recurrent (either local or distant) mast cell tumor following surgical excision. *Clin Cancer Res,* 15**,** 3856-3865.

LOOPER, J. S., MALARKEY, D. E., RUSLANDER, D., PROULX, D. & THRALL, D. E. 2006. Epidermal growth factor receptor expression in feline oral squamous cell carcinomas. *Vet Comp Oncol,* 4**,** 33-40.

LÖRZ, M., MEYER-BREITING, E. & BETTINGER, R. 1994. Proliferating cell nuclear antigen counts as markers of cell proliferation in head and neck cancer. *Eur Arch Otorhinolaryngol,* 251**,** 91-94.

LUI, V. W., THOMAS, S. M., ZHANG, Q., WENTZEL, A. L., SIEGFRIED, J. M., LI, J. Y. & GRANDIS, J. R. 2003. Mitogenic effects of gastrin-releasing peptide in head and neck squamous cancer cells are mediated by activation of the epidermal growth factor receptor. *Oncogene,* 22**,** 6183-6193.

LURJE, G. & LENZ, H. J. 2009. EGFR Signaling and Drug Discovery. *Oncol,* 77**,** 400-410.

MA, B. B. Y., POON, T. C. W., TO, K. F., ZEE, B., MO, F. K. F., CHAN, C. M. L., HO, S., TEO, P. M. L., JOHNSON, P. J. & CHAN, A. T. C. 2003. Prognostic significance of tumor angiogenesis, Ki 67, p53 oncoprotein, epidermal growth factor receptor and HER2 receptor protein expression in undifferentiated nasopharyngeal carcinoma - a prospective study. *Head Neck,* 25**,** 864-872.

MACY, D. W. & REYNOLDS, H. A. 1981. The Incidence , Characteristics and Clinical Management of Skin Tumours of Cats. *J Am Anim Hosp Assoc,* 17**,** 1026-1034.

MAGNE, M. L., RODRIGUEZ, C. O., AUTRY, S. A., EDWARDS, B. F., THEON, A. P. & MADEWELL, B. R. 1997. Photodynamic therapy of facial squamous cell carcinoma in cats using a new photosensitizer. *Lasers Surg Med,* 20**,** 202-209.

MALANCHI, I., PEINADO, H., KASSEN, D., HUSSENET, T., METZGER, D., CHAMBON, P., HUBER, M., HOHL, D., CANO, A., BIRCHMEIER, W. & HUELSKEN, J. 2008. Cutaneous cancer stem cell maintenance is dependent on β-catenin signalling. *Nature,* 452**,** 650-653.

MALINOWSKI, C. 2006. Canine and Feline Nasal Neoplasia. *Clin Tech Small Anim Pract,* 21**,** 89-94.

MAO, C., LIAO, R. Y. & CHEN, Q. 2010. Loss of PTEN expression predicts resistance to EGFR-targeted monoclonal antibodies in patients with metastatic colorectal cancer. *Br J Cancer,* 102**,** 940.

MAULDIN, G. N. 2001. Consultations of Feline Internal Medicine. Chapter 66, p 526-528, *In:* AUGUST, J. (ed.) *Consultations of Feline Internal Medicine,* Philadelphia: W.B. Saunders Company.

MELZER, K., GUSCETTI, F., ROHRER BLEY, C., SUMOVA, A., ROOS, M. & KASER-HOTZ, B. 2006. Ki67 reactivity in nasal and periocular squamous cell carcinomas in cats treated with electron beam radiation therapy. *J Vet Intern Med,* 20**,** 676-681.

MILANO, G., SPANO, J. P. & LEYLAND-JONES, B. 2008. EGFR-targeting drugs in combination with cytotoxic agents: from bench to bedside, a contrasted reality. *Br J Cancer,* 99**,** 1-5.

MILLER, M. A., NELSON, S. L., TURK, J. R., PACE, L. W., BROWN, T. P., SHAW, D. P., FISCHER, J. R. & GOSSER, H. S. 1991. Cutaneous neoplasia in 340 cats. *Vet Path,* 28**,** 389-395.

MINKE, J. M., SCHUURING, E., VAN DEN BERGHE, R., STOLWIJK, J. A., BOONSTRA, J., CORNELISSE, C., HILKENS, J. & MISDORP, W. 1991. Isolation of two distinct epithelial cell lines from a single feline mammary carcinoma with different tumorigenic potential in nude mice and expressing different levels of epidermal growth factor receptors. *Cancer Res,* 51**,** 4028-4037.

MOK, T. S., WU, Y.-L., THONGPRASERT, S., YANG, C.-H., CHU, D.-T., SAIJO, N., SUNPAWERAVONG, P., HAN, B., MARGONO, B., ICHINOSE, Y., NISHIWAKI, Y., OHE, Y., YANG, J.-J., CHEWASKULYONG, B., JIANG, H., DUFFIELD, E. L., WATKINS, C. L., ARMOUR, A. A. & FUKUOKA, M. 2009. Gefitinib or Carboplatin-Paclitaxel in Pulmonary Adenocarcinoma. *N Engl J Med,* 361**,** 947-957.

MONROE, M. M., ANDERSON, E. C., CLAYBURGH, D. R. & WONG, M. H. 2010. Cancer stem cells in Head and Neck Squamous Cell Carcinoma. *J Oncol,* Epub ahead of print 8 Nov 2010

MORRIS, J. & DOBSON, J. 2001. Chapter 7: Head and neck, p 94-124, *In:* MORRIS, J. & DOBSON, J. (eds.) *Small Animal Oncology*. 1st ed. Oxford: Blackwell Science Limited.

MORRIS, J. S., NIXON, C., BRUCK, A., NASIR, L., MORGAN, I. M. & PHILBEY, A. W. 2008. Immunohistochemical expression of TopBP1 in feline mammary neoplasia in relation to histological grade, Ki67, ER[alpha] and p53. *Vet J,* 175**,** 218-226.

MRHALOVA, M., PLZAK, J., BETKA, J. & KODET, R. 2005. Epidermal growth factor receptor-its expression and copy numbers of EGFR gene in patients with head and neck squamous cell carcinomas. *Neoplasma,* 52**,** 338-343.

MUKARATIRWA, S., VAN DER LINDE-SIPMAN, J. S. & GRUYS, E. 2001. Feline nasal and paranasal sinus tumours: clinicopathological study, histomorphological description and diagnostic immunohistochemistry of 123 cases. *J Feline Med Surg,* 3**,** 235-245.

MUNDAY, J. S., HOWE, L., FRENCH, A., SQUIRES, R. A. & SUGIARTO, H. 2009. Detection of papillomaviral DNA sequences in a feline oral squamous cell carcinoma. *Res Vet Sci,* 86**,** 359-361.

MUNDAY, J. S., KIUPEL, M., FRENCH, A. F., HOWE, L. & SQUIRES, R. A. 2007. Detection of papillomaviral sequences in feline Bowenoid in situ carcinoma using consensus primers. *Vet Dermatol,* 18**,** 241-245.

MWG. 2008. *siRNA design tool* [Online]. mwg. Available: www.ecom.mwgdna.com/cgi/siRNA_design2.cgi [Accessed 12.08. 2008].

NAGANE, M., LIN, H., CAVENEE, W. K. & HUANG, H. J. S. 2001. Aberrant receptor signaling in human malignant gliomas: mechanisms and therapeutic implications. *Cancer Lett,* 162**,** S17-S21.

NAITO, Y., YAMADA, T., UI-TEI, K., MORISHITA, S. & SAIGO, K. 2004. siDirect: highly effective, target-specific siRNA design software for mammalian RNA interference. *Nucleic Acids Res,* 32**,** W124-129.

NCBI. 2010a. *BLAST searches cat genome* [Online]. Available: http://www.ncbi.nlm.nih.gov/genome/guide/cat/ [Accessed 10.08 2010].

NCBI. 2010b. *Search for gene homology* [Online]. ncbi. Available: www.ncbi.nlm.nih.gov/sites/homologene [Accessed 10.08. 2010].

NCBI. 2010c. *Search for gene sequences* [Online]. ncbi. Available: www.ncbi.nlm.nih.gov/genbank/GenbankSearch.html [Accessed 10.08. 2009].

NCI. 2010. *Search for Clinical Trials* [Online]. Available: http://www.cancer.gov/search/SearchClinicalTrials.aspx [Accessed 18.11. 2010].

NEGRI, F. V., BOZZETTI, C., LAGRASTA, C. A., CRAFA, P., BONASONI, M. P., CAMISA, R., PEDRAZZI, G. & ARDIZZONI,

A. 2010. PTEN status in advanced colorectal cancer treated with cetuximab. *Br J Cancer,* 102**,** 162-164.

NESPECA, G., GREST, P., ROSENKRANTZ, W. S., ACKERMANN, M. & FAVROT, C. 2006. Detection of novel papillomaviruslike sequences in paraffin-embedded specimens of invasive and in situ squamous cell carcinomas from cats. *Am J Vet Res,* 67**,** 2036-2041.

NICHOLSON, R. I., GEE, J. M. & HARPER, M. E. 2001. EGFR and cancer prognosis. *Eur J Cancer,* 37 Suppl 4**,** S9-15.

NISSIM, A. & CHERNAJOVSKY, Y. 2008. Historical Development of Monoclonal Antibody Therapeutics. *In:* CHERNAJOVSKY, Y. & NISSIM, A. (eds.) *Therapeutic Antibodies.* Springer Berlin Heidelberg.

NORMANNO, N., BIANCO, C., DE LUCA, A., STRIZZI, L., GALLO, M., MANCINO, M. & SALOMON, D. A. 2008. Chapter 16 Expression and Prognostic Significance of the EGFR in Solid Tumours, p 221-234 *In:* HALEY, J. D. & GULLICK, W. J. (eds.) *EGFR Signaling Networks in Cancer Therapy.* 1 ed. New York: Humana Press.

NORTHRUP, N. C., SELTING, K. A., RASSNICK, K. M., KRISTAL, O., O'BRIEN, M. G., DANK, G., DHALIWAL, R. S., JAGANNATHA, S., CORNELL, K. K. & GIEGER, T. L. 2006. Outcomes of cats with oral tumors treated with mandibulectomy: 42 cases. *J Am Anim Hosp Assoc,* 42**,** 350-360.

NOZAWA, H., TADAKUMA, T., ONO, T., SATO, M., HIROI, S., MASUMOTO, K. & SATO, Y. 2006. Small interfering RNA targeting epidermal growth factor receptor enhances chemosensitivity to cisplatin, 5-fluorouracil and docetaxel in head and neck squamous cell carcinoma. *Cancer Sci,* 97**,** 1115-1124.

O'NEILL, S. H., NEWKIRK, K. M., ANIS, E. A., BRAHMBHATT, R., FRANK, L. A. & KANIA, S. A. 2010. Detection of human papillomavirus DNA in feline premalignant and invasive squamous cell carcinoma. *Vet Dermatol,* E-pub ahead of print.

ODA, D. & WATSON, E. 1990. Human Oral Epithelial Cell Culture I. Improved Conditions for Reproducible Culture in Serum-Free Medium. *In vitro Cell Dev Biol,* 26**,** 589-595.

OGILVIE, G. K. & MOORE, A. S. 1996a. Section V: Tumours of the Oral Cavity, p340-348. *In:* OGILVIE, G. K. & MOORE, A. S. (eds.) *Managing the Veterinary Cancer Patient A Practice Manual.* 1st ed. Trenton, New Yersey: Veterinary Learning Systems Company, Inc.

OGILVIE, G. K. & MOORE, A. S. 1996b. Section V: Tumours of the Skin and Surrounding structures, p 473-483. *In:* OGILVIE, G. K. & MOORE, A. S. (eds.) *Managing the Veterinary Cancer Patient A Practice Manual.* 1st ed. Trenton, New Jersey: Veterinary Learning Systems Company , Inc

OGILVIE, G. K., MOORE, A. S., OBRADOVICH, J. E., ELMSLIE, R. E., VAIL, D. M., STRAW, R. C., SALMON, M. D., KLEIN, M. K., ATWATER, S. W. & CIEKOT, P. E. 1993. Toxicoses and efficacy associated with administration of mitoxantrone to cats with malignant tumors. *J Am Vet Med Assoc,* 202**,** 1839-44.

OKAMOTO, A., CHIKAMATSU, K., SAKAKURA, K., HATSUSHIKA, K., TAKAHASHI, G. & MASUYAMA, K. 2009. Expansion and characterization of cancer stem-like cells in squamous cell carcinoma of the head and neck. *Oral Oncol* 45**,** 633-639.

OLAYIOYE, M. A., NEVE, R. M., LANE, H. A. & HYNES, N. E. 2000. The ErbB signaling network: receptor heterodimerization in development and cancer. *EMBO J,* 19**,** 3159-3167.

OWEN, L. M. 1980. TNM classification of tumours in domestic animals. *Geneva: World Health Organisation*.

PAI, S. I., LIN, Y. Y., MACAES, B., MENESHIAN, A., HUNG, C. F. & WU, T. C. 2006. Prospects of RNA interference therapy for cancer. *Gene Ther,* 13**,** 464-77.

PAOLONI, M. & KHANNA, C. 2008. Translation of new cancer treatments from pet dogs to humans. *Nat Rev Cancer,* 8**,** 147-156.

PARTRIDGE, M., GABALLAH, K. & HUANG, X. 2005. Molecular markers for diagnosis and prognosis. *Cancer Metastasis Rev,* 24**,** 71-85.

PATZEL, V., RUTZ, S., DIETRICH, I., KOBERLE, C., SCHEFFOLD, A. & KAUFMANN, S. H. E. 2005. Design of siRNAs producing unstructured guide-RNAs results in improved RNA interference efficiency. *Nat Biotech,* 23**,** 1440-1444.

PEASTON, A. E., LEACH, M. W. & HIGGINS, R. J. 1993. Photodynamic therapy for nasal and aural squamous cell carcinoma in cats. *J Am Vet Med Assoc,* 202**,** 1261-1265.

PETRIE, A. & WATSON, P. 2006a. Chapter 13.3 Sample size. *In:* PETRIE, A. & WATSON, P. (eds.) *Statistics for Veterinary and Animal Science.* 2nd ed. Oxford, UK: Blackwell Publishing Ltd.

PETRIE, A. & WATSON, P. 2006b. Chapter 14.6 Survival Analysis. *In:* PETRIE, A. & WATSON, P. (eds.) *Statistics for Veterinary and Animal Science.* 2nd ed. Oxford, UK: Blackwell Publishing Ltd.

PFAFFL, M. W. 2001. A new mathematical model for relative quantification in real-time RT-PCR. *Nucleic Acids Res,* 29**,** e45-51.

Pet Food Manufacturers' Association 2010. *Pet Population Figures 2010* [Online]. Available: http://www.pfma.org.uk/overall/pet-population-figures-.htm [Accessed 21.05 2010].

PICH, A., CHIUSA, L. & NAVONE, R. 2004. Prognostic relevance of cell proliferation in head and neck tumors. *Ann Oncol,* 15**,** 1319-1329.

PIRCHER, A., PLONER, F., POPPER, H. & HILBE, W. 2010. Rationale of a relaunch of gefitinib in Caucasian non-small cell lung cancer patients. *Lung Cancer,* 69**,** 265-271.

PONTIUS, J. U., MULLIKIN, J. C., SMITH, D. R., LINDBLAD-TOH, K., GNERRE, S., CLAMP, M., CHANG, J., STEPHENS, R., NEELAM, B., VOLFOVSKY, N., SCHAFFER, A. A., AGARWALA, R., NARFSTROM, K., MURPHY, W. J., GIGER, U., ROCA, A. L., ANTUNES, A., MENOTTI-RAYMOND, M., YUHKI, N., PECON-SLATTERY, J., JOHNSON, W. E., BOURQUE, G., TESLER, G. & O'BRIEN, S. J. 2007. Initial sequence and comparative analysis of the cat genome. *Genome Res,* 17**,** 1675-1689.

POSTORINO-REEVES, N. C., J.M., T. & WITHROW, S. J. 1993. Oral Squamous Cell Carcinoma in the Cat. *J Am Anim Hosp Assoc,* 29**,** 438-441.

PRIESTER, W. A. 1973. Skin tumors in domestic animals. Data from 12 United States and Canadian colleges of veterinary medicine. *J Natl Cancer Inst,* 50**,** 457-466.

PRIGENT, S. A. 2006. Chapter 11: Growth factors and their signalling pathways in cancer, p186-209. *In:* KNOWLES, M. & SELBY, P. (eds.) *Introduction to the Cellular and Molecular Biology of Cancer.* 4th ed. Oxford: Oxford University Press.

PRINCE, M. E., SIVANANDAN, R., KACZOROWSKI, A., WOLF, G. T., KAPLAN, M. J., DALERBA, P., WEISSMAN, I. L., CLARKE, M. F. & AILLES, L. E. 2007. Identification of a subpopulation of cells with cancer stem cell properties in head and neck squamous cell carcinoma. *Proc Natl Acad Sci U S A* 104**,** 973-978.

PRINCE, M. E. P. & AILLES, L. E. 2008. Cancer Stem Cells in Head and Neck Squamous Cell Cancer. *J Clin Oncol,* 26**,** 2871-2875.

QUEIROGA, F. L., PEREZ-ALENZA, D., SILVAN, G., PENA, L. & ILLERA, J. C. 2009. Positive correlation of steroid hormones and EGF in canine mammary cancer. *J Steroid Biochem Mol Biol,* 115**,** 9-13.

QUON, H., LIU, F. F. & CUMMINGS, B. J. 2001. Potential molecular prognostic markers in head and neck squamous cell carcinomas. *Head Neck,* 23**,** 147-159.

RATUSHNY, V., ASTSATUROV, I., BURTNESS, B. A., GOLEMIS, E. A. & SILVERMAN, J. S. 2009. Targeting EGFR resistance networks in head and neck cancer. *Cell Signal,* 21**,** 1255-1268.

RECILLAS-TARGA, F. 2006. Multiple strategies for gene transfer, expression, knockdown, and chromatin influence in mammalian cell lines and transgenic animals. *Mol Biotechnol* 34**,** 337-354.

REDEMANN, N., HOLZMANN, B., VON RUDEN, T., WAGNER, E. F., SCHLESSINGER, J. & ULLRICH, A. 1992. Anti-oncogenic activity of signalling-defective epidermal growth factor receptor mutants. *Mol cell biol,* 12**,** 491-498.

REUTER, C. W., MORGAN, M. A. & ECKARDT, A. 2007. Targeting EGF-receptor-signalling in squamous cell carcinomas of the head and neck. *Br J Cancer,* 96**,** 408-416.

REYNOLDS, A., LEAKE, D., BOESE, Q., SCARINGE, S., MARSHALL, W. S. & KHVOROVA, A. 2004. Rational siRNA design for RNA interference. *Nat Biotech,* 22**,** 326-330.

RHO, J. K., CHOI, Y. J., LEE, J. K., RYOO, B.-Y., NA, I. I., YANG, S. H., KIM, C. H. & LEE, J. C. 2009. Epithelial to mesenchymal transition derived from repeated exposure to gefitnib determines the sensitivity to EGFR inhibitors in A549, a non-small cell lung cancer cell line. *Lung Cancer,* 63**,** 219-226.

RITTÀ, M., ANDREA, M. D., MONDINI, M., MAZIBRADA, J., GIORDANO, C., PECORARI, G., GARZARO, M., LANDOLFO, V., SCHENA, M., CHIUSA, L. & LANDOLFO, S. 2009. Cell cycle and viral and immunologic profiles of head and neck squamous cell carcinoma as predictable variables of tumor progression. *Head Neck,* 31**,** 318-327.

ROBERTS, P. J. & DER, C. J. 2007. Targeting the Raf-MEK-ERK mitogen-activated protein kinase cascade for the treatment of cancer. *Oncogene,* 26**,** 3291-3310.

ROBERTS, W. G., KLEIN, M. K., LOOMIS, M., WELDY, S. & BERNS, M. W. 1991. Photodynamic Therapy of Spontaneous Cancers in

Felines, Canines, and Snakes With Chloro-aluminium Sulfonated Phthalocyanine. *J Natl Cancer Inst,* 83**,** 18-23.

ROCHE. 2009. *Roche Universal Probe Library Assay Design Centre* [Online]. Roche Ltd. Available: www.roche-applied-science.com [Accessed 19.04. 2009].

ROELS, S. L., VAN DAELE, A. J., VAN MARCK, E. A. & DUCATELLE, R. V. 2000. DNA ploidy and nuclear morphometric variables for the evaluation of melanocytic tumors in dogs and cats. *Am J Vet Res,* 61**,** 1074-1079.

ROGERS, S. J., HARRINGTON, K. J., RHYS-EVANS, P., O-CHAROENRAT, P., & ECCLES, S. A. 2005. Biological significance of c-erbB family oncogenes in head and neck cancer. *Cancer Metastasis Rev,* 24**,** 47-69.

RUTTEMAN, G. R., FOEKENS, J. A., PORTENGEN, H., VOS, J. H., BLANKENSTEIN, M. A., TESKE, E., CORNELISSE, C. J. & MISDORP, W. 1994. Expression of epidermal growth factor receptor (EGFR) in non-affected and tumorous mammary tissue of female dogs. *Breast Cancer Res Treat,* 30**,** 139-146.

SABATTINI, S., MARCONATO, L., ZOFF, A., MORINI, M., SCARPA, F., CAPITANI, O. & BETTINI, G. 2010. Epidermal growth factor receptor expression is predictive of poor prognosis in feline cutaneous squamous cell carcinoma. *J Feline Med Surg,* 12**,** 760-768.

SAHLGREN, C., GUSTAFSSON, M. V., JIN, S., POELLINGER, L. & LENDAHL, U. 2008. Notch signaling mediates hypoxia-induced tumor cell migration and invasion. *Proc Natl Acad Sci U S A,* 105**,** 6392-6397.

SAIK, J. E., TOLL, S. L., DITERS, R. W. & GOLDSCHMIDT, M. H. 1986. Canine and Feline Laryngeal Neoplasia: A 10-year Survey. *J Am Anim Hosp Assoc,* 22**,** 359-365.

SALOMON, D. S., BRANDT, R., CIARDIELLO, F. & NORMANNO, N. 1995. Epidermal growth factor-related peptides and their receptors in human malignancies. *Crit Rev Oncol Hematol,* 19**,** 183-232.

SANTISTEBAN, M., REIMAN, J. M., ASIEDU, M. K., BEHRENS, M. D., NASSAR, A., KALLI, K. R., HALUSKA, P., INGLE, J. N., HARTMANN, L. C., MANJILI, M. H., RADISKY, D. C., FERRONE, S. & KNUTSON, K. L. 2009. Immune-Induced Epithelial to Mesenchymal Transition In vivo Generates Breast Cancer Stem Cells. *Cancer Res,* 69**,** 2887-2895.

SASAOKA, T., LANGLOIS, W. J., LEITNER, J. W., DRAZNIN, B. & OLEFSKY, J. M. 1994. The signaling pathway coupling epidermal growth factor receptors to activation of p21ras. *J Biol Chem,* 269**,** 32621-32625.

SCHERER, L. J. & ROSSI, J. J. 2003. Approaches for the sequence-specific knockdown of mRNA. *Nat Biotech,* 21**,** 1457-1465.

SCHWARZ, D. S., HUTVAGNER, G., DU, T., XU, Z., ARONIN, N. & ZAMORE, P. D. 2003. Asymmetry in the assembly of the RNAi enzyme complex. *Cell,* 115**,** 199-208.

SHARMA, S. V., BELL, D. W., SETTLEMAN, J. & HABER, D. A. 2007. Epidermal growth factor receptor mutations in lung cancer. *Nat Rev Cancer,* 7**,** 169-181.

SHIN, D. M., RO, J. Y., HONG, W. K. & HITTELMAN, W. N. 1994. Dysregulation of epidermal growth factor receptor expression in premalignant lesions during head and neck tumorigenesis. *Cancer Res,* 54**,** 3153-3159.

SHINTANI, S., FUNAYAMA, T., YOSHIHAMA, Y., ALCALDE, R. E. & MATSUMURA, T. 1995. Prognostic significance of ERRB3 overexpression in oral squamous cell carcinoma. *Cancer Lett,* 95**,** 79-83.

SHIOMITSU, K., JOHNSON, C. L., MALARKEY, D. E., PRUITT, A. F. & THRALL, D. E. 2009. Expression of epidermal growth factor receptor and vascular endothelial growth factor in malignant canine epithelial nasal tumours. *Vet Comp Oncol,* 7**,** 106-114.

SHTIEGMAN, K., KOCHUPURAKKAL, B. S., ZWANG, Y., PINES, G., STARR, A., VEXLER, A., CITRI, A., KATZ, M., LAVI, S., BEN-BASAT, Y., BENJAMIN, S., CORSO, S., GAN, J., YOSEF, R. B., GIORDANO, S. & YARDEN, Y. 2007. Defective ubiquitinylation of EGFR mutants of lung cancer confers prolonged signaling. *Oncogene,* 26**,** 6968-6978.

SIBILIA, M., KROISMAYR, R., LICHTENBERGER, B. M., NATARAJAN, A., HECKING, M. & HOLCMANN, M. 2007. The epidermal growth factor receptor: from development to tumorigenesis. *Differentiation,* 75**,** 770-787.

SIGISMUND, S., ARGENZIO, E., TOSONI, D., CAVALLARO, E., POLO, S. & DI FIORE, P. P. 2008. Clathrin-Mediated Internalization Is Essential for Sustained EGFR Signaling but Dispensable for Degradation. *Dev Cell,* 15**,** 209-219.

SNYDER, L. A., BERTONE, E. R., JAKOWSKI, R. M., DOONER, M. S., JENNINGS-RITCHIE, J. & MOORE, A. S. 2004. p53 expression and environmental tobacco smoke exposure in feline oral squamous cell carcinoma. *Vet Path,* 41**,** 209-214.

SONG, J., CHANG, I., CHEN, Z., KANG, M. & WANG, C.-Y. 2010. Characterization of Side Populations in HNSCC: Highly Invasive, Chemoresistant and Abnormal Wnt Signaling. *PLoS ONE,* 5**,** e11456.

SONG, J. I. & GRANDIS, J. R. 2000. STAT signaling in head and neck cancer. *Oncogene,* 19**,** 2489-2495.

SORKIN, A. & GOH, L. K. 2009. Endocytosis and intracellular trafficking of ErbBs. *Exp Cell Res,* 315**,** 683-696.

STEBBINS, K. E., MORSE, C. C. & GOLDSCHMIDT, M. H. 1989. Feline oral neoplasia: a ten-year survey. *Vet Path,* 26**,** 121-128.

STELL, A. J., DOBSON, J. M. & LANGMACK, K. 2001. Photodynamic therapy of feline superficial squamous cell carcinoma using topical 5-aminolaevulinic acid. *J Small Anim Pract,* 42**,** 164-169.

STOICA, G., KIM, H. T., HALL, D. G. & COATES, J. R. 2004. Morphology, immunohistochemistry, and genetic alterations in dog astrocytomas. *Vet Path,* 41**,** 10-19.

TAKASAKI, S. 2010. Efficient prediction methods for selecting effective siRNA sequences. *Comput Biol Med,* 40**,** 149-158.

TANNEHILL-GREGG, S., KERGOSIEN, E. & ROSOL, T. J. 2001. Feline head and neck squamous cell carcinoma cell line: characterization, production of parathyroid hormone-related protein, and regulation by transforming growth factor-beta. *In Vitro Cell. Dev. Biol. Anim.,* 37**,** 676-683.

TANNEHILL-GREGG, S. H., LEVINE, A. L. & ROSOL, T. J. 2006. Feline head and neck squamous cell carcinoma: a natural model for the human disease and development of a mouse model. *Vet Comp Oncol,* 4**,** 84-97.

THARIAT, J., YILDIRIM, G., MASON, K. A., GARDEN, A. S., MILAS, L. & ANG, K. K. 2007. Combination of radiotherapy with EGFR antagonists for head and neck carcinoma. *Int J Clin Oncol,* 12**,** 99-110.

THEON, A. P., MADEWELL, B. R., SHEARN, V. I. & MOULTON, J. E. 1995. Prognostic factors associated with radiotherapy of squamous cell carcinoma of the nasal plane in cats. *J Am Vet Med Assoc,* 206**,** 991-996.

THIERY, J. P., ACLOQUE, H., HUANG, R. Y. J. & NIETO, M. A. 2009. Epithelial-Mesenchymal Transitions in Development and Disease. *Cell,* 139**,** 871-890.

THOMAS, R., DUKE, S. E., WANG, H. J., BREEN, T. E., HIGGINS, R. J., LINDER, K. E., ELLIS, P., LANGFORD, C. F., DICKINSON, P. J., OLBY, N. J. & BREEN, M. 2009. 'Putting our heads together': insights into genomic conservation between human and canine intracranial tumors. *J Neurooncol,* 94**,** 333-349.

THOMAS, S. M., COPPELLI, F. M., WELLS, A., GOODING, W. E., SONG, J., KASSIS, J., DRENNING, S. D. & GRANDIS, J. R. 2003. Epidermal growth factor receptor-stimulated activation of phospholipase Cgamma-1 promotes invasion of head and neck squamous cell carcinoma. *Cancer Res,* 63**,** 5629-5635.

THOMSON, M. 2007. Squamous cell carcinoma of the nasal planum in cats and dogs. *Clin Tech Small Anim Pract,* 22**,** 42-45.

TROMBLEE, T. C., JONES, J. C., ETUE, A. E. & DRU FORRESTER, S. 2006. Association between Clinical Characteristics, Computed Tomography Characteristics, and Histologic Diagnosis for Cats with Sinonasal Disease. *Vet Radiol Ultrasound,* 47**,** 241-248.

ULLRICH, A., COUSSENS, L., HAYFLICK, J. S., DULL, T. J., GRAY, A., TAM, A. W., LEE, J., YARDEN, Y., LIBERMANN, T. A., SCHLESSINGER, J., DOWNWARD, J., MAYES, E. L. V., WHITTLE, N., WATERFIELD, M. D. & SEEBURG, P. H. 1984. Human epidermal growth factor receptor cDNA sequence and aberrant expression of the amplified gene in A431 epidermoid carcinoma cells. *Nature,* 309**,** 418-425.

VALCOURT, U., KOWANETZ, M., NIIMI, H., HELDIN, C.-H. & MOUSTAKAS, A. 2005. TGF-{beta} and the Smad Signaling Pathway Support Transcriptomic Reprogramming during Epithelial-Mesenchymal Cell Transition. *Mol Biol Cell,* 16**,** 1987-2002.

VAN KRUININGEN, H. J. 1995. Gastrointestinal System. *In:* CARLTON, W. W. & MCGAVIN, M. D. (eds.) *Thomson's Special Veterinary Pathology.* 2nd ed. St. Louis: Mosby.

VISVADER, J. E. & LINDEMAN, G. J. 2008. Cancer stem cells in solid tumours: accumulating evidence and unresolved questions. *Nat Rev Cancer,* 8**,** 755-768.

WANG, Y.-N., YAMAGUCHI, H., HSU, J.-M. & HUNG, M.-C. 2010. Nuclear trafficking of the epidermal growth factor receptor. *Oncogene,* 29**,** 3997-4006.

WEICHSELBAUM, R. R., DUNPHY, E. J., BECKETT, M. A., TYBOR, A. G., MORAN, W. J., GOLDMAN, M. E., VOKES, E. E. & PANJE, W. R. 1989. Epidermal growth factor receptor gene amplification and expression in head and neck cancer cell lines. *Head Neck,* 11**,** 437-442.

WHEELER, D. L., DUNN, E. F. & HARARI, P. M. 2010a. Understanding resistance to EGFR inhibitors -impact on future treatment strategies. *Nat Rev Clin Oncol,* 7**,** 493-507.

WHEELER, D. L., HUANG, S., KRUSER, T. J., NECHREBECKI, M. M., ARMSTRONG, E. A., BENAVENTE, S., GONDI, V., HSU, K. T. & HARARI, P. M. 2008. Mechanisms of acquired resistance to cetuximab: role of HER (ErbB) family members. *Oncogene,* 27**,** 3944-3956.

WHEELER, S. E., SUZUKI, S., THOMAS, S. M., SEN, M., LEEMAN-NEILL, R. J., CHIOSEA, S. I., KUAN, C. T., BIGNER, D. D., GOODING, W. E., LAI, S. Y. & GRANDIS, J. R. 2010b. Epidermal growth factor receptor variant III mediates head and neck cancer cell invasion via STAT3 activation. *Oncogene,* 29**,** 5135-5145.

WILEY, H. S. 2003. Trafficking of the ErbB receptors and its influence on signaling. *Exp Cell Res,* 284**,** 78-88.

WILHELM, S., DEGORCE-RUBIALES, F., GODSON, D. & FAVROT, C. 2006. Clinical, histological and immunohistochemical study of feline viral plaques and bowenoid in situ carcinomas. *Vet Dermatol,* 17**,** 424-431.

WILLIAMS, B. R. 1999. PKR; a sentinel kinase for cellular stress. *Oncogene,* 18**,** 6112-6120.

WILLIAMS, R., KLINE, M. & SMITH, R. 1996. BSA and Restriction Enzyme Digestions. *Promega Notes* Promega Corporation.

WIRTZ-PEITZ, F. & ZALLEN, J. A. 2009. Junctional trafficking and epithelial morphogenesis. *Curr Opin Genet Dev,* 19**,** 350-6.

WITHROW, S. J. & STRAW, R. C. 1990. Resection of the Nasal Planum in Nine Cats and Five Dogs. *J Am Anim Hosp Assoc,* 26**,** 219-222.

XI, S., ZHANG, Q., GOODING, W. E., SMITHGALL, T. E. & GRANDIS, J. R. 2003. Constitutive activation of Stat5b contributes to carcinogenesis in vivo. *Cancer Res,* 63**,** 6763-6771.

XIA, H., CHEUNG, W. K. C., SZE, J., LU, G., JIANG, S., YAO, H., BIAN, X.-W., POON, W. S., KUNG, H.-F. & LIN, M. C. 2010. miR-200a regulates epithelial-mesenchymal to stem-like transition via ZEB2 and [beta]-catenin signaling. *J Biol Chem,* E-pub ahead of print.

YANG, D., BUCHHOLZ, F., HUANG, Z., GOGA, A., CHEN, C. Y., BRODSKY, F. M. & BISHOP, J. M. 2002. Short RNA duplexes produced by hydrolysis with Escherichia coli RNase III mediate effective RNA interference in mammalian cells. *Proc Natl Acad Sci U S A,* 99**,** 9942-9947.

YARDEN, Y. & SLIWKOWSKI, M. X. 2001. Untangling the ErbB signalling network. *Nat Rev Mol Cell Biol,* 2**,** 127-137.

YOUNG, B. & HEATH, J. W. 2002a. Epithelial tissues, p 80-96. *In:* HORNE, T. (ed.) *Wheater's Functional Histology.* 4th ed. Edinburgh: Churchill Livingstone.

YOUNG, B. & HEATH, J. W. 2002b. Oral tissues, p 237-248. *In:* HORNE, T. (ed.) *Wheater's Functional Histology.* 4th ed. Edinburgh: Churchill Livingstone.

YU, J. Y., DERUITER, S. L. & TURNER, D. L. 2002. RNA interference by expression of short-interfering RNAs and hairpin RNAs in mammalian cells. *Proc Natl Acad Sci U S A,* 99**,** 6047-6052.

YUAN, B., LATEK, R., HOSSBACH, M., TUSCHL, T. & LEWITTER, F. 2004. siRNA Selection Server: an automated siRNA oligonucleotide prediction server. *Nucl. Acids. Res.* **,** W130-W134.

ZHANG, N., ERJALA, K., KULMALA, J., QIU, X., SUNDVALL, M., ELENIUS, K. & GRÉNMAN, R. 2009. Concurrent cetuximab, cisplatin, and radiation for squamous cell carcinoma of the head and neck in vitro. *Radiother Oncol,* 92**,** 388-392.

ZHANG, Z., SCHWARTZ, S., WAGNER, L. & MILLER, W. 2000a. A greedy algorithm for aligning DNA sequences. *J Comput Biol,* 7**,** 203-214.

ZHANG, Z. F., MORGENSTERN, H., SPITZ, M. R., TASHKIN, D. P., YU, G. P., HSU, T. C. & SCHANTZ, S. P. 2000b. Environmental tobacco smoking, mutagen sensitivity, and head and neck squamous cell carcinoma. *Cancer Epidemiol Biomarkers Prev,* 9**,** 1043-1049.

ZHOU, H., ZENG, X., WANG, Y. & SEYFARTH, B. R. 2006. A Three-Phase Algorithm for Computer Aided siRNA Design. *Informatica,* 30**,** 357-364.

Appendix A: N2 media

Component	Quantity added	End concentration
DMEM/F12	-	Makes 10L (1X)
Sodium Bicarbonate	1.2 g	
Progesterone	156.25 µl	10 nM
Putrescine dihydrochloride	50 µl	50 µM
Sodium selenite	141.8 µl	15 nM
Apo-Transferrin (human)	25 ml	12.5 µg/ml
Insulin (bovine pancreas)	1 ml	10 µg/ml
EGF (recombinant human)	50 µl	5 ng/ml
bFGF (recombinant human)	50 µl	5 ng/ml
Methylcellulose	1.6 g/100ml	1.6%

Appendix B: Solutions & Buffers

Agarose gels: 1-1.2% small (35 ml) and large gels (100-120 ml) were made by adding 1-1.2g of agarose per 100 ml distilled water and microwaving until dissolved. The solution was allowed to cool, and nucleic acid labelling solutions were added before gel was poured into moulds and allowed to set.

Freezing media: 10% DMSO in FBS

Giemsa stain 10%: Add 5ml Giemsa stain to 45 ml distilled water and mix well.

imMedia™ Amp Blue sachets: Add content of one sachet to 200 ml distilled water and heat in microwave until dissolved. Allow to cool before pouring into plastic 10 cm dishes, makes 8-10 agar plates.

Laemmli Sample Buffer (2x): 120 mM Tris-HCl pH 6.8, 4% (w/v) sodium dodecyl sulphate (SDS), 20% (v/v) glycerol, 200mM DTT, 0.04% (w/v) bromophenol blue.

Luria broth base (Miller's LB broth base®, Invitrogen): powdered form, dissolve 25 g per litre of distilled water. Autoclave and allow to cool. Add

250 µl Ampicillin at a concentration of 100mg per ml to each 250 ml of LB broth. Typical formula per litre: 10 g Peptone 140, 5g Yeast Extract, 10 g sodium chloride.

Phosphate-buffered saline (PBS) (10x): purchased as 10x concentrate, made up with 100 ml 10x solution in 900 ml distilled water. Typical formula (g/l) sodium chloride (8g), potassium chloride (0.2g), di-sodium hydrogen orthophosphate (1.44g), potassium di-hydrogen orthophosphate (0.24g).

PBS/BSA 0.5% solution: Dissolve 100 mg BSA in 20 ml PBS and filter sterilise. Store at 2-8°C.

PBS Tween-20 (PBST): 0.01 M Phosphate, 0.154 M NaCl, and 0.1 % Tween-20, pH 7.4.

PBST blocking buffer: 5% Skimmed Milk in PBST.

Propidium Iodide: Frozen stock at 10mg/ml in water, kept in 20µl aliquots at minus 20°C. Working stock at 200µg/ml, make up by adding 980µl PBS, cover in foil and store in fridge.

Resolving gel: 8-10% acrylamide, 375 mM Tris-HCl pH 8.8, 0.1% SDS, 0.1% ammonium persulphate and polymerisation was initiated by adding 0.08% TEMED

SDS-PAGE running buffer (1x): 25 mM Tris, 190 mM glycine, 0.1% (v/w) SDS

Separation buffer for MACS sorting: PBS at pH 7.2, 0.5% BSA and 2mM EDTA. Filter sterilised and stored at 2-8°C.

Stacking gel: 5% acrylamide, 126 mM Tris-HCl pH 6.8, 0.1% SDS, 0.1% ammonium persulphate and polymerisation was initiated by adding 0.1% TEMED

TAE electrophoresis buffer (10x): Tris-HCl (0.4M, pH 8.0), sodium acetate (0.2M), EDTA (0.02M, pH 8.0).

TE buffer: 10mM Tris (pH 8.0), 1mM EDTA

Transfer buffer (1x): 25 mM Tris, 190 mM glycine, 20% (v/v) methanol

Tris-buffered saline Tween-20 (TBST): 20mM Tris-HCl, 0.15M NaCl, and 0.1% Tween-20.

TBST blocking buffer: 5% Bovine Serum Albumin (BSA) in TBST.

Urea lysis buffer: 7M Urea, 0.1 % DTT, 0.05% v/w Triton X-100, 25 mM NaCl, and 20 mM 4-(2-hydroxyethyl)-1-piperazineethanesulfonic acid (HEPES) (pH 7.5).

Appendix C: Questionnaire

CENTRE FOR SMALL ANIMAL STUDIES
Direct telephone: 08700 502540 Fax: 08700 502541
Oncology Unit
S Murphy BVM&S MSc (Clin Onc) MRCVS
Markus Clinician in Veterinary Oncology
Alison Hayes (Mrs) BVMS CertVR MRCVS
Clinician in Oncology
Prue Neath BSc(Hons), BVetMed,DACVS, MRCVS
ACVS Specialist in Veterinary Surgery

AMH
DATE XX/XX/XXXX

Dear Colleague

Our records show that you have submitted a sample to the Diagnostic Services Department, at the Animal Health Trust in the past three years, for a case of feline, oral squamous cell carcinomas (SCC).

As I am sure you are aware, squamous cell carcinoma is a devastating disease of the oral cavity in older cats, for which there is seldom a satisfactory treatment once the tumour has progressed to a stage where definitive surgery is not an option. All too often, cats present with advanced cancer and despite best supportive care, euthanasia is often required within a matter of weeks.

In order to gather more background information on this group of cats, we would be very grateful if you could spare the time to look back into your practice case notes and complete the enclosed questionnaire. Although most of these cats will have died, we hope access to their medical records will still be possible. The information that you provide will form the basis of a study involving further pathological analysis of your submitted samples.

You may not be able to answer all of the questions from your records. However, any information that you are able to provide will be useful to us, so please still return the form. I have enclosed a pre-paid envelope. Alternatively, you can fax the questionnaire back to Alison Hayes, at the Small Animal Centre. However you choose to reply, your prompt attention would be very much appreciated.

In helping to gather this information, you are contributing to an ongoing, multidisciplinary, research project. The information that we gain may provide a better understanding of the biology of this common cancer and may ultimately lead to new therapeutic options. We hope to conclude the study in the next 6 months and look forward to being able to share our findings directly with you.

Once again, thank you for taking the time to complete the enclosed questionnaire. All information will remain confidential and no cat owners will be contacted. If you have any further questions, I will be happy to discuss these with you.

Yours sincerely

Alison Hayes (Mrs) BVMS CertVR MRCVS
Clinician in Oncology

FELINE ORAL SQUAMOUS CELL CARCINOMA QUESTIONNAIRE

Re: Re: Lab No:

Where boxes are provided, please tick the relevant box ☑.
If a date is required, please enter the day/month/year format e.g for 26th October 2002 would be 26/OCT/2002.

THIS SECTION IS ABOUT THE AGE OF THE CAT

1. Was the date of the cat's birth known? Yes☐ If yes please state date of birth

--/---/----

1. Please go to question 3

No ☐ *Please go to question 2*

2. If date of birth was unknown, please give age in years at diagnosis …….
Is this approximate? Yes ☐
No ☐

THIS QUESTION IS ABOUT THE BREED/TYPE ***Please tick only one box***

3. What breed was the cat?

Domestic Short haired (DSH) ☐
Domestic Long haired (DLH) ☐
Unknown ☐
Pedigree ☐ *Please specify*
……

4. Colour:

Please state colour ……

Colour unknown ☐

THIS QUESTION RELATES TO GENDER ***Please tick only one box***

5. What was the sex?

Male ☐
Male neutered ☐
Female ☐
Female neutered ☐
Unknown ☐

THIS SECTION ASKS ABOUT THE DISEASE PRESENTATION

This disease may have presented before a definitive diagnosis was possible. Please answer the following questions.

6. What was the date of first presentation? --/---/----

7. What was the date of biopsy --/---/----

8. Was this problem discovered as part of a regular, routine or general health examination e.g. pre-vaccination examination?
   Yes ☐
   No ☐

9. Was the owner concerned about the general health of their cat?
   Yes ☐
   No ☐

10. Was the owner concerned about the oral health of their cat?
    Yes ☐
    No ☐

11. Please describe your findings on physical examination

……..……

……..……

……

12. Was there a history of stomatitis/dental disease?

    Yes ☐ Please go to question 13
    No ☐ Please go to question 14

13. Please give details

……..……

……..……

……

THIS SECTION IS ABOUT THE DISEASE PROGRESSION

14. Is this cat still alive?
    Yes ☐ If yes, please go to question 18
    No ☐
    Don't know ☐

15. Did the cat die or was euthanasia performed?
    Died ☐
    Euthanasia ☐

16. Date of death if known --/---/----

17. Was the cause of death/reason for euthanasia related to the oral SCC

Yes ☐
No ☐
Don't know ☐

Please add any further information about the cause of death or euthanasia.

……

……

MORE SPECIFICALLY ABOUT THE TUMOUR

As the disease progresses, large amounts of the mouth can become involved, and it is not always possible to say where the tumour originated.

18. When thinking about the site of the tumour within the oral cavity, please ***tick one*** of the following that best describes the tumour.

Sublingual	☐	
Tongue, other than sublingual	☐	
Mandible	☐	➔ go to question 19
Maxilla	☐	➔ go to question 19
Hard palate	☐	
Soft palate	☐	
Cheek (i.e. buccal mucosa)	☐	
Unknown site in the oral cavity	☐	
No tumour in the oral cavity	☐	

19. Within the mandible or maxilla please indicate the position. Please ***tick one*** box.

Rostral (i.e. incisors or canine teeth) ☐
Cheek teeth (i.e. premolar and molar) ☐
Exact location uncertain ☐

THIS QUESTION IS ABOUT THE SPREAD OF TUMOUR BEYOND THE ORAL CAVITY

The regional lymph nodes are in the retropharyngeal and submandibular areas.
When considering these regions, were the nodes

20. Enlarged?

Yes ☐
No ☐
Don't know ☐

21. Biopsied/needle aspirated?

Yes	☐	➔ go to question 22
No	☐	➔ go to question 23
Don't know	☐	➔ go to question 23

22. Were samples sent to a pathologist?

Yes☐
No☐

23. Were radiographs of the thorax obtained?

Yes☐ ➔ go to question 24
No☐ ➔ go to question 25
Don't know☐ ➔ go to question 25

24. Were there any signs of distant metastasis on the thoracic radiographs?

Yes☐ ➔ please describe below
No☐ ➔ go to question 25
Don't know☐ ➔ go to question 25

Please describe

……

……

THIS SECTION RELATES TO TREATMENT

These questions relate to **three** treatment periods before, during and after a diagnosis was made.

Before a histological diagnosis was made

25. Was any treatment attempted?

Yes☐ ➔ go to question 26
No☐ ➔ go to question 27
Don't know☐ ➔ go to question 27

26. Did treatment include any NSAID's? (eg Ketofen, Rimadyl, Metacam, etc)

Yes☐
No☐
Don't know☐

Please describe this and any other medication given prior to biopsy

……

……

Relating to treatment at the time of biopsy

27. At the time that the oral site was biopsied, was the cat receiving any medication?

Yes☐ ➔ go to question 28
No☐ ➔ go to question 29
Don't know☐ ➔ go to question 29

28. Did treatment include any NSAID's? (e.g. Ketofen, Rimadyl, Metacam, etc)

Yes☐
No☐
Don't know☐

Please describe this and any other medication being at the time of biopsy.

……

……..……

…….……

Relating to treatment after a histological diagnosis was made

29. Was any treatment attempted?

Yes☐ ➔ go to question 30
No☐ ➔ go to question 31
Don't know☐ ➔ go to question 31

30. Did treatment include any NSAID's? (eg Ketofen, Rimadyl, Metacam, etc)

Yes☐
No☐
Don't know☐

Please describe this and any other medication given after biopsy

……..……

……..…….

31. If any definitive treatment attempted, e.g. surgery, chemotherapy, radiotherapy, please describe treatment and outcome?

…….

……..……

……..

……

ANY OTHER INFORMATION

……..

……

……..

Signature …….

Print name ……...

Date …….

Please return completed questionnaire to Alison Hayes in the envelope provided to

Alison Hayes
Animal Health Trust,
Lanwades Park,
Kentford,
Newmarket, Suffolk CB8 7UU
Fax: 08700 502541

Thank you for completing this questionnaire

Appendix D: Feline EGFR sequence and alignment with the feline genome

BLAST search against feline whole genome shotgun sequences
Program: BLASTN 2.2.24+
Reference:
Zheng Zhang, Scott Schwartz, Lukas Wagner, and Webb Miller (2000), "A greedy algorithm for aligning DNA sequences", Journal of Computational Biology
2000; 7(1–2):203–14.

SCCF1 full tyrosine kinase region sequence

>Felis catus epidermal growth factor receptor (EGFR) tyrosine kinase
CTGCACAGGACGAGGACCAGACAGCTGCGTGCAGTGTGCACACTACATCGACGGCCCTCA
CTGCGTCAAGACCTGCCCGGCTGGCATCATGGGAGAAAACAACACCCTGGTCTGGAAGTT
TGCGGACGCCAATCGCATGTGTCACCTGTGCCATTCAAACTGTACCTACGGCTGTTCTGG
GCCAGGTCTTGAAGGCTGTGCTACAGATGGGCCCAAGATCCCATCCATCGCCACTGGGAT
TGTTGGGGGCCTCCTCTTGGTGGTGGTGGTGGCCCTTGGGGTGGGCCTCTTTCTGCGCCG
ACGCCACATCGTCCGCAAGCGCACACTTCGCAGACTGCTGCAGGAAAGAGAGCTTGTTGA
GCCTCTTACGCCCAGCGGAGAAGCTCCCAACCAAGCTCTCTTGAGGATCTTAAAGGAAAC
AGAATTCAAAAAGATCAAGGTGCTGGGCTCTGGAGCATTTGGCACAGTGTACAAGGGACT
CTGGATCCCAGAAGGTGAGAAGGTTAAAATTCCTGTGGCCATCAAGGAGTTACGAGAAGC
CACATCTCCAAAAGCCAACAAGGAAATCCTTGATGAAGCTTACGTGATGGCCAGTGTGGA
CAATCCCCACGTGTGCCGCCTCCTGGGCATCTGCCTGACGTCCACGGTCCAGCTCATCAC
ACAGCTCATGCCCTTCGGCTGCCTCCTGGACTATGTCCGCGAGCACAAGGACAACATTGG
CTCCCAGTACCTGCTCAACTGGTGTGTGCAGATTGCGAAGGGCATGAACTACCTGGAAGA
CCGGCGCTTGGTGCACCGTGACCTGGCAGCCAGGAATGTCCTGGTGAAGACGCCACAGCA
TGTCAAGATCACAGATTTTGGGCTGGCCAAACTGCTTGGTGCCGAGGAGAAAGAATACCA
CGCGGAAGGAGGCAAAGTGCCTATCAAGTGGATGGCTTTGGAATCAATTTTACACCGAAT
TTACACCCACCAAAGTGACGTCTGGAGCTATGGAGTCACCGTTTGGGAGTTGATGACCTT
TGGGTCTAAACCTTACGACGGAATCCCCGCAAGTGAGATCTCGACCATCCTGGAGAAAGG
AGAGCGCCTCCCGCAGCCACCCATATGCACCATCGATGTCTACATGATCATGGTCAAGTG
CTGGATGATAGATGCAGACAGTCGCCCGAAATTCCGTGAGTTGATCATTGAATTCTCCAA
AATGGCCCGAGACCCCCAGCGCTACCTTGTCATCCAGGGAGATGAGAGAATGCATCTGCC
AAGCCCTACAGACTCCAATTTTTACCGCGCCCTGATGGACGAAGAAGACATGGAAGACGT
CGTAGATGCC

Feline amino acid sequence

>Felis catus epidermal growth factor receptor (EGFR) tyrosine kinase
CTGRGPDSCVQCAHYIDGPHCVKTCPAGIMGENNTLVWKFADANRMCHLCHSNCTYGCSG
PGLEGCATDGPKIPSIATGIVGGLLLVVVVALGVGLFLRRRHIVRKRTLRRLLQERELVE
PLTPSGEAPNQALLRILKETEFKKIKVLGSGAFGTVYKGLWIPEGEKVKIPVAIKELREA
TSPKANKEILDEAYVMASVDNPHVCRLLGICLTSTVQLITQLMPFGCLLDYVREHKDNIG
SQYLLNWCVQIAKGMNYLEDRRLVHRDLAARNVLVKTPQHVKITDFGLAKLLGAEEKEYH
AEGGKVPIKWMALESILHRIYTHQSDVWSYGVTVWELMTFGSKPYDGIPASEISTILEKG
ERLPQPPICTIDVYMIMVKCWMIDADSRPKFRELIIEFSKMARDPQRYLVIQGDERMHLP
SPTDSNFYRALMDEEDMEDVVDA

Sequences producing significant alignments:	
Accession	Description
ACBE01065685.1	Felis catus c497001689.Contig1, whole genome shotgun sequence
AANG01387714.1	Felis catus cont1.387713, whole genome shotgun sequence
ACBE01065687.1	Felis catus c435901305.Contig1, whole genome shotgun sequence
AANG01738232.1	Felis catus cont1.738231, whole genome shotgun sequence
ACBE01065683.1	Felis catus c505502232.Contig1, whole genome shotgun sequence
AANG01387712.1	Felis catus cont1.387711, whole genome shotgun sequence
AANG01738233.1	Felis catus cont1.738232, whole genome shotgun sequence
ACBE01065684.1	Felis catus c490401688.Contig1, whole genome shotgun sequence
AANG01387767.1	Felis catus cont1.387766, whole genome shotgun sequence
AANG01738234.1	Felis catus cont1.738233, whole genome shotgun sequence

Query: our TK sequencing
Sbjct: feline genome shotgun sequence

```
Query  14    GGACCAGACAGCTGCGTGCAGTGTGCACACTACATCGACGGCCCTCACTGCGTCAAGACC  73
             ||||||||||||||||||||||||||||||||||||||||||||||||||||||||||||
Sbjct 4489   GGACCAGACAGCTGCGTGCAGTGTGCACACTACATCGACGGCCCTCACTGCGTCAAGACC  4430

Query  74    TGCCCGGCTGGCATCATGGGAGAAAACAACACCCTGGTCTGGAAGTTTGCGGACGCCAAT  133
             ||||||||||||||||||||||||||||||||||||||||||||||||||||||||||||
Sbjct  4429  TGCCCGGCTGGCATCATGGGAGAAAACAACACCCTGGTCTGGAAGTTTGCGGACGCCAAT  4370

Query  134   CGCATGTGTCACCTGTGCCATTCAAACTGTACCTACGG  171
             |||||||||||||||||||||||||||||||||||||
Sbjct  4369  CGCATGTGTCACCTGTGCCATTCAAACTGTACCTACGG  4332


Query  171   GCTGTTCTGGGCCAGGTCTTGAAGGCTGTGCTACAGATGGG  211
             |||| || ||||||||||||||||||||||||||||||||
Sbjct  2271  GCTGTTCTGGGCCAGGTCTTGAAGGCTGTGCTACAGATGGG  2215


Query  210   GGCCCAAGATCCCATCCATCGCCACTGGGATTGTTGGGGGCCTCCTCTTGGTGGTGGTGG  269
             ||||||||||||||||||||||||||||||||||||||||||||||||||||||||||||
Sbjct  4953  GGCCCAAGATCCCATCCATCGCCACTGGGATTGTTGGGGGCCTCCTCTTGGTGGTGGTGG  4894

Query  270   TGGCCCTTGGGGTGGGCCTCTTTCTGCGCCGACGCCACATCGTCCGCAAGCGCACACTTC  329
             ||||||||||||||||||||||||||||||||||||||||||||||||||||||||||||
Sbjct  4893  TGGCCCTTGGGGTGGGCCTCTTTCTGCGCCGACGCCACATCGTCCGCAAGCGCACACTTC  4834

Query  330   GCAGACTGCTGCAGGAAAGAGAG  352
             |||||||||||||||||||||||
Sbjct  4833  GCAGACTGCTGCAGGAAAGAGAG  4811


Query  351   AGCTTGTTGAGCCTCTTACGCCCAGCGGAGAAGCTCCCAACCAAGCTCTCTTGAGGATCT  410
             ||||||||||||||||||||||||||||||||||||||||||||||||||||||||||||
Sbjct  3941  AGCTTGTTGAGCCTCTTACGCCCAGCGGAGAAGCTCCCAACCAAGCTCTCTTGAGGATCT  3882

Query  411   TAAAGGAAACAGAATTCAAAAAGATCAAGGTGCTGGGCTCTGGAGCATTTGGCACAGTGT  470
             ||||||||||||||||||||||||||||||||||||||||||||||||||||||||||||
Sbjct  3881  TAAAGGAAACAGAATTCAAAAAGATCAAGGTGCTGGGCTCTGGAGCATTTGGCACAGTGT  3822
```

```
Query  471   ACAAGG  476
             ||||||
Sbjct  3821  ACAAGG  3816


Query  474   AGGGACTCTGGATCCCAGAAGGTGAGAAGGTTAAAATTCCTGTGGCCATCAAGGAGTTAC  533
             ||||||||||||||||||||||||||||||||||||||||||||||||||||||||||||
Sbjct  2302  AGGGACTCTGGATCCCAGAAGGTGAGAAGGTTAAAATTCCTGTGGCCATCAAGGAGTTAC  2361

Query  534   GAGAAGCCACATCTCCAAAAGCCAACAAGGAAATCCTTGATG  575
             |||||||||||||||||||||||||||||||||||||||||||
Sbjct  2362  GAGAAGCCACATCTCCAAAAGCCAACAAGGAAATCCTTGATG  2403


Query  575   GAAGCTTACGTGATGGCCAGTGTGGACAATCCCCACGTGTGCCGCCTCCTGGGCATCTGC  634
             ||||||||||||||||||||||||||||||||||||||||||||||||||||||||||||
Sbjct  3864  GAAGCTTACGTGATGGCCAGTGTGGACAATCCCCACGTGTGCCGCCTCCTGGGCATCTGC  3923

Query  635   CTGACGTCCACGGTCCAGCTCATCACACAGCTCATGCCCTTCGGCTGCCTCCTGGACTAT  694
             ||||||||||||||||||||||||||||||||||||||||||||||||||||||||||||
Sbjct  3924  CTGACGTCCACGGTCCAGCTCATCACACAGCTCATGCCCTTCGGCTGCCTCCTGGACTAT  3983

Query  695   GTCCGCGAGCACAAGGACAACATTGGCTCCCAGTACCTGCTCAACTGGTGTGTGCAGATT  754
             ||||||||||||||||||||||||||||||||||||||||||||||||||||||||||||
Sbjct  3984  GTCCGCGAGCACAAGGACAACATTGGCTCCCAGTACCTGCTCAACTGGTGTGTGCAGATT  4043

Query  755   GCGAAGG  761
             |||||||
Sbjct  4044  GCGAAGG  4050


Query  759    AGGGCATGAACTACCTGGAAGACCGGCGCTTGGTGCACCGTGACCTGGCAGCCAGGAATG  818
              ||||||||||||||||||||||||||||||||||||||||||||||||||||||||||||
Sbjct  18063  AGGGCATGAACTACCTGGAAGACCGGCGCTTGGTGCACCGTGACCTGGCAGCCAGGAATG  18004

Query  819    TCCTGGTGAAGACGCCACAGCATGTCAAGATCACAGATTTTGGGCTGGCCAAACTGCTTG  878
              ||||||||||||||||||||||||||||||||||||||||||||||||||||||||||||
Sbjct  18003  TCCTGGTGAAGACGCCACAGCATGTCAAGATCACAGATTTTGGGCTGGCCAAACTGCTTG  17944

Query  879    GTGCCGAGGAGAAAGAATACCACGCGGAAGGAGGCAAAGT  918
              |||||||||||||||||||||||||||||||||||||||||
Sbjct  17943  GTGCCGAGGAGAAAGAATACCACGCGGAAGGAGGCAAAGT  17904


Query  917   GTGCCTATCAAGTGGATGGCTTTGGAATCAATTTTACACCGAATTTACACCCACCA  972
             ||||||||||||||||||||||||||||||||||||||||||||||||||||||||
Sbjct  6313  GTGCCTATCAAGTGGATGGCTTTGGAATCAATTTTACACCGAATTTACACCCACCA  6368

Query  973   AAGTGACGTCTGGAGCTATGG  993
             |||||||||||||||||||||
Sbjct  6369  AAGTGACGTCTGGAGCTATGG  6389


Query  992    GGAGTCACCGTTTGGGAGTTGATGACCTTTGGGTCTAAACCTTACGACGGAATCCCCGCA  1051
              ||||||||||||||||||||||||||||||||||||||||||||||||||||||||||||
Sbjct  13724  GGAGTCACCGTTTGGGAGTTGATGACCTTTGGGTCTAAACCTTACGACGGAATCCCCGCA  13665
```

```
Query  1052   AGTGAGATCTCGACCATCCTGGAGAAAGGAGAGCGCCTCCCGCAGCCACCCATATGCACC  1111
              ||||||||||||||||||||||||||||||||||||||||||||||||||||||||||||
Sbjct  13664  AGTGAGATCTCGACCATCCTGGAGAAAGGAGAGCGCCTCCCGCAGCCACCCATATGCACC  13605

Query  1112   ATCGATGTCTACATGATCATGGTCAAGTG  1140
              |||||||||||||||||||||||||||||
Sbjct  13604  ATCGATGTCTACATGATCATGGTCAAGTG  13576


Query  1140  GCTGGATGATAGATGCAGACAGTCGCCCGAAATTCCGTGAGTTGATCATTGAATTCTCCA  1199
              ||||||||||||||||||||||||||||||||||||||||||||||||||||||||||||
Sbjct  198   GCTGGATGATAGATGCAGACAGTCGCCCGAAATTCCGTGAGTTGATCATTGAATTCTCCA  257

Query  1200  AAATGGCCCGAGACCCCCAGCGCTACCTTGTCATCCAGG  1238
              |||||||||||||||||||||||||||||||||||||||
Sbjct  258   AAATGGCCCGAGACCCCCAGCGCTACCTTGTCATCCAGG  296


Query  1234  CCAGGGAGATGAGAGAATGCATCTGCCAAGCCCTACAGACTCCAATTTTTACCGCGCCCT  1293
              ||||||||||||||||||||||||||||||||||||||||||||||||||||||||||||
Sbjct  1703  CCAGGGAGATGAGAGAATGCATCTGCCAAGCCCTACAGACTCCAATTTTTACCGCGCCCT  1762

Query  1294  GATGGACGAAGAAGACATGGAAGACGTCGTAGATGCC  1330
              |||||||||||||||||||||||||||||||||||||
Sbjct  1763  GATGGACGAAGAAGACATGGAAGACGTCGTAGATGCC  1798
```

Appendix E: Publications arising from the thesis

BERGKVIST, G. T., ARGYLE, D. J., PANG, L.Y., MUIRHEAD, R. & YOOL, D. A. 2011. Studies on the Inhibition of Feline EGFR in Squamous Cell Carcinoma: Enhancement of radiosensitivity and rescue of resistance to small molecule inhibitors. *Cancer Biol Ther*, 11 (11), 927-937.

BERGKVIST, G. T. & YOOL, D. A. 2011. Epidermal Growth Factor Receptor as a Therapeutic Target in Veterinary Oncology. *Vet Comp Oncol*, 9 (2), 81-94.

BERGKVIST, G. T., ARGYLE, D. J., MORRISON, L., MACINTYRE, N., HAYES, A. & YOOL, D. A. 2011. Expression of Epidermal Growth Factor Receptor (EGFR) and Ki67 in Feline Oral Squamous Cell Carcinomas (FOSCC). *Vet Comp Oncol*, 9 (2), 106-117.